Journal of Inorganic Biochemistry 242 (2023) 112154

Contents lists available at ScienceDirect

Journal of Inorganic Biochemistry

journal homepage: www.elsevier.com/locate/jinorgbio

Review Article

The inorganic chemistry of the cobalt corrinoids – an update

Helder M. Marques *

Molecular Sciences Institute, School of Chemistry, University of the Witwatersrand, Johannesburg 2050, South Africa

ARTICLE INFO

Keywords:
Cobalt corrinoids
Ligand substitution reactions
Biological chemistry of B_{12}
B_{12} redox chemistry
B_{12} photochemistry
Computational methods and B_{12} chemistry

ABSTRACT

The inorganic chemistry of the cobalt corrinoids, derivatives of vitamin B_{12}, is reviewed, with particular emphasis on equilibrium constants for, and kinetics of, their axial ligand substitution reactions. The role the corrin ligand plays in controlling and modifying the properties of the metal ion is emphasised. Other aspects of the chemistry of these compounds, including their structure, corrinoid complexes with metals other than cobalt, the redox chemistry of the cobalt corrinoids and their chemical redox reactions, and their photochemistry are discussed. Their role as catalysts in non-biological reactions and aspects of their organometallic chemistry are briefly mentioned. Particular mention is made of the role that computational methods – and especially DFT calculations – have played in developing our understanding of the inorganic chemistry of these compounds. A brief overview of the biological chemistry of the B_{12}-dependent enzymes is also given for the reader's convenience.

1. Introduction

Much has been written about almost every aspect of the chemistry of vitamin B_{12} and its derivatives, the cobalt corrinoids, in several edited volumes (for example, [1–5]), and in comprehensive reviews of their structural properties [6], general chemistry [7], biological chemistry [8–28], their intra-cellular trafficking [29,30], the B_{12} antivitamins [31–33], corrinoid-catalysed organic reactions [34], photochemistry and photobiology [35,36], and their function as riboswitches [37–39], for example. The importance of B_{12} in health and nutrition in humans (for example, [40–49]), in animals (for example, [50–52]), and in microbial communities [53,54] continues to attract attention. While cobalt in excess is toxic to humans [55–57], B_{12} deficiency has severe health consequences.

This review focusses on the inorganic chemistry of the cobalt corrinoids, particularly the thermodynamics and kinetics of their coordination chemistry and developments in the field since the publication in 1972 of Pratt's seminal book, *The Inorganic Chemistry of Vitamin B_{12}* [58]. This is a (belated) tribute to the memory of John Pratt (Fig. 1), a luminary in the B_{12} field, who sadly passed on in 2018, aged 84. A brief overview of the biological chemistry of B_{12} is also given for the reader's convenience – but the reader needs to appreciate this for what it is: a brief overview only.

While there are several cobalt-containing enzymes [59,60], the biological chemistry of cobalt is dominated by the chemistry of the cobalamins, derivatives of vitamin B_{12} [2,7,16]. Pernicious anaemia was a fatal disease characterised by neurological and haematological abnormalities that caused overwhelming fatigue; people that suffered from the disease had low red blood cell counts and hence were deficient in the carrying of oxygen to the tissues. The disease was formally described in 1824 by James Combe, who suggested that it could be related to a disorder of the digestive tract [61] although it was not until Thomas Addison provided a full clinical and pathological description that it began to be recognized as a distinct entity [62], and was referred to as 'Addisonian anaemia' [63]. The term "pernicious anaemia" appears to have been coined in Germany by Michael Biermer as the insidious course of the disease was then untreatable [64].

In the 1920s, George Whipple at the University of Rochester School of Medicine and Dentistry, began assessing the effects of treatments for anaemia caused by chronic blood loss. Treating dogs with raw liver showed much promise in the regeneration of blood [65]. George Minot and William Murphy, working in Boston, followed this up by using raw liver to treat cases of pernicious anaemia. The treatment caused rapid symptomatic improvement and an elevation of the red cell count [66]. William Castle showed that, to be absorbed, the antipernicious anaemia factor ("extrinsic factor") must interact with a substance in gastric juice or "intrinsic factor." We now know that this intrinsic factor (IF), also known as the gastric intrinsic factor (GIF) protein, coded in humans by the *GIF* gene, is a glycoprotein produced by the parietal cells of the stomach. It is required for the absorption of B_{12} in the ileum of the small

* Corresponding author.
E-mail address: Helder.Marques@wits.ac.za.

https://doi.org/10.1016/j.jinorgbio.2023.112154
Received 7 January 2023; Received in revised form 23 January 2023; Accepted 26 January 2023
Available online 3 February 2023

Fig. 1. John McDonald Pratt.

intestine [67].

Minot, Murphy, and Whipple received the Nobel Prize in Physiology or Medicine in 1934 for their development of liver therapy of pernicious anaemia. Somewhat ironically, two years later it became evident that the positive response of dogs to liver was because of the iron rather than the B_{12} content [68].

Liver extracts were used for intramuscular injection until the 1950s to treat cases of pernicious anaemia. In 1948 the "anti-pernicious anaemia factor" was isolated from liver and kidney by Smith [69] and by Folkers and co-workers [70] who named the factor vitamin B_{12}. They showed that the administration of a few micrograms could prevent relapse of the disease. It was identified as containing cobalt [69], a rare trace metal in biology, and, indeed, a relatively rare element in the Earth's crust [71].

The structure of B_{12} was determined by Dorothy Hodgkin and her colleagues using X-ray diffraction methods [72,73]. Its total synthesis by Woodward, Eschenmoser and co-workers remains a landmark in organic synthesis [74,75].

Although a number of other cobalt-requiring proteins are known [59,60] and in which typically the metal ion activates H_2O to catalyse a hydrolytic reaction [76], probably the most important function of cobalt in biology is in vitamin B_{12} and its derivatives. Exposure to cobalt compounds, almost always as Co(II) or Co(III)) from environmental, dietary, occupational or medical sources (most commonly from metal-on-metal hip implants) may have adverse neurological, cardiovascular and endocrine effects [77–80]. In addition to redox-active cobalt generating reactive oxygen species (ROS), it competes with other biologically essential ions, and its kinetic inertness amplifies this toxicity effect [76].

Probably the best known function of the cobalt corrinoids is in folate and fatty acid metabolism. They are essential micronutrients in animals, including humans, but not in plants or fungi. But the function of the corrinoids is diverse and continues to be elucidated. Surprising new discoveries include their role as a photo-receptor in light-dependent gene regulation [81] and in modulating the structure of microbial communities in the human gut [53].

Humans have two enzymes that require cobalamin: methylmalonyl CoA mutase, which requires adenosylcobalamin, [AdoCbl],[1] and converts methylmalonyl CoA into succinyl CoA, and 5-methyltetrahydrofolate-homocysteine methyltransferase (methionine synthase, MS), which requires methylcobalamin, [CH_3Cbl], and is required for recycling of tetrahydrofolate by means of methionine synthesis from homocysteine. B_{12} deficiency can result in damage to the myelin sheath of nerves because of the accumulation of methylmalonyl CoA, and megaloblastic anaemia because of an inability to regenerate tetrahydrofolate, which is required for thymine synthesis [82–88].

B_{12} is essential for the normal function of DNA and deficiency of the vitamin impairs the ability of cells to divide. The most rapidly dividing cells are found in the skin, hair follicles and lining of the gastrointestinal tract, and in bone marrow, where red blood cells are made. The effects of B_{12} deficiency on the skin and bowel are minimal; however, the inability of the bone marrow to produce red cells is the root cause of pernicious anaemia. As mentioned, the vitamin also plays an important role in the central nervous system and is essential for the production of the myelin that forms the protective sheath surrounding nerve cells.

B_{12} deficiency leads to conditions including megaloblastic anaemia, tingling and numbness of the extremities, gait abnormalities, visual disturbances, memory loss and dementia [89] and is also associated with developmental and neurological disorders [90,91]. Elevated homocysteine levels, indicative of impaired one-carbon metabolism that, *inter alia*, could be indicative of insufficient levels of B_{12}, have been associated with the onset and progression of Alzheimer's disease [92], in general cognitive decline [93], and may lead to brain abnormalities [94]. Thrombotic microangiopathy (TMA) induced by a cobalamin deficiency is rare and closely resembles the clinical features of thrombotic thrombocytopenic purpura (TTP) [95].

B_{12} deficiency is readily determined by a blood test and treatment entails supplementation, by injection, or uptake through the nasal passages [43]. Low levels of B_{12} can occur in the aged because of atrophy of the lining of the stomach that leads to the inadequate production of intrinsic factor. Dietary folate supplementation may ameliorate the anaemia, but not myelin damage or accumulation of homocysteine (a condition known as homocysteinuria [96]), which is thought to contribute to stroke and cardiac infarction. Deficiency usually results from deficit dietary uptake, absorption or transport of B_{12}, since non-vegan diets usually have sufficient quantities of B_{12}. People on strict vegan diets are at high risk of developing B_{12} deficiency unless they take B_{12} supplements [97]. There is a correlation between patients on metformin as an oral hypoglycaemic drug and B_{12} deficiency [98].

The role of B_{12} is some clinically-important diseases, such as its role in *Mycobacterium tuberculosis*, remains poorly understood [99]. Indeed, the complexities of the role that B_{12} and its derivatives play in biology, and the limits of our current understanding, are neatly illustrated by the case of *M. tuberculosis.* The bacterium has the ability to carry out the *de novo* synthesis of B_{12} but it is also able to scavenge corrinoids with an ATP-binding protein. Its genome encodes two B_{12} riboswitches and three B_{12}-dependent enzymes. One enzyme (MetH) is used in the biosynthesis of methionine; the second, MutAB, is used in propionate utilization; but the role of the third, a ribonucleotide reductase, remains unknown. The bacillus is clearly B_{12}-dependent and appears to have the competency to regulate function depending on the availability of B_{12}: either it scavenges it from its environment, or it switches on the metabolically expensive *de novo* synthesis route.

2. The structure of the cobalt corrinoids

2.1. Nomenclature

B_{12} and its derivatives contain a tetrapyrrole ligand, corrin (Fig. 2), with absolute *R* configuration at C1 and C19 [100]. Unlike a porphyrin, there is a direct bond between the A and D rings. The left-chiral asymmetry of the corrin at C1 distinguishes the "upper" (or β) and "lower" (or α) face.

In the so-called "complete corrinoids", the α ligand is part of a nucleotide loop that is attached to ring D at C17 (Fig. 3). The nucleotide loop does not appear to impart strain on the macrocycle [101]. The terminal bases may be purines or benzimidazoles [102]; a phenol may

[1] The term $[RCbl(X)]^{n+}$ will be used to refer to a cobalamin with R the axial ligand and X the oxidation state of cobalt. If the specific oxidation state (as here) is not given, then Co(III) is assumed. The term [Cbx] refers to any cobalt corrinoid.

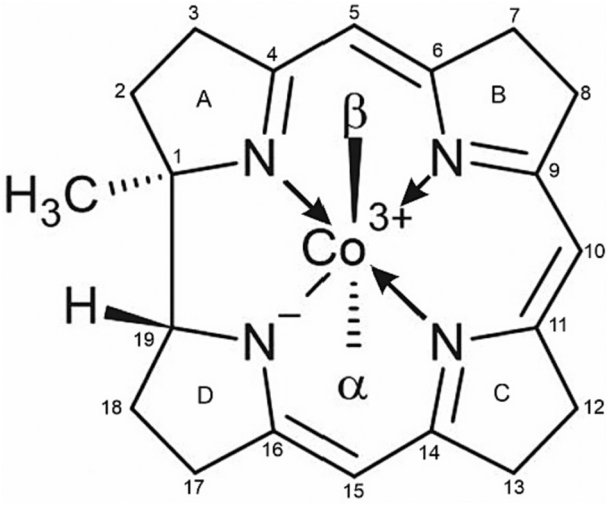

Fig. 2. The tetrapyrrole macrocyclic ligand of the cobalt corrinoids.

also occupy the terminal position of the nucleotide loop but does not coordinate the metal ion [103]. Acetamide substituents point to the β face at C2, C7 and C18, and propionamides point to the α face at C3, C6 and C13.

Cobalt complexes where the oxidation state of the metal ranges all the way from −3 to +6 are known [104]. In the cobalt corrinoids, however, the cobalt ion usually occurs in the low spin +3, +2 or + 1 oxidation state. The electrochemical oxidation of Co(III) in methylcobalamin ([MeCbl]) leads to the rapid cleavage of the Co—C bond, producing aquacob(III)alamin, $[H_2OCbl]^+$, and methanol [105]. DFT (BP86/6-31G*) and CASSCF/MC-XQDPT2 calculations suggest that cationic $[MeCbl]^+$ is best described as a metal with Co(III)/Co(IV) character and a corrin π radical cation, and has a considerably weakened Co—C bond [106].

Cobinamides lack the nucleotide tail, with hydrolytic cleavage of the nucleotide side chain at the phosphate group; the *d* side chain is therefore $CH_2CH_2CONHCH_2CH(CH_3)OH$. Compounds such as aquacyanocobinamide ($[ACCbi]^+$, or Factor B) will be present in solution as two diastereomeric coordination isomers, or diastereomers, α-aqua, β-cyano and α-cyano, β-aqua; the diastereomers of Factor B are not very readily separated and often interchange in solution, probably though intermediate formation of the diaqua and dicyano complexes. (The α and β isomers of other cobinamides can be separated chromatographically [107,108], as mentioned later, see Section 9.2). Compounds in which the C17 (or *f*) side chain retains the ribose 3-phosphate residue, but not necessarily the 5,6-dimethylbenzimidazole (bzm) base are termed cobamides. Cobyric acid is the hexamide with a propionic acid *f* side chain. In cobyrinic acid, all seven side chains of the corrin have been hydrolysed to carboxylic acids.

We will use the generic term *cobalt corrinoids* to refer collectively to all corrin species. There are IUB and IUPAC recommendations for the naming of the corrinoids [109] that have been succinctly summarised [110]. The numbering scheme used in shown in Fig. 4.

The two principal biologically active forms of the cobalt corrinoids are methylcobalamin $[CH_3Cbl]$ (or [MeCbl]), and 5′-deoxydenosylcobalamin (coenzyme B_{12}; [AdoCbl]) (Fig. 3). Cyanocobalamin ([CNCbl], vitamin B_{12}) is not biologically active and has to be converted to a functional form ($[CH_3Cbl]$, [AdoCbl]). Aquacobalamin, $[H_2OCbl]^+$, or vitamin B_{12a}, has H_2O as the upper (β) axial ligand; it loses H^+ to form hydroxocobalamin, [HOCbl] ($pK_a = 7.462(7)$ [111]).

Free forms of the cobalamins are usually found with bzm occupying the lower (α) coordination site (the "base-on" form). Protonation of bzm at low pH (pK_a for $[H_2OCbl]^+ = -2.13$ [112]; [MeCbl] = 2.89 [113]; [AdoCbl] = 3.67 [112]) leads to the "base-off" form [23]. Many proteins in which a cobalamin is the cofactor bind it with bzm displaced by a His

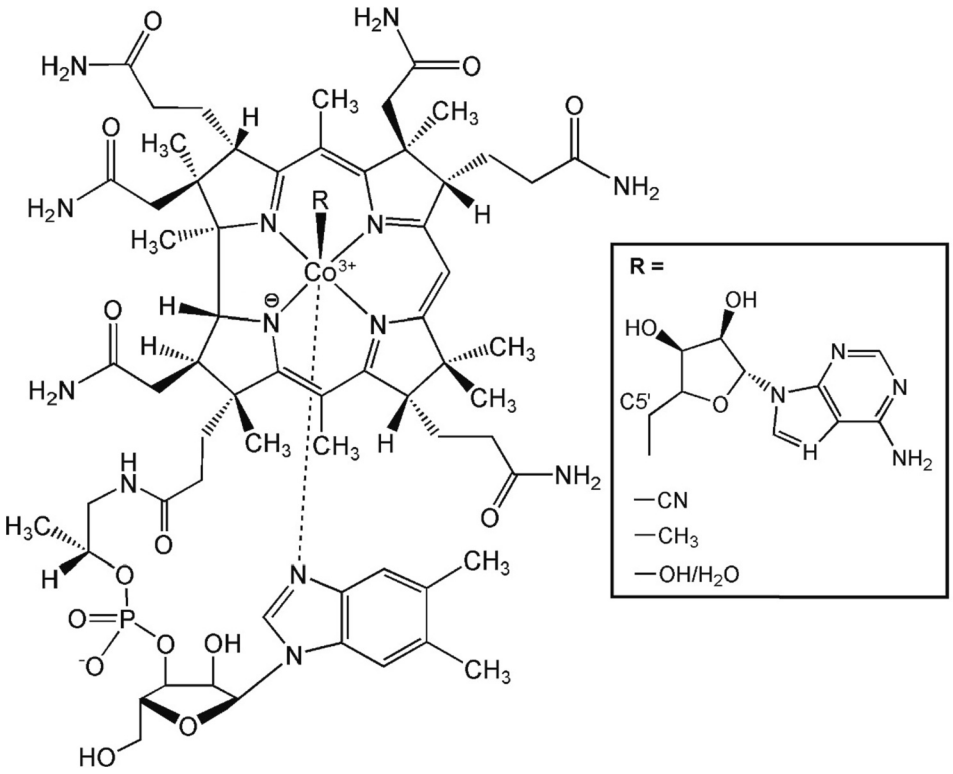

Fig. 3. The structure of the cobalamins. In adenosylcobalamin, [AdoCbl], or coenzyme B_{12}, $R = 5'$-deoxyadenosyl. Cyanocobalamin or vitamin B_{12} itself, [CNCbl], has $R = CN^-$. Methylcobalamin, $[CH_3Cbl]$ or [MeCbl], has $R = CH_3^-$; in aquacobalamin, or vitamin B_{12a}, $[H_2OCbl]^+$, $R = H_2O$ and in hydroxocobalamin, [HOCbl], $R = OH^-$.

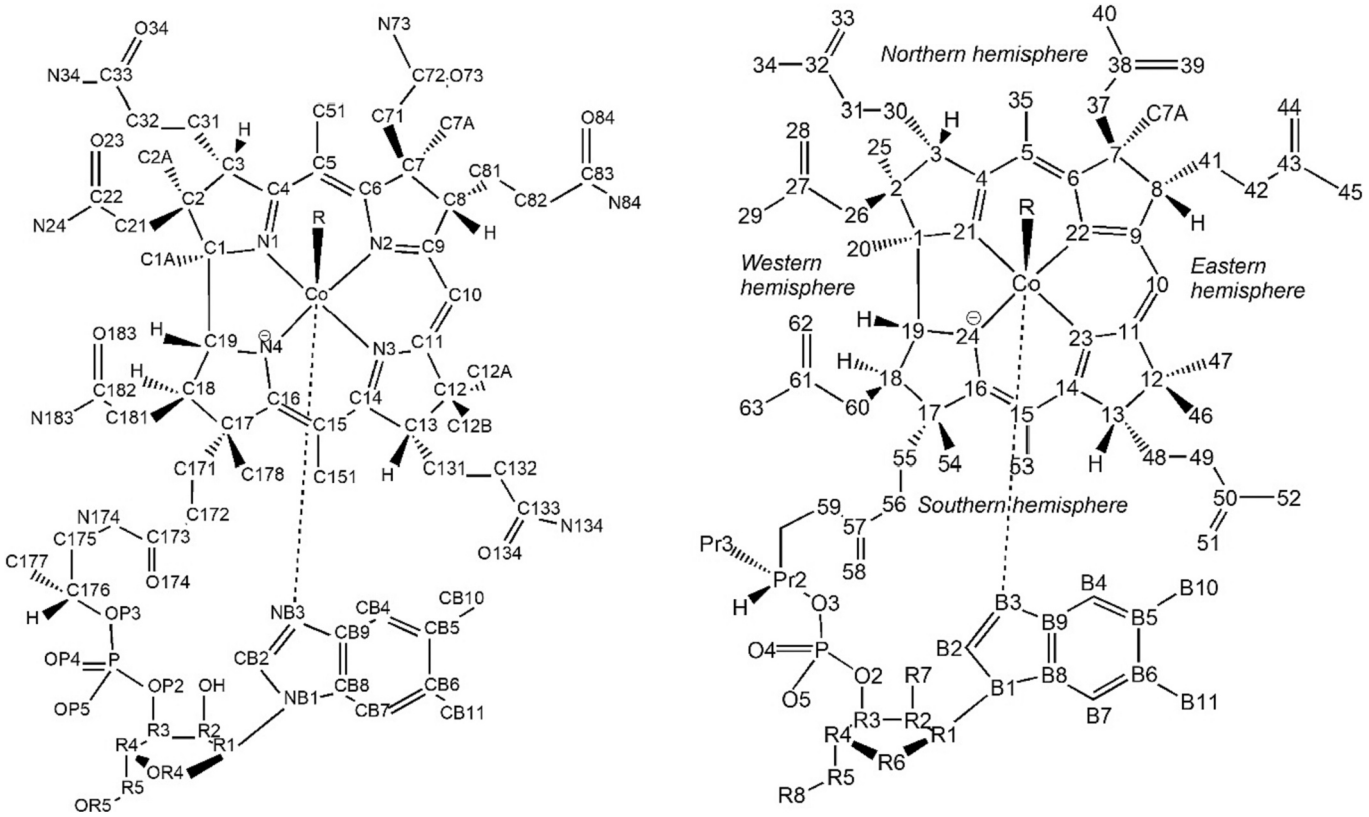

Fig. 4. The numbering of the cobalt corrinoids. That on the left accords with IUPAC and IUB recommendations; that on the right is the numbering commonly used in the earlier literature.

residue from the protein ("base-off/His-on") [114].

The cobalt ion is usually in the +3 oxidation state under aerobic conditions, and is six-coordinate. [CNCbl] features a strong Co—C bond, and a relatively weak bond to the axial bzm base. The Co—C bond in an alkylcobalamin such as [MeCbl] is considerably weaker [115].

A one-electron reduction produces the Co(II) form, cob(II)alamin, [Cbl(II)], or B_{12r}. It is often five-coordinate in neutral solution with a vacant β coordination site. If the β coordination site is occupied, then the bond to bzm is weakened and the pK_a for the base-off/base-on reaction is raised to 2.9 [116], 3.4 [117] and 4.8 [118] when the β ligand is H_2O, SCN^- and SO_2^-, respectively, for example. Protonated, base-off [Cbl(II)] is five-coordinate in a coordinating solvent, with a solvent molecule occupying an axial coordination site, as demonstrated by continuous wave EPR spectroscopy at X-band frequencies and pulse-EPR and ENDOR methods at X-, Q- and W-band frequencies [119]. A further one-electron reduction produces cob(I)alamin ($[Cbl(I)]^-$, B_{12s}; this is most often four-coordinate [58].

B_{12} cofactors with α-axial ligands other than bzm have also been observed [120], with the most common example being pseudo-B_{12} (Fig. 5), in which N7-linked adenine replaces bzm as the α-axial ligand [121]. Pseudo-B_{12} has no physiological functionality in humans but is physiologically important in *Salmonella enterica* serovar Typhimurium [122]. Factor III_m found in, for example, *Clostridium thermoaceticum,* has a methoxy group at position B5 and H at position B6 of the benzimidazole ligand [123].

Whilst interest in the chemistry of the cobalt corrinoids is aimed principally at reaching an understanding of their roles – and the mechanistic details underlying those roles – in biology, the physical and inorganic chemistry of these compounds are interesting in their own right and their study has made contributions to these branches of chemistry. This is the principal focus of this review.

Various spectroscopic methods have been used to elucidate the molecular and electronic structure of the cobalt corrinoids. NMR in particular (for example [124–136]) has been very useful for studying the compounds in solution, and electronic (uv-vis), electronic circular dichroism (ECD), x-ray absorption fine structure (EXAFS), x-ray absorption near edge structure (XANES), electron paramagnetic resonance (EPR) and resonance Raman (rR) spectroscopy have played an important role in probing their structure [137–145]. Detailed assignments of the uv-vis, rR and ECD spectra, often supported by computational

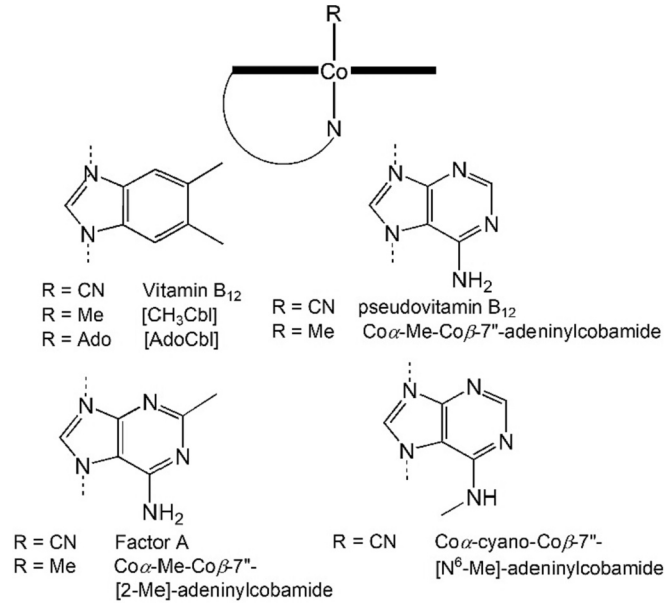

Fig. 5. Variability in the lower axial ligand of the cobalt corrinoids.

methods, are available (for example [142,143,146–151]).

ECD spectra of the cobalamins are quite sensitive to the identity of the β ligand [142,151]. The rR spectra depend on the oxidation state of the metal [150] because of differences in the extent of mixing between Co $3d_{xz}$ and $3d_{yz}$ orbitals and vacant corrin π^* orbitals in [CNCbl], [Cbl (II)] and $[Cbl(I)]^-$. There is an increase in the donation of electron density from the metal to corrin π^* orbitals as the oxidation state of the metal decreases; this leads to a weakening of the conjugated C—C and C—N bonds of the corrin and decrease in the frequency of their normal modes of vibration. Vibrations of principally the C—C and C—N bonds of the corrin along one axis of the corrin ring (the C1,C19–C10 axis for Co (III), the C5–C15 axis for Co(II) and Co(I)) couple to perpendicularly polarized electronic transitions.

The rR and resonance Raman optical activity (rROA) spectra, with excitation at 532 nm, of a number of cobalamins ([CNCbl], [HOCbl], [HCCPhCCCbl], [CN-10BrCbl]) have been reported [151]. The spectra are all quite similar as the dominant contributions are resonantly enhanced ring vibrations [138,151]. The substitution of the *meso* proton, the proton at C10, C10H, by Br, as expected, leads to significant differences between the rR spectra of [CNCbl] and [CN-10BrCbl] because of the change in the electronic structure of the corrin ring. The rROA spectra, on the other hand, are more sensitive to the nature of the axial ligand because of the contribution from electronically excited states that differ in energy and sign of their rotatory strengths [151]; they are also more intense for a chiral system such as a corrinoid when in resonance with multiple electronic excites states, allowing for measurements to be performed on solutions with concentrations as low as 10 μM [151].

Important and useful as these spectroscopic methods have been – and will undoubtedly continue to be – there is little doubt that, from the very early days of research into B_{12} and its derivatives [72,73], crystallography has played a central role in the chemistry of the cobalt corrinoids [152].

2.2. Co(III) corrinoids

A comprehensive review of the crystal structures of the cobalamins is available [153]. There are over one hundred such structures deposited in the database of the Cambridge Crystallographic Data Centre (CCDC),[2] but many are not particularly accurate, with large *R* factors, and considerable disorder in the corrin side chains, in the C ring, and in solvent molecules [152,154]. Of the deposited structures, 18 have *R* factors of <5% (Table 1). The Co—N, N—C and C—C bond lengths, their average, and standard deviation, obtained from these structures are listed in Table 1. (A domed, five-coordinate structure of the heptamethyl cobyrinate (cobester) with a (3-benzenesulfonyl)cyclobutyl ligand in the β coordination site and with $R = 3.15\%$ [155] has not been included.)

The Co—N1 and Co—N4 bonds are shorter than the Co—N2 and Co—N3 bonds because of the direct C1—C19 link of the A and D rings (Table 2). This also causes an elongation of the C4—C5 and C15—C16 bond lengths (1.448(6) Å, $n = 36$) compared to the other C—C of the delocalised π electron system (1.390(31) Å, $n = 90$). The bond lengths between the sp^3 carbon atoms vary between 1.513 and 1.592 Å (mean 1.555(17) Å, $n = 126$).

In studies of alkyl cobaloximes, once regarded as suitable models of the alkyl cobalamins, it was found that complexes with short Co—C bonds also have short Co—N bonds to a trans N-donor ligand [156,157], an effect described as an *inverse trans influence* [158] since it is usually observed in coordination chemistry that shortening the bond length between a ligand and a metal tends to increase the bond length between the metal and the trans ligand. An attempt to quantify the factors that affect the length of the Co—C bond in the alkyl cobaloximes indicate that the bond lengthens with an increase in the steric bulk of the ligand and its σ donor ability, and shortens as the Co—C—X bond angle increases, where X is a substituent on the donor C atom of the axial ligand [159].

The structural data for alkylcobalamins show that the trans $Co—N_{bzm}$ bond tends to lengthen as the Co—C bond to an alkyl β ligand increases. In Fig. 6 (insert) the crystallographic values of the Co—C bond length are plotted against the $Co—N_{bzm}$ bond length for all alkylcobalamins (i.e., where C is (formally) sp^3 hybridised as in $—CH_3$ and $—CH_2(CH_2)_2CH_3$, sp^2 hybridised as in $—CO(OCH_3)$, and sp. hydridised as in $—C \equiv C\text{-Ph}$. The data for CNCbl itself, and related structures, are included. There is a clear, albeit weak ($r^2 = 0.79$) correlation between the two parameters and steric effects (the bulk of the ligand and its probable interaction with the corrin and its side chains) and electronic effects (hybridisation, σ donor power, ability to act as a π acceptor) are likely to be important factors. The data in the main graphic of Fig. 6 are limited to those structures where the C donor atom is either CN^- or (formally) sp^3 hybridised (Table A1 of the Appendix). The weak correlation clearly persists. It should be appreciated, however, that there is considerable variability in crystallographically-determined structural parameters, as the standard deviations for the mean values of the axial bond lengths in [CNCbl] (35 structures), [CF_3Cbl] (2 structures), [CH_3Cbl] (5 structures), [CHF_2Cbl] (2 structures) and [AdoCbl] (5 structures), show, and caution needs to be exercised lest the data are over-interpreted. Moreover, the effect of crystal packing forces may not be negligible; indeed, as has been pointed out, structural features of the cobalt corrinoids, such as the corrin fold angle [160] (see Section 2.5) and the $Co—N_{bzm}$ bond length [161] can be very sensitive to these solid state effects. For example, [$CN—10NO_2$Cbl] crystallises in the monoclinic space group $P2_1$ with four molecules in the unit cell [162]. The Co—C bond length varies from 1.84 to 1.88 Å, the $Co—N_{bzm}$ bond length varies from 2.03 to 2.13 Å, while the fold angle varies from 11.6° to 26.5° in these four molecules! As the authors of this study point out, the values are strongly dependent of the position of each molecule within the unit cell and its interaction with occluded solvent acetone or water.

There is solid state NMR evidence showing that crystallisation conditions can lead to different polymorphs of [CNCbl] which have observable structural differences [163]. NOE-derived distant restraints molecular mechanics modelling of [MeCbl] in solution shows significant differences in the conformation of the nucleotide loop compared to that observed in the solid state because of interaction with solvent H_2O molecules [164]. Given the structure of the corrinoids, it is no surprise that they are very soluble in aqueous solution, and interact intimately with H_2O solvent molecules. (Detailed analyses of the structure of the solvent around [AdoCbl] determined by x-ray and neutron diffraction methods have been reported [165,166].) The effect of pressure on a crystal of [CNCbl] grown from aqueous solution has been explored, and pressure results in significant changes to the conformation of the amide side chains, and particularly to the ordering of occluded water molecules [167].

In the case of non-alkyl cobalamins [XCbl]'s (Fig. 7), where (A) the ligand X has an O or N donor atom or, (B) P, S or Cl, there appears to be no significant correlation between the $Co—N_{bzm}$ and the Co—X bond lengths, particularly if the value for nitrosylcobalamin, [NOCbl] [183], is omitted; the Co—NO bond length is 1.907 Å while the $Co—N_{bzm}$ bond length, 2.32–2.35 Å, is exceptionally long.

Given the rapid advances in computational power and the ever increasing availability of commercial and open source code, computational methods offer many possibilities of gaining significant insight into the chemistry of the cobalt corrinoids. Such studies will be referred to throughout this review; but as this is by no means the principal focus, no claim is made that the computational work is comprehensively reviewed. Density Functional Theory (DFT) has featured prominently in theoretical studies of the cobalt corrinoids [184]. However, some widely-used functionals, such as B3LYP, may not give reliable results because of errors associated with the Hartree-Fock exchange and the LYP functional itself [185]. With a judicious choice of methodology, semi-empirical methods can also yield useful results [186]. Molecular

[2] From a search of the CCDC in January 2021

Table 1
High resolution crystal structures of cobalt corrins.

CCDC Code	Description of structure	Year	Note	*R* /%	Temp /K	Radiation	Ref
ENAVAR	B_{12} with protonated phosphate; trifluoroacetate counter ion	2011		4.09	100	Mo *Kα* (0.71069 Å)	[160]
GIBMOU	B_{12}	2007	a	3.32	295	Mo *Kα* (0.71069 Å)	[168]
GIBMOU01	B_{12}	2009	b	3.40	90	Mo *Kα* (0.7107 Å)	[169]
GINNEY	Phenylethynylcobalamin	2013		4.91	233	Mo *Kα* (0.7107 Å)	[170]
GIZYOD	Chlorocobalamin	1998	c	4.86	100	Synchrotron, 0.8 Å	[171]
INIZUA	Diisopropylphophitocobalamin	2004	d	4.10	123	Mo *Kα* (0.7107 Å)	[172]
ISUKAI	Isoamylcobalamin	2004	e	4.26	123	Mo *Kα* (0.7107 Å)	[173]
MEDZAZ	Phenylcobalmin	2017		4.37	193	Mo *Kα* (0.7107 Å)	[174]
NEOVBT01	Cyano-13-epicobalamin; the *e* side-chain is epimerised and points upwards to the β face of the corrin	1996	f	4.04	295	Mo *Kα* (0.71073 Å)	[175]
NEVSAJ	Conjugate of B_{12} and [Pt(en)Cl(NC)] with a Co(III)—CN^-—Pt(II) link	2007	g	4.82	183	Mo *Kα* (0.71069 Å)	[176]
PAFBUV	AdoCbl	2009	h	4.80	23	Mo *Kα* (0.7107 Å)	[169]
QINJOO	Phenylethynylcobalamin	2013	i	4.22	100	Cu *Kα* (1.54178 Å)	[177]
RIKFUM	Aquacobalamin with Cl substituting H at C10	1997	j	4.26	295	Mo *Kα* (0.71073 Å)	[178]
SUNYEF	Aquacobalamin	1995	k	4.54	295	Synchrotron, 0.65 Å	[179]
WIKXUJ	B_{12}	2000	l	4.35	100	Synchrotron, 0.8 Å	[180]
YAKDIZ	B_{12} with hydroxyquinoline attached at the 5′-OH position of ribose	2011	m	4.92	183	Mo *Kα* (0.71069 Å)	[181]
YUCCAB	Ethylcobalamin	2009		4.62	293	Synchrotron (0.78468 Å)	[182]
YUCCEF	*n*-Butylcobalamin	2009	n	4.69	293	Synchrotron (0.78468 Å)	[182]

[a]One of the propanol solvent molecules is disordered. Charge density study. [f] Extensive disorder of water solvent molecules. [b] The solvent is extensively disordered. Multipole refinement based on the Hansen-Coppens formalism. [c] Solvent water molecules are disordered. [d] Three disordered water solvent molecules share a site with an acetone solvent molecule. [e] The alkyl ligand is disordered over two sites with occupancies 0.615:0.385. Water solvent molecules are disordered. [f] Four lattice water molecules are disordered. [g] The en ligand, Cl and Pt atom are each disordered over two sites with occupancies of 0.75:0.25. The trifluoroacetate counter anion, some of the acetone solvent molecules and some water solvent molecules are also disordered. [h] An ethanol and two water solvent molecules are disordered. Multipole refinement based on the Hansen-Coppens formalism. [i] Disorder in water and acetone solvent molecules. [j] Positions C12, C46 and C47 are disordered and modelled as an equilibrium between axial and equatorial positions of C46 and C47, with occupancy factors 0.75:0.25; H atom positions at C10, C11, C35, C36 and C53 are trigonally disordered; water molecules are disordered. [k] Ribose hydroxymethyl group is disordered. [l] The solvent is extensively disordered. Multipole refinement based on the Hansen-Coppens formalism. [m] Disorder in an acetone solvent molecule. [n] The n-butyl ligand is disordered over two sites with occupancies of 0.57:0.43. Some of the solvent water molecules are disordered.

Table 2
Mean bond lengths of the corrin core from eighteen high resolution crystal structures[a].

Bond	Bond length /Å	σ /Å	Bond	Bond length /Å	σ /Å	Bond	Bond length /Å	σ /Å
Co—N1	1.888	0.008	N4—C19	1.500	0.007	C11—C12	1.504	0.006
Co—N2	1.916	0.008	C1—C2	1.534	0.015	C12—C13	1.554	0.007
Co—N3	1.915	0.009	C2—C3	1.558	0.012	C13—C14	1.541	0.009
Co—N4	1.881	0.009	C3—C4	1.539	0.009	C14—C15	1.368	0.007
N1—C1	1.484	0.006	C4—C5	1.447	0.006	C15—C16	1.448	0.005
N1—C4	1.302	0.006	C5—C6	1.367	0.008	C16—C17	1.515	0.011
N2—C6	1.393	0.007	C6—C7	1.524	0.009	C17—C18	1.567	0.008
N2—C9	1.340	0.007	C7—C8	1.546	0.009	C18—C19	1.579	0.014
N3—C11	1.341	0.008	C8—C9	1.519	0.008	C19—C1	1.546	0.006
N3—C14	1.398	0.005	C9—C10	1.385	0.008			
N4—C16	1.297	0.007	C10—C11	1.383	0.009			

[a]See Fig. 4 for atom numbering.

mechanics (MM) methods have also been helpful, as will be discussed later.

In a comprehensive study to determine the origin of the normal and inverse trans influence in the cobalt corrinoids, Kuta and co-workers used the BP86 functional to calculate the gas phase equilibrium geometry of 28 alkylcobalamins, with bzm in the *α* coordination site [187]. All corrin side chains were truncated to H so results will be insensitive to interactions between the axial ligands and the side-chains. Nevertheless, the coordination sphere of the metal was reasonably well reproduced. Using a range of alkyl and fluoroalkyls as *β* ligand, where the donor atom to Co was an sp^3 C atom, they reproduced the inverse trans influence observed experimentally (Fig. 6).

The focus then turned to two sets of ligands. In the first set (—CH_3; —CH_2CH_3; —$CH(CH_3)_2$; —$C(CH_3)_3$), both the donor ability and the steric bulk increase across the series, whereas in the second set (—$C(CN)_3$, —$CCl(CN)_2$, —$CCl_2(CN)$, —CCl_3), the steric bulk is relatively constant while the electron withdrawing ability increases across the series.

For the first set, an analysis of the Kohn-Sham orbitals of the complexes showed that three MOs, a linear combination of Co d_z^2, C p_z and N_{trans} p_z, and their mixing with corrin *π*, Co d_{xy} and N_{trans} p_x and p_y orbitals, could be used to rationalise the inverse and normal trans influence. In agreement with a previous study [188], it was found that increasing the *σ* donor ability of the *β* ligand raises the energies of several of these MOs, diminishing the extent of the bonding and hence (perhaps counter-intuitvely) causes an elongation of the axial bond lengths. However, as steric bulk increases, an orbital which has strong anti-bonding character between the metal and the axial ligands decreases in energy. The increase in steric interaction weakens the overlap between Co d_z^2 and both C p_z and N_{trans} p_z, which diminishes the anti-bonding character of this orbital. There is therefore an interplay between electronic and steric effects.

For the second set, steric effects are minimal and the effect is virtually entirely electronic. An increase in the electron-withdrawing power

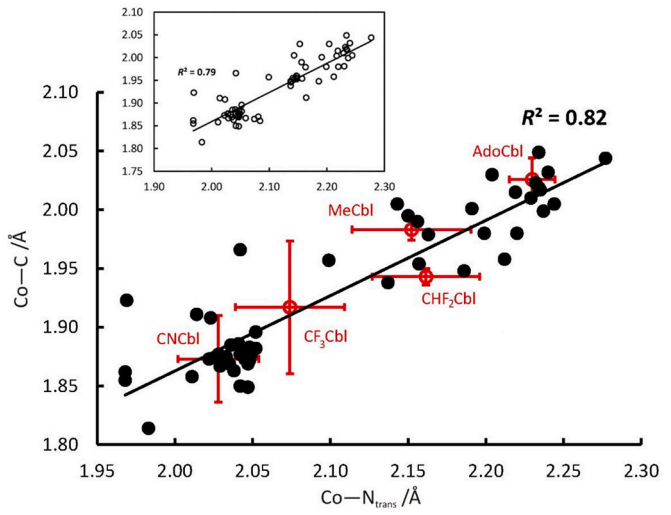

Fig. 6. Structural data for alkylcobalamins, [RCbl], suggest that trans Co—N_{bzm} bond length tends to increase with an increase in the length of the Co—C bond to an alkyl β ligand. The insert includes data for all [RCbl] where C is sp^3, sp^2 or sp–hybridised, including data for cyanocobalamins. The data in the main graphic are limited to those structures where the C donor atom is either CN^- or (formally) sp^3 hybridised (Table A1 of the Appendix). The variability in the crystallographically-determined bond lengths, indicated as standard deviations (in red) should be noted. (For interpretation of the references to colour in this figure legend, the reader is referred to the web version of this article.)

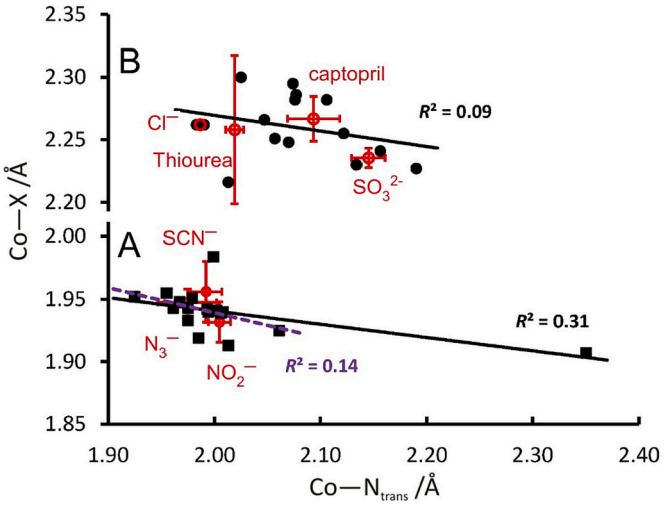

Fig. 7. Crystallographically observed correlation between a Co—X bond length to ligand X, where the donor atom is not C, in the β coordination site and the trans Co—N_{bzm} bond length. The donor atom in A is N or O; in B it is P, S or Cl.

of the ligands increases the positive charge on the metal; this in turn causes an attraction of the nitrogenous base but a repulsion of the alkyl group, i.e., a normal trans influence is seen.

The authors concluded that the reason why a normal trans influence has not been observed in the experimental data for alkylcobalamins is that complexes which would show this effect have yet to be prepared and their structure determined.

Some early DFT studies include a demonstration that the Co—N_{bzm} bond length has little influence on the homolysis of a CH_3 group in the β position [189] but the bond dissociation energy (BDE) for the heterolysis reaction to produce Co(I) and CH_3^+ decreases as the Co—N_{bzm} bond length increases [190]; the substrate radical-to-product rearrangement of the AdoCbl-dependent enzymes (i.e. modelling of the radical rearrangement step that occurs after Co—C bond homolysis using both DFT and DFT/MP2 methods) [191,192]; the electronic structure of the cobalt corrinoids [193,194]; their electronic spectra [195]; estimates of the energy for the homolysis of the Co—C bond in a series of model alkylcobalt corrin complexes [196]; and ^{14}N superhyperfine and nuclear quadrupole coupling constants [197,198].

Brunold and co-workers used a combination of MM methods and DFT (PBE/TZP) to produce accurate models of known cobalamin structures with a variety of β axial ligands (CH_3^-, CN^-, H_2O), treating the corrin core and axial ligands (including bzm) by DFT methods, and the side chains and nucleotide loop by MM methods [199]. The corrin fold angle was reasonably well-reproduced (within 3° for [MeCbl] and [CNCbl] but underestimated by 12° in $[H_2OCbl]^+$); bond lengths to CH_3^- and CN^- were within 0.03 Å (but over-estimated by 0.17 Å to H_2O); and the Co—N_{bzm} was reproduced to about 0.1 Å. The structure of the corrin was well reproduced (bond lengths within about 0.03 Å). Using this methodology, structures for the corresponding cobinamides (which have so far eluded crystallisation) were determined. The study showed how changing bzm to H_2O profoundly changes the energy of a Co $3d_{z^2}$-based orbital, other Co d orbitals, and the largely corrin-based π HOMO orbital.

A strategy that has been used is to augment existing empirical molecular mechanics (MM) force fields to model complete corrinoids [200]. Parametrisation usually relies on fitting parameters to reproduce a wide range of crystal structures. Parameters for the MM2 [201] and AMBER [202–204] force fields for modelling the cobalt corrinoids have been developed [205,206]. Bond lengths are typically reproduced to 0.03 Å or better, and angles, including the fold angle of the corrin ring, to 2° or better [207]. These methods can offer real insight into the solution structure of the cobalt corrinoids [208,209], especially when coupled with NMR-derived distance restraints in molecular dynamics simulations [210–214]. The Universal Force Field (UFF) [215] has also proved very useful in modelling the cobalt corrinoids [216]. MM methods have been used, for example, for exploring the interaction between cobalt corrinoids and their transport proteins TCII [217,218], BtuF [219] and BtuB [220]; conjugates of [CNCbl] with peptide nucleic acids [221]; and, coupled with QM calculations, to explore the structure of, for example, the reductive dehalogenase PceA [222] and the epoxyqueuosine reductase, QueG [223].

An analysis of the conformational flexibility of the corrin in the cobalt corrinoids based on a variety of methods including matrix partitioning, factor analysis, and surface accessibility calculations of solid state structures available at that time [224] showed that the corrin is very flexible along the Co—C10 vector with the northern hemisphere of the corrin being the most flexible. The extent of folding depends on the bulkiness of the axial ligands. More recently, MM studies have also highlighted the flexibility of the corrin, with the corrin fold angle varying by up to 45° in MD simulations at 300 K. The corrin undergoes a "breathing" motion in which C5, C10 and C15 oscillate above and below the mean corrin plane, in agreement with the findings of Pett et al. [224]. The pyrrole rings, and in particular the B and C rings, are also very flexible, with the acetamide and propionamide side chains visiting many locally-minimum energy conformations. There is less flexibility in the "western" half of the molecule, presumably because of the direct link between the A and D rings.

2.3. *Co(II) corrinoids`*

Crystal structures of Co(II) corrinoids are rare. Werthemann reported a dimer of Co(II) heptamethylester (cob(II)ester) bridged by iodide [225], where each Co(II) is displaced by 0.12 Å from the mean plane of the 4 N donors of the equatorial macrocycle towards the bridging ligand. Kräutler and co-workers determined the structure of five-coordinate monomeric cob(II)ester coordinated in the β coordination site by ClO_4^- [226] with a long Co—O bond (2.31 Å). The coordination geometry about the metal is not significantly different to that in dicyanocob(III) ester and the metal is displaced a mere 0.048 Å from the mean plane of

the four corrin N donor atoms, which, as was pointed out [226], is small compared to the displacement of Co(II) of 0.14 Å from the mean plane of the 4 N donors in Co(II) porphyrins.

The crystal structure of cob(II)alamin itself is known [227]. Low spin Co(II) is displaced by 0.12 Å from the mean plane of the four equatorial N donors towards bzm. As with the cob(II)ester structure, the coordination geometry around the metal does not differ significantly from Co(III) corrinoids. The five-coordinate structure of B_{12r} has more recently been confirmed using neutron diffraction, a study which was also able to elucidate the structure of solvent water around the cobalamin [228,229]. Both structures show that the Co—N bond to bzm in B_{12r} is elongated (2.131 Å [227] and 2.140 Å [229]) when compared to $[H_2OCbl]^+$ (1.925 Å [179] and 1.985 Å [230] in $[H_2OCbl]^+$; 1.967 Å in $[H_2O(10\text{-}Cl)Cbl]^+$ [178] and 1.975 Å in $[H_2O(10\text{-}Br)Cbl]^+$ [231]).

The electronic structure of base-off cob(II)alamin, with water replacing bzm, and of a four-coordinate cob(II)alamin, as found in the H759G variant of MetH, the 5-methyltetrahydrofolate-homocysteine methyltransferase methionine synthase found in bacteria, has been investigated by EPR, MCD, DFT(PBE/TZP) and a multi-reference *ab initio* treatment (Spectroscopy ORiented Configuration Interaction (SORCI) method) [232]. In the d^7 five-coordinate complex the unpaired electron density resides primarily in $3d_z^2$. In the four-coordinate complex there is mixing between $3d_z^2$ and $3d_{x^2-y^2}$ and there is configurational interaction between these two singlet electronic configurations. There are two low-lying excited states where unpaired electron density is largely found in $3d_{xz}$ and $3d_{yz}$, respectively, and these mix with the ground state through spin-orbit coupling. This leads to a multiconfigurational wavefunction for the ground state of this complex. This electronic structure, which could perhaps be described as an entatic state, favours rapid electron transfer by reductants, leading to cob(I)alamin, $[Cbl(I)]^-$.

2.4. Co(I) corrinoids

Cob(I)alamins are low spin, EPR-silent complexes with (formally) a Co d^8 electronic structure. No Co(I) corrinoids have been crystallised and their structure determined by diffraction methods, no doubt a consequence of their ready oxidation (for example, $[Cbl(II)]|[Cbl(I)]^- = -0.64$ (or -0.61 V), see Section 5.1). A crystal structure of the isoelectronic Ni(II) analogue of cobyrinic acid, nibyric acid, shows the metal to be four coordinate [233], as it is in the Ni(II) analogue of $[Cbl(I)]^-$, [Nibl] as deduced by NMR [233]. While it could be argued that this is precedence for assuming that Co(I) in $[Cbl(I)]^-$ is four coordinate, square planar Ni(II), with an effective ionic radius of 0.49 Å [234], is undoubtedly smaller than low spin Co(I) (the radius of which appears to be unknown; low spin Co(II) has an effective ionic radius of 0.65 Å [234]).

While similar indirect conclusions have been made from uv-vis spectroscopy [235,236] and electrochemical studies [237,238], the best experimental evidence available is from X-ray edge and EXAFS data [239] which shows that Co(I) in $[Cbl(I)]^-$ exists as a distorted four-coordinate complex (experimentally, 3.5(6) ligands; Co—N = 1.88(2) Å) in 35% glycerol, ≤ 150 K). This was confirmed by X-ray fluorescence measurements which ruled out a coordination number of 5 or a tetrahedral geometry. From an x-ray absorption spectroscopy/spectroelectrochemical study at room temperature, pH 1.4, Giorgetti and co-workers [240] concluded that Co(I) in $[Cbl(I)]^-$ is indeed four coordinate.

Computational work, using DFT [190,241–243], TD-DFT [244] and CASPT2 [245], gave a 4-coordinate species with two shorter and two longer Co—N bonds to the corrin N donors. However, if dispersion is taken into account (for example, using ωB97X-D/6–311++G(d,p), and as reviewed in [246]), then it becomes evident that Co(I) can form long axial bonds to hydrogen atoms, where the Co···HXR, X = N, O, C, interaction is a non-covalent interaction reminiscent of a hydrogen bond.

2.5. Corrins with metals other than cobalt

Of the structurally-related cyclic tetrapyrroles found in nature (corrin, porphine, hydrocorphin and chlorin, Fig. 8), each with its distinctive metal ion (Co, Fe, Ni and Mg, respectively), corrin has the smallest central cavity with a trans N···N distance of 3.93 Å, while porphine (4.17 Å), chlorin (3.99 and 4.35 Å, average 4.17 Å) and hydrocorphin (4.34 Å) are considerably larger [247]. It has been suggested that the small size of the corrin cavity is an important factor in selecting for the low spin state in octahedral Co(III), square pyramidal Co(II) and square planar Co(I) complexes of the cobalt corrins [248], the enzymatically active forms of the cobalt corrins in the B_{12}-dependent enzymes. However, the corrin ring is quite flexible, and can accommodate other metal ions. For example, low spin six-coordinate Co(III) has an ionic radius of 55 pm while that of six-coordinate Rh(III) is significantly larger, 67 pm [234]; yet both are readily accommodated in a corrin.

The Rh(III) analogue of chlorocobalamin [ClCbl], chlororhodibalamin [ClRhbl], was first reported by Koppenhagen et al. [249,250], who treated metal-free hydrogenobalamin, [Hbl], isolated from cultures of the acetogenic eubacterium *Chromatium thermoaceticum* grown in cobalt-free media, with $[Rh(CO)_2Cl]_2$. $[H_2ORhbl]^+$ could be prepared by precipitation of chloride with silver nitrate, and reduced to the Rh(I) complex by borohydride. Treatment with methyl iodide and 5′-iodo-5′-deoxadenosine produced the Rh analogues of [MeCbl] and [AdoCbl], respectively. None of the compounds were crystallised; their structure was inferred from the 3 proton signal of coordinated CH_3^- in $[CH_3Rhbl]$, and analysis of the decomposition products of [AdoRhbl] on treatment with excess CN^-. A much more efficient route is now available for the metal-free corrin hydrogenobyric acid, ([Hby], Fig. 9A) [251], which can be converted to the metal-free analogue of cobalamin, hydrogenobalamin [Hbl] [233].

A crystal structure of a Rh(III) complex of a corrin was obtained on treating hydrogenobyrinic acid a,c-diamide with $[Rh(CO)_2Cl]_2$ [252]. The Rh(III) complex has two axial Cl^- ligands. Compared to dicyanocobyrinic acid *a,c*-diamide [253], the central cavity of the corrin has expanded to accommodate the larger metal ion (Table 3). A crystal structure of [ClRhbl] is also available [254]. The bzm base is coordinated with a relatively long Co—N_{bzm} bond (2.063 Å, cf. 1.990 Å in [ClCbl] [171]), as is the bond to Cl^- (Co—Cl = 2.352 Å, but 2.262 Å in [ClCbl]).

[AdoRhbl] has been prepared by a combination of biological and chemical steps, and its solution structure (by NMR) and solid state structure (by XRD) fully explored [255], confirming its base-on structure. There are clear differences in the behaviour of [AdoRhbl] and [AdoCbl], not least of which is that the former is not sensitive to visible radiation, while the latter decomposes rapidly by homolysis of the Co—C bond. [AdoRhbl] is inactive in *in vivo* assays for methionine synthase and inhibits [AdoCbl]-dependent diol dehydratase [255]. The comparatively ready availability of [ClRhbl] makes it feasible to prepare [AdoRhbl] and [MeRhbl], as well as compounds such as iodorhodibalamin, [IRhbl] [254].

Incorporation of the larger low-spin Rh(III) into corrin results in longer metal—N_{corrin} bond lengths (by 0.082(5) Å) when compared to [AdoCbl], but a more modest increase of 0.035(5) Å in the axial bond lengths. The corrin is flatter in [AdoRhbl] than in [AdoCbl] (fold angles, defined as the angle between the mean planes through N1, C4, C5, C6, N2, C9, C10, and N4, C16, C15, C14, N3, C11, C10, respectively, [258], of 6.0° and 10.1°, respectively, Table 4), as is the B ring with the *c*-acetamide and *d*-propionamide in pseudo-equatorial positions, although NMR evidence shows that it has the same conformation as the B ring of [AdoCbl] in solution.

The corrin macrocycle is quite capable of accommodating the larger Rh(III) ion by adopting a smaller corrin fold angle. The helicity, *h*, of the corrin, the N1—N2—N3—N4 torsion angle about the pseudo-bond between N2 and N3 [251], is also smaller as a consequence of a flatter corrin ring.

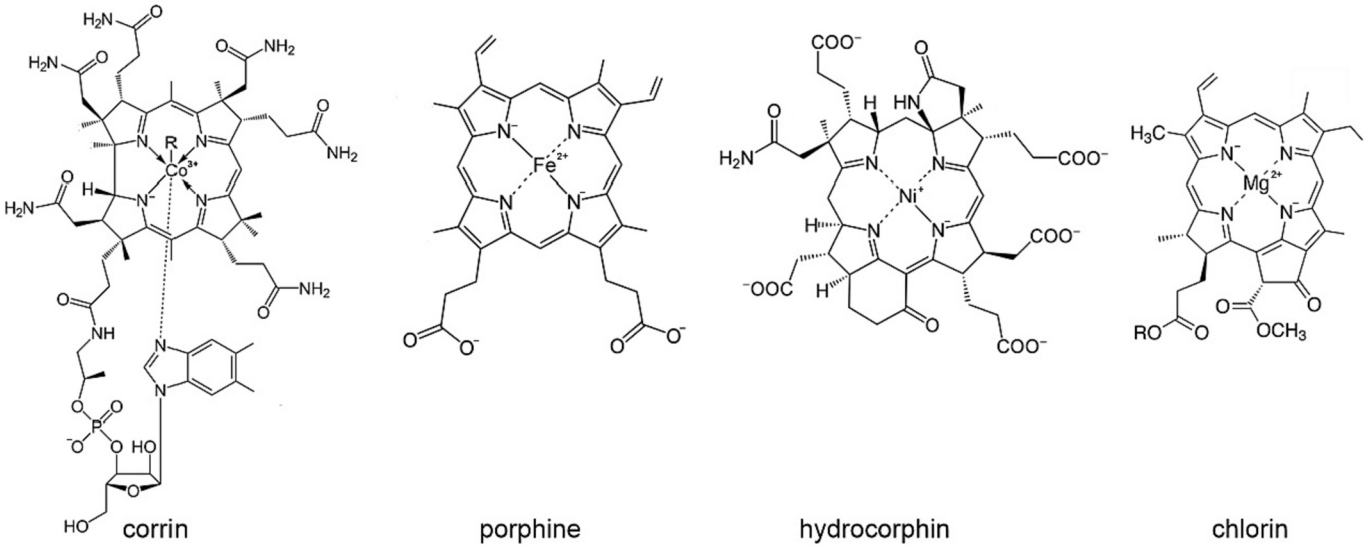

Fig. 8. The tetrapyrroles of nature.

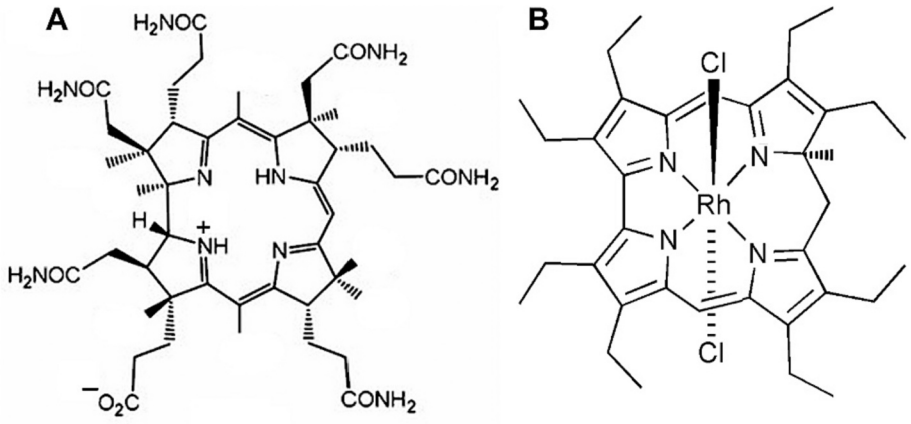

Fig. 9. A: Hydrogenobyric acid. In hydrogenobyric acid all side chains are hydrolysed to carboxylic acids. B: The structure of a Rh(III) complex of an oxidised corrin, a rhodalamine analogue (see Table 3).

Table 3
Comparison of the equatorial bond lengths in Co(III) and Rh(III) corrinoids.

	M^{3+}—N1 /Å	M^{3+}—N2 /Å	M^{3+}—N3 /Å	M^{3+}—N4 /Å	Ref
[AdoCbl]	1.875	1.913	1.900	1.880	[169][a]
[AdoRhbl]	1.956	2.001	1.989	1.955	[255][b]
[Cl_2Rhby-a,c-diamide]	1.953	1.998	1.978	1.956	[252][c]
[Cl_2Coby-a,c-diamide]	1.899	1.915	1.915	1.877	[256][d]
Rh(III) rhodalamine analogue [f]	1.935	1.991	2.002	1.941	[257][e]
[ClCbl]	1.882	1.917	1.922	1.893	[171][g]
[ClRhbl]	1.960	1.977	1.984	1.947	[254][h]

[a]CCDC ref. code PAFBUV; [b]URALOQ; [c]CNRHBR; [d]CYCOAM; [e]HULSUC; [f]Fig. 9B; [g]TUZPAI; [h]GIZYOD.

Various measures have been used to gauge the extent of deviation from planarity of the corrin ring (Fig. 10). The direct link between the A and D ring means that, unlike the porphines, the corrins will be markedly non-planar. One of these measures is the corrin fold angle [258] which is the angle between two east-west planes in the corrin (see above). A second – perhaps more appropriate for corrins in which the bzm base is either missing or uncoordinated [233] – is the interplane angle, ϕ, between the north-south N1—metal—N4 and N2—metal—N3 planes. A third is the helicity, h, of the corrin [251], as mentioned above. Yet another is the deviation of the metal ion from the mean plane for the four corrin N atoms, M⊥. To give a sense of the flexibility of the corrin, these values for some representative corrins are collected in Table 4.

Bröring et al. [257] showed that Rh(III) also fits comfortably into the cavity of an oxidised corrin (Fig. 9B). The Rh(III)—N bonds lengths in this complex are comparable to those in [AdoRhbl] [255] and [AdoCbl] [263] (Table 2). The central $Rh^{3+}(N)_4$-unit is nearly planar (mean deviation from planarity of 0.018 Å) and the corrole adopts a ruffled conformation with the C ring tilted at 16.1° to this mean plane.

The Ni(II), Pd(II), Pt(II), Zn(II), Mg(II) and Cd(II) complexes of a seco corrin, where the C1—C19 bond is missing and the bond between C1 and C24 is a double bond, have been prepared [264]. The efficiency of the photochemical cyclisation to the complete corrin depends on the identity of the metal. The crystal structures of the Ni(II), Pd(II) and Pt(II) complexes have been determined [264], but apparently not of the cyclised corrins.

Zn(II), Ni(II) and Cu(II) corrins have been known for some time (with Zn(II) corrins used as intermediates in the total synthesis of B_{12} [259,265–268]) and studied in their own right for their chemical and physical properties [269,270]. Treatment of solutions of two metal-free

Table 4
Measures of the flexibility of the corrin ring in metallocorrins.

	M	ionic radius /pm[†]	M-N21 /Å	M-N22 /Å	M-N23 /Å	M-N24 /Å	Ave M-N_{corrin}/Å	Fold angle /deg	helicity, *h* /deg	Interplane angle, ϕ /deg	M⊥ /pm	Ref
[Hyby]								11.6	12.9	13.4[¶]	2[¶]	[251][h]
[NiCor] [‖]	SqPl Ni (II)	49	1.851	1.913	1.884	1.847	1.87	9.9	10.2	11.2	1	[259,260][m]
[Niby]	SqPl Ni (II)	49	1.836	1.883	1.864	1.859	1.86	8.8	10.1	11.1	3	[233][j]
Cob(II)alamin	5C Co (II)	65[‡]	1.871	1.911	1.893	1.874	1.89	16.2	5.9	12.0	12	[227][n]
Cob(II)alamin	5C Co (II)	65	1.935	1.856	1.836	1.954	1.90	14.4	5.6	14.2	15	[229][f]
ClO_4cob(II) ester*	5C Co (II)	65	1.889	1.931	1.906	1.874	1.90	6.0	6.1	7.7	5	[226][k]
[Znby]	5C Zn (II)	68	2.039	2.030	1.986	2.054	2.03	6.4	8.0	27.9	62	[261][i]
[Cl_2Coby-a,c-diamide]	LS 6C Co(III)	55	1.899	1.915	1.915	1.877	1.90	8.2	6.1	6.6	1	[256][d]
[Cl_2Rhby-a,c-diamide]	6C Rh (III)	67	1.953	1.998	1.978	1.956	1.97	7.9	5.5	6.2	1	[252][c]
[CNCbl]	LS 6C Co(III)	55	1.886	1.919	1.922	1.900	1.91	15.9	4.2	4.8	2	[169][g]
[AdoCbl]	LS 6C Co(III)	55	1.875	1.913	1.900	1.880	1.89	10.1	3.3	3.5	0	[169][a]
[AdoRhbl]	6C Rh (III)	67	1.956	2.001	1.989	2.055	2.00	6.0	3.0	3.8	2	[255][b]
[ClCbl]	6C Co (III)	55	1.882	1.917	1.922	1.898	1.90	17.5	4.0	5.0	3	[171][o]
[ClRhbl]	6C Rh (III)	67	1.960	1.976	1.984	1.947	1.97	17.4	3.0	4.3	3	[254][e]

[a]CCDC ref. code PAFBUV; [b]URALOQ; [c]CNRHBR; [d]CYCOAM; [e]TUZPAI; [f]ARIWUU; [g]GIBMOU01; [h]SOLJAH; [i]POTWAZ; [j]KAHPAO; [k]FOGMAP; [m]NIMCOR; [n]KECWUK, [o]GIZYOD. *The heptamethyl ester, Co(II)-heptamethyl-cobyrinate with ClO_4^- in the β coordination site. [¶]Estimated using the centroid of N21, N22, N23 and N24 as the putative position of a coordinated metal ion.[†]Ionic radii from [234]. [‡]LS Co(II); the effective ionic radius of HS Co(II) is much larger, 75 pm [104,262]. [‖]The synthetic corrin 5, 8,13,13-pentamethyl-5-cyano-corrin.

corrins from *Chromatium*, tentatively identified as phenyl-hydrogenobamide (where phenyl is linked by an α—O—glycosidic bond to the C1 atom of the ribose moiety of an intact corrin) and hydrogenobyric acid ([Hby], Fig. 9A) with $CuSO_4$ produced the four-coordinate Cu(II) complexes, while treatment with $Zn(CH_3CO_2)_2$ produced a five-coordinate complex, with one axial coordination site likely occupied by H_2O [269]. The estimated Cu—N_{eq} bond length is 1.91 Å [271].

The growth of *Chromatium* in the presence of bzm produces α–(5,6-dimethylbenzimidazole)hydrogenobamide, or hydrogenobalamin, the metal-free version of B_{12}. Cu(II) and Zn(II) could be inserted into this metal-free corrin to produce the Cu(II) and Zn(II) analogues of B_{12}. The Cu(II) complex is four-coordinate, base-off, while the Zn(II) complex is five-coordinate with bzm coordinated above pH 2.7 [270].

More recently, the Zn(II) [261] and Ni(II) [233] analogues of cobyric acid and B_{12} have been reported. As established by NMR methods, [ZnCbl] is 5-coordinate, with bzm coordinated to the metal ion. The crystal structure of zincobyric acid, [Znby], shows a markedly domed structure with the metal ion out of the mean plane of the corrin, displaced towards the β face, and coordinated to a carboxylate of a neighbouring molecule (2.06 Å). The Zn(II)—N bonds lengths to N1 through N4 are, respectively, 2.030, 2.030, 1.985 and 2.054 Å.

As mentioned above, the crystal structure of cob(II)alamin [229] shows that low spin Co(II), as expected, is 5-coordinate. The structure is domed towards the bzm ligand on the α face on the macrocycle, with a Co—N bond length of 2.140 Å. The Co(II)—N bonds lengths to N1 through N4 are, respectively, 1.935, 1.856, 1.836 and 1.954 Å, somewhat shorter than in the Zn(II) complex, even though five-coordinate Zn (II) has a similar ionic radius (68 pm [234]) to low-spin five-coordinate Co(II) (67 pm [104]). Similar observations have been made [261] by comparing the structure of [Znby] with that of heptamethyl-cob(II) yrinate [226]. Since [Znby] and [Znbl] fluoresce (with emission at 552 and 560 nm, respectively), they are potentially interesting luminescence probes of B_{12}-dependent systems.

As expected for Ni(II) coordinated by a π-electron rich macrocyclic ligand, the metal adopts a low-spin four-coordinate pseudo square planar geometry in [Niby], as determined from its crystal structure, and in [Nibl], as deduced by NMR methods [233]; structurally, [Nibl] is therefore reminiscent of isoelectronic cob(I)alamin [238,246]. Accommodation of four-coordinate Ni(II) (ionic radius 49 pm [234]) causes a shrinkage of the cavity of the corrin and the Ni(II)—N bonds lengths to N1 through N4 are, respectively, 1.836, 1.883, 1.864 and 1.859 Å.

A Ni(II) complex of a cobalamin analogue but with conjugation interrupted between C5 and C6 (5,6-dihydroxy-5,6-dihydro-nibalamin, [5,6-DHNibl]) has been prepared [272]. It remains firmly four-coordinate in aqueous solution and fails to coordinate strong ligands such as CN^- and SCN^- [272]. The Ni(II) heptamethyl cobester analogue of [5,6-DHNibl], $[5,6\text{-DHNibs}]^+$ undergoes a reversible one electron electrochemical reduction to Ni(I), $E_{1/2} = -0.89$ V (vs SHE) in DMF (and −0.95 V in MeCN). This was corroborated by both spectroelectrochemical (reversible shifts in the electronic absorption spectrum accompanying reduction and re-oxidation) and EPR studies ($g\perp = 1.980$, $g_{||} = 2.194$). Electrochemically-generated [5,6-DHNibs] is a competent reductant of 2-chloroacetonitrile to acetronitrile and Cl^-. The system therefore mimics the activity of the Ni(I) form of the cofactor F_{430}. DFT calculations (B3LYP/6–31 + G(d)), with CPCM-simulated solvent (MeCN), suggest that the unpaired electron density of [5,6-DHNibs] resides predominantly on the metal ion, causing an expansion of the corrin core by elongation of the Ni(I)—N bonds.

DFT modelling (BP86 or PBE with def2-TZVP/D3) of 5-coordinate $[\alpha\text{-AcZnby}]^-$ and $[\beta\text{-AcZnby}]^-$ with an acetate ligand in the α and β coordination sites, respectively, of the corrin [261] produced a domed structure with Zn(II) significantly displaced from the mean corrin plane, the latter in good agreement with the crystal structure of [Znby], with its long bond between the metal and the carboxylate of a neighbouring moiety (Table 4). A model of 5-coordinate [ZnCbl] using the same

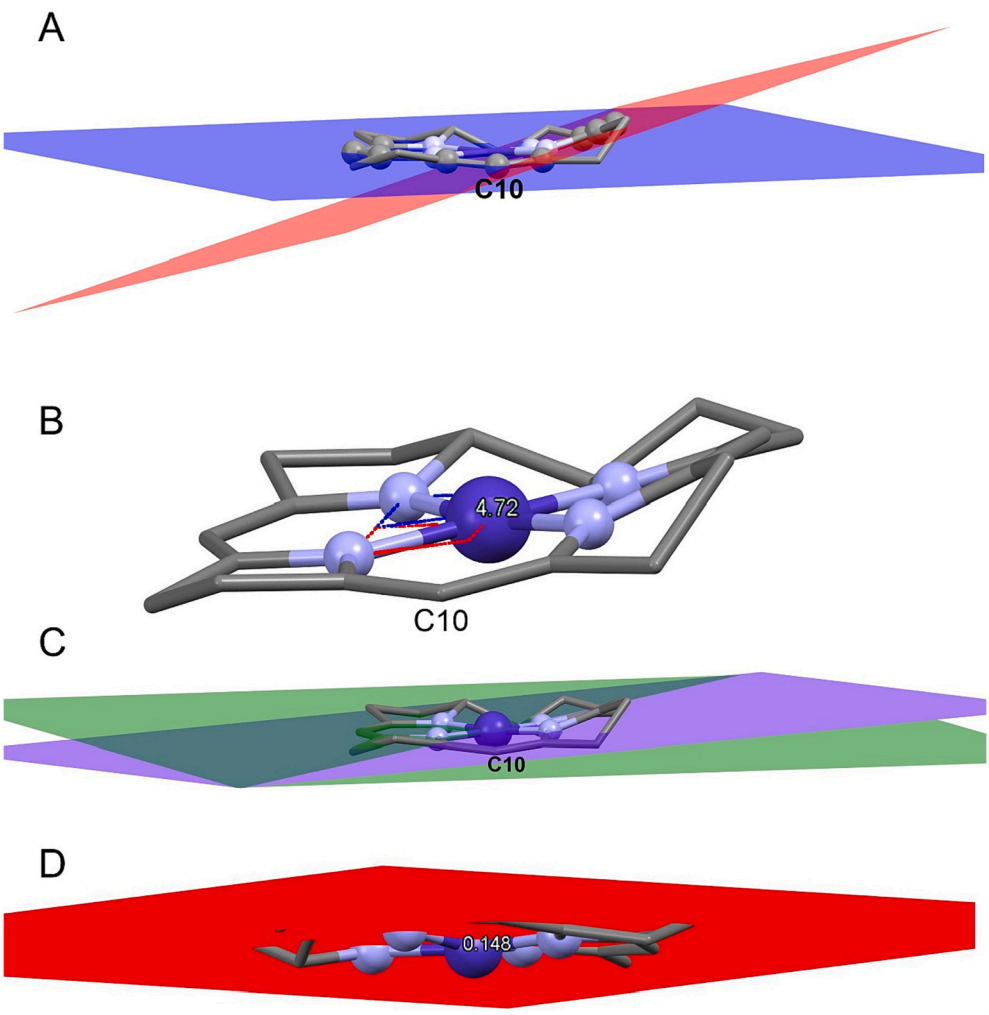

Fig. 10. A) The corrin fold angle viewed from the eastern hemisphere of the corrin: the angle between the mean planes through N1-C4-C5-C6-N2-C9-C10 (red) and C10-C11-N3-C14-C15-C16-N4 (blue). B) The helicity, *h*, of a corrin: the N1—N2—N3—N4 torsion angle about the pseudo-bond between N2 and N3. The value is in degrees. C) The interplane angle, ϕ, between the N1-Co-N4 (green) and N2-Co-N3 planes (blue). D) M⊥, the deviation of the metal ion from the mean plane for the four corrin N atoms (solid red surface). The value is in Å. (Illustrations A through C from [180]; D from [227].) (For interpretation of the references to colour in this figure legend, the reader is referred to the web version of this article.)

functional and basis set gave a structure with Zn(II) significantly displaced (by 0.46 Å) towards the bzm ligand coordinated in the α face of the corrin. Thus, while Zn(II) has a similar ionic radius to low spin Co(II) (Table 4) this closed shell ion is accommodated less comfortably in the cavity of the corrin macrocycle, with long Zn(II)—N_{corrin} bonds, and with large M⊥ values. This indicates that electronic interaction between open shell cobalt systems and the corrin is an important feature of the chemistry of the cobalt corrinoids.

The dependence of the average metal—N_{corrin} bond lengths on the effective ionic radius of the metal ion using the data of Table 4 is shown in Fig. 11. It is intriguing to note how reduction of six coordinate low spin Co(III) to five coordinate low spin Co(II) has virtually no effect on the Co—N_{corrin} bond lengths. This ensures there is virtually no influence on the reorganisation energy associated with the change in oxidation state, and hence clearly contributes to an efficient conversion between (formally) Co(III) and Co(II) in the [AdoCbl]-dependent enzymes.

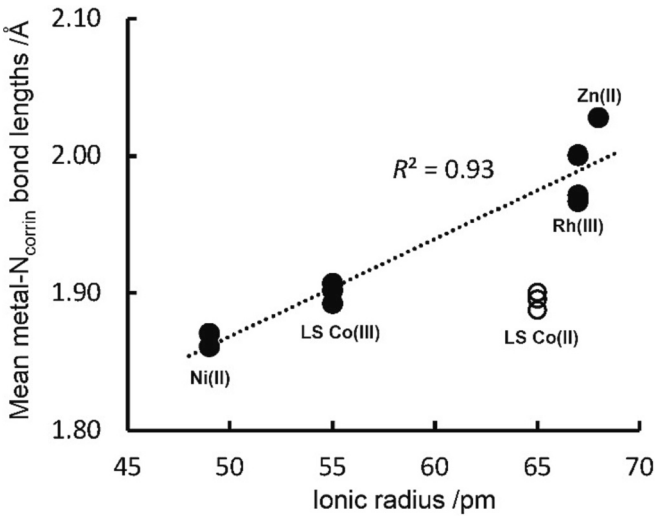

Fig. 11. The dependence of the mean bonds between the corrin N donors and the metal on the ionic radius of the metal ion.

3. A brief overview of B_{12}–requiring biochemistry

There are many reviews and compilations that summarise the biosynthesis, uptake, metabolism and biochemical reactions of the cobalamins, including specific enzymes, in biological systems (for example [1,2,7,9,10,23,29,273–284]). Only a very brief summary is provided here.

An overview of B_{12}–requiring biochemistry is shown in Scheme 1 (adapted from Bridwell-Rabb and Drennan [282]). An understanding of the biosynthetic pathways that lead to the production of B_{12} has opened up the prospect of devising new avenues for the industrial scale production of this essential vitamin, widely used in the medical and food industries [285].

Cobalamins are essential for three enzyme-catalyzed reactions:

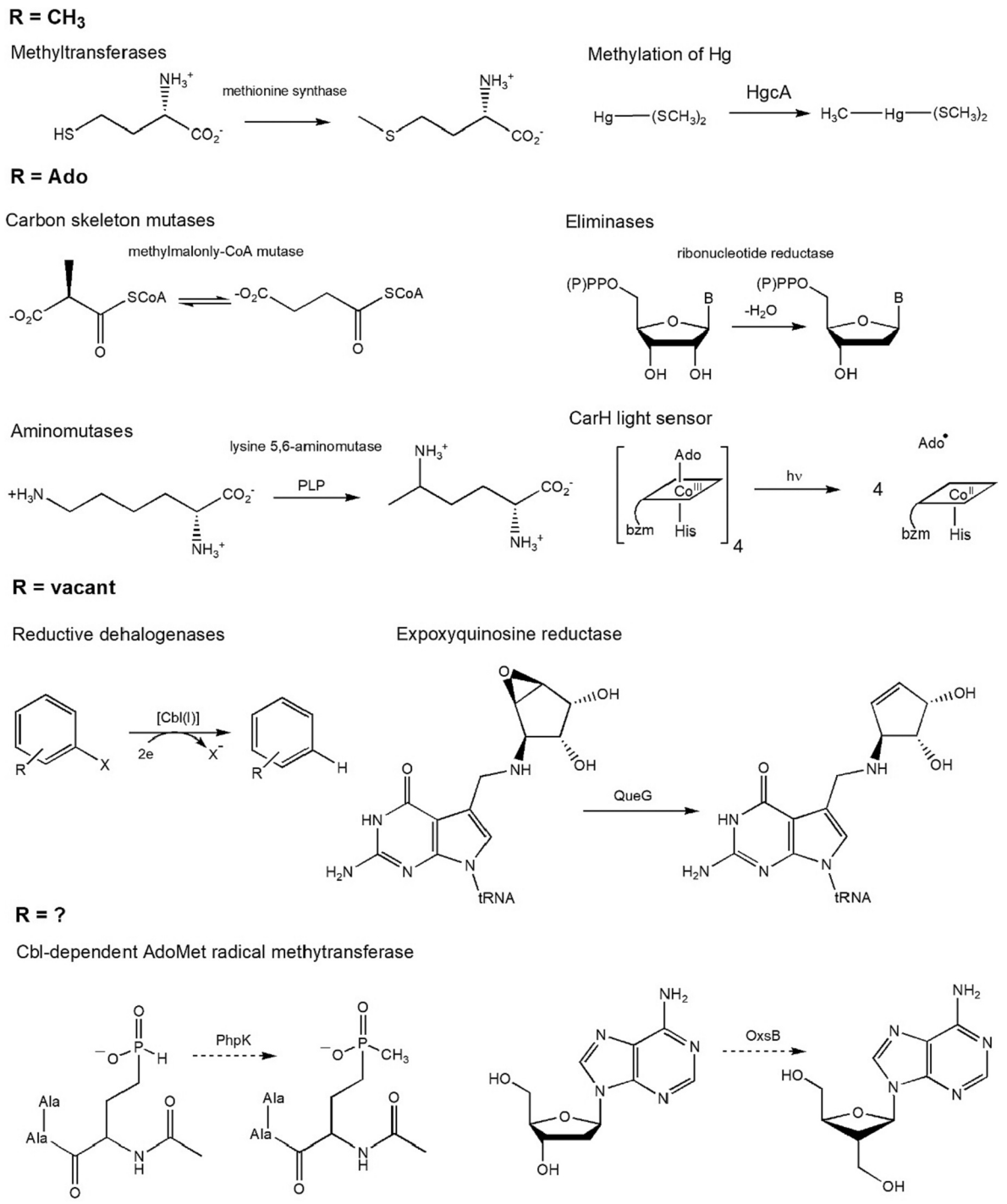

Scheme 1. Some examples of Cbl-dependent proteins as defined by the nature of the upper ligand (adapted from [282]). [MeCbl]-dependent methyl transferases include methionine synthase, which catalyses the transfer of a methyl cation to homocysteine and the mercury methylase HgcA, which is thought to catalyse transfer of a methyl anion to a Hg^{2+}-bis(thiolate) compound (represented as Hg-S(CH_3)$_2$), the most prevalent form of Hg^{2+} in methylmercury producers. [AdoCbl]-dependent enzymes include carbon skeleton mutases, eliminases, and aminomutases; the latter also requires pyridoxyl phosphate (PLP). Recently, [AdoCbl] has been shown to be involved in light-dependent gene regulation of the carotenoid (Car) biosynthetic operon via the transcriptional regulator CarH, adding a new function for this flavour of Cbl cofactor. A third class of Cbl-dependent enzymes, which includes the reductive dehalogenase PceA and the queuosine biosynthetic enzyme QueG do not have an upper axial ligand and are denoted as "open"-Cbl-dependent enzymes. The final class is made up of enzymes that appear to require the machinery for both S-adenosylmethionine (AdoMet) radical chemistry and a Cbl cofactor [288]. Examples include phosphinate methylase PhpK and oxetanocin-A biosynthetic enzyme OxsB.

methyltransferases, isomerases, and reductive dehalogenases [14,23,24,34,286,287]. There are also enzymes that require both S-adenosylmethionine (AdoMet) radical chemistry and a Cbl cofactor [288]. In the methyltransferases, a methyl group in transferred from a methyl donor to a methyl acceptor. These enzymes use [CH_3Cbl] as the cofactor. The isomerases catalyse rearrangements in which a hydrogen atom is directly transferred between two adjacent atoms with concomitant exchange of the second substituent, X, which may be a carbon atom with substituents, the oxygen atom of an alcohol, or an amine. The isomerases use [AdoCbl]. These radical-based transformations occur in

the mutases, dehydratases, deaminases, and class II ribonucleotide reductases.

3.1. The [CH_3Cbl]-dependent enzymes

[CH_3Cbl]-dependent enzymes catalyse the heterolytic cleavage of the Co—C bond to form what is often referred to as the "super-nucleophile" cob(I)alamin, $[Cbl(I)]^-$ [289] and a methyl carbocation that is transferred to a nucleophilic acceptor. The prototypical member of this class, [CH_3Cbl]-binding 5-methyltetrahydrofolate-homocysteine methyltransferase methionine synthase (also known as methionine synthase, MS, and termed MetH in bacteria), catalyses the transfer of a methyl group from 5-methyltetrahydrofolate (CH_3—THF) to homocysteine (Hcy) for methionine synthesis [14,290,291] (Scheme 2). The enzyme-catalysed reactions are accelerated by between some 10^6 to nearly 10^8 times compared to realistic protein-free methyl transfer reactions [292]. The role of the strictly conserved Ser-Asp-His triad (and where His replaces bzm in the α coordination site) is crucial [292].

MS forms part of the S–adenosylmethionine (SAM) biosynthesis and regeneration cycle. The form of this enzyme found in plants is cobalamin-independent; microorganisms express both cobalamin-dependent and cobalamin-independent forms.

Every 200–2000 enzyme cycle turnovers sees the oxidation of Co(I) by O_2 or reactive oxygen species (ROS) to inactive cob(II)alamin, [Cbl(II)] [293] (Scheme 2, in red). Activity is restored through reduction by methionine synthase reductase (MSR), a diflavin reductase that uses both FAD and FMN as intramolecular electron carriers during catalysis [294]. It also serves as a chaperone protein, enhancing incorporation of cobalamin into apo-MS [295]. Methionine formed by the methylation of homocysteine is converted to SAM by methionine adenosyltransferase. S-adenosylhomocysteine (SAH) is then hydrolysed to homocysteine and adenosine by SAH hydrolase to complete the cycle.

Glimpses into the structure of the SAM enzyme, methanogenesis marker protein 10 (Mmp10) from the archaea species *Methanosarcina acetivorans*, was recently reported [296], work which "identifies distinctive active site rearrangements to provide a structural rationale for the dual use of the SAM cofactor for radical and nucleophilic chemistry".

The enzyme complexes that activate, protect and perform catalysis on the reactive B_{12} cofactor of the methyl transferase in the acetogen *Moorella thermoacetica* have been elucidated thanks to x-ray crystal structures of the 220 kDa enzyme complex that contains all enzymes responsible for B_{12}-dependent methyl transfer reactions in this organism, a corrinoid iron-sulfur protein, CFeSP, and the methyltransferase [297]. The Fe_4S_4 cluster of CFeSP accepts an electron from a partner protein, delivering it to [Cbl(II)] to form $[Cbl(I)]^-$ (Eq. 1).

$$[4Fe-4S]^+ + Co(II) \rightarrow [4Fe-4S]^{2+} + Co(I) \quad (1)$$

$[Cbl(I)]^-$ initiates a nucleophilic attack on methyl-tetrahydrofolate, CH_3—THF (Eq. 2).

$$Co(I) + CH_3\text{–}THF \rightarrow CH_3 - Co(III) + THF \quad (2)$$

The methyl group is delivered to the active site A cluster, a $Ni_2Fe_4S_4$ metallocluster (A-cluster) of acetyl-CoA synthase and which then becomes the methyl of acetyl-CoA, and regenerating $[Cbl(I)]^-$ [298].

An interesting example of a cobalamin-dependent radical SAM methyltransferase is that responsible for the synthesis of *L*-phosphinothricin, $CH_3(P(O)O^-)CH_2CH_2CH(NH_3^+)(C(O)O^-)$, an amino acid that is the only known naturally-occurring entity with a C—P—C linkage,

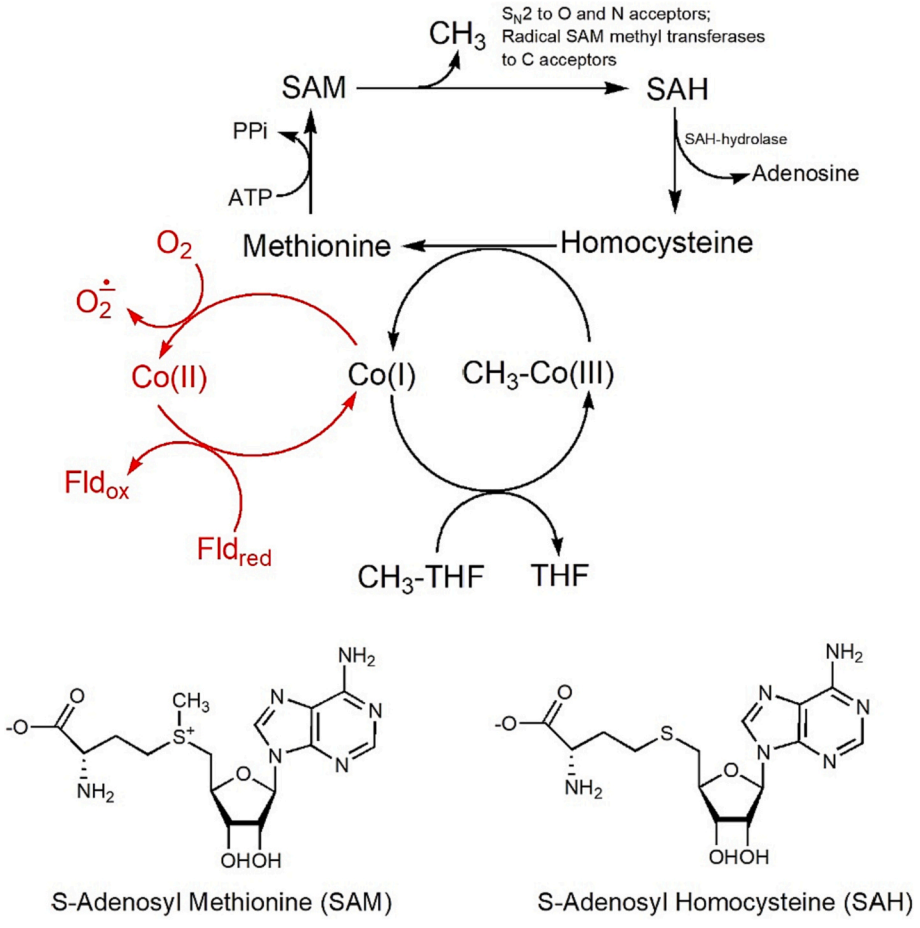

Scheme 2. The transfer of a methyl group from 5-methyltetrahydrofolate to homocysteine, producing methionine, catalysed by methionine synthase.

produced by the bacteria *Streptomyces hygroscopicus*, *Streptomyces viridochromogenes*, and *Kitasatospora phosalacinea* [299–301]. A *L*-glutamate analogue, it has herbicidal and antimicrobial properties. Another is that from the marine bacterium *Shewanella denitrificans* OS217, which catalyses the P-methylation of *N*-acetyl-demethylphosphinothricin and demethylphosphinothricin to produce *N*-acetylphosphinothricin and phosphinothricin, respectively [302].

MM methods can be very useful when coupled with quantum mechanical calculations (QM/MM methods) where the MM force field is used to model large structures, such as a protein, and QM or related methods are used for modelling the portion of the molecule, such as the cofactor, for which a reliable description of its electronic structure is sought [303,304]. Using QM/MM methods, Kumar and Kozlowski explored two possible pathways that lead to the transfer of a methyl group from the methyl group donor from CH_3—THF to $[Cbl(I)]^-$ during the catalytic cycle of MetH [305] (Scheme 3).

In the first pathway, Co(I) undertakes a nucleophilic attack on the methyl group of CH_3-THF; this is generally thought to be the mechanism of the reaction. In the ground state of $[Cbl(I)]^-$, the HOMO is in essence the Co $3d_z^2$ orbital, and $[Cbl(I)]^-$ is therefore predicted to have a closed shell $S = 0$ ground state with an electron pair in $3d_z^2$, consistent with the concept of its "supernucleophilic" nature. This electronic configuration was also found to be the predominant (but not only) contributor to the ground state wavefunction in a CASSCF/CASPT2 study [245]. This is in contrast to a B3LYP study which indicated that the ground state consists of a d^7 metal ion antiferromagnetically coupled to a corrin-based π radical [241]. The CASSCF/CASPT2 study indicated a modest 20% contribution to the ground state of the Co(II)-corrin $\pi^\bullet$ diradical configuration.

Kozlowski and co-workers used CASSCF/XMCQDPT2 calculations to show how the Co(I)—N bond length to an axial N-donor ligand (modelled using imidazole) affects the electronic structure of the metal [306]. At short bond lengths, the diradical contribution to the ground state wavefunction becomes important, while at longer bond lengths (> 2.5 Å) the dominant configuration is a closed shell d^8 configuration. This suggests that attack of Co(I) on the methyl group of CH_3—THF could proceed either by S_N2 nucleophilic attack of Co(I) or firstly by long-range electron transfer from Co(II) to the pterin ring, follow by $CH_3^\bullet$ transfer to the metal. Both pathways have a similar energy barrier of ca. 35 kJ mol^{-1} [305]. This flexibility, tuned by an interaction with an axial N-donor ligand, would allow for methyl transfer in situations where steric crowding might make nucleophilic attack on the pterin difficult. The S_N2 pathway, with an energy barrier of 33–38 kJ mol^{-1} is in line with the experimentally-observed rate constant for the reaction (7×10^4 M^{-1} s^{-1} at 37 °C [292,307]) provided that protonation of the methyl donor occurs before nucleophilic attack by the metal. In the absence of protonation, the activation energy is an untenable ≈160 kJ mol^{-1}. Thus proton transfer must occur prior to, or in concert with, methyl group transfer.

3.2. The [Ado-Cbl] dependent enzymes

The [AdoCbl]-dependent enzymes fall into three classes [7,308]. Carbon skeleton rearrangements in which the migrating group is a carbon fragment are catalyzed by the Class I enzymes, the mutases (for example, methylmalonyl-CoA mutase, Scheme 4a). The Class II enzymes include the eliminases, which catalyze the migration and subsequent elimination of an hydroxyl or amino group (Scheme 4b shows the reaction catalyzed by ethanolamine ammonia-lyase), and ribonucleoside-triphosphate reductase which catalyzes the reduction of ribonucleoside triphosphates (Scheme 4c). The Class III enzymes, the aminomutases, catalyze the migration of an amino group to an adjacent carbon (the reaction of lysine-5,6-aminomutase on *DL*-lysine is shown in Scheme 4d).

The Class I and Class III enzymes bind [AdoCbl] in a base-off/His-on form in which the bzm base and the nucleotide loop are buried in a hydrophobic pocket whilst the α coordination site is occupied by the imidazole side chain of a His residue. The proximal His ligand forms part

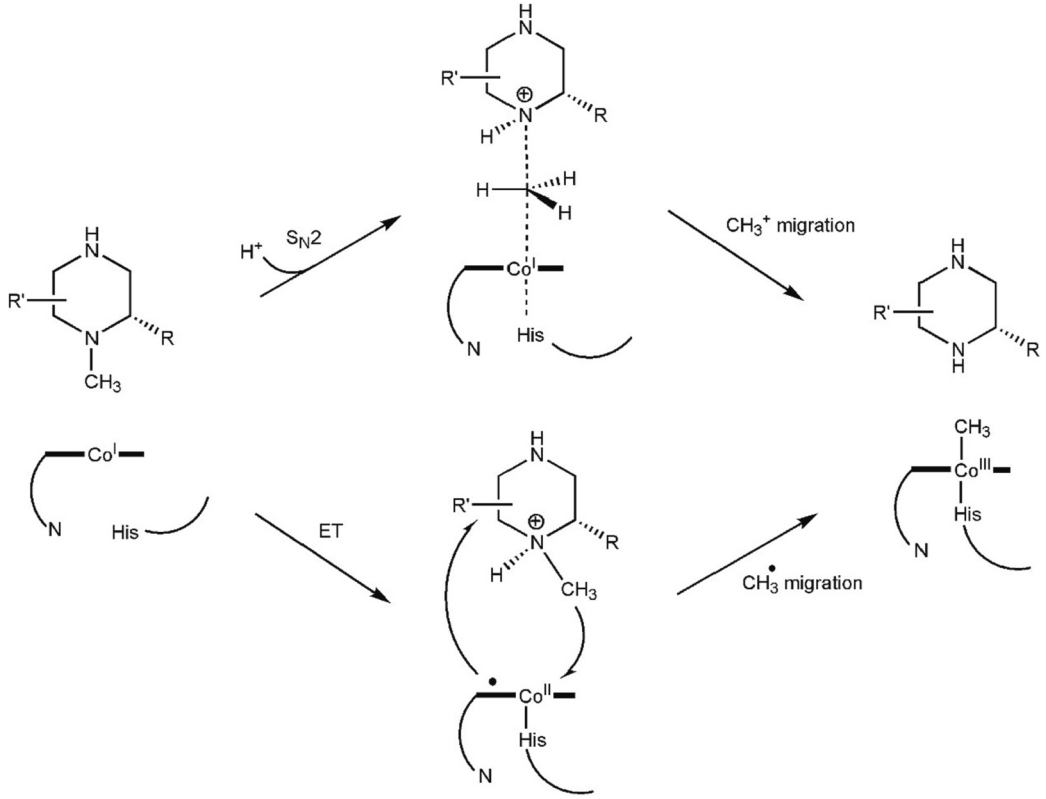

Scheme 3. Two possible routes for the transfer of methyl group from CH_3-THF (depicted schematically) to cob(I)alamin.

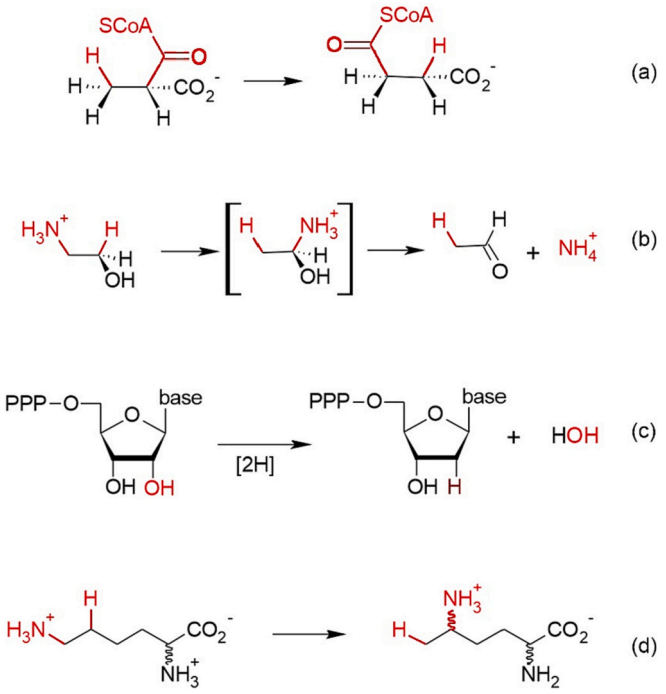

Scheme 4. (a) The conversion of *L*-methylmalonyl-CoA to succonyl-CoA, catalaysed by methylmalonyl-CoA mutase (MCM). (b) The conversion of ethanolamine to acetaldehyde and ammonia catalyzed by ethanolamine ammonia-lyase (EAL). (c) The reduction of a ribonucleoside triphosphate catalysed by ribonucleoside-triphosphate reductase. (d) The conversion of *DL*-lysine to 3,5-diaminohexanoate.

of a hydrogen-bonded network, the so-called catalytic triad, DXHXGXK (or DXHXGXN in 2-methyleneglutarate mutase) [309–311]. [CH_3Cbl] is bound in a similar manner in methionine synthase [114]. In the Class II enzymes, [AdoCbl] is bound with the axial bzm ligand coordinated to the metal.

The first step in the reaction catalysed by methylmalonyl–coenzyme A mutase (MCM) (Scheme 5), also known as methylmalonyl-CoA isomerase, and its relatives, which interconvert branched and linear acyl groups through carbon skeleton transformations, involves cleavage of the Co—C bond between Co and the adenosyl moiety [312,313]. The Ado$^\bullet$ radical abstracts H from the substrate to form a substrate radical, sub$^\bullet$ [314], a reaction that is accelerated by some 12 orders of magnitude by the enzyme [315–317]. How the enzyme produces this remarkable rate enhancement has been the subject of considerable debate and speculation [318–325]. It is suggested that the Gibbs energy released on substrate binding contributes to the lowering of the energy barriers required for the homolysis of the Co—C bond [323]. It is noteworthy that a detailed analysis of the electron densities of [AdoCbl] and [MeCbl] based on high resolution, low temperature x-ray diffraction studies followed by BP86/TZVP DFT calculations and analysis of the topological properties of the Co—C and Co—N_{bzm} bonds showed there is very little difference in the properties of the Co—C bonds of the two compounds [169]. That one undergoes homolytic bond cleavage in its biological reactions and the other heterolytical cleavage strongly suggest that it is the protein that controls these reactions. QM/MM simulations suggest that a mechanochemical switch, controlled by the protein, effects control of the radical intermediates [326]. In solution, $\Delta H^{\ddagger}$ for homolysis of the Co—C bond in [AdoCbl] is 133(3) kJ mol^{-1} while $\Delta S^{\ddagger} = 28(4)$ J K^{-1} mol^{-1} [316]. For ethanolamine ammonia-lyase, as determined (234–248 K, DMSO/water cryosolvent) by time-resolved, full-spectrum EPR, when extrapolated to 298 K, $\Delta H^{\ddagger} = 134(4)$ kJ mol^{-1}, identical to the aqueous solution value, but $\Delta S^{\ddagger}$ is ten times larger, 255 (25) J K^{-1} mol^{-1} [327]. In this enzyme, at any rate, the decrease in $\Delta G^{\ddagger}$ from 134 to 58 kJ mol^{-1}, a 13 order of magnitude increase in the rate of Co—C bond homolysis, is entirely entropy-driven. Entropic factors are also the driving force behind the formation of the Co(II)-cysteine thiyl radical ion pair in ribonucleotide triphosphate reductase [328], but it is enthalpy that drives the formation of the Co(II)-substrate radical pair in methylmalonyl CoA mutase [312].

Whether the α coordination site is occupied by bzm or imidazole, as deduced by comparing the properties of [AdoCbl] and [Ado(Im)Cbi], in which imidazole rather than bzm is the axial base, makes very little difference to the kinetics and thermodynamics of homolysis and heterolysis of the Ado ligand [329]. [Me(Im)Cbi] is destabilised relative to [MeCbl] for the transfer of methyl to a Co(III) electrophile, but abstraction by a Co(II) radical species is not significantly affected [330]. It does, however, have a much higher pK_a for the base off form, 4.3(1), than [MeCbl], 2.9 [113] (or 2.5 [331]).

Brunold and co-workers used QM/MM methods to investigate the effect altering the proximal His ligand has on the properties of the Co(II) product of the homolysis of the Co—Ado bond [332]. It is believed that stabilisation of the post-homolysis products, Co(II) and Ado$^\bullet$, contributes significantly to the rate increase effected by the enzymes (see [333] and references therein). Reduction in charge donation by the proximal ligand (which is probably achieved in the enzyme by proton uptake by the catalytic triad) leads to stabilisation of the 3d-based MOs of the Co(II) state. A QM/MM study by Jensen and Ryde [334] of glutamate mutase indicates that a number of factors are responsible for the rate increase. Firstly, the bond dissociation energy of the Co—C bond is significantly decreased in the enzyme when compared to free [AdoCbl];

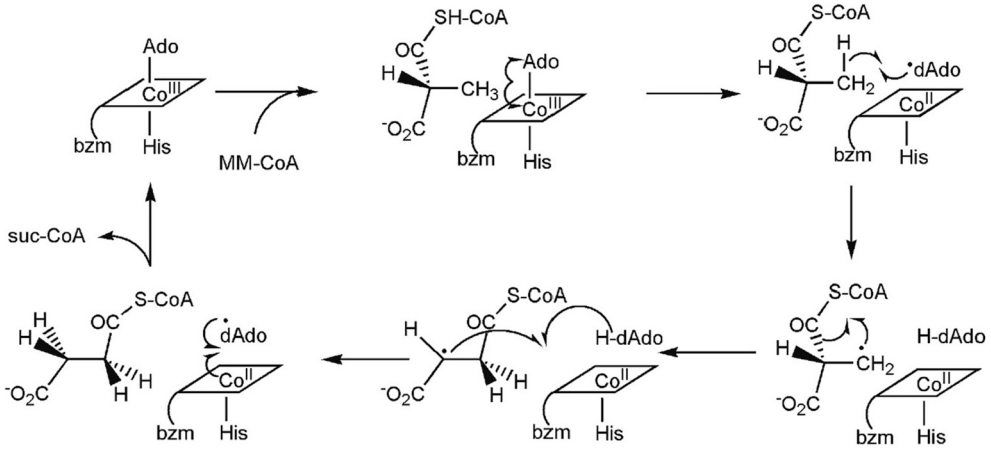

Scheme 5. The reaction catalysed by methylmalonyl-coenzyme A mutase (MCM)

secondly, the enzyme stabilises the dissociated state through van der Waals and electrostatic interactions; thirdly, the protein is moderately more stable when the cofactor is in its dissociated form; and fourthly, the coenzyme is deformed by steric interaction with protein residues.

3.3. The reductive dehalogenases

The reductive dehalogenases (RDases) catalyse reactions in which a halogen atom is removed from an organic substrate (Scheme 6) [335,336]. They degrade both naturally-occurring (from geological events or as a consequence of secondary metabolism in plants and microorganisms [337]) and anthropogenic (from their improper disposal or uncontrolled use) organohalogens in the environment [338]. Enzymes in this class have yet to be identified in humans. Several mechanisms, depending on the organic substrate, all involving $[Cbl(I)]^-$ as attacking nucleophile, have been proposed [335,339].

These enzymes typically contain two iron-sulfur clusters (either two [4Fe-4S] or one [4Fe-4S] and one [3Fe-4S]) and a cobalt corrinoid. The cofactor is bound with water (or hydroxide) in the β coordination site of Co. The reactions can be mediated by reduced metal ions (iron, tin, zinc) [340] or metal-containing porphyrinoids such as cobalamin, F_{430} and haemin [341] but for most RDases the physiological electron donor is unknown [337].

3.4. Functional diversity

Humans and other mammals rely on their diet to acquire B_{12} and, as far as is known at present, have two B_{12}-dependent enzymes (see Section 4). Bacteria are more versatile. Some can synthesise cobalamins *de novo*, and they use them as cofactors in a variety of enzyme reactions: $[CH_3Cbl]$ in the fixation of carbon dioxide through the acetyl-CoA pathway, methanogenesis and in methylation reactions; [AdoCbl] in several isomerases, amino mutases, diol dehydratase, ethanolamine ammonia lyase and a ribonucleotide reductase.

The cobalt corrinoids involved vary between organisms. Plants do not use corrins. In mammals and bacteria, cobalamins are involved in both the methylation of homocysteine [342] and in the Class B radical S-adenosyl methionine (SAM) methyl transferases, RSMTs [288]. In archaea, corrins other than cobalamin are involved. In the methanogenic archaea the methyl group is derived from methanol, acetate or CO_2; it is transferred to the sulfur atom of coenzyme M (2-mercaptanmethanesulfonate, $HS(CH_2)_2SO_3^-$) and ultimately ends up as methane. In the acetogenic anaerobes, the methyl group is derived from CO_2 and is transferred from CH_3-THF to carbon monoxide dehydrogenase to produced acetate [19,343].

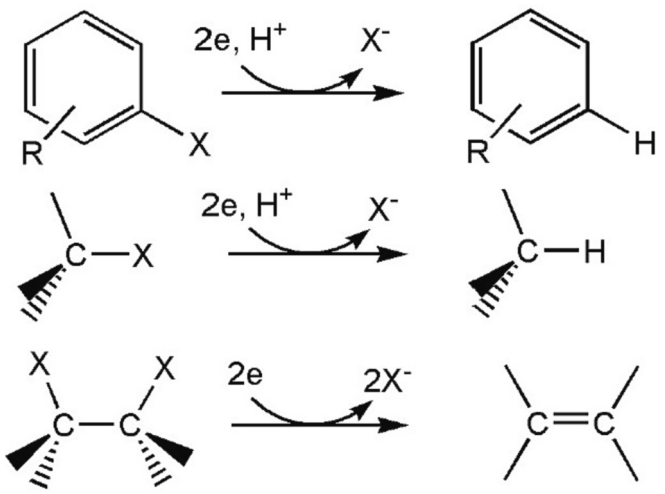

Scheme 6. Examples of reactions catalysed by the RDAses

The mode of binding of the corrinoid cofactor to the apoenzyme varies. As mentioned above, in many enzymes, including methionine synthase [114], methylmalonyl-CoA mutase [344], glutamate mutase [345] and lysine 5,6-aminomutase [346], His from a "catalytic triad" D-X-H-XX-G motif [114] provides the α ligand to cobalt (the "base-off/His-on" mode of binding), and evidence comes primarily from crystal structures determined by diffraction methods. The EPR spectrum of the paramagnetic cob(II)amide cofactor can also be extremely useful, with hyperfine couplings to ^{14}N or ^{15}N-labelled bzm showing the base-on binding in diol dehydratase [347–349], glycerol dehydratase [350] and ethanolamine ammonia-lyase [198,351,352].

The axial ligands are not the only feature of the cobalt corrinoids important for their catalytic action. There is evidence of the interaction of the acetamide *a* side chain with the adenosyl group to maintain the group in the catalytic position in diol dehydratase and ethanolamine ammonia-lyase [353]. The side chain swings between the original and catalytic positions in a synchronized manner with the radical shuttling between the coenzyme and substrate. If residues that interact directly or indirectly with the *a* side chain are mutated, the rate of unproductive side reactions increases and the enzyme turnover decreases. In a ribonucleotide reductase from *Thermotoga maritima*, the *e* side chain hydrogen bonds to the substrate GDP, locking it in proximity to the [AdoCbl] cofactor [354]. It has been suggested that hydrogen bonding between C19H and 3′-O of the ribose moiety of the Ado ligand aids in the formation of $Ado^\bullet$ [355], but the effect is likely to be very small [356].

3.5. Newer developments - riboswitches

A riboswitch is a regulatory segment of a mRNA molecule that binds a small molecule, resulting in a change in production of the proteins encoded by the mRNA [357–359]. These RNA-based elements are found mostly in bacteria and archaea as well as a few plants. The mediation of gene regulation is based on mRNA conformational changes that occur when ligands such as vitamins, amino acids, nucleotides, amino-sugars, or metals are bound. Riboswitches can therefore regulate transcription. The first discovered riboswitch and the second-most widespread is the [AdoCbl]-riboswitch [360–362]. This means that a riboswitch-containing mRNA is directly involved in regulating its own activity, in response to the concentrations of its effector molecule. For example, *E. coli btuB* mRNA [362] interacts with [AdoCbl] to control the synthesis of the BtuB transmembrane protein, which transports corrinoids across the outer membrane of the bacterium. At low [AdoCbl] concentrations, [AdoCbl] is not bound to the riboswitch and this allows the association of mRNA with the ribosome, permitting synthesis of the BtuB protein. At high concentrations of [AdoCbl], its binding to the riboswitch changes the three-dimensional structure of the mRNA in such a way that prevents it binding to the ribosome. Clearly, the concept of an "on" and "off" position is not binary and depends on the association constant between the riboswitch and the effector molecule. Recent evidence suggests that cobalamin riboswitches are quite promiscuous, responding to a wide range of corrinoids [39].

There is a less common $[H_2OCbl]^+$ riboswitch which, it has been speculated, may have evolved in marine organisms where there is high light exposure [363]. The cobalamin-dependent riboswitches therefore sense the presence of [AdoCbl] or $[H_2OCbl]^+$ to regulate the genes that are involved in the synthesis or uptake of cobalamins.

An interesting example is in *Rhodobacter capsulatus* [364], a photosynthetic purple bacterium where B_{12} performs a gene regulation function. The bacterium can grow in the dark under aerobic conditions. Under anaerobic conditions and in the presence of light, *R. capsulatus* produces bacteriochlorophyll and photosynthesis occurs through an anaerobic pathway. In the presence of oxygen the anaerobic pathway needs to be suppressed because it also produces $^1O_2$ [365]. The DNA that codes for the proteins that allow for bacteriochlorophyll synthesis can be repressed by the protein CrtJ binding to it [366]. The repressor action of CrtJ is modulated by the protein AerR. In the presence of light [AdoCbl]

(or [CH_3Cbl]) is photolysed to [H_2OCbl]$^+$ (or [HOCbl]). AerR binds [H_2OCbl]$^+$ (but not [AdoCbl] or [CH_3Cbl]). The [H_2OCbl]$^+$/AerR complex can then bind to CrtJ, displacing it from the DNA, and hence allowing bacteriochlorophyll synthesis to take place.

3.6. Newer developments - cobalamin-based photoreceptors

[AdoCbl]-dependent photoreceptors are used by some bacteria as a transcriptional repressor [81,367,368]. The prototype, CarH, mediates light-dependent expression of DNA coding for transcription of the proteins needed for synthesis of carotenes in some non-photosynthetic bacteria.

The discovery that light plays a role in B_{12} biology was surprising. In the gram-negative soil bacterium *Myxococcus xanthus*, light induces a transcriptional response that leads to carotenoid biosynthesis [369]. Carotenoids are found in several species of bacteria [370–372] and homologous sequences to the photoreceptor protein are found in the genomes of many others (for example [81,365,373–376]).

Although only discovered relatively recently [81], our knowledge of how the [AdoCbl] photoreceptors function has advanced quite rapidly [367,377–380]. In brief, the bacteria produce carotenoids, which are yellow-to-red pigments, to protect themselves from photo-oxidative damage by quenching the $^1O_2$ and other ROS produced on absorption of radiation [369,373]. The photoreceptor protein in, for example, *M. xanthus,* CarH, is coded by the *carH* gene [381]. CarH consists of a C-terminal region with an amino acid sequence similar to that of the [CH_3Cbl] binding region of MetH. [AdoCbl] is bound in the base-off/His-on form [81]. The N-terminal region can bind to DNA. Thus the C-terminal region is the light detector region and the N-terminal region allows for carotenoid synthesis. The control mechanism is exquisitely simple and is understood in some detail because the crystal structures of *T. thermophilus* CarH in its dark state, free and bound to operator DNA, and after exposure to light, have been reported [377].

In its repressor-active form, CarH is a tetramer (or dimer of dimers) and binds four [AdoCbl] moieties, but only when [AdoCbl] is present (Fig. 12). The tetramer binds to its cognate DNA operator, a 30 base-pair region between the region encoding for CarH itself, and the gene encoding CrtB, the operator that controls carotogenesis. The binding involves both hydrogen bonding and electrostatic interactions between the protein and the phosphate backbone of the DNA. This blocks the access of RNA polymerase, and hence the transcription of the proteins that are required to synthesise carotenoids.

When exposed to radiation of $< \approx 540$ nm, [AdoCbl] is photolysed; the product of this photolysis is exclusively (and unexpectedly) 4′,5′-anhydroadenosine [378]. This is likely to be the result of Ado$^\bullet$ being held in close proximity to cob(II)alamin due to a cage effect of the protein, possibly a defence mechanism on the part of the protein to prevent Ado$^\bullet$-induced damage. As has been demonstrated in viscous solvents [382–384], such a situation may lead to β-hydride elimination, producing the observed 4′,5′-anhydroadenosine and hydridocobalamin ([CblH], Co^{III}—H^- ↔ Co^{II}—H ↔ Co^{I}—H^+). Cob(I)alamin is in equilibrium with hydridocobalamin and H_2 [385]. In solution and under anaerobic conditions, hydridocobalamin rapidly dissociates to Co(II) and molecular hydrogen. In the case of a cobalamin firmly bound in a protein binding site it seems more likely that it would serve as a Brønsted acid and protonate water or a protein residue [368]. Under aerobic conditions Co(III) would be produced. (As an aside, it may be noted that reduction of [H_2OCbl]$^+$ and aquacyanocobinamide in glacial acetic acid with zinc dust produces a five-coordinate corrinoid with hydride as axial ligand [386]. Exposure of this to olefins led to the isolation and characterisation of ethylcobalamin and isopropylcobinamide, confirming the existence of a hydrido cobalt corrinoid.)

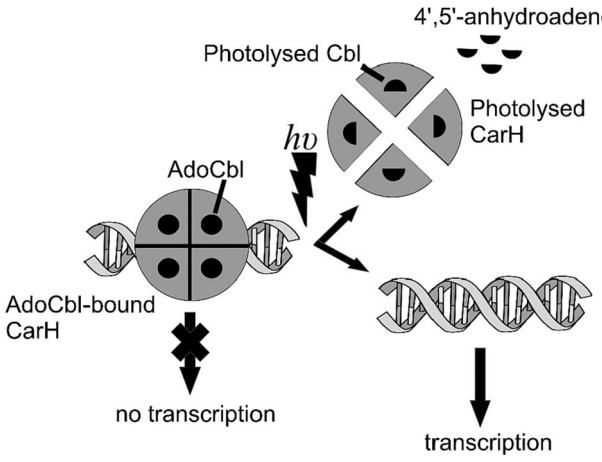

Fig. 12. A tetramer of [AdoCbl] bound to the CarH photoreceptor binds to operator DNA, preventing transcription. Photolysis releases the Ado ligand (as 4′,5′-anhydroadenosine), releasing the operator DNA so that transcription can proceed. After Jost, et al. [377]

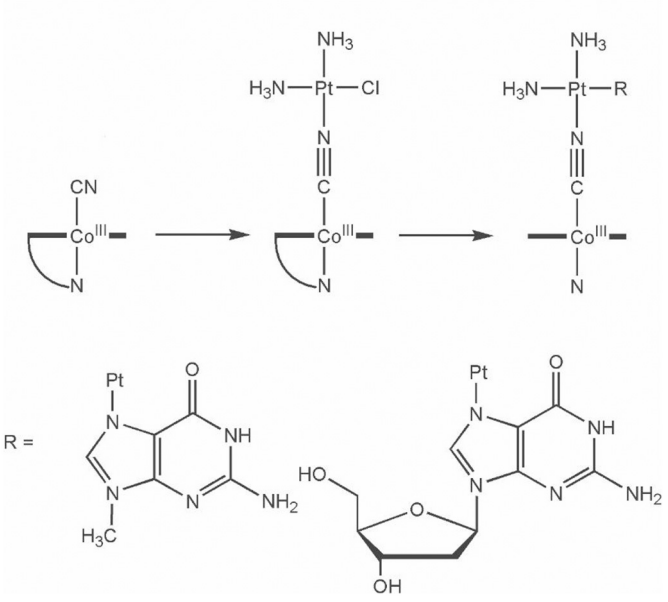

Fig. 13. Examples of cyanide-bridged B_{12}-cisplatin conjugates [425].

An alternative proposal, based on observations on the fs–s timescale [379] using ultrafast spectroscopy, suggests an (unprecedented) Co—C bond cleavage to Co(III) and Ado$^-$; β-elimination would then yield 4′,5′-anhydroadenosine and hydridocobalamin. It is conceivable that the protein modulates the properties of the Co—C bond to favour heterolytic cleavage (the Ado ligand has a somewhat different orientation than in the AdoCbl-requiring enzymes, but the Co—C bond length (2.2 Å) is not unusual).

After photolysis, Trp131 moves into the void arising from the loss of the Ado ligand and the imidazole from His132 occupies the β coordination site. This His, however, is not strictly required either for the formation of the tetramer or its light-induced collapse [367]. The concomitant, very significant, rearrangement of the protein disperses the tetramer; interaction with the DNA ceases, and gene expression is released. What remains to be elucidated is how the [AdoCbl] light sensor, which is biologically expensive to produce, is recovered for the next cycle.

Romine and co-workers [387] have recently reported the development of an affinity-based B_{12} probe (B_{12}–ABP) by attaching a group containing a diazirine (for irreversible photo-cross-linking to B_{12}-binding proteins) and an alkyne moiety (for appending fluoroprobes for analytical purposes) to the 5′-hydroxy position of the ribose in B_{12}. They used B_{12}–ABP to identify B_{12}-binding proteins in the non-phototropic

B_{12}-producing bacterium *Halomonas* sp. HL-48. *Halomonas* was known to require B_{12} as a cofactor for ethanolamine biosynthesis and as a riboswitch for the B_{12} salvage system [388]. They discovered a light-sensing transcriptional regulator that binds B_{12} and also found B_{12}-binding proteins that are involved in the metabolism of folate, methionine and ubiquinone where they are likely to act as allosteric effectors. Since these metabolic processes produce the precursors to the synthesis of DNA, RNA and proteins, it is suggested that B_{12} can be used to modulate growth and B_{12}-producing organisms may facilitate the coordination of community metabolism. B_{12}-ABP captured a total of 17 proteins, including 8 SAM-dependent enzymes, that are linked by methionine synthase in methionine, folate and ubiquinone metabolism, indicating significant roles in the control of methionine and 5-Me-THF.

4. A brief note on medical applications

Developments in medicinal applications of B_{12} have been reviewed (for example, [389–400]). As far as is known at present, humans have two B_{12}-dependent enzymes. [AdoCbl]-dependent methymalonyl coenzyme A mutase (MCM) catalyses the isomerisation of methymalonyl-CoA to succinyl-CoA [323]. [MeCbl]-dependent methionine synthase (MS) catalyses the synthesis of methionine by transferring a methyl group from CH_3-THF to homocysteine [401] (see Section 3). Genetic disorders in the metabolic pathways that lead to the assembly of the two enzymes lead to methylmalonic aciduria and homocystinuria [29]. The lack of Intrinsic Factor, one of the three B_{12} transport proteins in humans, leads to pernicious anaemia [402]. Elevated homocysteine levels have been associated with the onset of cognitive disorders such as Alzheimer's disease [92]. [CNCbl] taken as a supplement has to be converted to the active forms in the body, and much is known about the machinery that accomplishes this [403–405].

The high affinity of cobalt corrinoids for CN^- make compounds such as $[H_2OCbl]^+$ [406] and dinitrocobinamide [407] effective antidotes for cyanide poisoning. Aquanitrocobinamide, $[(H_2O)(NO_2)Cbi]^+$ can be absorbed by muscle tissue, whereas $[H_2OCbl]^+$ requires intravenous injection [407]. The complexation of cobalamins and cobinamides by human serum albumin (HSA), for example, may compromise their effectiveness as cyanide antidotes as shown in a detailed study of their reaction with bovine serum albumin, a HSA model [408]. The very obvious purple colour of $[(CN)_2Cbi]$ makes it effective for the spectrophotometric detection of cyanide in blood and other bodily fluids [409–413].

There has been considerable work on exploiting the sophisticated transport and accumulation pathway of B_{12} to develop modified cobalt corrinoids that are potentially useful in diagnostics and in therapy. Several reviews are available [395,414–418]. While showing potential, this approach has yet to lead to a commercialised product because of, among other issues, a limited uptake capacity (ca. 2.5 μg day^{-1}), lack of tissue specificity, and degradation of the conjugate [414].

The availability of crystal structures of the B_{12} transport proteins and both molecular mechanics and quantum mechanics methods for the reliable modelling of the cobalt corrinoids and their proteins has made *in silico* modelling of B_{12}-conjugate-transporter systems possible [218], which will undoubtedly assist in the design and eventually realisation of B_{12}-based delivery systems. For such systems to be viable, it is essential that the cobalamin is modified in such a way that this does not interfere with its transport and assimilation. The current understanding is that the 5′-OH moiety, and the metal itself, are the most suitable positions for modification [395,415]. Indeed, even attaching a very large moiety such as Rhodamine B to 5′-OH through a 14-atom PEG spacer did not significantly affect the binding kinetics or affinity of Intrisic Factor for the B_{12} complex [419,420]. Selected examples include conjugation of B_{12} with NIR light harvesting antennas [421]; with a ^{64}Cu complex potentially useful for PET imaging [422] and a ^{99m}Tc complex for targeting of cancer cells [423]; with peptides [424] and peptides and nucleic acids [221]; with cisplatin [425,426] (Fig. XX), ^{99m}Tc(I) and Re (I) [426], bridged to Co(III) through cyanide; with a variety of Pd(II) complexes bridged to Co(III) through cyanide [427]; with a Re(I) complex for receptor-mediated uptake and screening in lung cancer cells [428]; and with a photo-activated CO-releasing molecule for protection of fibroblasts under conditions of hypoxia [429].

The rationale for attaching anti-cancer drugs such as cisplatin to B_{12} is that rapidly proliferating cells take up B_{12} more rapidly than normal cells, thus achieving some measure of selectivity [425]. Release of the drug would occur on reduction of Co(III) to Co(II) through the action of the normal B_{12}-processing pathway.

B_{12} conjugates with fluorescent probes have been developed which target the cubilin receptor of cancer cells [428,430,431], so there is significant potential for both diagnostic and therapeutic purposes. A promising tactic is to attach an anticancer drug derivative, such as doxorubicin, to B_{12} through a Co—C bond, and then induce bond cleavage (and hence drug release) by photoirradiation [421].

As mentioned, because of its involvement in DNA synthesis, there is an increased demand for B_{12} in rapidly proliferating cell lines [432]. Antivitamins B_{12}, compounds that for example, inhibit B_{12}-dependent enzymes, hence occupying the physical but not the biological space of cobalamins [433], are therefore potentially attractive as therapeutic drugs [31,33,434]. Examples of such compounds are [RCbl]'s where R = 4-ethylphenyl [435] or R═C≡CH-Ph [170,177] and feature a strong Co—C bond; this feature of these "locked B_{12}" compounds [435] precludes their processing into enzymatically active forms. They are not very photolabile [436] (see Section 6); the conversion of [4-ethylphenylCbl] to [Cbl(II)] has a quantum yield <1%. DFT and TD-DFT calculations on a model complex (all side-chains replaced by H; bzm replaced by imidazole) indicate photodissociation involves lengthening of the Co—N_{Im} bond through metal-to-ligand charge transfer followed by lengthening of the Co—C bond through the ligand field state (a state in the S_1 potential energy surface of predominantly Co d → d character [437]; see Section 6).

5. Redox behaviour

Since the biological chemistry of the cobalt corrinoids features cobalt in the +3, +2 and + 1 oxidation states, the redox properties of the cobalamins, and the consequence of the oxidation state of the metal for its coordination chemistry and reactivity, is of considerable interest [438]. As comprehensive reviews are available [439,440], only particular aspects are highlighted in what follows, with an emphasis on more recent reports.

5.1. Electrochemical behaviour and redox chemistry

The reduction potential of the cobalt corrinoids depends on what axial ligands are present, and is a function of pH. In the case of $[H_2OCbl]^+$, its reduction potential between pH 2.9 and 7.8 in aqueous solution is +0.20 V (22 °C; all values vs SHE unless otherwise indicated) and moves to more positive values at lower pH as bzm is protonated and the base-off form is produced ($pK_a = -2.4$ [238], or −2.13 [112]), and to less positive values above pH 7.5 due to deprotonation of coordinated H_2O [238] and formation of [HOCbl], $pK_a = 7.462(7)$ [111]. The reduction potential of $[(H_2O)_2Cbi]^{2+}$, 0.51 V [441], is precisely the same as that of base-off $[H_2OCbl]^+$. Coordination of bzm therefore stabilises the metal against reduction. A Pourbaix diagram for $[H_2OCbl]^+$, adapted from [238], is shown in Fig. 14. Slightly different values were obtained in a later study [442], but the broad pattern of redox behaviour as a function of pH remains the same. Values in italics (in V) in Fig. 14 are from that study. The broad features of the diagram are quite well reproduced using DFT methods with the PBE functional [443].

The reduction potential of [Cbl(II)] is −0.61 V down to pH 4.7, then shifts to −0.49 V with the protonation of bzm ($pK_{base\text{-}off} = 2.9$ [116,238]). $[Cbl(I)]^-$ is normally 4 coordinate. Protonation of base-off bzm occurs with $pK_{base\text{-}off} = 4.7$ [238] (but reported as 5.6 from a

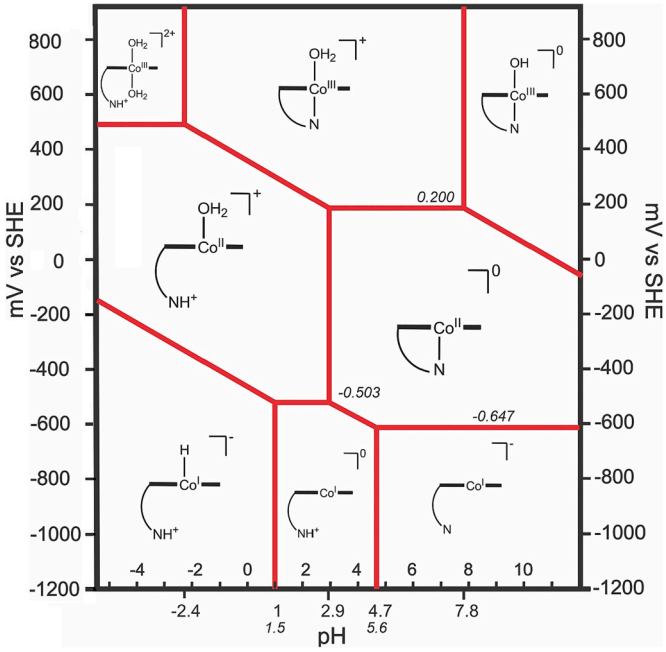

Fig. 14. The electrochemical behaviour of $[H_2OCbl]^+$ as a function of pH, adapted from [238]. Values in italics are from [442].

spectroelectrochemical study [442]). In strongly acidic solution, with a $pK_a \approx 1$ [238] (or 1.5 [442]), protonation of $[Cbl(I)]^-$, to form [HCbl(I)], occurs. The Co(II)|Co(I) potential for $[(H_2O)_2Cbi]^{2+}$ is −0.49 V [441], precisely the value determined for base-off $[H_2OCbl]^+$ (Fig. 12); unsurprisingly, $[(H_2O)_2Cbi]^{2+}$ and base-off $[H_2OCbl]^+$ have a similar electrochemical behaviour. The redox potential is more positive than for base-on $[H_2OCbl]^+$, reflecting the poorer σ donor power of H_2O compared to bzm.

In a DMSO-propanol solution, [CNCbl] is apparently electrochemically reduced directly to $[Cbl(I)]^-$ at −0.76 V because of the slowness of the first electron transfer step [444]. Its electrochemical behaviour in the presence of excess CN^- is complex because of the high affinity of Co(III) for CN^- [444].

Alkylcobalamins are more difficult to reduce because of electron density donation from the alkyl ligand to the metal. The reduction potential of base-on $[CH_3Cbl]$ is −1.36 V in DMF:propanol [238,445] and in DMSO [238] as determined by cyclic voltammetry. This shifts to −1.21 V for the base-off form [238]. Best fit values obtained by fitting the experimental data in 80:20 DMF:MeOH at room temperature to simulations gave values of, respectively, −1.35 V and −1.22 V for base-on and base-off $[CH_3Cbl]$ [446]. A value of −1.07 V for [AdoCbl] using double-potential-step chronoamperometry has been reported [447].

Crucial to understanding how the protein controls and modifies the properties of the cobalamin cofactor is the observation that the redox potential of the Co(II)|Co(I) couple in aqueous solution (−500 mV) is outside the range of biological reductants (−260 to −460 mV) [238,295,448]. Clearly, attenuation of the Co(II)|Co(I) couple is mandatory.

It is clear – and perhaps intuitively obvious – that the axial ligands have a significant effect on the redox potential of the cobalamins. This has been rationalised using DFT methods at the BP86/6–31+G* level of theory [449], accounting for the effect of solvent using the polarisable continuum model and the integral equation formalism variant (IEFPCM). Even though more recent work has suggested that the PBE functional is the most appropriate for reproducing the experimental redox properties of the cobalt corrinoids [443] – and hence, by implication, exploring experimentally unavailable, or not yet available, situations – this earlier work still provides interesting insights. Although the calculated redox potentials do not numerically reproduce the experimental values very well (for example, the experimental and calculated redox potentials for $[H_2OCbl]^+$; $[CF_3Cbl]$; and $[CH_3Cbl]$ are, respectively, 0.20 V [238] and −0.71 V; −1.03 V [129] and −1.30 V; and −1.23 V [447] and −1.52 V), the general trend is reproduced, with a redox potential becoming increasingly more negative as the donor power of the β ligand increases. Electron-donating alkyl and electron-withdrawing fluoroalkyl groups were then used as β ligands (trans to imidazole) to evaluate their effect on the redox potential. Electron-donating ligands tend to decrease the redox potentials while electron-withdrawing ligands increase them. Moreover, there is a good correlation between the E_{LUMO} values of the complexes and their redox potentials. Although the LUMO has a predominantly π^* character, its energy is modulated by the nature of the β ligand. As the electron donating ability of the β ligand increases, the E_{LUMO} increases (becomes less negative) and the redox potential decreases (becomes more negative). It was concluded that the E_{LUMO} value, which depends on the electronic character of the β ligand in alkylcobalamins, is a key determinant of the value of E^o.

Calculations with the PBE functional suggest that the Co(II) → Co(I) reduction is feasible if the reduction step is preceded by formation of a 4-coordinate Co(II) complex, thus rationalising, for example, the occurrence of 4-coordinate cob(II)alamins in two adenosyltrasferases, human adenosyltransferase (hATR) and CobA from *S. enterica* [450,451].

PBE-TZVP calculations on a square pyramidal 5-coordinate $[Cbl(I)]^-$ complex with H_2O as axial ligand, minimised to a structure where the H_2O ligand, originally placed at 2.2 Å from Co(I), moves well into the outer coordination sphere and where there is at best a long-range Co···H-OH interaction [243], reminiscent of the cobalamin structure in methionine synthase (MetH) [452]. The calculations show that the dissociation reaction of the square pyramidal complex in the gas phase has a ΔG of −8 kJ mol^{-1}, corroborating the well-established view that a square planar four coordinate geometry is the preferred geometry of $[Cbl(I)]^-$.

However, it has been pointed out that the PBE functional does not take dispersion into account so that it may underestimate the stability of a five-coordinate Co(I) complex [453]. A dispersion-corrected functional (B97-D and ωB97X-D with the 6–31++G(d,p) basis set) [453] modelling of $[Cbl(I)]^-$ (with all side chains truncated to H), and with an axial H_2O ligand, produced a structure with Co(I) forming a Co(I)···H—OH hydrogen bond (2.3 to 2.4 Å; Wiberg bond index 0.04 to 0.09), and $\Delta G_f = -2.5$ to 10 kJ mol^{-1} *in vacuo*; in a simulated solvent medium, using a polarisable continuum solvation model, $\Delta G_f > 0$ for all functionals used. The predicted ΔG_f values were significantly more exothermic (including in a simulated solvent) if the corrin side chains were included in the calculations, principally because of an N—H···OH_2 interaction with the *a* side chain amide, and became more negative as the dielectric constant of the medium decreased.

Interestingly, the redox potential of the Co(II)|Co(I) couple, as predicted by modelling with (BP86/6–31+G*), which reportedly gives reasonably good estimations of redox potentials [453], is significantly increased (i.e., less negative by between 0.10 V and 0.225 V) if the Co(I)···H—OH hydrogen bond is retained, which suggests a mechanism for its tuning to allow for electron transfer from reductants in biological processes [453].

In a QM/MM study (with a variety of dispersion-corrected DFT functions and a 6–31++G(d,p) basis set), Kozlowski and co-workers explored the feasibility of such a mechanism in a methyltransferase enzyme [454]. They used a polarisable continuum model to simulate the relatively hydrophobic environment of the protein ($\varepsilon = 4.7$) and based their modelling on the structure of the cob(II)alamin-bound MetH structure [452]. An H_2O molecule was placed in the vicinity of the β coordination site of the metal, as was phenol to mimic the Y1139 residue in the protein. ONIOM geometry optimisation of the Co(II) state produced a weakly-bound O-bound H_2O (Co—O 2.4 to 2.7 Å, depending on what functional was used, with dispersion-corrected functionals

producing shorter bond lengths), and which formed hydrogen bonds to residues Y1139 and E1097; the latter was also involved in a salt bridge interaction with R1094, which probably contributes to a strong pull effect on H_2O, weakening its interaction with the metal and in effect placing the metal in an entatic state.

In the Co(I) state, the axial H_2O interacted with the metal through H, forming a Co(I)···H—OH hydrogen bond (2.3–2.5 Å). This led to the intriguing suggestion that a conformation switch in H_2O, from O-bound to H-bound, may be a key feature in driving the reduction of Co(II), tuning the redox potential into an accessible range for biological reducing agents.

A second aspect of the Co(I) state that has received attention is the regeneration cycle in enzymes such as MetH and the corrinoid iron-sulfur protein CFeSP [455,456]. During enzyme turnover, reaction with ROS produces every 200–2000 catalytic cycles the catalytically-incompetent cob(II)alamin form (see Scheme 2) [457,458]. Spectroscopic studies (uv-vis, MCD, EPR) on mutated MetH [458] have suggested that regeneration of $[Cbl(I)]^-$ starts with displacement of the α His ligand by a conformational change in the protein and the occupation of the β coordination site by H_2O, thus maintaining the preferred five-coordinate geometry of the Co(II) state. Axially ligated H_2O interacts with Y1139. Binding of SAM causes an elongation or rupturing of the Co(II)—OH_2 bond, mediated by the Y1139 active site residue (or, based on the interpretation of the electron density in a crystal structure at 2.7 Å resolution, through hydrogen bonding of H_2O to both Y1139 and E1097 [452]). This raises the redox potential of the Co(II)|Co(I) couple, facilitating electron transfer from the reducing agent, flavodoxin. $[Cbl(I)]^-$ then acts as the attacking nucleophile on SAM.

More recent computational work (HF, BP86 and dispersion-correctional functionals/6-31G(d)5d) broadly confirm this model but suggests the increase in the reduction potential of the Co(II)|Co(I) couple stems from formation of a Co(I)···HOR hydrogen bond [291,459]. The modelling also suggests that the hydroxyl group of Y1139 rather than H_2O (which are equidistant from the metal in crystal structure of the cob(II)alamin complex [452]) may be the species that interacts with Co(I) [459].

The nature of the coordination environment of Co in a cobalt corrinoid cofactor is likely to fundamentally influence the chemistry of the metal ion. An interesting case is the corrinoid/iron-sulfur protein (CFeSP) from *Moorella thermoacetica* which contains the corrinoid Factor III_m. The cofactor is bound in the base-off form and the α ligand is therefore expected to play an important role when the cob(I)amide, $[Cbd(I)]^-$, reacts with CH_3—THF and when it transfers the methyl cation to the NiFeS of the A cluster. Stich et al. [460] addressed the problem of the nature of the coordination environment of the corrinoid in CFeSP using spectroscopic (uv-vis, CD, MCD, ESR, rR) and computational methods (QM/MM with VWN-LDA and Becke and Perdew gradient corrections for exchange and correlation, respectively; ADF-IV triple ζ basis set; and DFT and TDDFT calculations with the B3LYP/SVP for all atoms but TZVP for Co) when comparing the protein-bound and free cofactor. This study showed that [Cbd(II)] is five-coordinate with H_2O occupying one of the coordination sites and $[CH_3Cbd]$ is six-coordinate with H_2O trans to CH_3. The replacement of the 5′-methoxybenzimidazole ligand by H_2O increases the Co(II)|Co(I) couple by some 0.12 V, enabling the reduction of the cofactor by the iron-sulfur cluster of the CFeSP to regenerate the catalytically competent $[Cbd(I)]^-$ form. More recent DFT calculations [291] (density-corrected functionals as well as BP86 and BP98; 6–31++G(d,p) basis set) confirm that replacing an N-donor ligand by an O-donor ligand causes a cathodic shift of the Co(II)|Co(I) couple.

The Co—OH_2 bond in $[CH_3Cbd]$ is elongated by some 0.2 Å when the methylated cofactor is bound to the protein. There is evidence from other studies [461,462] that the nature of the trans ligand has a profound effect on how the Co—CH_3 bond is cleaved; N-donor ligands inhibit heterolytic cleavage whilst O-donor ligands do not. Moreover, the computational work in this study [460] showed that elongation of the Co—OH_2 stabilises the $3d_z^2$ orbital, allowing for its mixing with corrin frontier orbitals to generate a more Co(I)-like metal centre, which would facilitate the heterolytic cleavage of the bond. It is speculated that the elongation of the Co—OH_2 bond may also inhibit Co—CH_3 homolysis given the strong preference of Co(II) for a square pyramidal geometry.

Since usually (but not always) cobalt corrinoids are six-, five- and four-coordinate when the metal is in the +3, +2 and + 1 oxidation state, respectively, electron transfer is not a simple outer sphere process, but is accompanied by the breaking or the making of a metal—ligand bond [238,446,463]. As the affinity of Co(III) for the β ligand increases, the rate constant k_s for electron transfer at an electrode surface to a cob(III)alamin decreases and there is virtually a negative linear correlation between log k_s and log K for coordination of the ligand by $[H_2OCbl]^+$ [238] (H_2O < DMSO < pyridine < bzm < CN^-). At sufficiently high pH, when virtually all $[H_2OCbl]^+$ is converted to [HOCbl] ($pK_a = 7.462(7)$ [111]), electrochemical reduction occurs almost exclusively through the hydroxo complex, and there is a single wave observable in the cyclic voltammogram, corresponding to a 2e reduction of Co(III) to Co(I) due to a convergence of the Co(III)|Co(II) and Co(II)|Co(I) waves because of the slowness of the first reduction step [238]. Electron transfer to base-off cob(II)alamin is fast ($k_s > 0.1$ cm s^{-1}), but much slower for base-on cob(II)alamin ($k_s = 2 \times 10^{-4}$ cm s^{-1}) [237].

A plausible explanation for this has been advanced [238]. If it is assumed that electron transfer to Co(III) and departure of the axial ligand to form five-coordinate Cbl(II) is a concerted process, then the stretching of the cobalt—ligand bond is an important factor controlling the rate of electron transfer. Hence the reduction potential becomes more negative, and the rate of reduction slower, as the affinity of Co(III) for the axial ligand increases. A similar argument would apply to the Co(II)|Co(I) couple.

The kinetics of the electrochemical electron transfer to corrinoids with "inorganic" ligands such as CN^- and H_2O are rather different to those where the corrinoid carries an "organic" ligand such as CH_3^- and Ado^-. In the case of $[CH_3Cbi]^+$ [445], electron transfer is followed by rapid ($k = 14$ s^{-1} at −20 °C, and 2.5×10^3 s^{-1} at 19 °C) loss of $CH_3^\bullet$ and formation of [Cbi(I)]. The estimated ΔE_A from an Arrhenius plot is 79 kJ mol^{-1} for $[CH_3Cbi]^+$ (cf. a bond dissociation energy, BDE, of 150 kJ mol^{-1} for $[CH_3Cbl]$ [464]); electron transfer clearly markedly weakens the Co—C bond. $CH_3^\bullet$ then diffuses away to dimerise, react with solvent, or, on a HDME, to produce alkyl mercury compounds. This forms the basis for a catalytic cycle for dehalogenating hydrocarbons, with the rate-limiting step being the attack of $[Cbl(I)]^-$ on a second equivalent of the alkyl halide (*vide infra*). The initial product of the reduction of $[CH_3Cbl]$, base-off methylcob(II)alamin, is estimated to have a much weaker Co—C bond (ca. 50 kJ mol^{-1}) [464]. The consequence of the reduction of $[CH_3Cbl]$ ($E = -1.36$ V at −30 °C in DMF:*n*-propanol) is more complicated because decay of $[CH_3Cbl]^-$ occurs via a competition between loss of bzm before loss of $CH_3^\bullet$, or loss of $CH_3^\bullet$ followed by loss of bzm to form four coordinate $[Cbl(I)]^-$ [445]. The overall rate constant for decay of CH_3Cbl^- via the two pathways is 1.2×10^3 s^{-1} at −30 °C in DMF:*n*-propanol.

A detailed study of the mechanism of the reductive cleavage of the Co—C bond after electrochemical reduction has been reported [447]. Briefly, the rate-determining step that follows the electron transfer process is the formation of a solvent-separated alkyl radical and cob(I)alamin. In the case of $[CH_3Cbl]$ the model predicts a Co—C bond dissociation energy of 130 kJ mol^{-1}. Steric effects between the alkyl ligand in [RCbl] and the corrin appear to be important, with $E_{1/2}$ becoming more negative as the Co—C bond length decreases (estimated by DFT using B3LYP/LANL2DZ), i.e. $E_{1/2}$ becomes more negative in the order *i*-Bu > *i*-Pr > *n*-Pr = Et ≈ *n*-Bu > Me.

Two factors can be expected to influence the redox potential of a cobalt corrinoid: the nature of the axial ligands, and the molecular structure of the corrinoid framework [465]. The effect of the axial ligand is readily discerned from the data in Table 5 which lists the electrochemically-determined reduction potentials of some

Table 5
Electrochemically-determined $E_{1/2}$ values for some cobalt corrins.

Cobalt corrin	$E_{1/2}$vs. SHE /V	Process	Experimental conditions	Ref
$[H_2OCbl]^+$	0.20	Co (III) → Co (II)	Spectroelectrochem. on Pt; 22 °C, Britton-Robinson buffer, pH 7	[469]
	−0.61	Co(II) → Co (I)	CV on HMDE; 22 °C, Britton-Robinson buffer, pH 7	[237]
$[(H_2O)_2Cbi]^{2+}$	0.51	Co (III) → Co (II)	Spectroelectrochem. on Pt; 22 °C (?), pH 1.6 ($HClO_4$) & 3.8 (Britton-Robinson buffer)	[441]
	−0.49	Co(II) → Co (I)	CV on HMDE; 22 °C, Britton-Robinson buffer, pH 9	[441]
$[(CN)_2Cbl]^-$	−0.63	Co (III) → Co (II)	Spectroelectrochem. on Pt or Au; 22 °C (?). In the presence of 1 M CN^- The product is cyanocob(II) alamin	[444]
[CNCbl]	−0.76	Co (III) → Co (I)	CV on HMDE; 22 °C. Two electron cathodic wave with reduction along an ECE sequence	[444]
base-off cob (II)alamin	−0.54	Co(II) → Co (I)	Reference to unpublished results	[238,444]
base-on cob(II) alamin	−0.88	Co(II) → Co (I)	Reference to unpublished results	[238,444]
$[CH_3Cbi]^+$	−1.23	Co (III) → (Co (II))¶ → Co (I) + $CH_3^\bullet$	CV on HMDE; −20 to 19 °C in DMF:n-propanol	[445]
$[CH_3Cbl]$	−1.36	Co (III) → (Co (II))¶ → Co (I) + $CH_3^\bullet$	CV on HMDE; −30 °C in DMF:n-propanol	[445]
$[CH_3Cbl]$	−1.27*	Co (III) → (Co (II))¶ → Co (I) + $CH_3^\bullet$	CV on Ag amalgam; 20 °C in 60:40 methanol:DMF	[447]
[AdoCbl]	−1.11	Co (III) → Co (I) + Ado$^\bullet$	CV on Ag amalgam; 20 °C in 60:40 methanol:DMF	[447]

¶Intermediate that rapidly decays. *Under these conditions other alkylcobalamins have $E_{1/2}$ values of −1.16 V (EtCbl); −1.15 V (*n*-PrCbl); −1.16 V (*n*-BuCbl); and −1.12 V (*i*-BuCbl) [447].

representative cobalt corrinoids, and other examples given above. Increasing the conjugation of the corrinoid by changing it from corrin to didehydrocorrin (DDHC) and to tetradehydrocorrin (TDHC) (Fig. 15) tends to facilitate reduction.

For base-off $[(H_2O)_2Cbl]^+$ [441] and with (presumably) H_2O in the two axial sites of the dehydrocorrins (pH 7.0, 0.1 M phosphate, 25 °C) the Co(III)|Co(II) redox potential changes from 0.51 V, to 0.45 V, and to 0.59 V, while the Co(II)|Co(I) potential changes from −0.50 V to −0.49 V, and to −0.07 V [465]. Cobaloximes and the related monooxime known as Costa's complex [466] (Fig. 16) have been explored

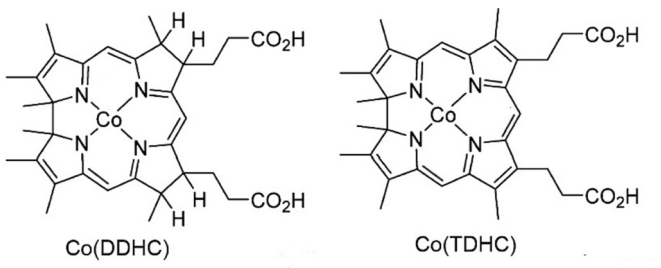

Fig. 15. The structure of the Co complexes of didehydrocorrin (DDHC) and tetradehydrocorrin (TDHC).

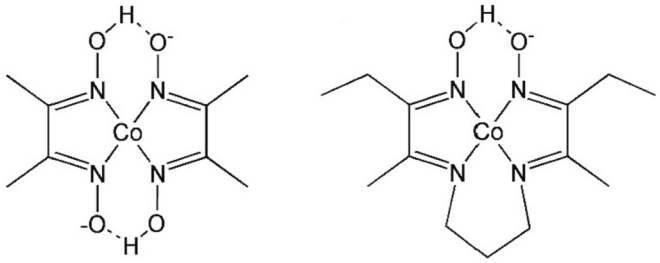

Fig. 16. Structure of the cobaloximes (left) and Costa's complex (right).

as model B_{12} complexes but they do not reproduce the redox properties of the cobalt corrins very well [467,468].

A very common procedure for the preparation of alkylcobalamins is to reduce $[H_2OCbl]^+$ to $[Cbl(I)]^-$ with, for example, $NaBH_4$, and then exploit the strong nucleophilicity of $[Cbl(I)]^-$ to displace a halide from an alkylhalide. An alternative, and synthetically much cleaner procedure, utilises the electrochemical generation of a Co(I) corrinoid at controlled potentials near the Co(II)|Co(I) couple [439,462].

5.2. Chemical redox reactions

The reduction of $[H_2OCbl]^+$ can be carried out chemically by a wide variety of reducing agents including ascorbic acid, sodium borohydride, sodium formate, a number of thiols and zinc amalgam [113,116,470–472]. $NaBH_4$ is very widely used and, depending on its concentration and the reaction time, can generate Co(II) or Co(I) [113]. Under aerobic conditions, the macrocycle is usually destroyed by the H_2O_2 that is produced by reaction of oxygen with reduced cobalamins [470]. A recent report [473] shows that $[H_2OCbl]^+$ does reversibly coordinate H_2O_2, with $\log K = 3.6$ at pH 7, dropping to 3.1 at pH 9. Co(III)-coordinated HO_2^- is protonated in acid solution ($pK_a \cong 5$), so no coordination is observed below pH 4.

5.2.1. Reactions of [CNCbl] with reduced flavin mononucleotide

All forms of B_{12} ingested from dietary or supplement sources undergo intracellular processing whereby the β ligand is removed before active forms of (in humans) [AdoCbl] and [MeCbl] are assembled [474,475]. The removal of CN^- from [CNCbl] is effected by the MMACHC protein coded by the *cblC* gene using reduced flavin mononucletide, $FMNH_2$, as reducing agent [476]. [CNCbl] is reduced to Co(II); the propensity of [Cbl(II)] for a five-coordinate metal ion [444] results in release of CN^-. The mechanism of this reaction in solution has recently been explored [477]. A ten-fold excess of $FMNH_2$ (37 °C, pH 6.8) only partially reduces [CNCbl] to [Cbl(II)] with rate constants (from the pH dependence of the reaction explored between pH 4.5 and 9.2) of 0.7(2) $M^{-1}\,s^{-1}$ for reaction with $FMNH_2$ and 7.4(5) $M^{-1}\,s^{-1}$ for the reaction with $FMNH^-$. By contrast, the reaction with aquacyanocobinamide, $[ACCbi]^+$, proceeds within the mixing time of the reagents. This suggests that the reduction of [CNCbl] requires the initial displacement of bzm by $FMNH_2$ followed by rapid inner sphere electron transfer. That the reduction does not go to completion could be a consequence of oxidation of [Cbl(II)] to $[H_2OCbl]^+$ by FMN, formed by the disproportionation of $FMNH^\bullet$ to FMN and $FMNH_2$. $[H_2OCbl]^+$ presumably reverts to [CNCbl] by picking up free CN^- formed from the initial reduction step.

5.2.2. Reactions of Co(III) with formate and formyl species, and singlet oxygen

A good example of the chemical reduction of $[H_2OCbl]^+$ is its reaction with formate (and related formyl species) [471]. From the pH-dependence of the reaction rate, the active species are $[H_2OCbl]^+$ and HCO_2^- (Eq. 3a) A deuterium kinetic isotope effect is consistent with hydride migration from coordinated formyl to cobalt to yield a protonated Co(I) species (Eq. 3b) which rapidly [478] comproportionates

with Co(III) to produce two equivalents of Co(II) (Eq. 3c).

$$[H_2OCbl]^+ + HCO_2^- \rightleftharpoons [(OCHO)Cbl]\ K = 4.6\ M^{-1} \quad (3a)$$

$$[(OCHO)Cbl] \rightarrow CO_2 + [HCbl(I)] \rightleftharpoons [Cbl(I)]^- + H^+\ k = 0.016\ s^{-1} \quad (3b)$$

$$[Cbl(I)]^- + [H_2OCbl]^+ \rightarrow 2[Cbl(II)] + H_2O \qquad k = 10^7\ M^{-1}\ s^{-1} \quad (3c)$$

Pyrocobester (the hexamethyl cobester with a missing *c* side chain and a double bond between C7 and C8) [479] undergoes photooxygenation, with cleavage of the C5—C6 bond, and formation of a dioxo species with C=O bonds at C5 and C6 [480].

A thorough investigation of the reaction of pyrocobester with O_2 in O_2-saturated CCl_4 (and with a thermal source of $^1O_2$) [481] showed that (i) irradiation of the corrinoid between 350 nm and 800 nm induces its photooxygenation with reaction rates proportional to its molar absorptivity at the wavelength of the irradiation; (ii) $^1O_2$ ($^1\Delta_g$) is an intermediate in the reaction, as established by solvent effects, H/D isotope effects, competition experiments, and quenching of the reaction with *β*-carotene. A (simplified) reaction scheme is shown in Eq. 4a,b. ([PyrCbs] = pyrocobester).

$$^1[PyrCbs] + h\nu \rightarrow {}^1[PyrCbs]^* \xrightarrow{k_{ISC}} 3[PyrCbs]^* \quad (4a)$$

$$^3[PyrCbs]^* + {}^3O_2 \rightarrow {}^1[PyrCbs] + {}^1O_2 \rightarrow [dioxoPyrCbs] \quad (4b)$$

Irradiation of $[(CN)_2Cbl]^-$ in an O_2-saturated solution of CD_3OD (−70 °C, tungsten lamp) in the presence of methylene blue (an $^1O_2$ sensitiser) leads to formation of the C5,C6 (10%) and the C14,C15 (24%) dioxo species, with 31% recovery of the starting cobalamin [482,483]. The reaction occurs considerably more slowly in CH_3OH [483].

5.2.3. Reactions of Co(III) with thiols, disulfides, nitrogen oxides and related species

Thiolatocobalamins play an important role in biology. For example, glutathionylcobalamin, [GSCbl], is probably the precursor of both [AdoCbl] and [CH_3Cbl] in humans [484]. Glutathione reacts rapidly with $[H_2OCbl]^+$ ($k \approx 18.5\ M^{-1}\ s^{-1}$ at pH 7.4) to form a very stable complex (log $K \approx 9.7$) [485]. It has been suggested that formation of [GSCbl] prevents the depletion of B_{12} by xenobiotics [486]. It is also thought that [GSCbl] is useful in treating conditions related to oxidative stress [89,92,487–490].

The reaction of $[H_2OCbl]^+$ with thiols can lead to relatively stable complexes (for example, with pentafluorothiophenol [491], *N*-acetylcysteine [492], glutathione [493], glutamylcysteine [494] and captopril [495]). Their uv-vis spectra are of the "atypical" type (see Section 7.2). In alkaline solution, a slow reduction to Co(II) and a disulfide occurs [496] whereas in acidic media the thiol is slowly protonated and released from the coordination sphere of the metal, reforming $[H_2OCbl]^+$ [497]. Both dithiothreitol [496] and cysteine [472] (less rapidly) readily reduce Co(III). Oxidised thiols such as hypotaurine and cysteinesulfinic acid also coordinate to $[H_2OCbl]^+$, producing atypical spectra [498]. Selenocysteine (SeCys) reacts with $[H_2OCbl]^+$ but the selenocyanato complex rapidly reduces Co(III) to Co(II) and only kinetic evidence of its existence was found [499]. The reaction between $[(H_2O)_2Cbi]^{2+}$ and thiols leads to relatively unstable complexes [500,501] although glutathionylcobinamide has been successfully prepared [502].

Thiolatocobalamins are not common; while the reactions of $[H_2OCbl]^+$ with a wide variety of thiols have been reported (see the comprehensive reference list in [503]), they usually reduce Co(III) to Co(II) at rates which increase with thiol concentration and pH. There are exceptions. Slow addition of thiophenol to $[H_2OCbl]^+$ in acetone at −15 °C under Ar (red light conditions) produced [C_6F_5SCbl], which was characterised by FAB-MS, and ^{1}H and ^{19}F NMR [491]. $[H_2OCbl]^+$ reacts with glutathione in neutral and acidic aqueous solution to form stable [GSCbl] [504], log $K = 9.7$ [485]. Cyclohexylthiolatocobalamin and cysteinylcobalamin have also been prepared [503]. The depletion of B_{12} *in vivo* by exposure to xenobiotics such as chloroprene and 1,3-butadiene is probably a consequence of their reaction with $[Cbl(I)]^-$ [486]. Glutathione may protect against this by forming [GSCbl] [486]. [GSCbl] reacts with SeCys through two pathways [505]. In the first, there is rapid formation of a complex between [GSCbl] and SeCys; this is followed by rate-determining ligand exchange and then rapid reduction of Co(III) to Co(II) with formation of $SeCys^\bullet$ (which then dimerises to $(SeCys)_2$). In the second pathway, SeCys displaces GS from the coordination sphere of Co(III), and then rapidly reduces Co(III) to Co(II).

When diaquacobyrinic acid heptamethyl ester $[(H_2O)_2Cbs]^{2+}$ is reacted with thiophenol under anaerobic conditions in the dark, $[(C_6H_5S)(H_2O)Cbs]^+$ is produced [506], presumably with the thiolate in the upper coordination position, although this was not explicitly demonstrated. Both photolysis of $[(C_6H_5S)(H_2O)Cbs]^+$ ($\lambda > 420$ nm, 80 min) and its thermolysis (50 °C, 4 h) lead to homolytic cleavage of the Co(III)—S bond to form the Co(II) complex and the phenyl thiyl radical.

The reaction of alkylcobalamins with 2-mercaptoethanol in alkaline solution involves the nucleophilic attack of the thiolate on coordinated alkyl to form an alkylthioether and cob(II)alamin in a reaction that is presumed to proceed via intermediate formation of Co(I) [507,508]. The reaction of (carboxymethyl)cobalamin with 2-mercaptoethanol was investigated as a function of pH [508]. At low pH, with the base-off form of the corrinoid, the reaction is moderately fast ($k = 2 \times 10^{-2}\ s^{-1}$ at 43 °C, pH 1.0) and involves a reductive cleavage of the Co—C bond by the thiol to produce acetate and Co(II). The reaction is slower in alkaline solution ($k = 1 \times 10^{-3}\ s^{-1}$ at 43 °C, pH 12.5) and entails nucleophilic attack of the thiolate on the Co—methylene carbon to form (eventually) Co(II) and *S*-(carboxymethyl)mercaptoethanol. The difference in the behaviour of the base-on and base-off forms was emphasised by showing that the reaction of 2-mercaptoethanol with a (carboxymethyl)cobamide in which the N3 of bzm is methylated produced acetate across the entire pH range (pH 2.1 to 10.2; *k* is virtually pH-invariant and ranges between 1.0×10^{-3} and $2.4 \times 10^{-3}\ s^{-1}$).

Nitric oxide reacts with [GSCbl] ($k = 2.82 \times 10^3\ M^{-1}\ s^{-1}$ between pH 4 and 10, with a slight increase in rate above pH 9), probably through intermediate formation of a *S*-nitrosoglutathionyl complex, to produce [NOCbl] [509].

Dithionite ($S_2O_4^{2-}$) reduces $[H_2OCbl]^+$. The actual reductant is the radical anion $SO_2^{-\bullet}$, formed from the dissociation of dithionite. This produces cob(II)alamin and SO_2 [118] after electron transfer; the second order rate constant for the reaction is $1.46(5) \times 10^3\ M^{-1}\ s^{-1}$ at 25 °C. In the presence of excess dithionite, [Cbl(II)] complexes $SO_2^{-\bullet}$ to produce a rare 6-coordinate Co(II) complex, $[SO_2Cbl(II)]^-$, with a $pK_{base\text{-}off} = 4.8$ (1), and in which the unpaired electrons on the ligand and the metal are antiferromagnetically coupled. A DFT-assisted assignment of its absorption and resonance Raman spectrum concluded that the (predominantly) $\pi \rightarrow \pi^*$ transitions of the *γ* band are partially mixed with a *π* orbital of coordinated $SO_2^{-\bullet}$, giving rise to a S=O stretch (at 987 cm^{-1}) in resonance with the *γ* band [510]. The same species is also generated when sulfoxylate (SO_2^{2-}) [511] and hydroxymethanesulfinate (HMS, $HOCH_2SO_2^{2-}$) [440,512] are used as reductants.

On exposure to O_2, $[SO_2Cbl(II)]^-$ is oxidised back to $[H_2OCbl]^+$ without significant attack on or destruction of the corrin [513]. Addition of two equivalents of H_2O_2 to $[SO_2Cbl(II)]^-$ produces a mixture of $[H_2OCbl]^+$ and two so-called stable yellow corrinoids, hydroxylated at C5 and C15, respectively (Fig. 17), isolated chromatographically as the dicyano complexes, in an approximate ratio of 1:2:2 [513]. The initial rate constant of the reaction is $1.8(1) \times 10^2\ M^{-1}\ s^{-1}$. The stable yellow corrinoids are also produced on treating [CNCbl] with HMS [514]. The reaction of $[SO_2Cbl(II)]^-$ with one equivalent of tertiary-butyl hydrogen peroxide produces $[SO_3Cbl]^-$, and no stable yellow corrinoids, with an initial rate constant of 13(1) $M^{-1}\ s^{-1}$ [513].

The rate of reduction of [CNCbl] with dithionite and HMS at pH 11.4 shows saturation kinetics at high reductant concentrations [515]. The saturating rate constant ($3.0 \times 10^{-2}\ s^{-1}$ at 25 °C) and the activation

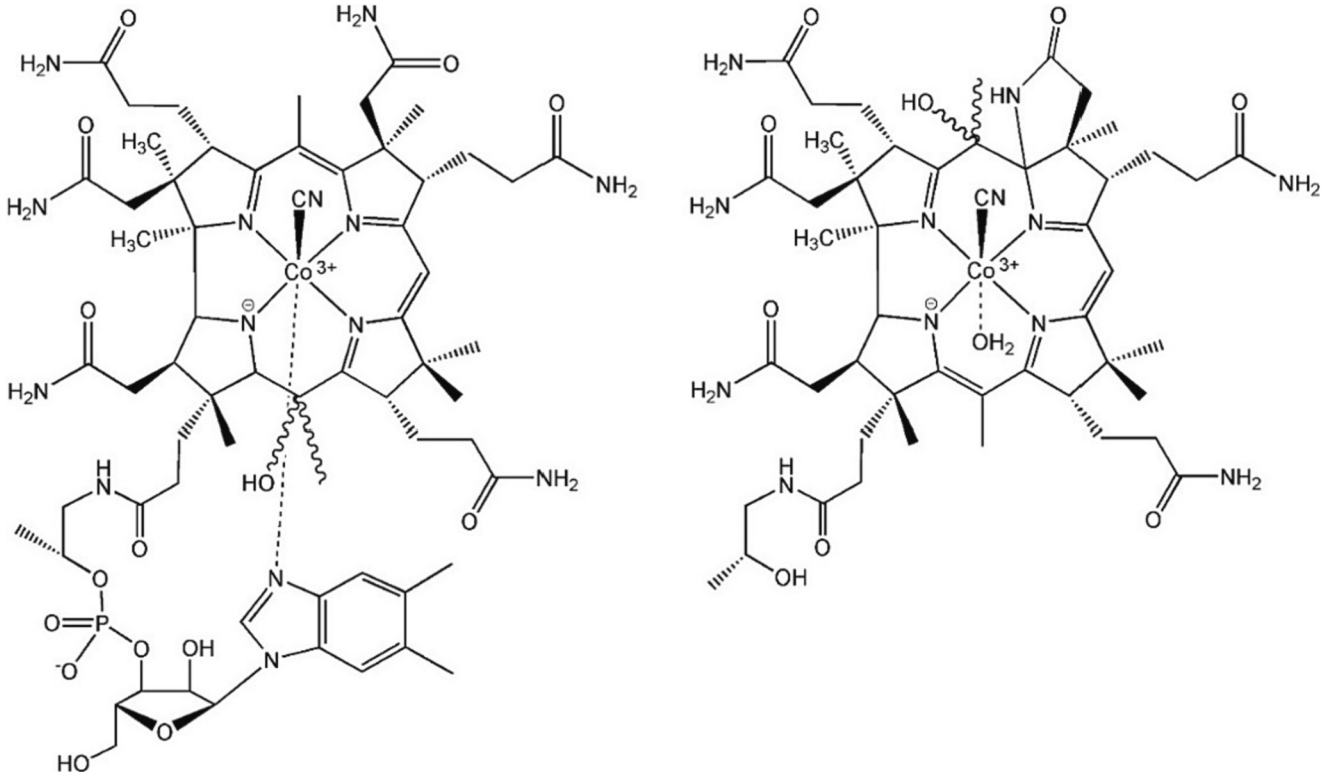

Fig. 17. Two stable yellow corrinoids (shown as the mono-cyano complex) formed in the reaction of [CNCbl] with NaHMS, $Na(HOCH_2SO_2)$. (For interpretation of the references to colour in this figure legend, the reader is referred to the web version of this article.)

parameters ($\Delta H^{\ddagger} = 103(6)$ kJ mol^{-1}; $\Delta S^{\ddagger} = 82(6)$ J K^{-1} mol^{-1}) are within experimental error identical to those for the dissociation of bzm trans to CN^- (4.2×10^{-2} s^{-1} at 25 °C; $\Delta H^{\ddagger} = 105(2)$ kJ mol^{-1}; $\Delta S^{\ddagger} = 81(6)$ J K^{-1} mol^{-1} [516]). Very similar results were obtained with dithionite. This strongly suggests that the rate-determining step is displacement of bzm by the reducing agent, followed by inner sphere electron transfer.

The reaction of H_2S with $[H_2OCbl]^+$ is complex [517]. Both H_2S and HS^- displace H_2O from $[H_2OCbl]^+$ (but not OH^- from [HOCbl], which, as has been known for a long time [471,518–521], is inert to substitution). This is followed by inner sphere electron transfer, a process which occurs significantly faster for the base-off form of [HSCbl]. Reaction with a second equivalent of H_2S follows to form $[HS_2Co(II)Cbl]^{2-}$ (or $[H_2S_2Co(II)Cbl]^-$, depending on pH) which then dissociates to HS_2^{2-} and [Cbl(II)]. In the case of the cobinamide, and in the presence of a sufficiently high concentration of H_2S, a stable $[(^-HS)_2Cbi]$ species can be formed [522].

Thiols are effective reductants for alkyl corrinoids. In principle, the reduction could occur by (i) an outer-sphere electron transfer from the thiol to the corrinoid which, at least initially, produces a corrin-based radical anion (Scheme 7) [523]; (ii) by coordination of the thiol to one of the coordination sites of the metal (*cf*. the reduction of [CNCbl] by HMS, *vide supra*); or (iii) by direct attack of the thiol on the alkyl ligand. Reduction of alkylcob(III)alamin to Co(II) increases the rate of homolysis of the Co—C bond some 10^{15} times, producing Co(I) and an alkyl radical, or, under acidic conditions, Co(II) (Scheme 7).

The chemical reduction of a corrinoid in which one of the ligands is H_2O and which involves coordination of the reducing agent should be dependent on pH since OH^- is inert to substitution [471,520,521].

The oxidation of 2-mercaptoethanol to the disulfide, which may be generalised as shown in Eq. 5, is an example of a reaction where reduction of the metal proceeds by an inner-sphere mechanism. There is

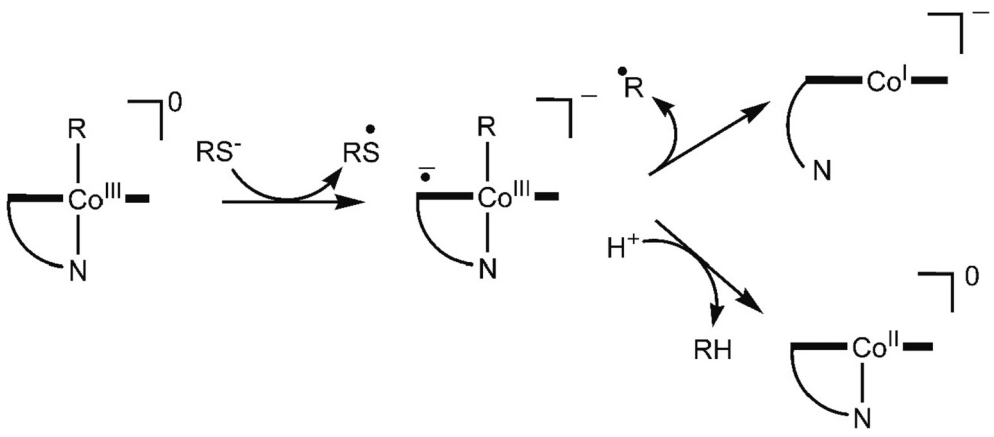

Scheme 7. One possible route of the reaction of an alkylcobalamin and a thiol.

indirect evidence for the formation of a [Cbl(I)] intermediate [524]. The probable reaction mechanism is shown in Scheme 8 (for an alkylcobalamin, such as R = CH_3, Ado; an equivalent mechanism is readily envisaged for an alkylcobinamide).

$$2\,RSH + O_2 \rightarrow\ RSSR + H_2O_2 \quad (5)$$

The reaction begins with displacement of bzm by the thiolate. The alkyl thiolate complex reacts with a second equivalent of the thiolate to produce a disulfide product and an alkylcob(I)alamin. Oxidation of the reduced corrinoid by O_2 forms H_2O_2 and regenerates the alkylcob(III)alamin. Methyl iodide inhibits the reaction, probably by trapping the corrinoid as an alkylmethyl complex. Irradiation of the system with visible light releases the inhibition and the rate of O_2 consumption increases markedly as $[H_2OCbl]^+$ (which is a better catalyst for these reactions than alkylcobalamins) is produced. N-donor ligands inhibit the reaction by competing for the axial coordination sites of the metal.

The analogous reaction catalysed by $[H_2OCbl]^+$ is only weakly inhibited by methyl iodide, suggesting that aquacob(II)alamin, $[H_2OCbl]$, rather than Co(I), is produced. Reaction of $[H_2OCbl]$ with O_2 is expected to produce superoxide, O_2^-, and indeed the reaction rate is significantly decreased in the presence of superoxide dismutase.

In the third reaction, RS^- initiates an S_N2 attack on a coordinated alkyl group, leading to the heterolytic cleavage of the Co—C bond (Scheme 9). This is generally thought to be the key step in the transfer of a methyl group from homocysteine to methionine catalysed by methyl transferase [292]. However, an alternative mechanism, in which the cofactor is initially reduced by deprotonated homocysteine – as in Scheme 7 – to form a corrin-based radical, followed by a radical coupling between coordinated R and $RS^\bullet$ to yield the thioether and Co(I), has been proposed [523] and shown by QM/MM calculations to be feasible [525]. CASSCF calculations show that the Co—C and Co—N_{bzm} bonds are significantly elongated and therefore weakened when models of [MeCbl] (all side chains truncated to H; imidazole as β ligand) is reduced [526]. More recent DFT calculations (BP86/TZVP with the polarizable continuum model (PCM) to simulate solvent water) suggest that methyl transfer from methyl halides to $[Cbl]^-$ (modelled with all side chains truncated to H) proceeds through an S_N2 reaction. If the alkyl halide is bulkier (^{i}Pr, ^{t}Bu) then the electron transfer radical pathway is favoured [527].

$[Cbl(I)]^-$ reacts rapidly with a disulfide to produce the corresponding thiol and [Cbl(II)] [528]; the overall reaction stoichiometry is given in Eq. 6.

$$R_2S_2 + 2[Cbl(I)]^- + 2H^+ \rightarrow 2RSH + 2[Cbl(II)] \quad (6)$$

The rate of the reaction depends on the state of protonation of the disulfide. For example, for cystine, k_2 (23 °C, $M^{-1}\,s^{-1}$) increases from 4.0 (5) × 10^4, to 2.9(2) × 10^5, to 4.2(2) × 10^5 for the unprotonated, monoprotonated, and diprotonated oxidant, respectively. The rate-determining step is the initial attack of $[Cbl]^-$ on R_2S_2. Two mechanisms can be envisaged. The first (Eq. 7.1) involves homolysis of the disulfide with the $RS^\bullet$ formed reacting with a second equivalent of $[Cbl(I)]^-$. The Co(II) sulfide intermediate then decomposes to the thiolate and [Cbl(II)].

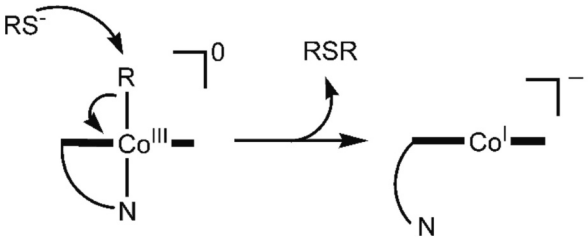

Scheme 9. An alternative pathway for the reaction of a thiol with an alkylcobalamin.

$$R_2S_2 + [Cbl(I)]^- \rightarrow [RSCbl(II)]^- + RS^\bullet \quad (7.1a)$$

$$RS^\bullet + [Cbl(I)]^- \rightarrow [RSCbl(II)]^- \text{ (fast)} \quad (7.1b)$$

$$2[RSCbl(II)]^- \rightarrow 2RS^- + 2[Cbl(II)] \text{ (fast)} \quad (7.1c)$$

Alternatively, heterolysis of the S—S bond produces RS^- and a Co(III) sulfide (Eq. 7.2), which is then reduced by $[Cbl(I)]^-$.

$$R_2S_2 + [Cbl(I)]^- \rightarrow [RSCbl(III)] + RS^- \quad (7.2a)$$

$$[RSCbl(III)] + [Cbl(I)]^- \rightarrow [RSCbl(II)]^- + [Cbl(II)] \text{ (fast)} \quad (7.2b)$$

$$[RSCbl(II)]^- \rightarrow RS^- + [Cbl(II)] \text{ (fast)} \quad (7.2c)$$

Reactions of disulfides with [Cbl(II)], on the other hand, are slow and incomplete.

Protonation of the disulfide increases the rate of the reaction. Fitting of the experimental data over the pH range studied (pH 4 – pH 10.5) allowed the second order rate constants for the unprotonated, monoprotonated and deprotonated forms of the oxidant to be deduced. For example, for cystine^{2-} ($(SCH_2CH(NH_2)CO_2^-)_2$), Hcystine$^-$, and H_2cystine, k_2 = 4.0(5) × 10^4, 2.9(2) × 10^5 and 4.2(2) × 10^5 $M^{-1}\,s^{-1}$ (25 °C; $LiClO_4$, μ = 0.2 M), respectively. Since protonation of some of the disulfide increases the rate of the reaction, this suggests that protonation weakens the S—S bond (for example, by intramolecular hydrogen bonding to the protonated carboxylate of dithioacetic acid) or by

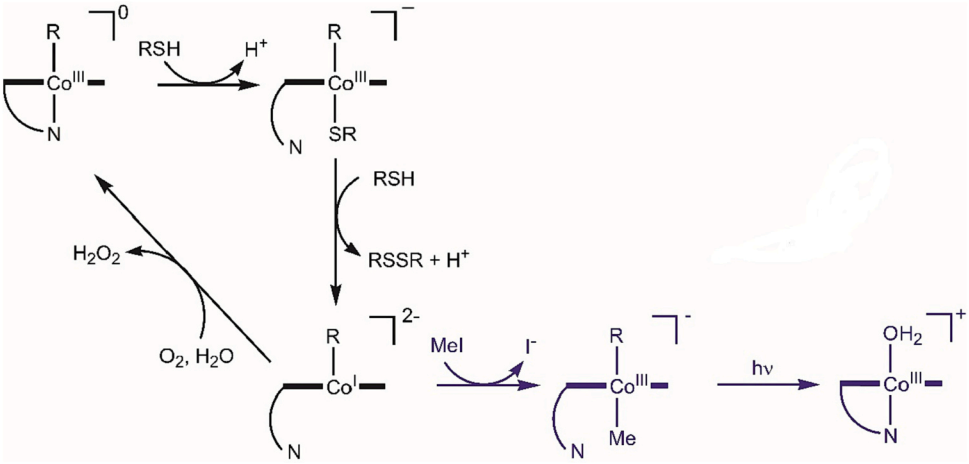

Scheme 8. The course of the reaction of an alkylcobalamin and a thiol. Methyl iodide inhibits the reaction.

stabilising the leaving thiyl group, or both. The intimate mechanism of the reaction involves, as rate-determining step, the nucleophilic attack of $[Cbl(I)]^-$ on the S—S bond. This could cleave homolytically to form $[(RS^-)Cbl(II)]^-$ and $RS^\bullet$ which then rapidly reacts with a second equivalent of $[Cbl(I)]^-$. $[(RS^-)Cbl(II)]^-$ would then dissociate to RS^- and [Cbl(II)]. Alternatively, the initial attack cleaves the S—S bond heterolytically, to form $[(RS^-)Cbl(III)]$ and RS^-; this would be reduced by $[Cbl(I)]^-$ to form RS^- and [Cbl(II)].

Sulfoxylate, SO_2^{2-} (or HSO_2^-) can be prepared by the anaerobic decomposition of thiourea dioxide, $(NH_2)_2CSO_2$ in alkaline solution [529,530]. Sulfoxylate will react with [HOCbl] to produce $[SO_2Cbl]^-$, the same product produced by the reaction with dithionite (*vide infra*). It is usually thought of as a hexacoordinate complex between $SO_2^{\bullet-}$ and Cbl (II), although DFT calculations (BP86/6-31G**) suggest the complex may have a protonated ligand and is best described as $[HSO_2^-Co(II)]$ [511]. The apparent second order rate constant at 25 °C, pH 13, is $1.95 \times 10^3\ M^{-1}\ s^{-1}$. If it is assumed that [HOCbl] is indeed inert to substitution and the rate-determining step is displacement of H_2O from the metal, then correcting for inert [HOCbl] gives $k = 3.1 \times 10^8\ M^{-1}\ s^{-1}$. There is a further, slow, reduction to $[Cbl(I)]^-$ ($k_{app} = 2.3\ M^{-1}\ s^{-1}$) [511] but this is preceded by an induction period, indicative of the occurrence of a complex redox process.

Nitric oxide does not react with $[H_2OCbl]^+$ around pH 7 [531] but does so, with high affinity (log $K = 8.9$, pH 7.4, 25 °C), with cob(II)alamin [116]. DFT (PW91/6-31G(d), B3LYP/6-31G(d)) and molecular orbital (HF/6-31G(d)) calculations on models of Co(II) and Co(III) corrins with NO suggest that Co(III) coordinates H_2O much more strongly than does Co(II), militating against coordination of NO by Co(III) [532]. By contrast, the poor affinity of Co(II) for H_2O, and the poor solvation of NO, leads to their reaction and the formation of [NOCbl], which the HF calculations indicate is best described as a Co(III)—NO^- complex. There is also resonance Raman evidence for a Co—NO bond based upon a vibrational band shift on ^{15}NO substitution [533].

Although it had been claimed that NO does react with the base-off form of $[H_2OCbl]^+$ [534], later work [535] demonstrated that this is not the case and that what had been observed was likely to have been a reaction with HNO_2, produced at low pH from nitrite impurities ubiquitously present in aqueous solutions of NO [531]. Once $[NO_2Cbl]$ is formed, it reacts with NO to produce [NOCbl] [535], but the reaction is complex and details are yet to be fully understood. Nevertheless, a plausible mechanism for the reaction at pH ≈ 1, consistent with all available kinetic data, has been proposed [535] and shown in Eqs. 8a – 8 g. (Hbzm refers to the protonated base-off form of the cobalt corrinoid) [116].

$$[H_2OCbl]^+ + HNO_2 \rightleftharpoons [NO_2Cbl] + H^+ \quad (8a)$$

$$[NO_2Cbl] + H^+ \rightleftharpoons [(Hbzm)NO_2Cbl]^+ \quad (8b)$$

$$[(Hbzm)NO_2Cbl]^+ + NO \rightleftharpoons [(Hbzm)(NO)(NO_2)Cbl]^+ \ (K^I) \quad (8c)$$

$$[(Hbzm)(NO)(NO_2)Cbl]^+ + H^+ \rightleftharpoons [(Hbzm)(NO)Cbl] + HNO_2 \ (k_1, k_{-1}) \quad (8d)$$

$$[(Hbzm)(NO)Cbl] + NO \rightleftharpoons [(Hbzm)(NO)_2Cbl] \quad (8e)$$

$$[(Hbzm)(NO)_2Cbl] + H_2O \rightleftharpoons [(Hbzm)NOCbl]^+ + HNO_2 \quad (8f)$$

$$[(Hbzm)NOCbl]^+ \rightarrow [NOCbl] + H^+ \ (pK_a = 5.1) \quad (8g)$$

The overall stoichiometry of the reaction between $[NO_2Cbl]$ and NO is given in Eq. 9

$$[NO_2Cbl] + 2NO + H_2O \rightleftharpoons [NOCbl] + 2HNO_2 \ (K) \quad (9)$$

The good fits obtained to an expression based on this mechanism provides a measure of confidence. The values obtained were $K = 0.6 \pm 0.2$, and $k_{NO} = Kk_1 = 7 \pm 2\ M^{-1}\ s^{-1}$.

$[H_2OCbl]^+$ reacts directly with Piloty's Acid (PA, benzenesulfonylhydroxamic acid, $PhSO_2NHOH$) between pH 3.5 and 10.3 to form a complex, $[PACbl]^+$, which rapidly deprotonates and loses $PhSO_2^-$ to produce nitrosylcobalamin, [NOCbl] [536].

Despite the very similar uv-vis spectra of alkylcobalamins and thiolatocobalamins [537], little was known about the photolability of the latter, in contrast to extensive studies on the former, until an elegant study by Lawrence and co-workers clarified matters [538]. Starting with $[H_2OCbl]^+$ they functionalised the OR5 hydroxyl of the ribose (Fig. 4) with ethylenediamine which provided a handle on which to attach fluorophores. They then replaced coordinated H_2O with *N*-acetyl-L-cysteine (NAcSH). [NAcSCbl] is stable in the dark and its photolysis at 360 nm produced $[H_2OCbl]^+$ at a rate about three orders of magnitude slower than the photolysis of $[CH_3Cbl]$. Photolysis was also carried out at 405 nm and 546 nm, with smaller quantum yields, and in all cases several orders of magnitude lower than for $[CH_3Cbl]$ at these wavelengths, despite rather similar molar absorptivities and theoretical evidence that the Co—S bond in glutathionylCbl has a smaller homolytic dissociation energy (110 kJ mol^{-1}) than the Co—C bond in $[CH_3Cbl]$ (155 kJ mol^{-1}) [7], possibly because of a more efficient radical recombination step. Appending a variety of fluorophores to [NAcSCbl] resulted in up to an order of magnitude increase in the quantum yield, a consequence of an increase in the absorptivity of the complex. That the thiyl radical is a product of the photolysis was demonstrated by radical trapping and EPR analysis. The study also showed that that fluorophores can act as photon antennas to modulate the rate of thiolato-Cbl photolysis.

Diazeniumdiolates (X–NONOates, Fig. 18) are extremely useful as NO precursors in the study of NO-dependent biological process, the importance of which was only appreciated in the late 1980's [539]. Diethylamino-NONOate, DEA-NONOate (X = Et_2N in Fig. 18) reacts directly with $[H_2OCbl]^+$ ($k_{obs} = 3.2 \times 10^{-5}\ s^{-1}$, pH 10.8; 50 μM $[H_2OCbl]^+$, 10 mM DEA-NONOate), with a 1:1.2 stoichiometry to produce nitrosylcobalamin, [NOCbl] and Et_2N–NO [540,541]. The rate-determining step is the decomposition of the initial adduct between DEA-NONOate and Co(III) to [NOCbl] (estimated $k = 0.63\ M^{-1}\ s^{-1}$), Scheme 10.

Interest in the chemistry of azanone (nitroxyl, HNO) arises in part because of its *in vivo* generation from the action of nitric oxide synthases on *L*-arginine, or the oxidation of *N*-hydroxy-L-arginine (see for example [542,543] and references therein), which can lead to nitrosative stress. There is also considerable interest in the use of HNO for therapeutic purposes (for example [544–546]). In aqueous solution, HNO rapidly dimerizes and decomposes to N_2O and H_2O, so studies with HNO are usually performed by using HNO donors such as sodium trioxodinitrate (Angeli's salt, $Na_2N_2O_3$). Between pH 4 and 8 $HN_2O_3^-$ decomposes to HNO and NO_2^-; at lower pH it is primarily an NO donor ([543] and references therein).

HNO reacts with both $[H_2OCbl]^+$ [543] and [Cbl(II)]. Below pH 9.9, $[H_2OCbl]^+$ reacts with $HN_2O_3^-$ to form NOCbl. The reaction is pH-dependent and, after accounting for the ionisation of $[H_2OCbl]^+$

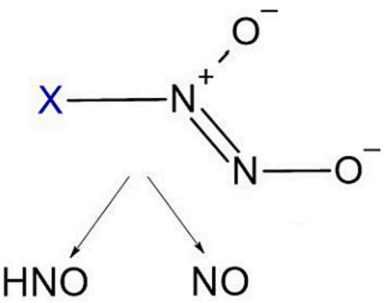

Fig. 18. Diazeniumdiolates (X–NONOates), precursors to NO.

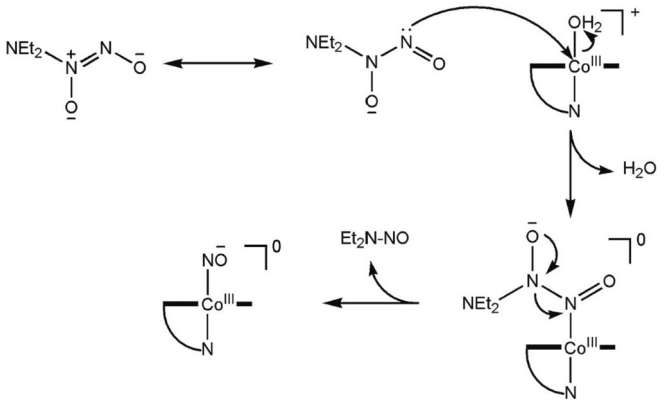

Scheme 10. The reaction of diethylamino-NONOate and $[H_2OCbl]^+$

($pK_a = 7.462(7)$) and $HN_2O_3^-$ ($pK_a = 9.48$), yielded a pH-independent value of $k = 123(5)\ M^{-1}s^{-1}$ for the reaction of $[H_2OCbl]^+$ with $HN_2O_3^-$. The proposed initial product, $[(HONO^-)ON—Co(III)]$ then decomposes to $[NO^-Cbl(III)]$ and NO_2^- [543]. At high pH, the rate determining step becomes the decomposition of $HN_2O_3^-$ to HNO, which then reacts with $[H_2OCbl]^+$, or possibly with [HOCbl], but details of the reaction were not established.

$[H_2OCbl]^+$ will react with nitrosothiols (RSNO) such as S-nitrosoglutathione (SNG) and S-nitroso-N-acetylpenicillamine (SNAP) (Fig. 19) [547]. There is an initial formation of a Cbl(III)–RSNO adduct, bound either through S or N (Scheme 11). The decomposition of the nitrosothiol produces with the thiolatocobalamin or [NOCbl]. The latter is the main cobalamin product (pH 7.4). In route B of Scheme 11, the decomposition of the nitrosothiol occurs via heterolytic S—NO bond cleavage followed by oxidation of a second equivalent of the nitrosothiol [547].

5.2.4. *Reactions with potent oxidants*

Cobalt corrinoids may be destroyed while reacting with potent oxidants such as HOCl [548–550]. The reaction of [CNCbl] with HOCl was reported to be complex [548]; at pH 7 it involves an initial lag phase, the origin of which is unclear, followed by a fairly rapid phase ($k_1 = 0.24\ s^{-1}$ on reaction of 11 μM [CNCbl] with 1 mM HOCl), possibly involving the displacement of bzm trans to CN^- by, surprisingly, Cl^- rather than OCl^- (supported by LC-MS evidence), followed by a slower phase ($k_2 = 0.11\ s^{-1}$ under the same conditions). Both phases increase exponentially with HOCl concentration and are therefore unlikely to be single, simple bimolecular process. This is followed by slow bleaching of the spectrum ($k = 2 \times 10^{-5}\ M^{-1}s^{-1}$), indicative of destruction of the corrin. Complete destruction of the corrin, with release of CN^-, requires a 28 M excess of the oxidant. The liberated CN^- reacts with HOCl to form cyanogen chloride, CNCl. A recent study has provided better insight into the processes involved [551]. In near neutral solutions, [CNCbl] undergoes chlorination of the C10 position and the *c* side chain forms a lactone between C6 and C7. Above pH 9.9, formation of this complex was not observed. The initial reaction involves the rapid formation of an (unidentified) complex between [CNCbl] and HOCl. This complex either rapidly reacts with a second equivalent of HOCl which clorinates the C10 position, or, more slowly, chlorinates C10 directly. Both pathways ultimately lead to formation of [CN-10ClCbl], with a rate law $k_{obs} = k'[HOCl]^2 + k''[HOCl]$. The pH dependence of k' is sigmoidal, varying from ca. $6 \times 10^4\ M^{-2}s^{-1}$ at pH 5.5 to near zero at pH 8.7, with an inflection at ca. 7.5, very close to the pK_a of HOCl which is 7.4 [552]. Clearly, the active reactant is HOCl and not OCl^-. In addition, minor products from destruction of the corrin were also observed. By contrast, [GSCbl] is much more resistant to modification of the corrin on reaction with HOCl [553]; $[H_2OCbl]^+$ is produced, and there is no evidence of chlorination of the corrin ring. It is suggested that HOCl oxidises both the amino and thiol groups of glutathione, which then dissociates from the metal ion.

HOCl rapidly oxidises [Cbl(II)] to form [HOCbl] in alkaline solution with a 1:1 stoichiometry [554]. In the process, $Cl^•$ is produced, which abstracts H from the corrin. This results in the formation of small quantities of corrinoids with two to four H atoms fewer than the parent cobalamin. The presence of [Cbl(II)] prevents HOCl-induced damage to bovine serum albumin, indicating that [Cbl(II)] is an efficient HOCl trapping agent.

The reaction of $[(CN)_2Cbi]$ with HOCl proceeds through the initial sequential displacement of CN^- by OCl^- ($k = 2 \times 10^{-3}$ and $2 \times 10^{-4}\ M^{-1}s^{-1}$, respectively, pH 7.4), followed by destruction of the corrin [549].

The reaction of the carbonate radical, $CO_3^{•-}$, with [HOCbl] between pH 9 and 11.5 occurs in two steps [555]. The first step of the reaction is essentially independent of pH and proceeds with $k_2 = 4.5(2) \times 10^8\ M^{-1}s^{-1}$. The rate of the second reaction is independent of [HOCbl] and increases marginally with pH, from $1.8 \times 10^3\ s^{-1}$ at pH 9.0 to $3.5 \times 10^3\ s^{-1}$ at pH 11.5. The first step is ascribed to H abstraction from multiple sites of the corrin not involved in the π conjugated system. The resulting radical complex undergoes rapid intramolecular transfer of the unpaired electron density to the metal centre for about 50% of these complexes to form the corresponding Co(II) carbocation complex. Subsequent complex and competing pathways lead to formation of corrinoid complexes with two fewer hydrogen atoms, and lactone derivatives.

5.2.5. *Alkylation of Co(II)*

Co(II) corrinoids can be slowly alkylated by direct reaction with alkyl iodides in aqueous solution, but the reactions are considerably faster in the presence of a thiol. Pratt et al. investigated the methylation of cob(II)alamin and cob(II)inamide by CH_3I in the presence of several thiols (dithiothreitol, 2-mercaptoethanol, thioglycolic acid) [556]. Methylation occurred in the order cob(II)inamide + RSH >> cob(II)alamin (with or without RSH) >> cob(II)inamide only (no detectable reaction). There was no detectable formation of Co(I) below the pK_a of the relevant thiol (i.e. the reaction $Co(II) + RSH \rightarrow Co(I) + {}^1/_2RSSR + H^+$ appears to require a significant concentration of RS^- to occur at any appreciable rate). The pseudo first-order rate constant for formation of $[CH_3Cbi]^+$ in the presence of dithiothreitol (DTT) and CH_3I reached a saturating value of $1.8 \times 10^{-2}\ s^{-1}$ at [DDT] > 30 mM and $[CH_3I] > 10$ mM, suggesting that formation of an intermediate, presumably $[RSH—Co(II)—CH_3I]^{2+}$,

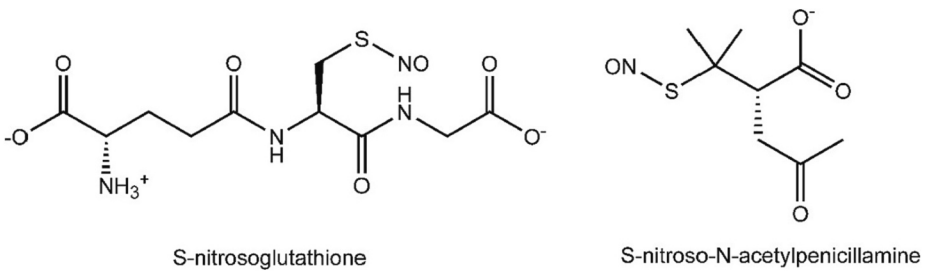

S-nitrosoglutathione S-nitroso-N-acetylpenicillamine

Fig. 19. Examples of nitrosothiols, oxidants of cob(II)alamin.

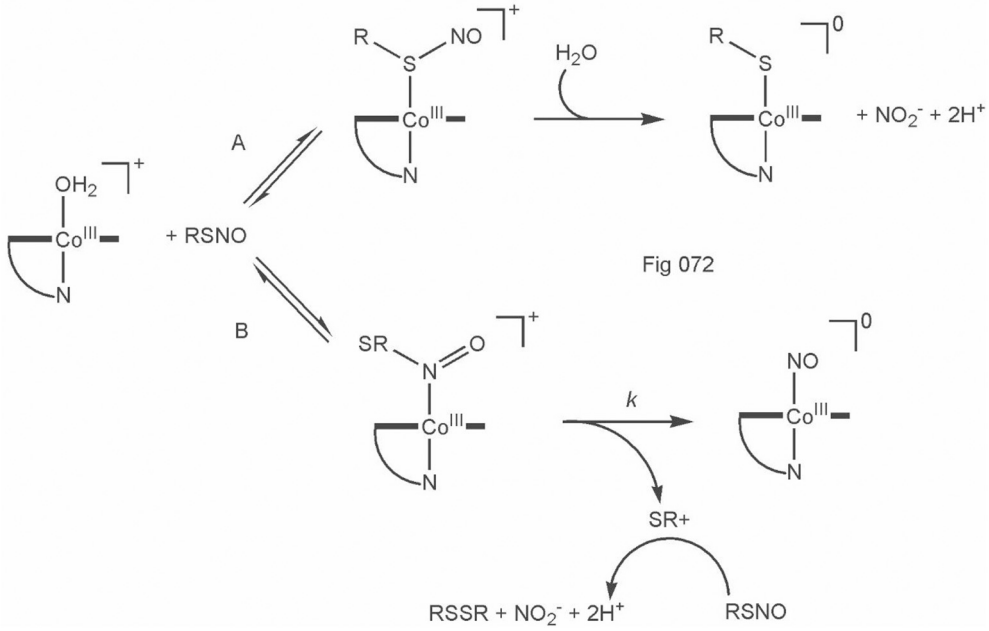

Scheme 11. The possible pathways for the reaction of $[H_2OCbl]^+$ and a nitrosothiol at pH 7.4.

occurs before electron transfer and decomposition into CH_3Cbi, $RS^\bullet$, H^+ and I^-.

Reducing $[H_2OCbl]^+$ with sodium formate in the presence of 4-ethylphenyldiazonium (4-EtPhN_2^+) as the tetrafluoroborate salt, leads to direct alkylation of [Cbl(II)] to produce [β-4-EtPhCbl] [170]. Presumably [Cbl(II)] reduces the diazonium ion with release of N_2 and the phenyl radical then combines with a second equivalent of [Cbl(II)] (Scheme 12). An alternative is to reduce $[H_2OCbl]^+$ to [Cbl(II)] electrochemically, then add the alkylating agent (for example, methyl bromoacetate) to produce [(methoxycarbonyl)methyl]cob(III)alamin) [557].

The crystal structure of [β-4-EtPhCbl], obtained using synchrotron radiation, shows that Co is displaced by 0.03 Å towards the alkyl ligand with a Co—C bond length of 1.981 Å, and a bond of 2.230 Å to the bzm ligand. The axial bond lengths are as expected for alkylcobalamins (see Fig. 6). The arylcorrin is thermally very stable; the pK_a for protonation of bzm is 3.7(1).

If the reaction is carried out in the presence of diphenyliodium chloride (with reduction of $[H_2OCbl]^+$ using either formate or sodium borohydride), both [β-PhCbl] and [α-PhCbl] are produced in 3:1 to 1:1 ratios [174] and they can be separated on a reverse phase column. The reaction of $[Cbl(I)]^-$ with phenylacetylene [133] also produces the two diastereomers of phenylvinylcobalamin; they can also be separated chromatographically (See Section 5.2.7).

Cob(II)inamides react directly with 1,1-dimethylpropyl hydroperoxide by means of a Fenton type reaction [558] to produce a mixture of the diastereomers α- and $[\beta\text{-}CH_3CH_2Cbi]^+$ (Eq. 10) [559].

$$\text{cob(II)inamide} + EtC(CH_3)_2OOH \rightarrow [(OH)(H_2O)Cbi]^+ + EtC(CH_3)_2O^\bullet \text{ (slow)} \quad (10a)$$

$$EtC(CH_2)_2O^\bullet \rightarrow Et^\bullet + CH_3COCH_3 \text{ (fast)} \quad (10b)$$

$$Et^\bullet + \text{cob(II)inamide} \rightarrow \alpha - \text{and } [\beta - EtCbi]^+ \text{ (fast)} \quad (10c)$$

Hence methylation of Co(II) corrinoids can occur by (a) reduction of Co(II) to Co(I) and attack on R—X by the 'supernucleophile' Co(I) (for example, [560]); (b) abstraction of the halide, followed by reaction of the alkyl radical with a second equivalent of Co(II), as demonstrated by Halpern [561]; (c), as demonstrated by Pratt [556], and for which additional evidence has been provided subsequently [562], in the case of a cobinamide, intermediate formation of an adduct between the corrinoid, a thiol and the alkyl halide; and (d) direct reaction with a hydroperoxide via Fenton type chemistry [559].

5.2.6. *Oxidation of Co(II)*

Co(II) corrinoids are readily oxidised to Co(III) by a wide variety of oxidants. The reaction with O_2 proceeds via intermediate formation of coordinated superoxide [563], a species that can be detected by EPR [563–566]. Superoxocobalamin has been crystallised and its crystal structure determined (at 96 K; Co—O = 1.93(1) Å; O—O = 1.32(2) Å; Co—O—O = 120(1)°) [567]. It decomposes to Co(III), H_2O_2 and O_2 (Eq. 11).

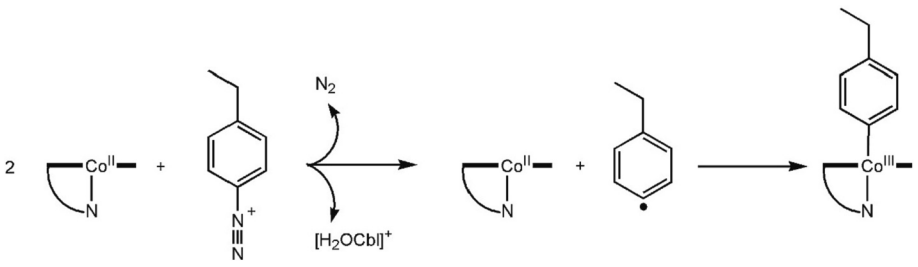

Scheme 12. The alkylation of cob(II)alamin, [Cbl(II)], with a phenyldiazonium cation.

$$[\text{bzm—Co(II)(corr)}] + O_2 \rightleftharpoons [\text{bzm—Co(III)(corr)—}O_2^-] \quad (11a)$$

$$2[\text{bzm—Co(III)(corr)—}O_2^-] + 2H_2O + 2H^+ \rightarrow 2[\text{bzm—Co(III)(corr)—}OH_2]^+ + H_2O_2 + O_2 \quad (11b)$$

Cob(II)alamin reacts rapidly ($k_2 \approx 7 \times 10^8\ M^{-1}\ s^{-1}$) with superoxide to produce H_2O_2 [568,569] (Eq. 12).

$$[\text{bzm—Co(II)(corr)}] + O_2^- \rightleftharpoons [\text{bzm—Co(III)(corr)—}O_2^{2-}] \quad (12a)$$

$$[\text{bzm—Co(III)(corr)—}O_2^{2-}] + 2H^+ + H_2O \rightarrow [\text{bzm—Co(III)(corr)—}OH_2]^+ + H_2O_2 \quad (12b)$$

The reaction of cob(II)inamide, [Cbi] with O_2^- is also fast, with $k_2 = 1.9 \times 10^8\ M^{-1}\ s^{-1}$ [501]. Under the experimental conditions (pH 7.1, 37 °C) the trans ligand is presumably H_2O. Under the same conditions, the reaction with cob(III)inamide, (i.e., predominantly with $[AHCbi]^+$ since the $pK_a = 5.91$ [570]) is also fast with $k_2 = 1.1 \times 10^8\ M^{-1}\ s^{-1}$.

Cob(II)alamin reacts with H_2O_2 to produce [HOCbl] and the hydroxyl radical $OH^\bullet$ which destroys the corrin [470]. In the presence of glucose and glucose oxidase, $[H_2OCbl]^+$ is reduced to [Cbl(II)] (pH 6.3, 37 °C), but with bleaching of the spectrum. Since catalase prevents this, it appears that the system generates H_2O_2 which destroys the corrin [571].

A recent investigation [513] of the reaction of [Cbl(II)] and H_2O_2 showed the reaction proceeded in two steps, the second of which led to bleaching of the spectrum. The rate constant for the first step is 2.63 (5) $\times 10^2\ M^{-1}\ s^{-1}$. The products of this step were identified (on addition of excess cyanide) to be $[(CN)_2Cbl]^-$, and the stable yellow corrinoids shown in Fig. 17, now in an approximate ratio of 4:3:2. The addition of DMSO, isopropanol and *D*-ribose, all hydroxyl radical traps, did not affect the yield of $[(CN)_2Cbl]^-$ and the stable yellow corrinoids; hence reaction with $OH^\bullet$ is not the only mechanism for producing stable yellow corrinoids. Oxidation of [Cbl(II)] with tertiary-butyl hydroperoxide (in the ratio of 1:2) forms $[H_2OCbl]^+$ in 80% yield, with a rate constant of 87(7) $M^{-1}\ s^{-1}$; there are trace amounts of stable yellow corrinoids, and some destruction of the corrin [513].

Akatov and co-workers [572] have shown that [HOCbl] (or, more likely, $[H_2OCbl]^+$) enhances the cytotoxicity of diethyldithiocarbamate (DDC, $Et_2NCS_2^-$) in tumor cells in a reaction that is slowed down by catalase. The main product of the reaction of [HOCbl] and DDC is disulfiram $Et_2NCS—S—SCSNEt_2$ and its oxidised forms. A possible mechanism for the reaction is shown in Scheme 13.

Cob(II)alamin is oxidised by $[Co(III)(NH_3)_5\times]^{n+}$ (R = Cl^-, Br^-, I^-, N_3^-, NSC^-, pyrazine) and $[Co(III)(bipy)_3]^{3+}$ to form $[H_2OCbl]^+$ and the corresponding Co(II) inorganic complex [573], which rapidly hydrolyses in aqueous solution. $[Co(III)(bipy)_3]^{3+}$ must necessarily effect electron transfer through an outer sphere mechanism. The oxidation by $[Co(III)(NH_3)_5I]^{2+}$ occurs through an iodide-bridged transition state. This may also apply to the other halide complexes. When X = NSC^- the reaction is independent of pH ($k_2 = 55(5)\ M^{-1}\ s^{-1}$); with X = halide or N_3^-, and for reaction with $[Co(III)(bipy)_3]^{3+}$, the rate decreases with pH. For example, for X = Br^-, $k_2 = (93(28) + 47(1)[H^+]^{-1})\ M^{-1}\ s^{-1}$. Since the pK_a for bzm in [Cbl(II)] = 2.9 [116], this suggests that the base-on form of [Cbl(II)] is the better reductant. The rate constants for the reaction of base-on [Cbl(II)] with X = Cl^-, Br^-, N_3^- and for the reaction with $[Co(III)(bipy)_3]^{3+}$ are (25 °C) 3×10^2, 4×10^4, 5×10^2 and $40\ M^{-1}\ s^{-1}$, respectively.

Other oxidants of Co(II) include sodium nitroprusside (Na_2[Fe(II)

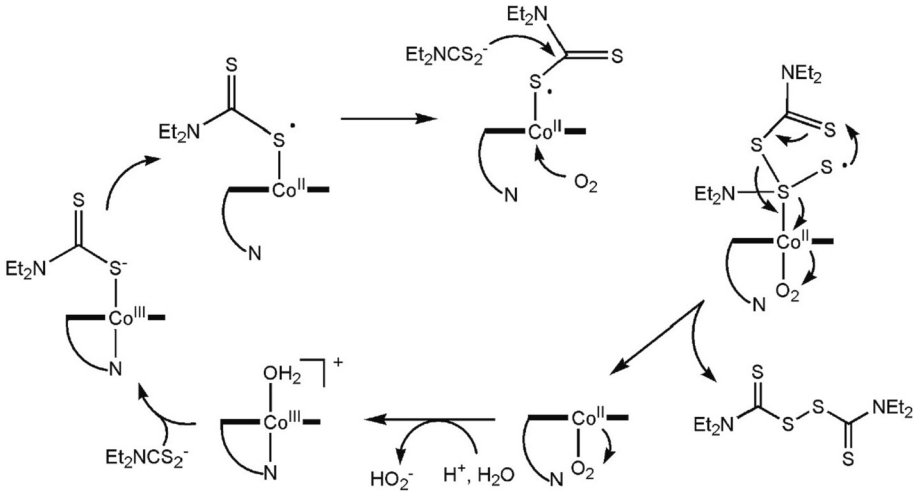

Scheme 13. Proposed scheme for the catalytic oxidation of diethyldithiocarbamate by $[H_2OCbl]^+$ (or [HOCbl]). The H_2O_2 produced probably reacts with Cbl(II), generating ROS that oxidise disulfiram.

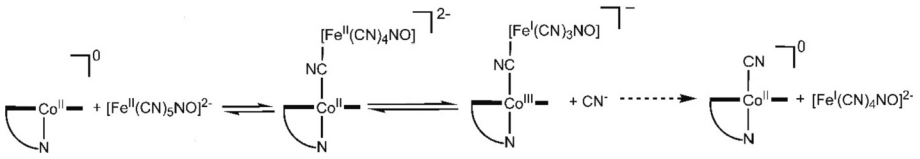

Scheme 14. The reaction between [Cbl(II)] and the nitroprusside anion.

$(CN)_5NO]$), peroxynitrous acid (ONOOH), NO_2, nitroxyl (azanone, HNO), periodate, and the carbonate radical anion $CO_3^{\bullet-}$. The reaction with nitroprusside proceeds through an initial complexation of [Fe(II)$(CN)_5NO]^{2-}$ by Co(II) and inner sphere electron transfer with release of CN^-. This then produces [CNCbl] (Scheme 14) [574].

At pH 1, SO_2 reacts with [Cbl(II)] to form the (protonated base-off) $[^-SO_2Cbl(III)]^{2+}$ complex [575] which then reacts with a second equivalent of SO_2 to produce $[^-S_2O_4Cbl(III)]^{2+}$.

The final product of the reaction of periodate with [Cbl(II)] between pH 10.1 and 12.3 is $[H_2OCbl]^+$, and there is no modification of the corrin [576]. The reaction is first order in $[IO_4^-]$ and [Cbl(II)] with a $[IO_4^-]$:[Cbl(II)] stoichiometry of 1:2. The reaction rate increases with a decrease in pH, and in the pH range of the study, the probable oxidants of [Cbl(II)] are $H_4IO_6^-$, $H_3IO_6^{2-}$ and $H_2IO_6^{3-}$. The rate constants for the reaction of [Cbl(II)] with the first two species (25 °C) were found to be $1.2(1) \times 10^8$ and $8(1) \times 10^4\ M^{-1}\ s^{-1}$, respectively. The rate constant for the reaction with $H_2IO_6^{3-}$ was indistinguishable from zero within the uncertainty of the experimental data. The proposed mechanism of the reaction within the pH range investigated envisages the formation of an iodine(VI) radical as an intermediate (Eq. 13).

$$Cbl(II)] + H_4IO_6^- \ (\text{or } H_3IO_6^{2-}) \rightarrow [H_2OCbl]^+ + H_2IO_5^{2-\bullet} \quad (13a)$$

$$Cbl(II)] + H_2IO_5^{2-\bullet} \rightarrow [H_2OCbl]^+ + IO_3^- \quad (13b)$$

A detailed account of the reaction of [Cbl(II)] and $[Cbl(I)]^-$ with HNO, which arises from the decomposition of Piloty's acid, PA, $PhSO_2NHOH$, has appeared [577]. At pH 10, the rate-determining step is the decomposition of PA, and this results in the clean oxidation of [Cbl(II)] and formation of [NOCbl]. Since the reaction stoichiometry is 2PA:[Cbl(II)], the reaction must involve multiple steps. It was suggested that HNO reduces [Cbl(II)] to $[Cbl(I)]^-$, producing $NO^\bullet$. $[Cbl(I)]^-$ then reduces a second equivalent of HNO, and the [Cbl(II)] thus produced reacts rapidly with $NO^\bullet$ to form the observed product, [NOCbl], with N_2 as a likely byproduct. To determine the feasibility of $[Cbl(I)]^-$ as an intermediate, its reaction with PA was examined under anaerobic conditions. This showed that $[Cbl(I)]^-$ indeed reacts with HNO, producing [Cbl(II)], and ultimately [NOCbl], with the decomposition of PA the rate determining step.

5.2.7. *Reactions of Co(II) with oxides of nitrogen*

The ability of cob(II)alamin to react with a wide variety of species that are responsible for nitrosative and oxidative stress confers on it antioxidant properties which may be important in biological systems [578]. The reaction between [Cbl(II)] and NO has received considerable attention because of the importance of NO in biology. Cobalt corrinoids are important in the inhibition of nitric oxide-induced physiologies and pathologies (for example [579–587]). NO inhibits methionine synthase and methylmalonyl-CoA mutase in mammals, probably by formation of [NOCbl], by reacting with both $[Cbl(I)]^-$ (the active form of cobalamin in the methyl transfer reaction) and [Cbl(II)] (which occurs when $[Cbl(I)]^-$ is oxidised and an S-adenosyl methionine-dependent pathway is required to restore function (Scheme 2) [588–591]. An N_2O-dependent inactivation mechanism is also possible [592,593]. NO will bind to [Cbl(II)] but will not displace H_2O from $[H_2OCbl]^+$ [594].

[NOCbl] (variously referred to as nitroxylcobalamin, nitrosylcobalamin and nitrosocobalamin) is air-sensitive and will react with O_2 to form $[NO_2Cbl]$ and $[H_2OCbl]^+$ via a Co(III) peroxynitrito

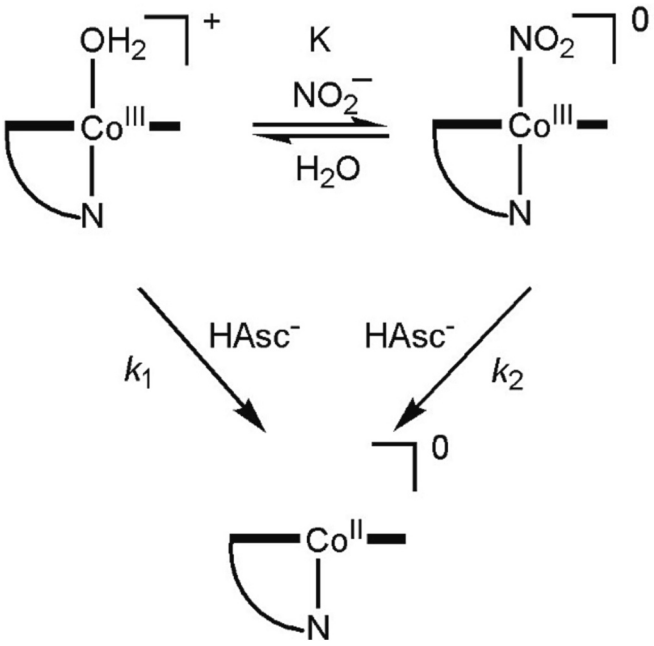

Scheme 15. The reaction of $[H_2OCbl]^+$ with ascorbate.

intermediate, $[ONO_2Cbl]$ [595]. Only base-on [NOCbl] reacts with O_2 and rates approach zero at low pH, i.e., the reaction requires a strong σ donor ligand. (This is corroborated by a recent study that shows that nitrosylcobinamide, where, given the strong trans influence of NO, the trans coordination site is occupied by water and a significant fraction of the complex is five coordinate, is much more resistant to aerobic oxidation, while introducing trans ligands such as imidazole or cyanide increases the rate of oxidation [596]). Correction of the apparent second order rate constants for the reaction between O_2 and [NOCbl] for the base-on/base-off equilibria of the reactant and product) leads to a rate constant of $9.3(2) \times 10^2\ M^{-1}\ s^{-1}$ at 25 °C, with $\Delta H^{\ddagger} = 29(1)$ kJ mol^{-1} and $\Delta S^{\ddagger} = -94(4)\ J\ K^{-1}\ mol^{-1}$, and an apparent equilibrium constant for the reaction of $\log K = 3.21(8)$.

The structure of [NOCbl] was determined on three different crystal batches [183]. The Co—N—O bond angle (119.4—120.3°) is consistent with a Co(III)—NO^- complex with a lone pair on N and the N—O bond length (1.12—1.14 Å) is consistent with a N═O bond. This confirms an earlier report that surface-enhanced Raman scattering (SERS) shows a significant change on adding NO to [Cbl(II)], consistent with reductive nitrosylation [591]. The Co—N_{bzm} bond length is remarkably long (2.32–2.35 Å), consistent with the strong σ donor (and moderate π acceptor) properties of NO^-. The strong trans influence of NO^- is also manifested in a high value of $pK_{base\text{-}off} = 5.1$.

$[NO_2Cbl]$ reacts with ascorbate ($HAsc^-$, pH 7.2, 25 °C), to produce [Cbl(II)] under anaerobic conditions [597,598]. In the system, $[H_2OCbl]^+$ and $[NO_2Cbl]$ are in equilibrium ($\log K = 5.3$), and reduction of $[H_2OCbl]^+$ proceeds over 100 times faster than reduction of $[NO_2Cbl]$ (Scheme 15), with $k_1 = 17.3(4)\ M^{-1}\ s^{-1}$ (in reasonable agreement with a value of $24\ M^{-1}\ s^{-1}$ reported previously [470]) and $k_2 = 0.13(1)\ M^{-1}\ s^{-1}$. At pH < 5, where ascorbate is present as H_2Asc and $HAsc^-$, and

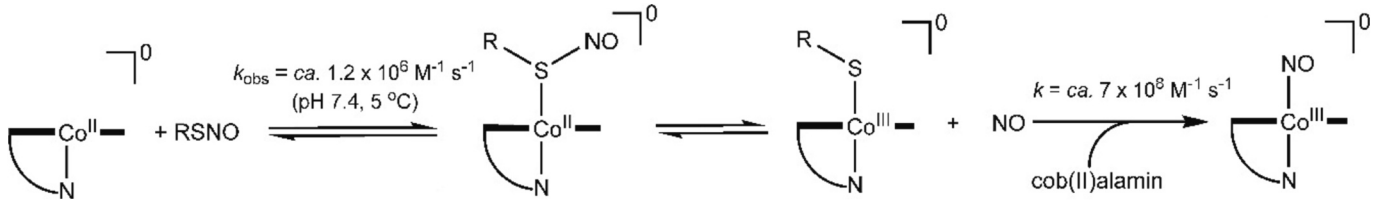

Scheme 16. The oxidation of cob(II)alamin by S-nitrosogluthanione (SNG) through an inner sphere electron transfer mechanism leading to the formation of nitrosylcobalamin.

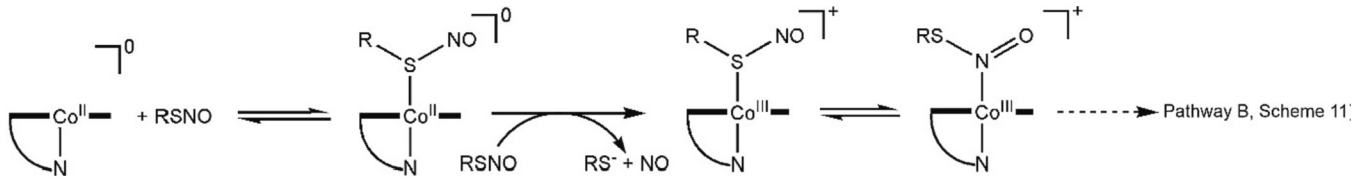

Scheme 17. The oxidation of cob(II)alamin by and S-nitroso-N-acetylapenicillamine (SNAP) through an outer sphere electron transfer mechanism.

is therefore a significantly weaker reductant, the reaction proceeds differently. $[H_2OCbl]^+$ and NO_2^- (which are in equilibrium with $[NO_2Cbl]$) are reduced by $HAsc^-$ to [Cbl(II)] and $NO^\bullet$ which combine to produce [NOCbl].

Cob(II)alamin is oxidised to Co(III) on reaction with nitrosothiols (RSNO) such as S-nitrosogluthanione (SNG) and S-nitroso-N-acetylapencilillamine (SNAP) (Fig. 19) [547]. The reaction with SNG is thought to proceed through initial formation of the S-bound nitrosothiol. This significantly lowers the Co(III)|Co(II) couple from 0.16 V (vs SHE) to ≈ −0.78 V, enabling oxidation of Co(II) to Co(III) bound to a thiolate, and release of NO. NO reacts rapidly with cob(II)alamin to form nitrosylcobalamin (Scheme 16).

At least under the conditions where the reaction of cob(II)alamin with SNAP was studied [547], the dependence of the reaction rate on $[SNAP]^2$ indicates that the oxidation of the metal proceeds through an outer-sphere mechanism (Scheme 17), rather than the inner sphere mechanism of Scheme 16). The oxidised product may rearrange to the N-bound nitrosothiol and produce nitrosylcobalamin and RSSR (as in pathway B of Scheme 11). The termolecular rate constant (25 °C, pH 7.4) for the process that leads to formation of SNAP bound to Co(III) is $1.5(3) \times 10^4\ M^2\ s^{-1}$ [547].

The reaction with nitrite will also oxidise Co(II) to Co(III) [440], apparently due to decomposition of HNO_2 to NO^+ and NO_2^-; NO^+ oxidises cob(II)alamin to cob(III)alamin, producing NO which itself does not react with $[H_2OCbl]^+$ (see Section 5.2.2) [531].

The rapid reaction of [Cbl(II)] with NO_2 ($k = 3.5 \times 10^8\ M^{-1}\ s^{-1}$) produces $[NO_2Cbl]$ [599]. ONOOH reacts with Co(II), forming [HOCbl] and NO_2, and NO_2 then reacts with Co(II) to produce $[NO_2Cbl]$. The rate-determining step is oxidation of [Cbl(II)] by ONOOH to [HOCbl] ($k = 3.70 \times 10^5\ M^{-1}\ s^{-1}$ at pH 7.4) [600].

HNO can be generated in situ from the decomposition of trioxodinitrate (sodium trioxodinitrate, Angeli's Salt, $Na_2N_2O_3$). HNO reacts with cob(II)alamin in an overall 2:1 ratio [601]. Cob(III)alamin was shown not to be an intermediate. Hence the first step is proposed to be the reduction of Co(II) to Co(I), which produces NO. Co(I) is then oxidised by HNO to form Co(II) and N_2, while the NO of the first step reacts with Co(II) to form [NOCbl]. The rate-determining step is the decomposition of $HN_2O_3^-$ (Eq. 14).

$$HN_2O_3^- \rightarrow HNO + NO_2^- \quad (14a)$$

$$Co(II) + HNO \rightarrow Co(I) + NO + H^+ \quad (14b)$$

$$Co(I) + HNO + H^+ \rightarrow Co(II) + {}^1/_2\ N_2 + H_2O \quad (14c)$$

$$Co(II) + NO \rightarrow [NOCbl] \quad (14d)$$

The overall reaction stoichiometry is therefore given by Eq. 15.

$$2Co(II) + 4\ HN_2O_3^- \rightarrow 2[NOCbl] + 4NO_2^- + N_2 + 2H_2O \quad (15)$$

The reaction of $ONOO^-$ with CO_2 produces the nitrosoperoxycarbonate anion $ONOOCO_2^-$; homolytic cleavage of the peroxo bond generates the carbonate radical anion $CO_3^{\bullet-}$ [602]. Brasch and coworkers [555] used pulse radiolysis methods to study the reaction of $CO_3^{\bullet-}$ with cob(II)alamin. It reacts rapidly with Co(II) to produce [HOCbl] ($k = 2.0 \times 10^9\ M^{-1}\ s^{-1}$) (Eq. 16).

$$[Cbl(II)] + CO_3^{\bullet-} + H_2O \rightarrow [HOCbl] + HCO_3^- \quad (16)$$

Subsequent slower reactions produce modified corrinoids after H-atom abstraction by $CO_2^{\bullet-}$.

Co(II) will reduce dehydroascorbic acid (DHA) to the ascorbyl radical in the presence of a thiolate such as cysteine [603]. It is thought that the initial step of the reaction is formation of the (5 coordinate) thiolato complex, with displacement of bzm. DHA then interacts with this complex – either by (weak) coordination to the vacant coordination site or in an outer sphere complex – and is reduced to the ascorbyl radical, leaving a thiolato complex of Co(III), which may hydrolyse to $[H_2OCbl]^+$. The ascorbyl radical disproportionates to ascorbate and dehydroascorbate.

5.2.8. Reactions of Co(I)

Cob(I)alamin, $[Cbl(I)]^-$, is an exceptionally strong nucleophile (nucleophilicity $n = 14.4$ on the Pearson scale [385]). Other Co(I) corrinoids are also powerful nucleophiles; for example, the methylation of some Co(I) corrinoids by methyl transfer from methanol and dimethylaniline has been reported [604].

Theoretical calculations (CASSCF/CASPT2 [245]; CASSCF/MC-XQDPT2 [306]) suggest the ground state wavefunction of $[Cbl]^-$ is an admixture of d^8 Co(I) and d^7 Co(II)/corrin π radical, the contribution of each configuration depending on the level of theory used [245,306]. The significant destabilisation of $3d_z^2$ as well as the partial biradical nature of the Co(I) state may be an important reason for its high reactivity, often referred-to as its 'supernucleophilicity'.

$[Cbl(I)]^-$ will complex H^+ in acid media ($pK_a \approx 1$ [238,605], or 1.5 [442]), to form hydridocobalamin [HCbl(I)], which decomposes to cob(II)alamin with evolution of molecular hydrogen.

$[Cbl(I)]^-$ reacts with simple alkyl halides such as methyl iodide [606] or a trimethyl sulfur derivative such as trimethylsulfoxonium iodide, $[(CH_3)_3SO]I$ [607] to produce almost exclusively $[CH_3Cbl]$ with the methyl ligand occupying the β coordination site. However, its

reaction with some electrophiles such as phenylacetylene [133] produces two isomers of phenylvinylcobalamin, with the organic ligand either in the β or in the α coordination site, which can be separated chromatographically. The β isomer has been crystallised and its structured determined by x-ray diffraction [133].

The strong nucleophilicity of $[Cbl(I)]^-$ allows it to readily react with oxides of nitrogen. The reaction with NO_2^- yields NH_2OH as product [608]. The dependence of the kinetics on pH indicates that HNO_2 ($HNO_2|N_2\,E = 1.45$ V, pH 0) and not NO_2^- ($NO_2^-|N_2\,E = 0.41$ V, pH 14,) is the oxidant. At pH 7, $k_{app} = 1.7 \times 10^3\ M^{-1}\ s^{-1}$. Fitting the observed rate constant to the experimental data between pH 10.7 and 6.5, assuming that only HNO_2 reacts with $[Cbl(I)]^-$, gives a pH-independent second order rate constant $k_2 = 1.15(8) \times 10^7\ M^{-1}\ s^{-1}$. It was proposed that the rate determining step in the reaction is a 2e oxidation of Co(I) to $[H_2OCbl]^+$, producing HNO. This rapidly oxidises a second equivalent of Co(I) to $[H_2OCbl]^+$, producing NH_2OH. Co(III) and Co(I) comproportionate, giving cob(II)alamin as the observed product. Overall, 4 equivalents of Co(I) react with one equivalent of HNO_2 (Eq. 17), and the overall reaction is given in Eq. 18 [609].

$$2H^+ + HNO_2 + [Cbl(I)]^- \rightarrow [H_2OCbl]^+ + HNO\ (\text{rate determining}) \quad (17a)$$

$$HNO + 2H^+ + H_2O + [Cbl(I)]^- \rightarrow [H_2OCbl]^+ + NH_2OH\ (\text{fast}) \quad (17b)$$

$$2[Cbl(I)]^- + 2[H_2OCbl]^+ \rightarrow 4[Cbl(II)] + 2H_2O\ \left(k = 3.2 \times 10^7\ M^{-1}\ s^{-1}\right) \quad (17c)$$

$$4[Cbl(I)]^- + HNO_2 + 4H^+ \rightarrow 4[Cbl(II)] + NH_2OH + H_2O \quad (18)$$

$[Cbl(I)]^-$ reacts with NO_3^- under acidic conditions [610] up to neutral pH (but with rates decreasing sharply with increasing pH [608]) in a reaction in which 8 equivalents of $[Cbl(I)]^-$ are oxidised to [Cbl(II)] by NO_3^- (Eq. 19).

$$8[Cbl(I)]^- + NO_3^- + 10H^+ \rightarrow 8[Cbl(II)] + NH_4^+ + 3H_3O \quad (19)$$

The mechanism of the reaction is not well understood. Since the product is NH_4^+ rather than NH_2OH, it appears likely that the first step is a 1e oxidation of $[Cbl(I)]^-$ rather than the 2e oxidation proposed in the reaction with NO_2^-. If (as with HNO_2) the oxidant is HNO_3 ($pK_a = -1.19$), then this leads to a pH-independent rate constant of $3.2 \times 10^5\ M^{-1}\ s^{-1}$ (25 °C, $\mu = 0.11$ M [610]) or $3.9 \times 10^5\ M^{-1}\ s^{-1}$ (25 °C, $\mu = 1.5$ M [608]).

$[Cbl(I)]^-$ is oxidised by both ONOOH and $ONOO^-$ ($k_2 = 1.6 \times 10^8$ and $1.4 \times 10^5\ M^{-1}\ s^{-1}$, respectively) to produce, initially cob(II)alamin and NO_2. This is followed by a number of rapid steps that lead ultimately to the oxidation of 5 equivalents of $[Cbl(I)]^-$ to cob(II)alamin, producing N_2 [611].

One equivalent of hydrogen peroxide or tert-butyl hydroperoxide oxidises two equivalents of $[Cbl(I)]^-$ to [Cbl(II)] with little or no degradation of the corrin [513].

The reaction of ^{15}NO with $[Cbl(I)]^-$ at an electrode surface showed, from a mass spectroscopic analysis of the sampled headspace above the reaction solution, that $^{15}N_2$ and $^{15}N_2O$ are reaction products [591]. This suggests that $[Cbl(I)]^-$ can effect 2e reductions of NO and N_2O, the stoichiometry of which can be written as in Eq. 20.

$$2[Cbl(I)]^- + 2NO + 2H^+ \rightarrow 2[Cbl(II)] + N_2O + H_2O \quad (20a)$$

$$2[Cbl(I)]^- + N_2O + 2H^+ \rightarrow 2[Cbl(II)] + N_2 + H_2O \quad (20b)$$

$[Cbl]^-$ attacks, and is methylated by, $PhNMe_3^+$, a reaction that may be relevant to the formation of [MeCbl] with *N*-methyltetrahedrofolate as methyl donor (see Section 3.1) [612].

The reduction of a variety of substituted hydroxylamine derivatives to the corresponding amine by $[Cbl(I)]^-$ has been reported [613] (Scheme 18).

As with HNO_2 and HNO_3, it is suggested that in the pH range studied (pH 1–2) the reductant is $[Cbl(I)]^-$ (rather than [HCbl(I)]), and the oxidant is the protonated hydroxylamine. In some cases, as with hydroxylamine itself, the reaction is independent of pH. In others, as with $NH(SO_3)OH^-$, the reaction rate depends approximately linearly on $[H^+]$. It was argued that this is a consequence of the protonated form of the oxidant being a better electron acceptor than the unprotonated form, and where the pK_a is below the pH range of the study. The absence of any effect of alcohols (which are efficient traps for putative radical intermediates such as $NH_3^{\bullet+}$) is evidence that the reaction is likely to involve heterolysis of the N—O bond, Eq. 21.

$$[Co(I)]^- + HO\text{—}NHR_2^+ + 2H^+ \rightarrow [H_2OCbl]^+ + NH_2R_2^+ \quad (21)$$

This is followed by comproportionation between $[Cbl(I)]^-$ and $[H_2OCbl]^+$ to yield the stoichiometrically observed two equivalents of [Cbl(II)] per equivalent of hydroxylamine reduced. Rate constants are modest (between about 1 and 50 $M^{-1}\ s^{-1}$) with the notable exception of NH_2OSO_3H ($> 2 \times 10^4\ M^{-1}\ s^{-1}$); this is probably a consequence of $-OSO_3H$ being an exceptionally good leaving group so that nucleophilic attack, assuming that that is indeed the mechanism of the reaction, would involve attack on N rather than O.

The oxides of sulfur are also oxidants of $[Cbl(I)]^-$. In a comprehensive study, Dereven'kov and co-workers explored the oxidation of $[Cbl(I)]^-$ and [Cbi(I)] by $S_2O_3^{2-}$, SO_3^{2-} and $S_2O_4^{2-}$ [614]. Given that $[Cbl(I)]^-$ is most likely 4-coordinate, as expected there was no appreciable difference in the observed reactions rates of these oxidants with the two corrinoids.

The reaction of $[Cbl)]^-$ with $S_2O_3^{2-}$ is pH-dependent and rates → 0 at pH > 8 [614]. The experimental data are well-fitted to an equation that assumes the only oxidant is $HS_2O_3^-$ ($pK_a = 1.74$), and gives a pH-independent rate constant of $6.25(4) \times 10^7\ M^{-1}\ s^{-1}$ (and $5.0(1) \times 10^7\ M^{-1}\ s^{-1}$ for the reaction with [Cbi(I)]). The available evidence is consistent with a reaction that proceeds initially with a 1 e reduction of $S_2O_3^{2-}$ and S—S bond cleavage to produce either HS^- and $SO_3^{\bullet-}$ (or possibly $S^{\bullet-}$) and HSO_3^-. The S-based radical then reacts with a second equivalent of $[Cbl(I)]^-$ to produce SO_3^{2-} (or possibly S^{2-}, which would be protonated, $pK_a > 14$ and 6.9).

The reaction between $[Cbl(I)]^-$ and SO_3^{2-} shows a complex dependence on pH and it is likely that SO_3^{2-}, HSO_3^- and $S_2O_5^{2-}$ are all oxidants of $[Cbl(I)]^-$ [614]. The reactions are fast (10^6 to $10^9\ M^{-1}\ s^{-1}$), and based on the assumption that these are indeed the oxidants, rate constants

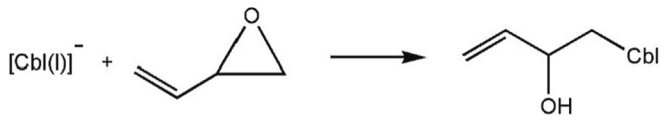

Scheme 19. The reaction of $[Cbl(I)]^-$ with an epoxide

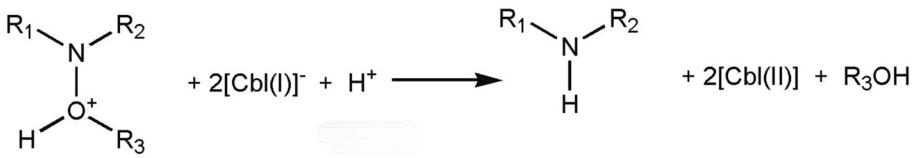

Scheme 18. The reduction of an hydroxylamine to an amine by $[Cbl(I)]^-$ at low pH.

have been estimated.

Dithionite, $S_2O_4^{2-}$, is a powerful oxidising agent that will oxidise [Cbl(I)]$^-$, as will its monomer, $SO_2^{\bullet-}$ [614], Eq. 22.

$$S_2O_4^{2-} \rightleftharpoons 2SO_2^{-} \quad (K = 1.4 \times 10^{-9}\ \mathrm{M}, 25^{\circ}\mathrm{C}) \tag{22a}$$

$$S_2O_4^{2-} + [\mathrm{Cbl(I)}]^- \rightarrow S_2O_4^{3-} + [\mathrm{Cbl(II)}] \tag{22b}$$

$$S_2O_4^{3-} + [\mathrm{Cbl(II)}] \rightarrow [SO_2\mathrm{Cbl}]^- + SO_2^{2-} \tag{22c}$$

$$SO_2^{-} + [\mathrm{Cbl(I)}]^- \rightarrow [\mathrm{Cbl(II)}] + SO_2^{2-} \tag{22d}$$

Sulfoxylate, SO_2^{2-}, (and its protonated species SO_2H^-, $S(OH)_2$) will reduce [Cbl(II)] and $[SO_2Cbl]^-$ to [Cbl(I)]$^-$, Eq. 23. The rate constants for the reduction reactions have been determined at pH 10 and, for the oxidation reactions, at pH 13 [511,614].

$$[SO_2\mathrm{Cbl}]^- + SO_2^{2-} \rightarrow [\mathrm{Cbl}(I)]^- + 2SO_2^{-} \tag{23a}$$

$$[\mathrm{Cbl(II)}] + SO_2^{2-} \rightarrow [\mathrm{Cbl}(I)]^- + SO_2^{-} \tag{23b}$$

The strong nucleophilicity of [Cbl(I)]$^-$ enables it to displace a halide from an alkyl halide to produce an alkylcobalamin, [Cbl(I)]$^- + RX \rightarrow [RCbl] + X^-$. The reaction with the artificial sweetener sucralose [615] is an example of such a reaction. The nucleophilicity of [Cbl(I)]$^-$ also permits it to react with epoxides (an example is shown in Scheme 19) [616].

The reaction of [Cbl]$^-$ with HNO, obtained from the decomposition of Piloty's acid, was discussed in Section 5.2.5.

The deleterious effects of mercury on human health are well known [617–619], as indeed is the role played by [MeCbl] in the methylation of mercury [620–624]. Ag(I) can remove CN^- and Hg(II) can remove an alkyl group from Co(III) corrinoids [625]. The transfer of a methyl group from a methylcobamide to mercury is thought to proceed by transfer of a CH_3^+ cation, as is usually found for the cobalamin-dependent methyltransferases [19]. Zhou et al. [626] used DFT methods (BP86-D with the SDD ECP and basis set for Hg, 6–311++G(d,p) basis set for all other atoms) to examine the ligand exchange reaction between a model corrinoid (all side chains truncated to H; $C_2H_5S^-$ as axial ligand to model Cys) and $(Et)_2Hg$. Their calculations showed that the reaction proceeds in a step-wise manner, with initial cleavage of the Co—C bond, and that the transfer of both a methyl radical and a methyl carbanion to the Hg(II) substrate is feasible, but carbanion transfer is energetically more favourable. In sharp contrast, Kozlowski and co-workers [627], incorporating spin-orbit coupling effects in their calculations, found that the exchange of CH_3 bound to a model Co(III) corrinoid (also with all side chains truncated to H and either imidazole or Cys as axial ligand) and CH_3S^- in $Hg(SCH_3)_2$ (modelled with SO-ZORA/BP86-D3/TZ2P, COSMO/H_2O) proceeds through a single transition state in a concerted manner. The exclusion of relativistic effects (BP86-D3/TZ2P, COSMO/H_2O) produced a rather different potential energy surface (PES) consistent with the initial heterolytic cleavage of the Co—C bond to produce CH_3^-. The main difference between the PES where the axial base is Cys and where it is His is that the transition state in the first case occurs at a significantly lower energy than in the second. The difference between the predicted mechanism with and without relativistic effects was found to lie in the electronic structure of Hg(II). The 6 s orbital decreases in energy and the 6p orbitals split into two spinors. They mix, and accommodate the CH_3 and two SCH_3 moieties in a T-shaped structure. The absence of relativistic effects makes the 6p orbitals inaccessible in the transition state; CH_3S^- is then released and the reaction proceeds in an energetically less favourable concerted manner.

5.2.9. Catalysis

The cobalt corrinoids have been used for a variety catalytic applications [7,34,628,629], including, for example, the photochemical deprotection of allyloxyarenes [630]; the dehalogenation of mono-and polyhalogenated compounds [631–637]; the hydrogenation of alkenes and alkynes [638]; the fluoroalkylation of heteroarenes [639]; the formation of alkyl radicals from strain-release reagents via intermediate formation of a Co(III)-alkyl complex followed by light-induced homolytic cleavage of the Co—C bond [155]; radical C—C bond forming reactions [640–643]; and as asymmetric catalysts for, for example, the enantioselective cyclopropanation of alkenes [644], isomerisation of achiral epoxides to optically active allylic alcohols [645,646] and achiral aziridines to optically active allylic amines [647], and the reduction of α,β-unsaturated esters [648]. An understanding of their electrochemical behaviour has permitted their use in a variety of catalytic systems. Corrinoids have been shown to be more robust electrocatalysts than cobalt porphyrins as the latter are comparatively rapidly oxidised and deactivated [632].

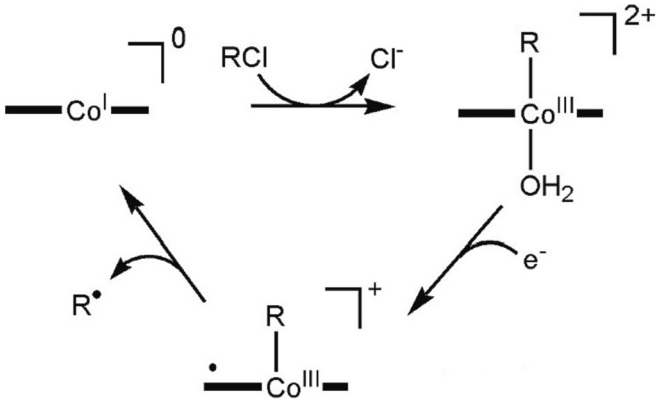

Scheme 20. The catalytic dehalogenation of an alkylhalide by cob(III)ester.

A few examples of the use of corrinoids as catalysts are given below only for the purpose of illustration as recent and comprehensive reviews are available [629,649], including a personal account by Hisaeda and Shimakoshi of their many outstanding contributions in this area [650].

Hisaeda and co-workers [651] studied the electrochemical dechlorination of DDT mediated by heptamethyl cobyrinate (cob(III)ester) on platinum. The reaction presumably proceeds by initial reduction of the Co(III) to Co(I). The formation of an alkylcorrinoid intermediate was shown spectrophotometrically; this decomposed into a Co(I) corrinoid and an alkyl radical as shown by spin trapping with PBN (Scheme 20). A similar reaction with other organic halides has also been reported [652].

The use of B_{12} covalently bound to agarose with a C_8 spacer, and with titanium(III) citrate as bulk reductant for the reductive dechlorination of tri- and tetrachloroethylene, has been reported [653]. The use of an immobilised catalyst makes this a potentially useful system for treatment of chlorinated solvent-contaminated effluent. The reaction with tetrachloroethylene proceeds by two parallel pathways, one involving initial reductive β-elimination to form dichloroacetylene, the other by hydrogenolysis to form initially trichloroethylene (Scheme 21).

The electrocatalytic reduction of vicinal dibromoalkanes by [Cbl(I)]$^-$ to alkenes in room temperature ionic liquids has been reported [654]. The stoichiometry of the reaction is given in Eq. 24.

$$2[\mathrm{Cbl(I)}]^- + \mathrm{RBr_2} \rightarrow \mathrm{alkene} + 2\mathrm{Br}^- + 2[\mathrm{Cbl(II)}] \tag{24}$$

Co(II) corrinoids may be reduced to Co(I) photochemically. Irradiation of $[Ru(II)(bpy)_3]^{2+}$ with sacrificial oxidation of triethanolamine produces $[Ru(I)(bpy)_3]^+$. Since $E^o(Ru(II)|Ru(I)) = -1.11$ V [655], this can reduce cob(II)ester to cob(I)ester ($Co(II)|Co(I) = -0.41$ to -0.37 V [656]). The cob(I)ester dehalogenates an alkyl chloride (such as DDT). Irradiation with visible light produces Co(II) and hence leads to a catalytic system as outlined in Scheme 22 (S = solvent or H_2O; reaction carried out in EtOH); it has a high conversion rate and reasonable turnover number (99% conversion of DDT to a variety of dechlorinated products; TN = 77). A similar system with Rhodamine B as

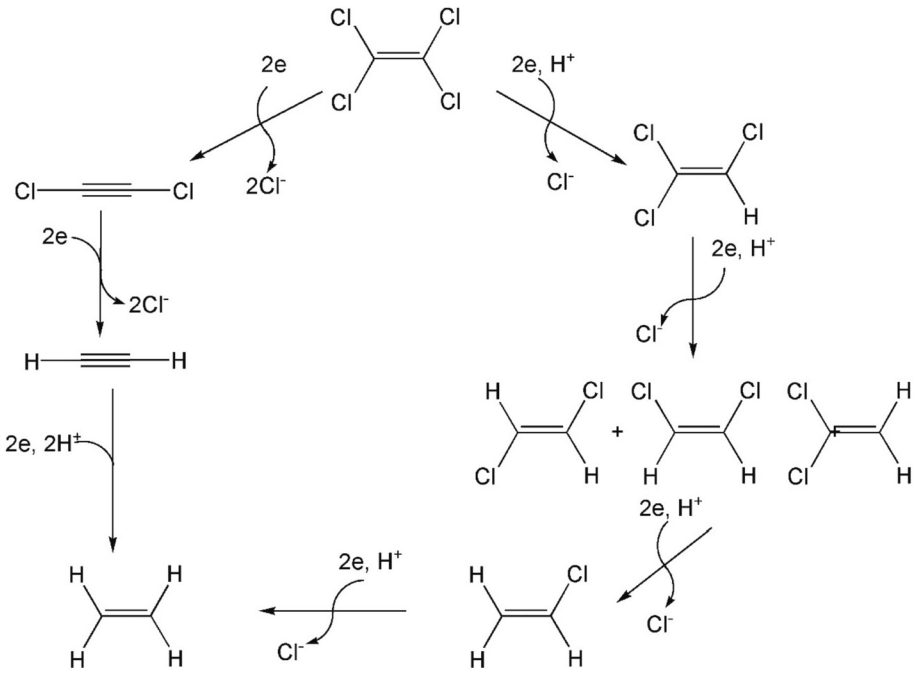

Scheme 21. Dechlorination of tetrachloroethylene by B_{12} immobilised on titanium citrate

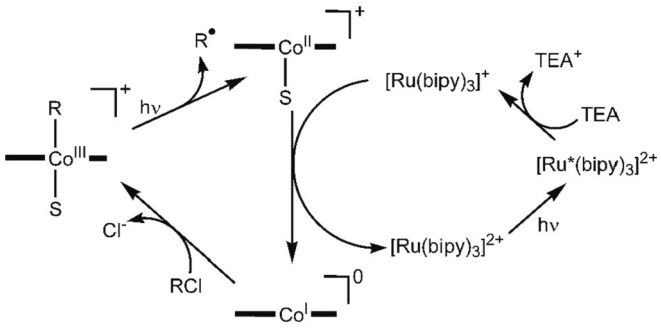

Scheme 22. Photocatalytic dehalogenation of an alkylchloride by a Co(III) corrinoid (S = solvent).

photosensitiser has been reported [657]. Other cobalt corrinoid-based methods for dehalogenation of alkyl halides are known (for example [657–662]).

[CNCbl] is reported to act a water oxidation catalyst (WOC) in sodium phosphate buffer (pH 7) at an overpotential of 0.58 V and with a Faradaic efficiency of 97.5% [663]. The reaction is thought to be initiated by loss of coordinated CN^-, and a proton-coupled oxidation of Co(III) to Co(IV) below pH 7 (to form a Co(IV)—OH^- complex). Above pH 7, the process becomes pH independent (i.e., becomes a simple electron transfer process) between pH 7.5 and 10, with the observed $pK_a \approx 7$ consonant with the pK_a of $[H_2OCbl]^+$ ($pK_a = 7.462(7)$ [111]). Hence in mildly alkaline solution the active catalytic species is [HOCbl] which is oxidised to the Co(IV)—OH^- complex. There is a linear dependence of the catalytic current density on catalyst concentration at the onset potential of 1.20 V (vs Ag|AgCl) in neutral sodium phosphate buffer. The normalised cyclic voltammograms ($j/v^{1/2}$) of the oxidation

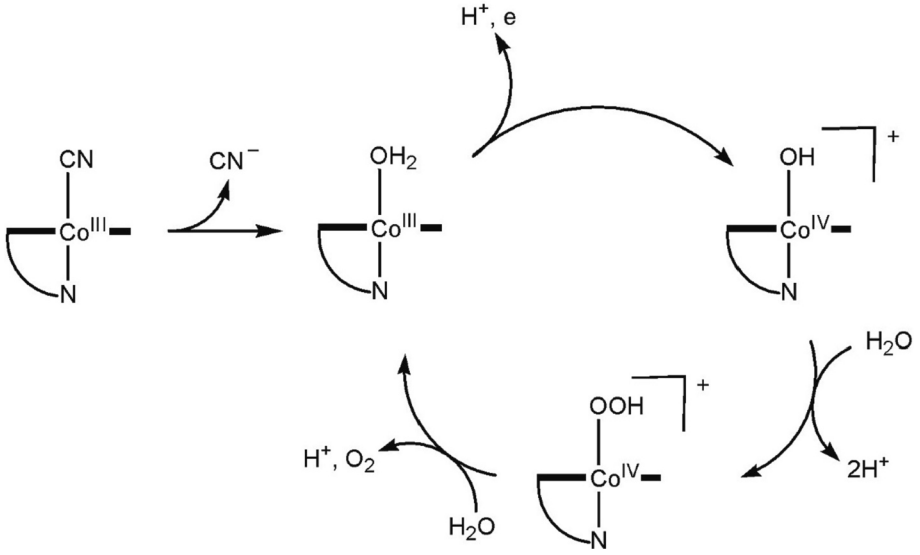

Scheme 23. The water oxidation reaction catalysed by $[H_2OCbl]^+$ derived from [CNCbl].

peak at 1.20 V indicates diffusion-controlled electrochemical behaviour, while the inverse dependence of the normalised current on the scan rate is indicative of catalytic behaviour. It was suggested that the rate-determining step was formation of an O—O bond from coordinated OH^- and a water molecule. Phosphate serves as the proton acceptor in the proton-coupled electron transfer process and so enhances the rate of the oxygen evolution reaction. Importantly, no evidence was found of degradation of the cobalamin after 11 h of controlled potential electrolysis. The assumed reaction mechanism is depicted in Scheme 23.

The mechanism of this reaction has recently been explored using DFT calculations (B3LYP-D3/6-31G(d,p)/SDD(Co)) [664]. There is overall agreement with the general mechanism proposed, including the role of HPO_4^{2-} as proton acceptor. The study does suggest that the corrin ring is a participant in the reaction; the results may not be very reliable, however, possibly because of the functional and/or the basis set used. The DFT energy-minimised structure of $[H_2OCbl]^+$ indicates that H_2O does not coordinate Co(III) and is, instead, hydrogen-bonded to the acetamide of the *c* side chain. The triplet state of $[H_2OCbl]^+$, featuring the metal formally in the +2 oxidation state and a radical on the corrin – which then becomes a participant in the reaction – is found to be lower in energy than the well-established Co(III) singlet state.

In sharp contrast to these results is a recent study on the use of [CNCbl] as a catalyst in oxygen evolution from water using in situ electrochemical liquid transmission electron microscopy (EC-LTEM), EXAFS, XANES and uv−vis spectroelectrochemistry at pH 11 [665]. This study showed that [CNCbl] in fact decomposes on the working electrode (a bare fluorine-doped tin oxide-coated glass slide (FTO)) and that the formation of cobalt oxyphosphate nanoparticles $Co(PO_4)_yO_x$ on the FTO interface in the presence of phosphate buffer is the initial step of the catalytic pathway. Treatment of the FTO with EDTA removes these catalytic entities. The authors of this study concluded that [CNCbl] is in fact unstable under their conditions and decomposes on the electrode surface.

In an interesting, if preliminary, study the Gryko group explored the influence of modifications to the *c* and *d* side chains, and substituents at the C10 position, on the function of the corrinoids as catalysts for C—C bond formation reactions, using the reaction of 1,1-diphenylethylene with ethyl diazoacetate as a model reaction [666]. This is shown in Scheme 24, as is the proposed mechanism.

The substitution of C10H by Br, Cl or NH_2 had little effect on the overall yield of the reaction, but did have a modest effect on the ratio of the final mixture of alkene and alkane produced, i.e., the selectivity of the reaction. Modification of the *c* and *d* side chain substituents had a very significant effect on both the yield and the selectivity of the reaction. The presence of an hydroxyl group in the *c* side chain significantly increased the yield and the selectivity (in favour of the alkene product), suggesting that hydrogen bonding with the reactant promotes the selectivity for the alkene over the alkane. The work emphasises the importance of both steric and electronic effects in the overall course of a cobalt corrinoid-catalysed reaction.

The immobilisation of [CNCbl] on reduced graphene oxide produces a system capable of effecting the electrochemical reduction of CO_2 to CO [667]. While there is clear evidence of the efficacy of the system (at an overpotential of 690 mV, pH 7.2, a Faradaic efficiency of 94.5% was obtained for converting CO_2 to CO with a CO partial current density (j_{CO}) of 6.24 mA cm^{-2} and a turnover frequency of up to 28.6 s^{-1}) the precise mechanism of the reaction was not established, and neither was it established whether the integrity of [CNCbl] on the catalyst was maintained. A similar comment can be made about a study of a catalyst for the reduction of O_2 to H_2O and H_2O_2 at a cathodic surface. The catalyst was prepared by pyrolysing [CNCbl] and carbon black in an N_2 atmosphere at 700 °C for 1 h [668]. This almost certainly led to the destruction of the corrin.

By contrast, [CNCbl] was immobilised on reduced nitrogen-doped graphene under mild conditions (sonication in DMF in an ice bath for 2 h) [669], which suggests the retention of its structural integrity; this

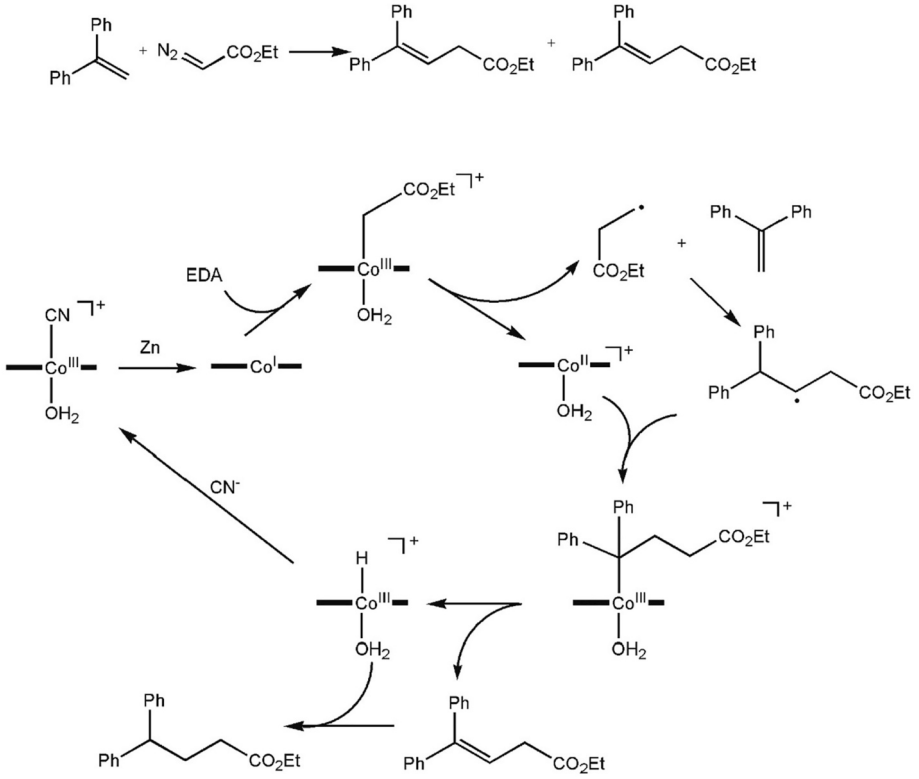

Scheme 24. The reaction of 1,1-diphenylethylene and ethyl diazoacetate (EDA) catalysed by a Co(I) corrinoid, and the proposed mechanism. The starting cobalt corrinoid was aquacyanocobester. The reactions were performed in acetonitrile so the identity of the ligand trans to coordinated alkyls and hydride is uncertain, and the coordination site may be vacant.

was confirmed by uv-vis, Raman and XPS analyses. [CNCbl] is likely to adhere to graphene through π–π interactions as demonstrated with cobalt phthalocyanines [670] and cobalt bis(benzenedithiolate) complexes [671]. Given the steric barriers to interaction between graphene and the corrin, it seems likely that the adherence to the material involves (base-off) bzm, but this was not probed. The [CNCbl]-modified graphene was bound to a glassy carbon electrode using Nafion as a binder. Electrochemical studies of the behaviour of the modified electrode showed it performed well in evolving hydrogen in 0.5 M H_2SO_4 (−0.096 V vs. reversible hydrogen electrode, a low Tafel slope of 60.35 mV/decade – diagnostic of fast electrode kinetics – and an overpotential requirement of a modest −0.210 V for 10 mA cm^{-2}). Co(III) is reduced to Co(I) which then is likely to act as the source of reducing equivalents for the rate-determining step of the hydrogen evolution reaction, $H_{ads} + H_3O^+ + e^- \rightarrow H_2 + H_2O$ (the Heyrovsky reaction). The electrode also performed usefully as an H_2O_2 sensor with a sensitivity of 430 mA mM^{-1} and a detection limit of 20 nM.

6. Photochemistry

Because the Co—C bond of alkylcobalamins is readily cleaved on exposure to light below about 580 nm, and as cleavage of this bond is essential in various catalytic cycles in which the cobalt corrinoids are involved [35], the photolysis of the alkylcorrinoids has been extensively studied using both experimental and theoretical methods [36,672–680]. Moreover, interest in the photochemistry of B_{12} has been heightened with the discovery of light-activated molecular switches [81] and the CarH photoreceptor that regulates carotenoid biosynthesis [377,379] (see Sections 3.5 and 3.6). Cobalamins have also been used for photolysis-mediated drug delivery systems [681]. It is interesting to note that the photolability of a Co—C bond is by no means limited to the alkyl corrinoids. For example, $[Co([14]aneN_4)(OH_2)(CH_3)]^{2+}$ and $[Co[14]tetraeneN_4)(OH_2)(CH_3)]^{2+}$ undergo homolysis with large quantum yields, a process which is virtually wavelength independent [682–684].

Non-alkyl cobalamins, like $[H_2OCbl]^+$ and [CNCbl] are usually photo-stable [678,685], with ultrafast internal conversion to a low-lying state of metal-to-ligand (MLCT) or ligand-to-metal (LMCT) charge transfer character which decays to the ground state with elongation of the axial bonds but without their cleavage [686]. (Dicyanocorrinoids can photogenerate $^1O_2$, which cleaves the corrin ring between C5-C6 and C14-C15 – see Section 5.2.2.) Recovery of the ground state is often within 2–7 ps [679], showing little if any homolysis of the Co—β bond [678], although [HOCbl], when exposed to radiation of <300 nm, produces hydroxyl radicals [687,688]; this has been exploited for the cleavage of super-coiled DNA by $OH^\bullet$. [CNCbl] is reasonably photostable [689] because the S_1 state, the lowest excited electronic state, involves a LMCT with elongation of the Co—C and Co—N_{bzm} bonds (confirmed more recently with XANES [144,690]) with a very low barrier of c. 12 kJ mol^{-1} (predicted to be 20 kJ mol^{-1} from theoretical calculations [686]) for internal conversion to the S_0 ground state [691], but which is sensitive to solvent polarity [692]. $[N_3Cbl]$ and $[H_2OCbl]^+$ exhibit similar behaviour [693]. Prolonged photoirradiation of [CNCbl], $[H_2OCbl]^+$ and [HOCbl] in the presence of ascorbic acid does lead to complete bleaching of the solution, evidence of oxidative cleavage of the corrin [694].

Irradiation of a base-on alkylCbl with uv-vis light rapidly produces an intermediate with a cleaved or weakened bond to the base, followed by homolysis of the Co—C bond. The result is a caged [Cbl(II)]:$R^\bullet$ pair [676,695], and competition between geminate recombination and radical escape determines the photolysis yield. This is dependent on factors such as the presence of species like O_2 that can react with the radical, and cage effects around the caged pair [696]. From flash photolysis experiments of [MeCbl] in deaerated aqueous and isopropanol solutions, the rate constant for recombination of [Cbl(II)] and $CH_3^\bullet$ is ca. $2 \times 10^9\ M^{-1}\ s^{-1}$ [697]. In aerated solutions, $CH_3^\bullet$ reacts rapidly with O_2 ($k_2 = 4.7 \times 10^9\ M^{-1}\ s^{-1}$ [698]) to produced $CH_3O_2^\bullet$ which then reacts with [Cbl(II)] ($k_2 \approx 2.4 \times 10^9\ M^{-1}\ s^{-1}$) to form the peroxo complex $[CH_3O_2Cbl]$ [697].

If the bzm is displaced by H_2O, for example in acidic solution, and as demonstrated with [AdoCbl], [MeCbl] and [propylCbl], the electronic structure of the corrin is altered and a fast non-radiative channel that competes with bond homolysis becomes available [699]. For example, the quantum yield for bond homolysis drops from near unity for [propylCbl] and [AdoCbl] to 0.2 and 0.12, respectively. An EPR study of the photolysis of $[MeCbi]^+$ and $[AdoCbi]^+$ (560–580 nm, 77 K and 300 K, methanol) in the presence of phosphines or pyridines showed that homolysis of the Co—C bond occurs to form the Co(II) species which then reacts with the phophine or pyridine ligands [700].

The fate of the $Ado^\bullet$ radical after photolysis of [AdoCbl] depends on environmental conditions. It can recombine with cob(II)alamin (k_R) or, after cage escape (k_E) and under anaerobic conditions, cyclise to 5′,8-cycloadenosine 8. In the presence of oxygen it produces adenosine 5′-aldehyde and 5′-peroxyadenosine (Scheme 25) [673,677,701–703].

In aqueous solution, $k_R = 1.43(2)\ ns^{-1}$, $k_E = 0.57(6)\ ns^{-1}$ and the quantum yield $\Phi = 0.20$–0.24 [676,704,705]. Cage escape is very dependent on solvent viscosity [706]; in ethylene glycol, for example, $k_E = 0.11(3)\ ns^{-1}$ which reduces Φ to 0.08 [704]. For [AdoCbl], Φ is not very sensitive to the excitation wavelength [707,708].

The intermediates that follow after photoexcitation and before bond cleavage depend on environmental factors. The singlet S_1 state corresponds to a corrin $\pi \rightarrow$ Co $3d_z^2$ LMCT state [143,148]. In aqueous solution, this leads to an intermediate in which the Co—N_{bzm} bond is either

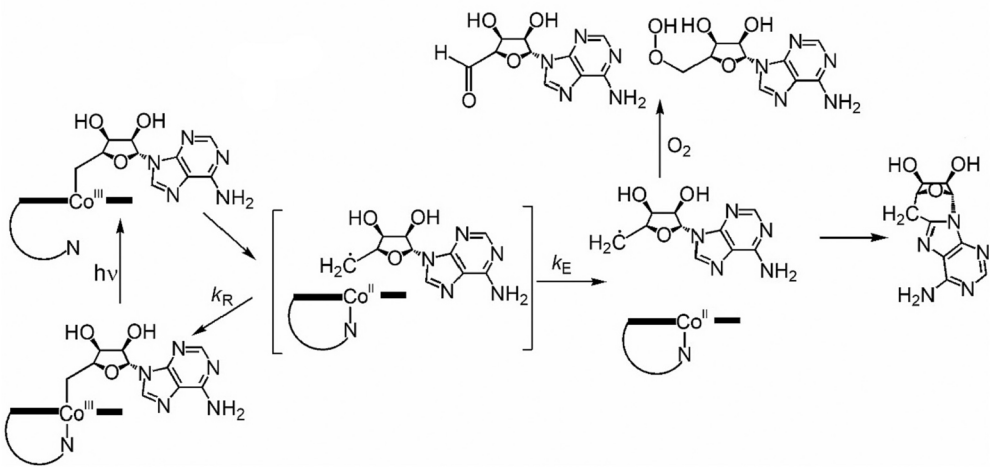

Scheme 25. The fate of [AdoCbl] upon photolysis.

broken or significantly weakened [676,678], whereas in a viscous solvent such as ethylene glycol, production of a caged radical pair proceeds without this intermediate [704]. In a protein environment, such as in glutamate mutase (in which [AdoCbl] is in the base-off/His-on form) the S_1 state appears to arise from a corrin $\pi \rightarrow$ Co 3d $\rightarrow$ Ado MLCT state brought about by mixing of Co 3d and Ado C 2 s and 2p orbitals [692,708]. TD-DFT calculations show there are two minima on the S_1 surface [709]; the first is associated with elongated axial ligands and the second is a MLCT minimum, corresponding to the pre-homolysis species in aqueous solution and the state that is stabilised by the protein environment, respectively.

The quantum yield Φ will decrease with a decrease in the size of the β ligand and with weakening or breaking of the bond to the bzm α ligand as this increases the relative rate of internal conversion to the ground state. Under aerobic conditions the $CH_3^{\bullet}$ radical that results from photolysis of [CH_3Cbl] eventually forms formaldehyde and smaller amounts of methanol, formic acid and CO_2; in the absence of oxygen a mixture of formaldehyde, methane, and ethane, as well as smaller amounts of methanol and formic acid are formed [672].

The response of [CH_3Cbl] to radiation is somewhat different to that of [AdoCbl] and is wavelength dependent [710,711]. The S_1 state is consistent with MLCT and electron density on the CH_3 ligand [675,692,711–714]. It can be accessed with green light (520 nm), resulting in ca. 15% radical pair production while the remainder of the excited state molecules return to the ground state by internal conversion. If blue light (400 nm) is used, then a higher energy state is accessed; 75% decays to the same S_1 state as accessed by green light and 25% produces radical pairs directly, with the additional translational energy mitigating against geminate recombination [35]; hence, unlike for [AdoCbl], Φ for [CH_3Cbl] is wavelength dependent. A similar mechanism is operative in ethyl- and *n*-propylcobalamins as well.

Alkynylcobalamins, with β ligand Co—C ≡ C—R, are very stable against photolysis and thermolysis (for example [170,715–717]), with efficient internal conversion to the ground state. In 4-phenylethylcobalamin, the Co—Ph(4-Et) bond, by contrast, is photolabile, although with $\Phi < 1\%$ [436]. An exploration of the two systems using TDDFT methods (BP86/TZVPP), but with all side chains replaced by H and bzm replaced by imidazole as axial ligand, suggests that while there is a path for radical formation from the S_1 state for [(4-EtPh)Cbl], involving cleavage of the Co—N_{Im} bond, the energetically most favourable path for return of photoexcited Co—C ≡ C–R to the ground state involves internal conversion [718]. A more recent investigation of the factors affecting the photolytic stability of alkynylcobalamins used ultrafast spectroscopic studies to show that the dynamics of the excited state and conversion to the ground state occurs through Co—N_{bzm} vibration and deformations of the corrin, and are the vehicle responsible for ground state recovery within 100 ps [719]. The stability of the Co—C bond of alkynylcobalamins is due to the π orbitals of the axial ligand interacting with corrin orbitals, shortening and stabilising the Co—C bond, a stabilisation that survives photochemical excitation to the S_1 state.

After formation of a radical pair, conversion between a singlet (S) and triplet ($T_{\pm 1}$) radical pair state is possible. Since geminate recombination can only occur from the S state, and since spin-interconversion is magnetic in origin, application of a magnetic field can remove accessibility to the $T_{\pm 1}$ states and hence influence the rate of geminate recombination. These magnetic field effects (MFEs) have been very useful is showing how radical quenching by protein dynamics can contribute to the catalytic power of a cobalamin-dependent enzyme [720]; this has been comprehensively reviewed [721–723].

The combination of a large β ligand and the coordination of an axial base (either bzm or His), preceded by the S_1 state in which bonding to the axial ligands is weakened [35], has clearly primed [AdoCbl] for the formation of radical pairs. A smaller axial ligand such as CH_3, or where the axial ligand is either displaced or only weakly bonding, mitigates against radical pair formation with the formation of an alternate excited state referred to as a Type II MLCT S_1 state, and so avoiding radical chemistry. The sequence of events that follows the absorption of radiation by [AdoCbl] has been elegantly delineated using XANES and broadband uv-vis transient absorption [724]. Initial sequential expansion of the Co—N_{corr} bonds, first along the *y*-direction perpendicular to the transition dipole, and then very soon afterwards along the *x*-direction, is followed by expansion of the axial bonds as the molecule moves out of the Frank-Condon active region of the potential energy surface. This is accompanied by electronic changes and the appearance of a band at 340 nm in the uv-vis spectrum. Intermediates in the photolysis of [CH_3Cbl] using time-resolved XAS have also been observed [725]. The first, in the picosecond time range, also involves marginal relaxation of the corrin and expansion of the Co—C bond. Radical escape leads to $[H_2OCbl]^+$, as expected. Recombination of the radical products, captured in the microsecond time range, sees an intermediate with recombined Co—C bond, and an elongated Co—N_{bzm} bond.

Warncke and co-workers [726] have reported incorporating $[MeCbi]^+$ into the $(\beta\alpha)_8$ TIM barrel protein, EutB, from ethanolamine ammonia lyase and using this as a photocatalyst in a visible-light (520 nm) photosensitizer/sacrificial electron donor system (Eosin Y as photosensitizer and triethanolamine (TEOA) as sacrificial reductant [727]) for production of H_2 from water at neutral pH. The Co(II)|Co(I) couple for a cobinamide, −0.50 V (vs SHE), Fig. 14, is thermodynamically competent to drive the production of water at pH 7 ($2H^+|H_2 = -0.42$ V). Under the conditions used, formation of the Co(I) species, [Cbi(I)], was observed spectrophotometrically. Turnover numbers, however, were low (maximum $4.4 \times 10^{-3}\ h^{-1}$) and 100-fold lower than when using a cobalt dimethylglyoxime complex, $[Co(dmgH)_2pyCl]$ as catalyst. The reaction proceeds by formation of [Cbi(I)] and its protonation to form $[HCbi(I)]^+$, which then acts as the reductant towards H^+ to produce H_2; a number of possible mechanisms for the reduction steps have been proposed [726]. Whilst photoreduction of $[MeCbi]^+$ to [Cbi(I)] clearly occurs, the low pK_a for its protonation (p$K_a = 1$, Fig. 12), is thought to be the reason for the low turnover numbers generated by this as a catalyst in neutral aqueous solution.

In contrast to the alkylcobalamins, comparatively little is known about the photolytic properties of thiolatocobalamins. Early reports suggest that they are photosensitive but provided little information [494,506,560]. A fairly comprehensive study of the photolysis of *N*-acetyl-*L*-cysteine cobalamin, [NAcSCbl], has since appeared [538]. A comparison of the exposure of [MeCbl] and [NAcSCbl] to radation of ≈ 360 nm, pH 5.5, showed that photolysis of [NAcSCbl] to produce $[H_2OCbl]^+$ occurs three orders of magnitude slower than photolysis [MeCbl] with Φ values of approximately 5×10^{-4}, 1×10^{-4} and 2×10^{-5} at 360, 405 and 546 nm, respectively, compared to values of 0.30, 0.30 and 0.15 for [MeCbl] at the same wavelengths, while the molar absorptivities of the two at these wavelengths are comparable. Given that the homolysis bond dissociation energy of, for example, glutathionylcobalamin (110 kJ mol^{-1}) is significantly lower than that of [MeCbl] (155 kJ mol^{-1}) [464,728,729], the comparative resistance of thiolatocobalamins to photolysis is remarkable. Presumably the recombination rate of the radical pair is much more favourable for a thiyl radical than for an alkyl radical. If, however, a fluorophore is appended to the thiolatocobalamin structure (for example, by derivatisation of the 5′-OH ribose group [538]) the rates of photolysis increase by an order of magnitude, largely due to an increase in the molar absorptivity of the compound since values of Φ increase only modestly. In the case of [NAcSCbl] and derivatives containing a fluorophore appended to the ribose, the use of a radical trap (PBN, *N*-tert-butyl-α-phenylnitrone) and EPR showed conclusively that photolysis leads to formation of a thiyl radical [538].

7. Coordination chemistry

The coordination chemistry and the ligand substitution reactions of the Co(III) corrinoids have been studied for many years, with coordination chemists attracted to it very soon after the isolation and

elucidation of the structure of vitamin B_{12} and the realisation that a number of derivatives could be prepared. There are several reasons for this, among them [331] their high molar absorptivity, which means the chemistry can be studied using small volumes (< 2 mL) of low concentration (< 50 μM) solutions by uv-vis spectroscopy; their high solubility in aqueous solution in which (unlike many porphyrins and phthalocyanines [730]) they remain monomeric; the coordination of the equatorial site by a macrocycle which prevents cis-trans isomerisation; being in most cases firmly octahedral complexes, the uncertainty sometimes surrounding the number of ligands bound, inherent in the chemistry of square planar complexes, is avoided; and chemical equilibria that are usually relatively rapidly established. There is one drawback with cobalt corrinoids in which the bzm ligand is absent. If the two axial ligands are not identical, then diastereomers may well occur in solution which may complicate the analysis and interpretation of the experimental results. Equilibrium constants for substitution of a single ligand, such as H_2O in aquahydroxocobinamide ($[AHCbi]^+$) for example, will very often refer to an equilibrium where reactants and products are mixtures of diastereomers. The solution structures of the two diastereomers of Factor B (aquacyanocobinamide, $[ACCbi]^+$) and of aquacyanocobyrinic acid heptamethyl ester, the cobester, $[ACCbs]^+$, have been determined by 2-dimensional ^{13}C and ^1H NMR methods [731]. The same methodology has been applied to a study of the solution structure of dicyanocobinamide and dicyanocobalamin [134].

7.1. Analytical applications

The distinctive uv-vis spectra of the cobalt corrinoids, and other factors mentioned above, have led to methods used for the determination of cobalt corrinoids in a wide variety of samples, and to their application as analytical reagents. Some are mentioned here for illustration. A relatively recent review of optical spectroscopy methods for the determination of B_{12} is available [732].

The cobalt corrinoids have a high affinity for CN^-. For example, log $K = 14.1$ [444] for coordination of CN^- by $[H_2OCbl]^+$, making it an effective antidote against cyanide poisoning [406], although it requires intravenous injection. The final product is $[(CN)_2Cbl]^-$, for which $\varepsilon_{368nm} = 3.04 \times 10^4\,M^{-1}\,cm^{-1}$ [733–735]. Recent work [736] has shown, however, that it is not a simple matter of the corrinoids competing with, for example, cytochrome oxidase for CN^- as they cannot compete with the protein in direct head-to-head competition experiments. That they are demonstrably effective cyanide antidotes means the reactions involved under physiological conditions are much more complex and have yet to be fully understood.

While formation of [CNCbl] from CN^- and $[H_2OCbl]^+$ is quite rapid ($k_2 = 2.36 \times 10^2\,M^{-1}\,s^{-1}$ [519]), the conversion to the dicyano complex is relatively slow ($k_1 = 4.2 \times 10^{-2}\,s^{-1}$ for replacement of bzm by H_2O trans to CN^- which is rate limiting; this is followed by rapid ($k_2 = 8.4 \times 10^4\,M^{-1}\,s^{-1}$) replacement of H_2O by CN^- [737]) albeit with a high affinity (log $K = 8.3$ [737]). $[(CN)_2Cbl]^-$ has a distinctive purple colour, with, as mentioned, $\varepsilon = 3.04 \times 10^4\,M^{-1}\,cm^{-1}$ for the γ band at 367 nm. This provides a convenient and widely-used method for quantification of the concentration of cobalamins in solution, especially in laboratory applications. Reaction with cobinamides are faster because of the absence of bzm, and the use of aquahydroxocobinamide as a cyanide antidote has been suggested [738], as has the use of dinitrocobinamide [407]. The very obvious purple colour of $[(CN)_2Cbi]$ has been exploited to develop fast and reliable indicators for the presence of cyanide in foods such as cassava [395,739–741] and in blood [409–413]. A summary of methods for the determination of B_{12} in foodstuffs is available [742].

An interesting application is the grafting of corrinoids onto a quartz crystal microbalance, used to sense CN^- and SCN^- in solution [743]. Another very common procedure used in the analysis of corrinoids is HPLC (for example [744–749]). An attractive alternative, especially if the corrinoid is unstable under the HPLC conditions commonly used, is to use the distinctive ^1H NMR signals of the aromatic region [750].

A variety of analytical electrochemical methods have been described. A graphene electrode was used to oxidatively decompose B_{12} and oxidise all nitrogen to NO_3^- (1.3 V vs. Ag|AgCl, 15 min); NO_3^- was then determined by reduction at a copper oxide nanocrystal coated graphene electrode [751]. An electrochemical sensor, consisting of Au-SnO_2 nanoparticles electrophoretically deposited on indium tin oxide, and differential pulse voltammetry, was used to electrocatalytically determine B_{12} in solution; the validity of the method was confirmed by analysing the B_{12} content of cow's milk [752]. A voltammetric method for determination of Co(II) in the presence of azo dyes gave comparable results to atomic absorption spectroscopy when applied to the determination of B_{12} in commercial vitamin supplements [753]. There are some unusual applications of corrinoids as analytical reagents. For example, silver nanoparticles functionalised with B_{12} have been used to detect Fe(III) in food samples [754].

The very nucleophilic character of $[Cbl]^-$ has been exploited for the detection of toxic electrophiles such as oxiranes (1,2-epoxides) of alkenes [616,755,756] (Scheme 26). The products are readily detected using LC-MS.

7.2. The corrin macrocycle

As mentioned, a distinctive feature of the cobalt corrinoids is their intense and characteristic uv-visible spectra. While a description of the origin of the spectra is beyond the scope of this review, a few observations are in order since uv-visible spectroscopy has played such a central role in the chemistry of the cobalt corrinoids. Fig. 20 shows three examples, the spectra of $[H_2OCbl]^+$, [MeCbl] and $[SO_3Cbl]^-$.

Species such as $[H_2OCbl]^+$ and [CNCbl] show so-called "typical" spectra with the α band around 550 nm, the β band at around 500 nm, a shoulder towards the higher energy of the β band, the weak D and E bands near 400 nm, and the most intense band in the near uv-vis spectrum, the γ band, at around 350 nm. Soft donor ligands such as CH_3^- and

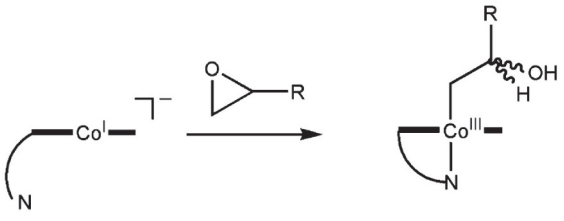

Scheme 26. Exploiting the high nucleophilicity of $[Cbl]^-$ to trap an oxirane.

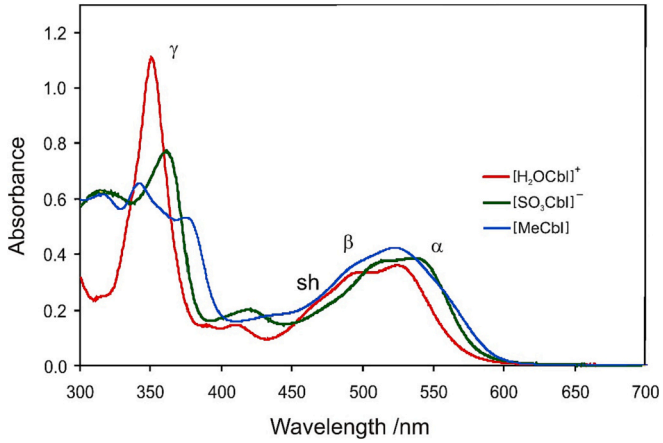

Fig. 20. Representative uv-vis spectra of the cobalamins.

SO_3^{2-} produce "atypical spectra" in which the γ band is red-shifted, split, and appears to be significantly less intense.

The shift of the α, β and γ bands in the spectrum to longer wavelengths [757,758] correlates approximately with the position of the donor atom in the nephelauxetic series [759] (F < O < N < Cl ≈ C < Br < I < S < Se). The correlation is a consequence of the increasing polarizability of the ligands and their donation of charge density to the metal through the σ bond [760].

The uv-vis spectra of eleven cobalamins [XCbl] (X = H_2O, CN^-, CH_3^-, N_3^-, Cl^-, $(i\text{-Pr})_2PO$, *i*-amyl, NO_2^-, SCN^-, $SeCN^-$, SO_3^{2-}) were empirically analysed by fitting the spectra with the minimum possible number of Gaussian functions [761]. The $\alpha\beta$ region could be adequately described by the overlapping of between three and five Gaussians. The γ region was best modelled as the overlapping of three Gaussians which are clearly not a vibrational progression, as proposed by earlier workers [762,763]. This is in agreement with TD-DFT calculations [142] where, for example, the γ region of the spectrum of $[H_2OCbl]^+$ was shown to arise from at least three different electronic transitions. The distinction between the "typical" and "atypical" spectrum of a cobalamin was shown to be arbitrary, as the differences stem from the components that together constitute the "γ-band" moving apart in response of the donation of electron density by the axial ligand. This is a good example of a cis influence in the chemistry of the cobalt corrinoids given that virtually all the prominent electronic transitions that are responsible for the uv-vis spectra of these compounds involve the corrin ligand.

The $\alpha\beta$ region, and the shoulder towards the higher side of the β band, may arise from several transitions [764,765] or predominantly from a vibrational progression of a single electronic transition [766]. Given that the broad structure of this region of the spectrum persists in metal-free corrins [251] and in [Znby] [261] (where Zn(II) replaces cobalt in a cobinamide, section 2.5), the transition(s) clearly have predominantly $\pi \rightarrow \pi^*$ chararcter. A study of the fluorescence of cobalamins with β alkynyl ligands indicates that – at least in the case of these compounds – a vibrational progression of a single excited state accounts for much of the absorption intensity in the $\alpha\beta$ region [767].

TD-DFT methods have been invaluable in providing insight into the electronic transitions responsible for these spectra. Briefly, soft donor ligands increase electron density on the metal ion which raises the energy of the metal 3d orbitals. They are therefore able to mix with corrin π orbitals which increases the number of electronic transitions that occur in the γ region of the spectrum. By contrast, in compounds that present with a "typical" spectrum, the transitions in the γ region are largely corrin $\pi \rightarrow \pi^*$ in origin, but virtually all electronic transitions are likely to involve at least some contribution from metal d orbitals [768].

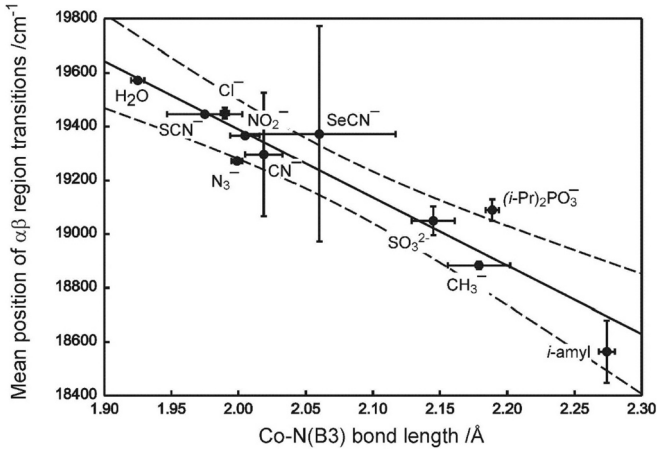

Fig. 21. Correlation between the mean positions of the Gaussians used to fit the $\alpha\beta$ region of the uv-vis spectrum of some cobalamins and the crystallographically-observed Co—N_{bzm} bond length. The labels refer to the β ligand. The broken lines are the 10% confidence intervals.

A plot of the mean position of the Gaussian functions used to fit the $\alpha\beta$ region of eleven cobalamins against the Co—N_{bzm} bond length ($r^2 = 0.90$) [761] is shown in Fig. 21 The horizontal error bars are drawn at $\pm 3\bar{\sigma}$ where $\bar{\sigma} = \sqrt{\sum_i \sigma_i^2}$ and σ_i is the e.s.d. of the crystallographically determined bond length, found from the crystallographic CIF file of each structure deposited in the CSD. The vertical error bars are the cumulative errors from the Gaussian fits of the spectrum. There is a clear correlation between the trans influence of the axial ligand and its cis influence. Brunold and co-workers [142] have shown that the contribution of the Co $3d_z^2$ to the HOMO, which is largely corrin-based, increases with the σ donor strength of the β ligand. This induces an antibonding interaction between the metal and bzm. The increased electron density on the metal is partially transferred to corrin-based π orbitals, narrowing the gap between the orbitals which are involved in the electronic transitions, predominantly of $\pi \rightarrow \pi^*$ character, that give rise to the $\alpha\beta$ region of the uv-vis spectrum of the cobalamins.

A similar explanation accounts for the "atypical" spectra of thiolatocobalamins. Like the alkyl ligands of the alkylcobalamins, the thiolate ligand is strongly σ-donating towards Co(III); this increases the energy of the $3d_z^2$ orbital, which is then able to effectively mix with corrin π orbitals, shifting the electronic transitions that give rise to the γ region of the spectrum to lower energy [537,729].

A weak band in the NIR region, referred to as band A [758], has been observed [522,757,758,761] particularly noticeable, for example, for iodocobalamin at 740 nm [757]. This region of the electronic spectrum of a wide range of cobalamins has been examined in some detail; it was found that the position of the A band is inconsistent with the nephelauxetic series but rather follows the spectrochemical series (I < Br < SCN < Cl < F < N < O < NCS < C < P). This band is predominantly due to a LMCT transition, corrin $\pi \rightarrow$ Co $3d_z^2$ [758]. It is a feature observed in the CD spectrum of $[H_2OCbl]^+$ at a lower energy than the $\alpha\beta$ region and assigned, on the basis of DFT calculations, to such a transition [142].

In a Gaussian analysis of the uv-vis spectra of several alkylcobalamins [769] it was reported that three low intensity Gaussian bands occur at approximately 500 nm, 460 nm and 400 nm. They were attributed to spin-allowed, Laporte-forbidden d-d transitions of the metal ion. However, this could not be unequivocally verified [761] and it is generally accepted that d-d transitions of Co in the cobalt corrinoids have low intensity and cannot be reliably detected by uv-vis spectroscopy [236].

As might be expected, perturbing the electronic structure of the corrin ring itself alters the position of the main bands in the uv-visible spectrum, given the very prominent involvement of the corrin π orbitals in these electronic transitions. The C10H of a corrin can be replaced by other groups [162,178,231,551,770–773]. Reaction of [CNCbl] with NOCl produces 10-nitrosocyanocobalamin [770–772]. This can be reduced with $NaBH_4$ to 10-aminocobalamin [771]. The reaction of [CNCbl] with HNO_3/Ac_2O at −10 °C for 3 h leads to [CN(10NO_2)Cbl in modest yields [162]. This is readily reduced to [CN-10NH_2Cbl] by borohydride which then provides a route to -N=CHR, -NHR and -NHCOR at C10 [162]. [CH_3Cbl] [771] and $[H_2OCbl]^+$ [231] react with *N*-bromosuccinimide to replace C10H with Br. [CNCbl] reacts with choloramine-T to produced 10-chlorocobalamin [771] but with a *c* lactone ring, and the reaction of chloramine-T with [CH_3Cbl] also replaces the C10H with Cl, producing [CH_3-10ClCbl] but without a *c* lactone [178]. [CNCbl] reacts with HOCl to form 10-chlorocobalamin; this rapidly reacts with HOCl which abstracts the C8H to form the *c*-lactone [551]. Methods for the synthesis of $[H_2O$-10BrCbl$]^+$ using *N*-bromosuccinimde as brominating agent have been described [231,774].

The corrin ring is not stable in alkaline solutions. For example, the amides of the corrin side chains of [CNCbl] can be hydrolysed and the bzm-containing moiety cleaved [775,776]; dehydroB_{12}, featuring a *c* ring lactam, formed [775]; the B ring can be opened between C7 and C8 to form the blue corrinoid 7,8-seco-cyanocobalamin which features a

Table 6
Position of the main bands in the spectrum of the cobalt corrinoids as a function of the substitutent, Z, at the C-10 position of the corrin ring.

Z	σ_P^a	α axial ligand	β axial ligand	Band position /nm			Ref
				γ	β	α	
NO	0.91	CN^-	CN^-	356	530	568	[772]
H	0	CN^-	CN^-	367	550	580	[58]
NH_2	−0.66	CN^-	CN^-	379	610	655	[771]
NO	0.91	bzm	H_2O	345	507	535	[772]
Cl	0.23	bzm	H_2O	355	536	558	[231]
Br	0.23	bzm	H_2O	356	539	555	[231]
H	0	bzm	H_2O	351	527	554	[787]
$NHCH_2$(4-MeOPh)	−0.70 [c]	bzm	CN^-	371	≈560	586	[162]
NH_2	−0.66	bzm	CN^-	376	611–615 [b]		[162]
N=CH-(4-MeOPh)	−0.54	bzm	CN^-	375	≈564	598	[162]
H	0	bzm	CN^-	361	520	550	[162]
$NHCO(CH_2)_2CONHBn$	0 [d]	bzm	CN^-	362	531	559	[162]
Cl	0.23	bzm	CN^-	364	546	576	[178]
Br	0.23	bzm	CN^-	365	550	576	[788]
NO_2	0.78	bzm	CN^-	354	521	541	[162]

[a] [789]. [b]Broad maximum observed. [c]Value for NHMe. [d]Value for NHCOMe.

C=C bond at C7 and a carbonyl group at C8 [777]; and deprotonation of C8 leads to the formation of an anionic reducing agent that reduces Co (III) to Co(II) [778]. Other sites of possible deprotonation are at C3 and C13 [779]. A detailed study of the reaction of OH^- with [CNCbl] in DMSO and isopropanol under anaerobic conditions has recently appeared [779]. The initial reaction leads to the deprotonation of C8, and the carbanion reduces Co(III) to Co(II). The CN^- released reacts with [CNCbl] to form $[(CN)_2Cbl]^-$. A lactone ring is formed on ring *c*. With excess OH^-, the carbanion is reduced to Co(I) with formation of $OH^\bullet$.

Modified corrinoids in which the main conjugated ring has been cleaved between C5 and C6 or between C14 and C15 are known [780,781]; the implication of this for the thermodynamics and kinetics of ligand substitution reactions at the axial coordination sites are discussed later in this review. Several corrins where the B ring has been cleaved have been synthesised and characterised [777,782]. The replacement of the *d* side chain in the cobester by a ketone, extending the conjugation of the corrin ring, causes a red shift in the uv-vis spectrum [783]. Other modifications to the *c* and *d* side chains of ring B have been described [784,785]. There are many accounts (for example [107,181,786]) of the modificiation of the chain linking the *f* side chain and the α base (bzm, imidazole, or one of their derivatives), but these are not considered in this review.

Table 6 gives the dependence of the γ, β and α bands on the substituent, Z, at the C-10 position of the corrin. The red shift of the bands as the donor power of the C10 substituent increases is clear.

The estimated (see the original report for details [162]) oxidation potential of the Co(I)|Co(III) couple correlates well with the Hammett parameter σ_P of the C10 substituemt, varying from ca. 0.8 V for [CN-10NH_2Cbl] to 1.4 V for [CN-10NO_2Cbl].

In some early work, Murakami et al. demonstrated the effect that changing the electronic structure of the macrocycle of the corrin has on the properties of their Co complexes [790,791]. They synthesised cobalt complexes of the modified corrins 8,12-diethyl-1,2,3,7,13,17,18,19-octamethyl-AD-didehydrocorrin (BDHC) and its tetradehydro analogue, TDHC) and compared their properties to those of the cobalt corrinoids. The macrocyclic skeleton of these and of corrin itself are shown in Fig. 22.

Table 7
Position of the principal bands (nm) in the uv-vis spectrum of [$(CN)_2$corrinoid] complexes.

Corrinoid[a]	γ	β	α
Corrin	367	544	578
BDHC	377	525	562
TDHC	397	678	753

[a]Data from [790]; corrin and BDHC in aqueous solution; TDHC in methanol

The extended conjugation of TDHC compared to BDHC and the cobamide has a significant effect on the position of the absorption maxima in the uv-vis spectrum. For example, while the position of the γ, β and α bands of the dicyano complexes of a cobamide and BDHC are similar (Table 7), those of TDHC are markedly red shifted. Like [Cbl(II)] [563], the Co(II) complex of BDHC forms a superoxo Co(III) complex on exposure to O_2; both this complex and the complexes of [Cbl(II)] and $[Co(II)(BDHC)]^+$ with pyridine have similar EPR spin Hamiltonian parameters, indicative of a similar electronic structure. Furthermore, the pK_a for ionisation of coordinated H_2O in the diaqua complexes of a Co (III) cobinamide and of BDHC are very similar (6.0 [331] and 6.2, respectively). This is understandable since the double bonds between C2 and C3, and between C17 and C18 are not part of the extended delocalised π electron system between N1 and N4. (There are steric

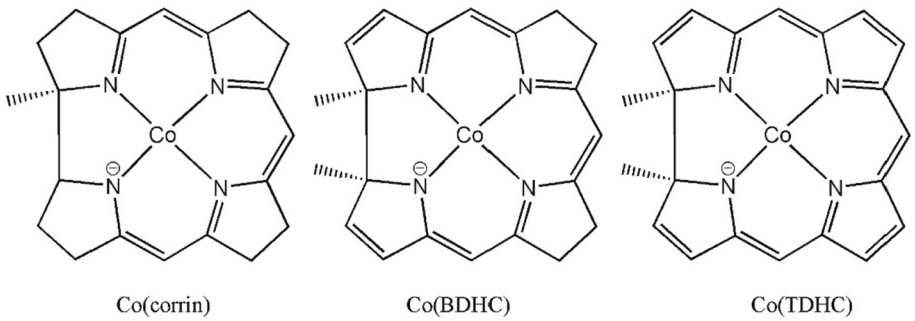

Fig. 22. The macrocyclic skeleton of the cobalt complexes of corrin, A,D-didehydrocorrin BDHC and its tetradehydro analogue, TDHC. The charge on Co is not specified as various oxidation states of the metals were examined [790].

consequences of having a methyl group at C19 [790,791].)

Extending the conjugated system by introducing double bonds between C7 and C8, and C12 and C13 does have a significant effect. The Co(III)|Co(II) and Co(II)|Co(I) couples of the Co complexes of BDHC and TDHC are observable by cyclic voltammetry in methanol; the values for [Co(TDHC)] are more positive: +0.59 V vs +0.47 V (vs SCE); and − 0.25 V vs −0.71 V. For the dicyano complexes, only a 2e process is observed (see Section 5.1). The Co(III)|Co(I) values in DMF for [$(CN)_2$Cbi], [$(CN)_2$Co(BDHC)] and [$(CN)_2$Co(TDHC)] are −1.14 V, −1.38 V and − 0.58 V, respectively. The extended conjugation of TDHC makes its cobalt complexes more easily reducible.

A DFT and TD-DFT study of dicyano complexes of the type [CN-[Co^{3+}–corrin(C10–X)]-CN] using the BP86 functional in which C10H was replaced by substituents X with Hammett σ_P constants varying between 0.91 (for X = NO) and − 0.66 (X = NH_2) to assess the cis effect on the equatorial ligands has been reported [792]. The BP86 functional reproduced the essential features of the experimental spectra of the dicyano cobalt corrins and the gap between the α and γ bands (204 nm) reasonably close to that observed experimentally in the uv-vis spectrum of [$(CN)_2$Cbl]$^-$ (213 nm), and much better than other functionals (B3LYP, CAM-B3LYP, PBE1PBE, M06 where the gap was found to be between 155 and 167 nm). The α band of the simulated spectrum corresponds to a transition between the HOMO (π_{corrin}/σ_{CN}) and the LUMO ($\pi^*_{corrin}/3d_{yz}$) and therefore is associated with the transfer of electron density from the axial ligand to the corrin, as also demonstrated by Andruniow and co-workers [195]. The α band shifts to longer wavelength as the HOMO–LUMO gap narrows with increasing electron donation by X. The study also showed that the ionic character of the Co—CN bond decreases with the electron withdrawing power of the C10 substituent; the bond becomes stronger and as a consequence the C ≡ N stretching frequency increases towards that of free CN^-.

Similar calculations on models of the type [NH_3–[Co^{3+}–corrin (C10–X)]-Me]$^+$ [793] showed that as X becomes more electron-donating, the weaker of the two axial bonds to the metal – the Co(III)—NH_3 bond – is elongated. This allows for a strengthening of the Co—CH_3 bond, as evidenced by the electron density at its bond critical point (from a QTAIM analysis). The Co—CH_3 bond length shortens marginally; there is therefore a normal trans influence between the axial ligands. Perhaps somewhat surprisingly, the BDE of Co—CH_3 (and ΔG for the homolysis reaction) decreases as the bond strengthens, emphasizing that they are not necessarily synonymous [794]. After cleavage of the Co—CH_3 bond, the Co(II)—NH_3 bond shortens, the extent of which increases as the electron donation ability of X increases. The effect of an increase in donation of electron density by the C-10 substituent is to differentially stabilise the five-coordinate complex. Stabilising the Co—N_α bond in the five coordinate product may be an important factor in modulating the BDE to a Co—C_β bond [795,796].

In DFT modelling of compounds of the type [H_3N−[$Co^{3+}N_4$]−Me]$^{n+}$, where N_4 = bis(dimethylglyoxime), porphyrin, corrin, and corrole, the nature of the tetraaza equatorial ligand can change the BDE values by over 30 kJ mol^{-1} [796]. For N_4 = bis(dimethylglyoxime) the BDE is significantly larger than for the other three systems, among which differences in BDE are quite small (≈10 kJ mol^{-1}). The differential stabilization of the five-coordinate product by the shrinking of the Co—N_α bond (in corrin and in corrole) or its elongation (in porphyrin and in bis(dimethylglyoxime)) is an important factor in determining the BDE of these systems. Corrin has the longest and weakest Co—C_β bond; this, together with a significant contraction of the Co—N_α in the post-homolysis product, appears to be the origin of its relatively low BDE.

There is also experimental evidence for the effect of perturbing the electronic structure of the corrin on the thermodynamics (log K values for coordination of ligands in the axial site, typically, substitution of H_2O by an exogenous ligand, L), and on the kinetics of this process, as discussed later in this review.

There is no convincing evidence for a ground state cis influence of corrin (i.e., the effect of the equatorial ligand on the structure of the complex, and in particular its impact on the axial ligands). A search of the CSD [797] produced 11 corrins with CN^- trans to CN^- for which the atomic coordinates have been deposited. There is no statistically significant difference between the Co—$(CN)_\alpha$ bond length, 1.931(17) Å, and the Co—$(CN)_\beta$ bond length, 1.922(18) Å; the average is 1.926(17) Å. This is indistinguishable from an average of 1.926(22) Å in bis-cyano porphyrin complexes (n = 7), or bis-cyano phthalocyanines (1.928(25) Å, n = 24). The three bis-cyano cobaloximes have a somewhat shorter Co—CN bond (1.908(10) Å) while the nine complexes where N_4 is a macrocyclic ligand have somewhat longer Co—CN bonds (1.969(10) Å). The 22 complexes where the equatorial ligand is an open chain have on average Co—CN bond lengths of 1.925(14) Å, again statistically indistinguishable from the bond lengths of the bis-cyano corrinoids. When comparing these statistics, apart from the rather large standard deviations, one also needs to keep in mind the relatively large uncertainty in the bond lengths of cobalt corrins. For instance, of the 11 bis-cyano corrins, only two have esd's between 0.006 and 0.01 Å; one has an esd > 0.03 Å; and the majority have 0.01 < esd < 0.03 Å. Also see the caveats in Section 2.2. It is therefore unwise to use the available structural data to attempt to make definitive conclusions about ground state cis structural effects in Co(III) complexes.

Table 8
Axial bond lengths of alkyl Co(III) complexes with the alkyl ligand trans to a N-donor of a fused 5- and 6-membered ring system.

Alkyl ligand		n	Co—C /Å (mean(σ))	Co—N(5,6 bicycle) /Å (mean(σ))
CH_3	Corrin	4	1.986(8)	2.167(22)
	Other complexes	4	2.004(11)	2.080(17)
CH_2R	Corrin	16	2.012(26)	2.213(37)
	Other complexes	9	2.015(43)	2.076(35)
CHR_2	Corrin	2	1.947(7)	2.162(35)
	Other complexes	5	2.039(44)	2.058(42)

There are not many other axial ligand combinations that are well represented for a variety of Co(III) complexes. The data for alkylcobalamins trans to an N-donor ligand consisting of a fused 5- and 6-membered ring system, such as bzm, are summarised in Table 8.

One might tentatively conclude that there is little difference in the Co—C bond lengths between alkyl Co(III) corrins and alkyl Co(III) complexes with other N_4 equatorial ligand systems; but, firstly, the caveat given above about the precision of the data, secondly, the relatively large value of the standard deviation of the data, and, thirdly the relative paucity of data, means such a conclusion needs to be treated with caution.

There is some structural evidence that perturbing the electronic structure of the corrin affects the bond lengths to the axial ligands, but the differences are small, may not be statistically significant, and no clear-cut trends emerge. Replacing the C10—H with Cl or Br (both π donors to the corrin) causes the Co—OH_2 bond length of H_2O in [H_2OCbl]$^+$ to shorten marginally from 1.952 Å [179] to 1.948 Å in [H_2O-10ClCbl]$^+$ [178] and to 1.933 Å and 1.943 Å in the two molecules in the asymmetric unit of [H_2O-10BrCbl]$^+$ [231], while the Co—N bond to bzm increases from 1.925 Å to 1.967 Å, and to 1.975 and 1.961 Å, respectively. In [MeCbl] the Co—CH_3 bond length is reported as 1.979 Å [180] and 1.990 Å [169], while the Co—N_{bzm} bond lengths are 2.613 and 2.156 Å, respectively. In [Me-10ClCbl] [178], the axial bond lengths to CH_3 remain essentially unchanged (1.979 Å and 2.200 Å). In [CN-10ClCbl], the Co—CN bond length at 1.97 Å is longer while the Co—N_{bzm} bond length, at 2.04 Å, is essentially the same as in [CNCbl] itself (1.867 and 2.029 Å [180]; 1.886 and 2.041 Å [180]; and 1.877 and 2.028 Å [798]). In [N_3(10-Br)Cbl], both axial ligands are shorter than in [N_3Cbl] itself (1.942 Å for Co—N_3 and 1.974 Å for Co—N_{bzm} [231], *vs.* 1.983 Å and 1.999 Å [171]).

7.3. The ligand substitution reactions: equilibria

7.3.1. The nature of Co(III) in the cobalt corrinoids

Co(III) in the cobalt corrinoids does not behave like a typical low spin d^6 metal ion. As discussed in Section 9, its ligand substitution reactions are surprisingly fast; this may arise from the transfer of electron density from the electron rich delocalised π electron system of the corrin macrocycle to the metal ion, conferring on it a measure of labile Co(II) character. One way of probing this is to examine the reaction of Co(III) in $[H_2OCbl]^+$ with ambident nucleophiles. Replacement of H_2O by $SeCN^-$ and NO_2^- [799,800], and $S_2O_3^{2-}$ [799] shows (from the structures determined by x-ray diffraction methods) that the ligands are coordinated through the softer available donor in each case (Se, N, S). In one study SCN^- in solid [SCNCbl] was found coordinated through N, but there is ^{13}C NMR evidence that in solution the compound exists as a mixture of the two linkage isomers [799]. In a second report, [SCNCbl] was found to crystallise as a mixture of the S- and N-bound species in a ratio of 3:2 [800]. This structural evidence, together with values of log *K* for ligand substitution (Section 7.3.3) and the kinetics discussed in Section 9, indicates that the metal has some measure of softness, or a borderline class *b* character [757,801].

7.3.2. The trans influence: the base-on/base-off equilibrium

Perhaps the simplest ligand substitution reaction of the cobalamins is the displacement of bzm, to form an equilibrium mixture of a five coordinate complex and one where, in a coordinating solvent, the α coordination site is occupied by a solvent molecule; the ratio of the two can be altered by increasing pressure which will favour the more compact six coordinate species [802,803].

The trans influence and the trans effect have played an important role in coordination chemistry and many reviews have appeared (for example [794,804–811]). We discuss the trans influence in cobalt corrinoid chemistry here, and look at the trans effect in Section 9.

Cobalamins exist in a variety of forms in solution, depending on pH, as illustrated schematically in Scheme 27. In addition to the species shown in the scheme, it has been suggested there may be a species in which the bzm in protonated, yet remains coordinated to the metal ion [812]. If that is indeed the case, the site of protonation is unclear and the species is likely to be a very minor contributor to the species present at any pH.

In acidic aqueous solution, protonation of bzm will lead to its displacement to form the six coordinate base-off complex with H_2O in the α coordination site. However, if X is a strong σ donor such as, for example, vinyl, methyl, sulfite, or dialkyl phosphite, a significant fraction of the base-off species may be five coordinate [802,813–820]. Increasing temperature favours the five-coordinate form in both cobalamins and cobinamides [819]; as shown in the case of diethylphosphitocobalamin, an increase in pressure favours the base-on form [818].

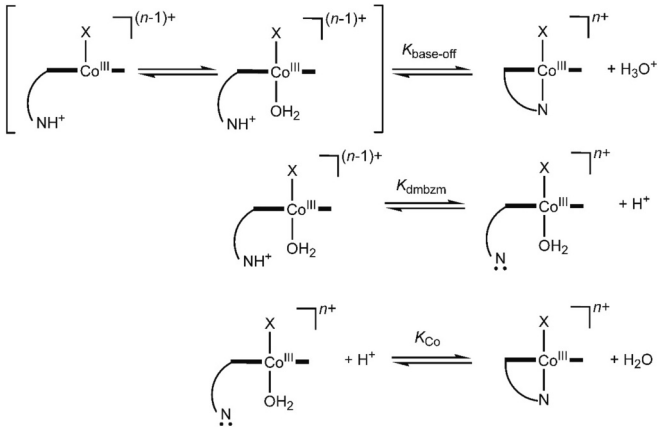

Scheme 27. The base-on/base-off equilibria of the cobalamins

There is evidence of an interaction between the uncoordinated base and the corrin in the base-off species, probably through formation of a hydrogen bond between the (unprotonated) B3 nitrogen of the nucleotide and a side chain amide of the corrin [821,822].

The on-off equilibrium of bzm can be monitored by ^{31}P NMR [112,127,823,824]; coordination of bzm to the metal induces changes in the OP2—P—OP3 bond angle, a strain which is relieved on displacement of the base from the metal [175,825]. Indeed, there is a good correlation between the Co—N_{bzm} bond length and the position of the ^{31}P resonance [175,183]. In the absence of a crystal structure, and certainly for cobalamins in which the side chains have not been epimerized from their usual positions, the ^{31}P chemical shift of the phosophodister moiety is a very useful way of estimating the Co—N_{bzm} bond length [175].

NMR-restrained molecular dynamics simulations of the base-off form of [NOCbl] indicated that there are two major forms in solution. In the first, the bzm is perpendicular to the corrin, and the B3 nitrogen, while >3 Å from the metal, points directly at it. In the second, bzm is parallel to and tucked beneath the corrin D ring. There is NMR evidence that in the base-off, bzm-deprotonated form of organocobalamins, the B3 nitrogen atom is hydrogen-bonded to an N—H of the *e* side-chain [826].

It follows from Scheme 27 that $K_{base\text{-}off} = (1 + K_{Co})K_{bzm}$ [113,827]. If it is assumed that $pK_{bzm} = 5.56$ [113], the value for free α-ribazole, then values of $pK_{base\text{-}off}$, K_{Co} and $-\Delta G_{Co}$ can be deduced, some of which are summarised in Table 9.

There is a good correlation between the Gibbs energy, $-\Delta G_{Co}$ for the coordination of bzm and the Co—N_{bzm} bond length (Fig. 23); this is a reflection of the affinity of the metal ion for the bzm ligand, which is subject to the trans effect of the β ligand. It is likely that electronic effects (the inductive power of the β ligand) are modulated by steric factors (the interaction between the β ligand and the corrin [816,817]). The position of the equilibrium towards the base-off form increases with the steric bulk of the alkyl group (Me < Et ≈ Pr < ^{i}Bu ≈ cyclobutyl < neopentyl ≈ cyclopentyl < ^{i}Pr ≈ cyclohexyl). At 25 °C [MeCbl] is ca. 5% in the base-off form in aqueous solution whereas [^{i}PrCbl] is ca. 80% base-off.

The structure of the loop connecting the *f* side chain to the α axial base is likely to play a role as well. Comparison of the base-on/base-off equilibria of two B_{12} mimics with imidazole as potential α axial base showed that addition of an additional methyl group to C176 (Pr2, Fig. 4) steers the imidazole towards coordination ($\Delta\Delta G^o = -4$ kJ mol^{-1}) [836].

The pressure-dependence of the spectra of vinylcobinamide, and of $[CH_3Cbl]$ in 0.5 M $HClO_4$ ($pK_{base\text{-}off} = 2.89$ [113]) has been investigated [803]. Under ambient conditions the two species are, respectively, 70% and 90% in the five-coordinate form [814]. Increasing pressure (up to 150 MPa) favours the six-coordinate form in both instances, with, from a plot of ln $K_{base\text{-}off}$ against *p*, $\Delta V = -12(1)$ cm^3 mol^{-1} in both cases, within experimental error of the theoretical value of -13.1 cm^3 mol^{-1} [837] for uptake of an H_2O ligand by a metal to form an octahedral complex.

7.3.3. The trans influence: substitution of coordinated H_2O

The substitution of coordinated H_2O in $[H_2OCbl]^+$, Factor B (aquacyanocobinamide, $[ACCbi]^+$), diaquacobinamide ($[(H_2O)_2Cbi]^{2+}$, DAC) and aquahydroxocobinamide ($[AHCbi]^+$) by an exogenous ligand was known from the very early years of the study of B_{12} chemistry. There were early reports on the substitution of H_2O in $[H_2OCbl]^+$ by, for example, CN^- [838–841]; SO_3^{2-}, H_2S, CNO^-, Cl^-, NO_2^- and Br^- [839]; SCN^- [841–843]; I^- [843]; NH_3 and histidine [841,844]; imidazole, pyridine, MeCN, NO_2^-, N_3^-, $[Fe(CN)_6]^{4-}$, $[Fe(CN)_6]^{3-}$ and $[Co(CN)_6]^{3-}$ [841]. The substitution of H_2O in $[ACCbi]^+$ by a variety of neutral and anionic ligands was also reported [841].

The first comprehensive study of substitution of H_2O in $[H_2OCbl]^+$ by an exogenous ligand appears to have been that by Hanania and Irvine in 1964 [845], who determined the equilibrium constant for the reaction with imidazole (HIm) spectrophotometrically as a function of pH and

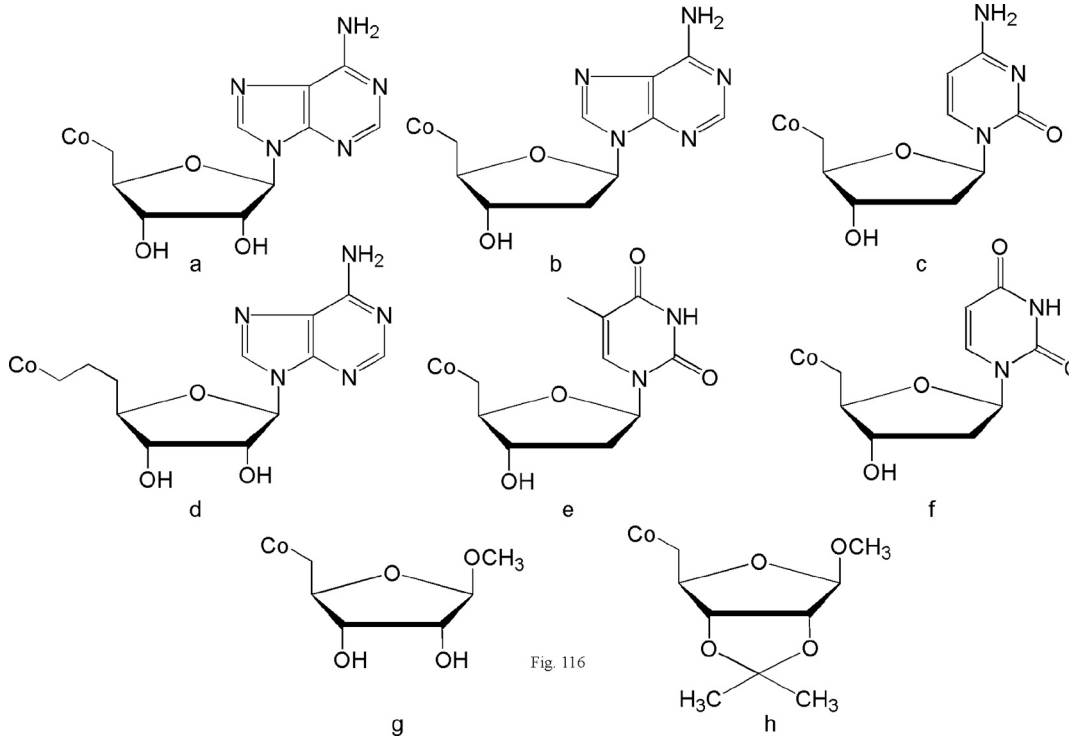

Fig. 116

Scheme 28. Structure of the β ligand of 5′-deoxynucleosidylcobalamins referred to in Table 9. a: Ado, 5′-deoxyadenosyl; b: 2′,5′-dideoxyadenosyl; c: Cyt, 2′,5′-dideoxycytidyl; d: AdePr, 5′-deoxyadeninylpropyl; e: Thy, 2′,5′-dideoxythymidyl; f: Urd, 2′,5′-dideoxyurinidyl; g: Rib, 5′-deoxylribosyl; h: isoRib, 5′-deoxy-2,3-isopropylidene-ribosyl

temperature. Three reactions are pertinent: the ionisation of coordinated H_2O; the deprotonation of H_2Im^+ to form Him; and deprotonation of coordinated HIm to form the imidazolate complex (Eq. 25, where it is understood the the α coordination site is occupied by bzm).

$$CoH_2O^+ \rightleftharpoons CoOH + H^+ \quad K_{Co} \tag{25a}$$

$$H_2Im^+ \rightleftharpoons HIm + H^+ \quad K_1 \tag{25b}$$

$$CoHIm^+ \rightleftharpoons CoIm + H^+ \quad K_2 \tag{25c}$$

The observed pH-dependent equilibrium constant, K_{obs}, is related to the equilibrium constant, K, for the reaction of Eq. 26 by Eq. 27.

$$CoH_2O^+ + HIm \rightleftharpoons CoHIm^+ + H_2O \quad K \tag{26}$$

$$K = \frac{K_{obs}(K_{Co} + [H^+])(K_1 + [H^+])}{K_1(K_2 + [H^+])} \tag{27}$$

A plot of the experimentally-determined values of log K_{obs} as a function of pH with the best-fit line determined using log $K = 4.60(3)$, p$K_{Co} = 7.72$, p$K_1 = 7.06$ and p$K_2 = 10.31$ is shown in Fig. 24.

Determination of K as a function of temperature between 10 °C and 30 °C yielded, from a van't Hoff plot of log K against $1/T$, values of $\Delta H = -30 \pm 3$ kJ mol^{-1} and $\Delta S = -13 \pm 8$ J K^{-1} mol^{-1}.

A more comprehensive study of the coordination of imidazole and its derivatives was reported more recently [846] and demonstrated factors that can make the system quite complex, depending on the structure of the entering ligand. (It should be emphasised, though, that the absolute values of log K values reported in that study may not be very reliable because of the use of KCl as ionic strength adjustor ($\mu = 1.0$ M)). Although K for coordination of Cl^- is small (3.3 [331]), it is not zero; so the reactive cobalamin species was not only $[H_2OCbl]^+$ as assumed, but also [ClCbl].)

The observed equilibrium constant, K_{obs}, is a function of pH and can be written as shown in Eq. 28, where the parameters α, β and γ depend on the structure of the imidazole.

$$K_{obs} = \frac{K_1\alpha}{(1 + K_{Co}/[H^+])\beta\gamma} \tag{28}$$

Protonation of the N-donor of an imidazole to form an imidazolium cation will prevent its coordination by $[H_2OCbl]^+$. Substitution at the α position sterically hampers coordination of an imidazole; hence the apparent log K for coordination of 2-methylimidazole by $[H_2OCbl]^+$ at pH 7.00 is 0.16 but 4.13 for coordination of imidazole itself.

In the case of an asymmetrically substituted imidazole, such as 4(5)-methylimidazole, and based on the very low binding constant observed for 2-methylimidazole, it is reasonable to assume that coordination to $[H_2OCbl]^+$ will occur almost exclusively through the 5-tautomer (Scheme 29), and $K_T = $ [4-tautomer]/[5-tautomer] must be taken into account [847]. A generalised scheme for the coordination of an imidazole by $[H_2OCbl]^+$ is shown in Scheme 30 [846,847].

For a pH range above the pK_a of the acid functionality of the side chains of imidazole lactic and histidine, it follows that for imidazole and 2-methylimidazole, $\alpha = 1 + K_z/[H^+]$, $\beta = 1 + [H^+]/K_L$ and $\gamma = 1$; for *N*-methylimidazole and 1,5-dimethylimidazole, $\alpha = \gamma = 1$ and $\beta = 1 + [H^+]/K_L$; in the case of 4(5)-methylimidazole and imidazole lactic acid, $\alpha = 1 + K_z/[H^+]$, $\beta = 1 + [H^+]/K_L$ and $\gamma = 1 + K_T$; for imidazole lactic acid, $\alpha = 1 + K_z/[H^+]$, $\beta = 1 + [H^+]/K_L$ and $\gamma = 1 + K_T$; and for histidine and histamine, $\alpha = 1 + K_y/[H^+] + K_yK_z/[H^+]^2$, $\beta = 1 + [H^+]/K_L + K_R/[H^+]$ and $\gamma = 1 + K_T$. Non-linear least squares fitting to the appropriate equation yielded values of the equilibrium constants (Table 10). Three representative fits are shown in Fig. 25 (data from [846].)

Excluding the value for sterically hindered 2-methylimidazole, log K_1 increases with the pK_a (i.e., the σ donor power) of the imidazole. Coordination of histamine and histidine decrease the pK_y values of the pendant amino group by ca. 1.1 units. The deprotonation to form, in the case of histamine, a neutral side chain, and in the case of histidine, a side chain carrying a -1 charge, increases the affinity of the ligand for the

Table 9
p$K_{base\text{-}off}$ and K_{Co} values of [XCbls][a].

X	p$K_{base\text{-}off}$	log K_{Co}	$-\Delta G_{Co}$ /kJ mol^{-1}	ΔH /kJ mol^{-1}	ΔS /J K^{-1} mol^{-1}	Ref
Cob(III)alamins						
H_2O	−2.4 (2)	8.0	45			[331]
H_2O	−2.13	7.69	43.8			[112]
NO_2^-	< −0.15 [b]					[132]
CN^-	0.02(4)	5.5	32 [c]			[828]
CN^-	0.1	5.5	31			[331]
CN^-	0.1	5.5	31			[824]
CN^-	0.11 [d]	5.5	31			[737]
CCH^-	0.7	4.9	28			[331]
p^1 [e]	< 1.1					[829]
$P(OMe)_3$	1.25(3)	4.32	24.6			[830]
CF_3^-	1.44	4.12	23.5	−29(1)	−20(5)	[113]
$P(OEt)_3$	1.46(4)	4.10	23.4			[830]
$HO_2CCH_2^-$	1.5	4.1	23			[58]
$CH(CN)_2^-$	1.6	4.0	23			[831]
$P(OMe)(F)O^-$	1.6	4.0	23			[832]
$NCCH_2^-$	1.81	3.75	21.4			[827]
SO_2^-	1.9	3.7	20			[575]
SO_3^{2-}	2.0	3.6	20			[787]
CF_2H^-	2.15	3.41	19.5	−29(2)	−31(6)	[113]
$CHClCH^-$	2.3	3.3	19			[633]
$P(OMe)_2O^-$	2.3	3.3	19			[829]
$CH_3OCOCH_2^-$	2.36	3.20	18.3	−36(2)	−61(6)	[113]
CH_2CH^-	2.4	3.2	18			[633]
isoRib$^-$ [f]	2.45	3.11	17.7			[833]
$P(OEt)_2O^-$	2.45(1)	3.11	17.7			[830]
CH_3^-	2.5	3.1	18 [g]			[331]
$CF_3CH_2^-$	2.60	2.96	16.9	−34(3)	−56(10)	[113]
Cyclopropyl$^-$	2.86(6)	2.70	15.4			[816]
CH_3^-	2.89	2.67	15.2	−31(2)	−54(6)	[113]
$P(O^iPr)_2O^-$	3.12(3)	2.44	13.9			[830]
AdePr$^-$ [f]	3.31	2.25	12.8			[175]
$CH_3OCOCH_2CH_2^-$	3.33	2.23	12.7	−32(2)	−71(6)	[113]
Rib$^-$ [f]	3.40	2.16	12.3			[833]
Thy$^-$ [f]	3.4	2.2	12			[834]
Ado$^-$ [f]	3.5	2.1	12			[834]
Urd$^-$ [f]	3.5	2.1	12			[834]
Cyt$^-$ [f]	3.5	2.0	12			[834]
$NCCH_2CH_2CH_2^-$	3.50	2.06	11.8	−32(1)	−67(7)	[113]
Ado$^-$ [f]	3.67	1.89	10.8			[112]
Cyclopropyl$^-$	3.7	1.86	10.6			[835]
Cyclobutyl$^-$	3.8	1.8	10			[835]
$CH_3CH_2CH_2^-$	4.10	1.46	8.33	−30(3)	−73(11)	[113]
$(CH_3)_2CHCH_2^-$	4.15(5)	1.41	8.04			[816]
$CH_3CH_2^-$	4.16	1.4	8.0	−37(3)	−99(10)	[826]
Cyclobutyl$^-$	4.17(4)	1.39	7.93			[816]
$(CH_3)_2CH^-$	> 4.5					[816]
Cyclopentyl$^-$	> 4.5					[816]
$(CH_3)_3CCH_2^-$	4.55	1.01	5.76			[835]
$(CH_3)_3CCH_2^-$	4.7	0.86	4.9			[816]
Cyclohexyl$^-$	4.7(2)	0.86	4.9			[816]
NO^-	5.1	0.56	2.6			[116]
13-epi Cob(III) alamins[h]						
CN^-	−0.90	6.5	37	−44(1)	−26(5)	[820]
CF_3^-	0.47	5.1	29	−36(3)	−22(10)	[820]
$NCCH_2$	0.85	4.7	27	−35(1)	−27(3)	[820]
$CF_3CH_2^-$	1.82	3.74	21.3	−38(1)	−54(4)	[820]
CH_3^-	2.15	3.41	19.5	−39(2)	−67(4)	[820]
$NCCH_2CH_2CH_2^-$	2.81	2.75	15.7	−36(2)	−67(4)	[820]
$CH_3CH_2^-$	3.51	2.05	11.7	−37(2)	−88(4)	[820]
8-epi Cob(III) alamins[i]						
CN^-	0.50	5.1	29	−33(2)	−13(8)	[820]
CF_3^-	1.75	3.81	21.7	−27.2(4)	−19(1)	[820]
$CF_3CH_2^-$	3.08	2.48	14.1	−32(3)	−59(4)	[820]
$CH_3CH_2^-$	4.62	0.940	5.36	−29(2)	−92(2)	[820]
Cob(II)alamins						
H_2O	2.9					[116]
SCN^-	3.4(4)					[117]
SO_2^-	4.8(1)					[118]

[a] See Scheme 27 for definitions. 25 °C unless otherwise indicated; $K_{base\text{-}off} = (1 + K_{Co})K_{bzm}$; p$K_{bzm} = 5.56$ [113]. [b] Hydrolysis of $[NO_2Cbl]$ to $[H_2OCbl]^+$ precluded a precise measurement. [c] $\mu = 1.0$ M. [d] Using p$K_{bzm} = 5.56$ rather than 5.0 used in [737]. [e] P^1 = 4-ethyl-2,6,7-trioxa-1-phosphabicyclo[2.2.2]octane (illustrated below). [f] See Scheme 28. [g] In 0.2 M acetate. [h] The *e* propionamide side-chain is epimerised from the lower to the upper face of corrin. [i] The *d* propionamide side-chain is epimerised from the lower to the upper face of corrin.

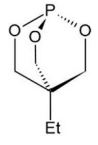

P^1

metal centre (i.e., log $K_3 >$ log K_1). Based on precedents from Fe(III) chemistry [848–850], this was attributed to a decrease (in the case of histamine) and (in the case of histsidine) an increase in coulombic repulsion and attraction, respectively, between the side chain and the residual +2 charge at the metal centre. This means that affinity of the Co(III) centre of $[H_2OCbl]^+$ and an imidazole (log K_3 for histamine and histidine; log K_1 for the other imidazoles in Table 10) is rather insensitive to the σ donor power of the ligand. There is, nevertheless, a clear linear trend between log K_2, the binding constant for a second ligand with the displacement of bzm, and pK_L.

There have been many studies subsequent to this. The relevant equation can be written in summarised form as Eq. 29.

$$\text{X-Co-Y} + \text{Z} \rightleftharpoons \text{X-Co-Z} + \text{Y} \quad (29)$$

For the purposes of illustration, Table 11 gives some examples of log K values. More complete details – but no claim is made that the Table covers all log K values ever reported! – can be found in Table A of the Appendix. The range of log K values is enormous, spanning nearly 14 orders of magnitude for substitution of H_2O trans to bzm, and some 8 orders of magnitude for its substitution trans to CN^-. (It should be borne in mind that aquacyanocobinamide exists in solution as a mixture of two stereoisomers, viz., α-aqua-β-cyano and α-cyano-β-aqua; this may be the case of alkylcobinamides as well, especially if the alkyl ligands is sterically undemanding.) An alkyl group has a very strong trans influence, and log K values are very small.

The polarity of the solvent will affect the values of log K. For example, log K for the coordination of imidazole and pyrazole trans to X in $[XCbs]^+$, X = CN^-, SO_3^{2-}, vinyl, increases with the polarity of the solvent (water > methanol > DMSO > DMF) [861]. This is probably a predominantly entropic effect, but unfortunately log K values were only determined at 25 °C.

The high affinity of Co(III) in $[H_2OCbl]^+$ for a range of relatively soft ligands such as CN^-, S^- and aromatic N-donors, and its relatively low affinity for hard ligands such as O-donors, indicates the metal has a borderline class *b* character [757,801] (see also Section 7.3.1).

An important point that emerged early on in these studies is the existence of a thermodynamic trans influence, i.e., ligand X can have a profound effect on the equilibrium constant for the replacement of the trans ligand Y by an incoming ligand Z; this is readily discerned from the results listed in Table 11. Further illustrative examples are brought together in Table 12.

The data in Tables 11 and 12 indicate that as X becomes a better donor to Co(III), the bond to the trans ligand weakens; secondly, as the donor power of Z increases, so does log K for its coordination to Co(III) – and in some instances (for example [846,858]) a clear linear correlation between the pK_a of Z and log K has been demonstrated); and thirdly, at the steric bulk of X increases, log K for coordination of Z decreases [858,863] (but π back bonding effects from CN^-, for example, are likely to be important as well [827,864,865]).

In a series of papers, Finke and co-workers explored in detail the

coordination of a variety of bases trans to 5′-deoxyadenosyl in $[AdoCbi]^+$, prompted by the novel evidence at time of the binding of [AdoCbl] in the base-off/His-on form in a number of coenzyme B_{12} dependent enzymes [863,866–868].

The coordination of a series of isosteric pyridines of variable basicity (as inferred from their pK_a in aqueous solution) to the α coordination site of $[AdoCbi]^+$ in ethylene glycol showed low affinity for the bases (K values from <0.2 to 2.5 M^{-1}, with ΔH from −14 to −27 kJ mol^{-1}, and ΔS from −46 to −84 J K^{-1} mol^{-1}), about an order of magnitude lower than $K_{Co} = 14.3$ for the intramolecular coordination of bzm in the same solvent (Scheme 27) [315]. The affinity increases with the basicity of the pyridine, and a compensation effect between ΔH and ΔS was noted (i.e. as ΔH becomes more negative, and the reaction enthalpically favourable, so does ΔS, making the reaction entropically less favourable). Based on an analysis of products of Co—Ado bond cleavage at 110 °C trans to pyridine and to *p*-dimethylaminopyridine, it was found that the basicity of the base has no effect on the rate of Co—C bond homolysis but increases the rate of hetereolysis of this bond [866]. *N*-methylimidazole also binds trans to Ado with a very modest $K = 0.4\ M^{-1}$; while the binding is more enthalpically favoured ($\Delta H = -33(2)$ kJ mol^{-1}) it is much more entropically disfavoured, with $\Delta S = -117(4)$ J K^{-1} mol^{-1} [867]. The thermodynamic parameters are unsurprising given the smaller steric demands of an imidazole compared to a pyridine. The binding of *N*-methylimidazole makes heterolysis of the trans Co—C bond competitive with homolysis, which led to the suggestion that to suppress heterolysis in the base-off/His-on form the Co—N bond must be long, i.e., close to that expected for the Co(II) oxidation state [867], although a later study concluded that there is no correlation between the ratio of homolysis to heterolysis and the Co—N bond length [868]. Sterically hindered bases such as 1,2-dimethylimidazole, 2-methylpyridine, and 2,6-dimethylpyridine do not bind detectably to Co(III) trans to Ado ($K < 0.03$). Uv-vis evidence was found for their coordination by [Cbl(II)] but the presence of both α and β diastereomers made quantification of binding constants (which are likely to be small) impossible [868].

If factors such as those discussed above are indeed important in determining the trans influence of a ligand in cobalt corrinoid chemistry, then there may be supporting structural evidence.

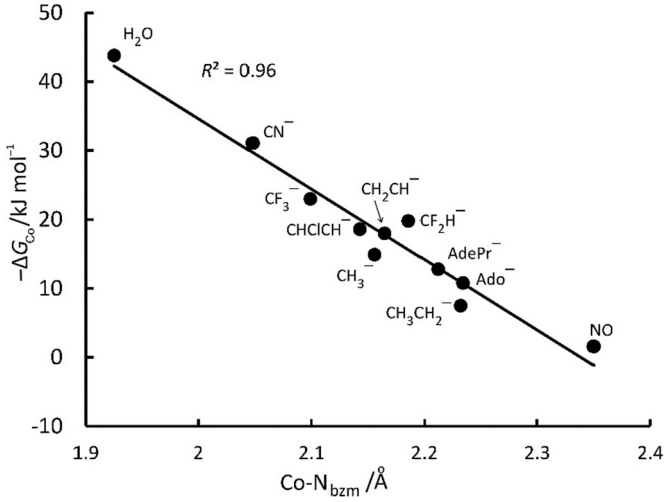

Fig. 23. Correlation between $-\Delta G_{Co}$ (see Scheme 27) and the crystallographically-observed Co—N_{bzm} bond length. The labels refer to the β ligand.

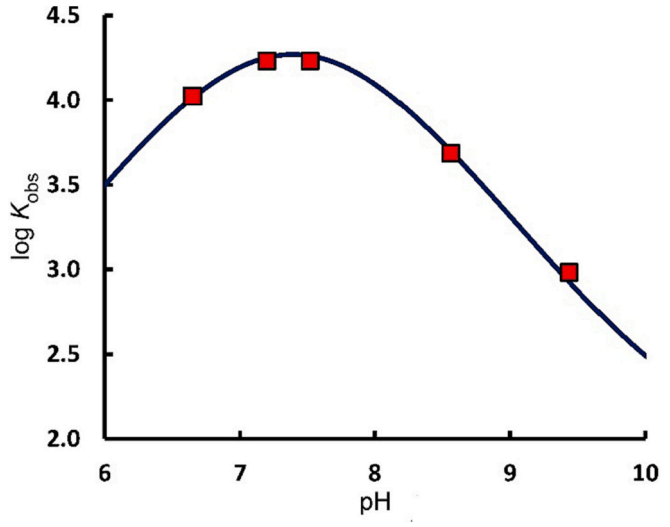

Fig. 24. The dependence of the observed equibrium constant, K_{obs}, on pH for the substitution of H_2O by Him in $[H_2OCbl]^+$. Constructed using data from [845].

7.3.4. *Structural evidence for the trans influence*

Crystal structures of many cobalt corrins are available; over 150 are listed in the CSD (see Section 2). Of these, 14 structures have both axial coordination sites of Co(III) occupied by CN^- and another 55 structures have CN^- in one of the axial coordination sites. There are 31 structures in which one of the coordination sites is occupied by an alkyl, ethenyl or ethynyl group. So, cobalt corrinoids with at least one Co—C bond should provide a statistically meaningful data set for exploring structural trends.

Studies of alkyl cobaloximes, which have sometimes been advanced as suitable models for the alkylcobalamins, showed that complexes with short Co—C bonds also have short Co—N bonds to a trans N-donor ligand [156,157], an effect described as an inverse trans influence. Attempts to quantify the factors that affect the length of the Co—C bond in the alkyl cobaloximes indicate that the bond lengthens with an increase in the steric bulk of the ligand and its σ donor ability, and shortens as the Co—C—X bond angle increases, where X is a substituent on the donor C atom of the axial ligand [159].

The structural data for [RCbl]'s with R trans to bzm show that the Co—N_{bzm} bond length tends to lengthen as the Co—C bond length increases. In Fig. 26 (insert) the crystallographic values of the Co—C bond length are plotted against the Co—N_{bzm} bond length for all [RCbl]'s (i.e., where C is (formally) sp^3 hybridised as in —CH_3 and —$CH_2(CH_2)_2CH_3$, sp^2 hybridised as in —CO(OMe), and sp. hybridised as in —C ≡ C-Ph); the data for [CNCbl] itself, and related structures, are included, yielding 101 structures. There is a clear, albeit weak ($r^2 = 0.79$), correlation between the two parameters and steric effects (the bulk of the ligand and its probable interaction with the corrin and its side chains) and electronic effects (hybridisation, σ donor power, ability to act as a π acceptor) may be important factors. The data in the main graphic of Fig. 26 are limited to those structures where the C donor atom is either in CN^- or (formally) sp^3 hybridised to obviate against such effects. The inverse trans influence correlation clearly persists ($r^2 = 0.82$). As has

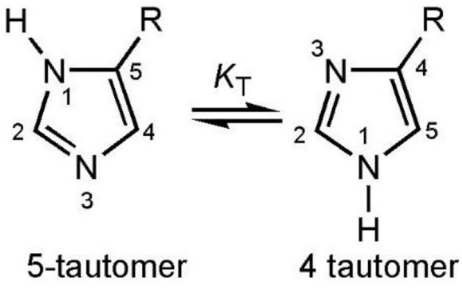

Scheme 29. The tautomerisation of an imidazole.

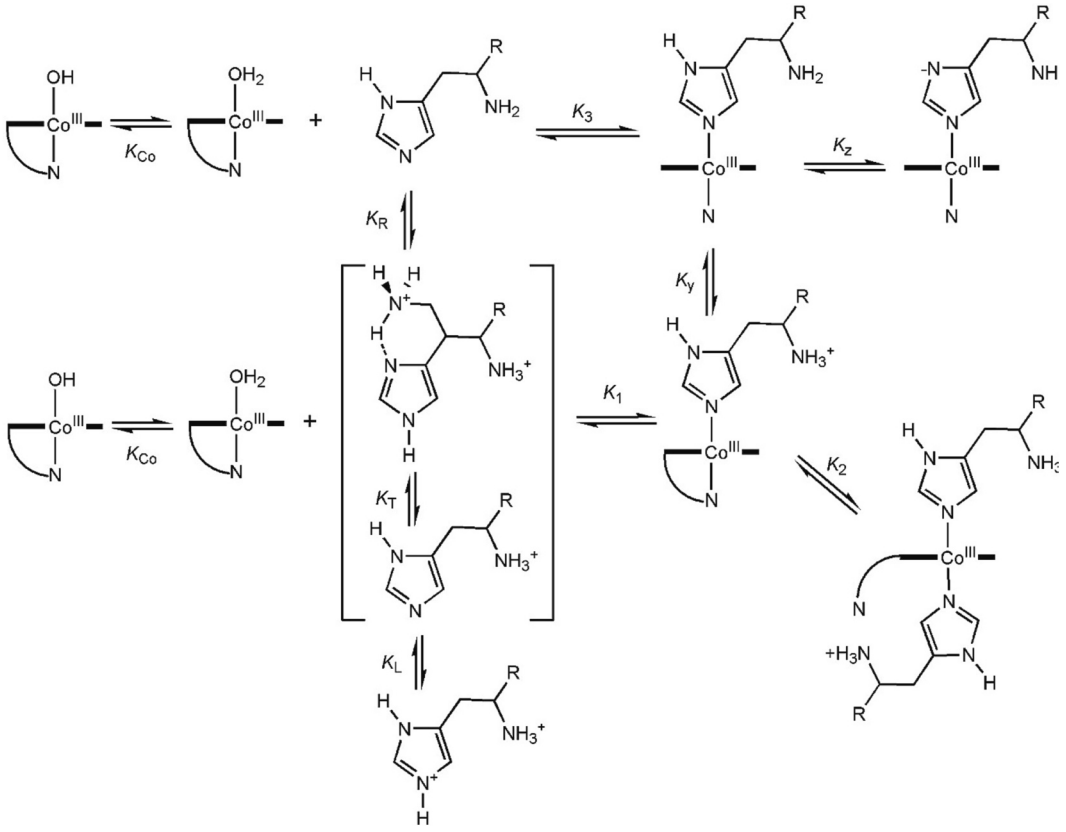

Scheme 30. Generalised scheme for the substitution of H_2O in $[H_2OCbl]^+$ by an imidazole derivative.

Table 10
Equilibrium and acid dissociation constants for the binding of imidazole and its derivatives by aquacobalamin at 25 °C, $\mu = 1.0$ M.

Ligand	pK_L	log K_1	log K_2	log K_3	pK_y	pK_z
histidine	6.23	4.30 (3)	< −1	4.60 (6)	7.99 (5)	10.06 (9)
histamine	6.41	4.41 (2)	−0.9	4.71 (3)	8.89 (5)	9.89(9)
2-methylimidazole	7.21	1.15 (6)				
N-methylimidazole	7.21	4.63 (5)	0.2			
imidazole	7.24	4.59 (1)	0.6			9.85(4)
imidazole lactic acid	7.39	4.86 (4)	0.9			10.20 (8)
4(5)-methylimidazole	7.76	4.90 (3)	1.3			10.4(2)
1,5-dimethylimidazole	7.97	4.82 (2)	1.4			

already been mentioned, there is considerable variability in crystallographically-determined structural parameters, as the standard deviations for the mean values of the axial bond lengths in [CNCbl] (57 observations in 49 crystal structures), [CF_3Cbl] (2 structures), [MeCbl] (4 structures), [CHF_2Cbl] (2 structures) and [AdoCbl] or structurally related complexes (8 structures), shown as error bars in Fig. 24, reveal, and caution needs to be exercised lest the data are over-interpreted.

In the case of non-alkyl cobalamins [XCbl]'s (Fig. 27), where (A) the ligand X is an O or N donor or, (B) P, S or Cl, there appears to be no significant correlation between the Co—N_{bzm} and the Co—X bond lengths (or perhaps a hint of a normal trans influence), particularly if the value for nitrosylcobalamin, [NOCbl] [183], is included; in this

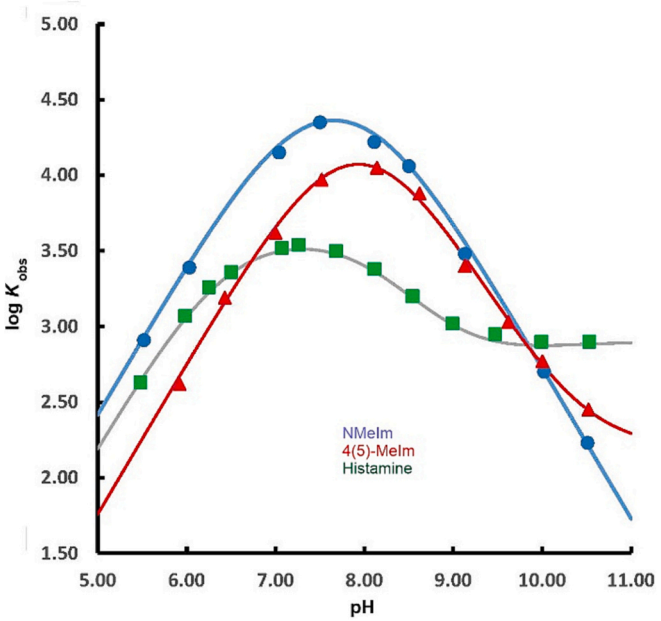

Fig. 25. The dependence of log K_{obs} on pH for substitution of H_2O in $[H_2OCbl]^+$ by by three representative imidazole derivatives: NMeIm (blue circles); 4(5)-MeIm (red triangles); and histamine (green squares). (For interpretation of the references to colour in this figure legend, the reader is referred to the web version of this article.)

structure the Co—NO bond length is 1.907 Å while the Co—N_{bzm} bond length is 2.32–2.35 Å, the longest bond to bzm yet observed.

Table 11
Representative log *K* values for substitution of H_2O by Z trans to X (Eq. 29).

Z	X	log *K*	Ref	Z	X	log *K*	Ref	Z	X	log *K*	Ref
CN^-	bzm	14.1	[17]	imidazolate	CN^-	≈8	[625]	CN^-	CH_3^-	2.4	[851]
Glutathione		9.7	[485]	CN^-		6.25	[852]	4-NH_2 pyridine		1.38	[321]
NH_3		7.0	[625]	benzimidazolate		5.0	[625]	4-Me pyridine		1.06	[321]
NH_2CH_3		ca. 6	[853]	imidazole		4.7	[625]	imidazole		1.04	[851]
histidine		5.8	[854]	SO_3^{2-}		4.6	[787]	pyridine		0.95	[855]
NO_2^-		5.5(1)	[856]	imidazole		4.1	[857]	*N*-Me imidazole		0.70	[851]
N_3^-		4.9(1)	[856]	NH_2CH_3		3.4	[853]	N_3^-		0.62	[321]
imidazole		4.63(7)	[856]	NH_3		3.35	[625]	NH_3		−0.7	[855]
$SeCN^-$		3.93(3)	[856]	NH_2CH_3		3.4	[858]	ethanolamine		−1.5	[851]
$S_2O_3^{2-}$		3.86	[757]	NH_2OH		2.5	[858]	imidazole	$C_2H_5^-$	−0.5	[859]
HS^-		3.83	[517]	NH_2NH_2		3.1	[858]	imidazole	$C_3H_7^-$	−1.0	[851]
SCN–		3.4(2)	[856]	$NH(CH_3)_2$		2.0	[853]	4-NH_2 pyridine	benzyl	0.96	[321]
isonazid		3.02(2)	[860]	$N(CH_3)_3$		≈0	[853]	imidazole		0.85	[321]
OCN^-		2.72	[757]	pyridine		2.6	[625]	4-Me pyridine		0.78	[321]
pyridine		1.23(7)	[856]	pyridazine		2.6	[858]	pyridine		0.72	[321]
$CH_3CO_2^-$		0.65	[787]	4-aminopyridine		4.6	[858]	N_3^-		0.64	[321]
				4-$N(CH_3)_2$pyridine		4.8	[858]	4-NH_2 pyridine	neopentyl	−0.96	[321]
				MeNC		2.8	[787]	imidazole		−0.28	[859]
				N_3^-		2.7	[787]	pyridine		−1.4	[321]
				benzimidazole		2.3	[625]	imidazole	isopropyl	< −2	[859]
				SCN^-		2.08	[852]	imidazole	cyclohexyl	< −2	[859]

Table 12
Illustrative examples of the thermodynamic trans Influence in the ligand substitution reactions on Co(III) in the cobalt corrinoids[a].

Y	Z	X	log *K*	Ref	Y	Z	X	log *K*	Ref
bzm	CN^-	CN^-	4.89(3)	[736]	H_2O	N_3^-	bzm	4.9(1)	[856]
		CCH^-	2.7	[331]			OH^-	3.45	[570]
		$CHCH_2^-$	0.7	[331]			CN^-	2.7	[787]
		CH_3^-	0.1	[331]			CH_2CH^-	0.68	[787]
					H_2O	SCN^-	H_2O	4.03	[117]
H_2O	CN^-	H_2O	≥14	[331]			bzm	3.15(3)	[485]
		bzm	14.1	[444]			OH^-	2.79	[117]
		CN^-	6.25(6)	[852]			SCN^-	2.13	[117]
		Me	3.0(2)	[331]					
		CCH^-	≥ 6.8	[188,862]	H_2O	SO_3^{2-}	H_2O	≈11	[787]
							bzm	7.3	[787]
H_2O	NH_3	H_2O	≥ 9	[625]			CN^-	4.6	[787]
		bzm	7	[625]					
		CN^-	3.35	[625]	H_2O	*N*-methylimidazole	OH^-	6.06	[570]
		SO_3^{2-}	ca. 0.6	[625]		imidazole	CN^-	3.10(2)	[861]
		CH_3^-	< −0.7	[855]			SO_3^{2-}	1.23(2)	[861]
		$CHCH_2^-$	−0.06	[853]			$CHCH_2^-$	1.15(2)	[861]

[a]Substitution of Y by Z trans to X (Eq. 29).

7.3.5. *Insights from DFT calculations*

DFT calculations are useful in providing insight into these data. Calculations using the BP86 functional reproduce the experimentally observed axial bond lengths in [MeCbl], [AdoCbl], [CNCbl] and [HOCbl] quite well [709]. For example, a BP86/def2-SVP level energy minimization using the COSMO solvation model ($\varepsilon = 80$) gave the Co—C bond length as 2.032 Å and the Co—N_{bzm} bond length as 2.206 Å in [AdoCbl]. The average Co—C bond length in six structures of [AdoCbl] and closely-related compounds is 2.016(22) Å while the Co—N_{bzm} bond length is 2.224(18) Å. The computational values fall well within the experimental ranges observed.

Interesting insights have been provided [158,187,194]. An increase in the steric bulk of a β alkyl ligand causes an increase not only in the Co—C_β bond length, but also in the Co—N_{trans} bond length, as the steric interaction between the β ligand and the corrin macrocycle itself induces a steric interaction between the macrocycle and the trans α ligand [194]. A study of the properties of the Co—C bond in phenylvinylcobalamin using a quantum theory of atoms in molecules (QTAIM) analysis [869,870] at the bond critical point from the wavefunction generated by BP86/TZVP modelling, and which reproduced the solid state structure reasonably well [133], showed the bond has significant elipticity, which is diagnostic of multiple bond character [871]. Thus both steric and electronic effects will be factors affecting the coordination sphere in a cobalt corrinoid [158,194].

In a comprehensive study to determine the origin of the normal and inverse trans influence in the cobalt corrins, Kozlowski and co-workers used the BP86 functional to calculate the equilibrium geometry of 28 alkylcobalamins in the gas phase [187]. All corrin side chains were truncated to H so results will be insensitive to interactions between the axial ligands and the side-chains. Nevertheless, the coordination sphere of the metal was reasonably well reproduced. Using a range of alkyl and fluoroalkyls as β ligand, where the donor atom to Co was an sp^3 C atom, they reproduced the inverse trans influence that is observed experimentally (Fig. 24).

They then focussed on two sets of ligands. In the first set (—CH_3; —CH_2CH_3; —$CH(CH_3)_2$; —$C(CH_3)_3$), both the donor ability and the steric bulk increase across the series, whereas in the second set (—$C(CN)_3$, —$CCl(CN)_2$, —$CCl_2(CN)$, —CCl_3), the steric bulk is relatively constant while the electron withdrawing ability increases.

An analysis of the Kohn-Sham orbitals of the complexes in this study showed that three MOs, a linear combination of Co d_z2, C p_z and N_{trans} p_z, and their mixing with corrin π orbitals, Co d_{xy} and N_{trans} p_x and p_y, could be used to rationalise the inverse and normal trans influence. In agreement with a previous study [188], it was found that increasing the

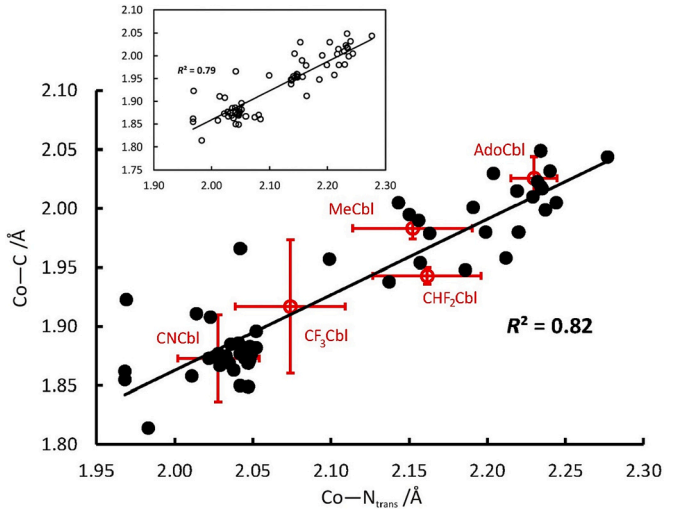

Fig. 26. Correlation between the crystallographically Co—C bond length and the Co—N_{bzm} bond lengths in [RCbl]'s where R is CN^- or a ligand with an sp^3 C as donor atom. The insert shows data for all [RCbl]'s where the ligand X has C as donor atom.

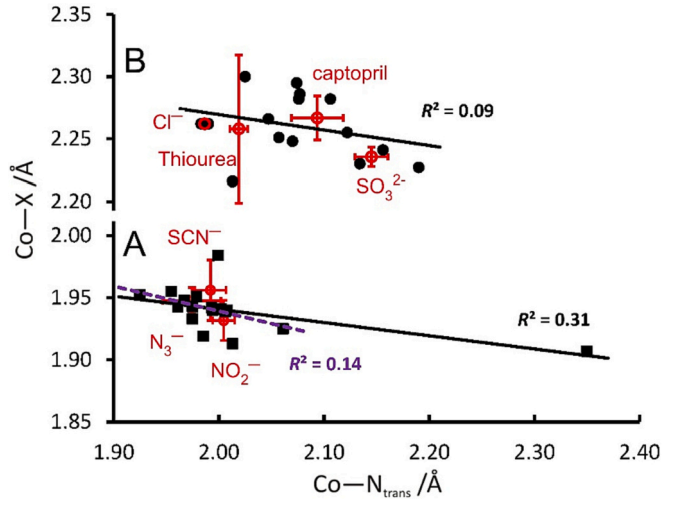

Fig. 27. Correlation between the Co—X bond length (where (A) X has O or N as donor atom and (B) where X has P, S or Cl as donor atom) in [XCbl]'s at the Co—N_{bzm} bond length.

σ donor ability of the β ligand raises the energies of several of these MOs, diminishing the extent of the bonding and hence causing an elongation of the axial bond lengths. However, as steric bulk increases, an orbital which has strong anti-bonding character between the metal and the axial ligands decreases in energy. The increase in steric interaction weakens the overlap between Co d_z2 and both C p_z and N_{trans} p_z, which diminishes the anti-bonding character of the orbital. There is therefore an interplay between electronic and steric effects.

For the second set, steric effects are minimal and the effect is virtually entirely electronic. An increase in the electron-withdrawing power of the ligands increases the positive charge on the metal; this in turn causes an attraction of the nitrogenous base but a repulsion of the alkyl group, i.e., a normal trans influence is seen.

They concluded that the reason a normal trans influence has not been observed in the experimental data for alkylcobalamins is that complexes which would show this effect have yet to be prepared and their structures determined.

Based upon this, it is probably reasonable to conclude that the trans influence seen in the data in Table 12 does indeed have its origins largely in electronic effects, and that the donor power of one ligand causes the bonding to the trans ligand to weaken.

7.3.6. *Steric effects of the corrin*

The nature of the side chains of the corrin will affect log *K* values for substitution of coordinated H_2O by an exogenous ligand. This is probably a steric effect, although the possibility of hydrogen bonding between, for example, the *c* side chain amide and H_2O coordinated on the β face of the corrin should not be underestimated. The value of log *K* for the coordination of imidazole by aquacyanocobinamide (amide side chains), 4.14, decreases to 3.95 for coordination by aquacyanocobester (methyl ester side chains), and to 3.57 when the side chains are propyl esters [625,845,872,873]. Electrostatic effects are also important, of course. For example, the value of log *K* for coordination of CN^- by aquacyanocobinamide, aquacyanocobester and aquacyanocobyrinic acid (carboxylate side chains) decreases from 6.25(6), to 6.13(5), and to 5.1(4) (21 °C, pH 7.5) as the interaction of coordinated CN^- changes from an attractive interaction with an amide side chain(s), to a hydrophobic interaction, and then to a repulsive interaction [852].

As mentioned several times, cobalt corrinoids such as cobinamides, with two different axial ligands X and Y, will exist in solution as diastereomers, [(β-X-α-Y)Cbi], and [(β-Y-α-X)Cbi] and they may interconvert [874,875]. They are readily prepared from [CNCbl] by, for example, treatment with CF_3SO_3H [876].

The thermolysis of the Co—C bond of an alkylcobinamide leads to formation of a [Co(II)][R$^\bullet$] solvent-caged pair [316,317,382,383,877,878]. The viscosity-dependence of the thermolysis reactions allows for an estimation of the ratio of the in-cage recombination rate constants to the α and β faces, k_c^α/k_c^β. In the case of $R = NCCH_2^-$, $k_c^\alpha/k_c^\beta = 2.6(6)$, which predicts a kinetically-controlled product distribution of 72%:28% of the α and β diastereomers, respectively, in excellent agreement with the 73%:27% observed for the oxidative addition of $NCCH_2Br$ to cob(II)inamide [874].

The two faces of the corrin have different steric demands; the upper face, with three acetamide side chains, is less sterically crowded than the lower face with its four propionamide side chains. These different steric demands have been demonstrated by the kinetics of the formation and the decomposition of α- and β-alkylCbi$^+$s [559,879–881]. The interconversion of α- and [β-$NCCH_2$Cbi]$^+$ shows that coordination to the α face is thermodynamically favoured by 7.5 kJ mol^{-1} but entropically disfavoured by 35 J K^{-1} mol^{-1} so that $K = 3.3$ at 25 °C for the $\alpha \rightarrow \beta$ conversion [880]. The entropic effect arises from the thermal mobility of the side chains [559,879,881]. The determination of binding constants for coordination of imidazole and pyridine to α- and [β-$NCCH_2$Cbi]$^+$ as a function of temperature confirmed that the α coordination site is enthalpically preferred but this has a larger negative value of ΔS [882]. The interplay between the two factors means that log *K* for coordination of pyridine in the α coordination site is larger than for coordination to the β site (1.26 compared to 0.93, based on the values of ΔH and ΔS determined from the temperature dependence of *K* between 5 °C and 45 °C) but the converse is true for imidazole (1.44 vs 1.96). Qualitatively similar results were obtained in the case of α- and [β-CF_3Cbi]$^+$, although entropy changes were found to be positive (Table A1 of the Appendix). The sterically more demanding $NCCH_2^-$ ligand overrides the preference of the nitrogenous bases for the sterically less crowded β coordination site.

By manipulation of the reaction conditions, the kinetically-controlled product distribution of the addition of $CH_3CH_2^\bullet$ (produced from the Fenton-like reaction of a Co(II) corrinoid and $Et(CH_3)_2COOH$, section 5.2.4) to a Co(II) corrinoid (cobinamide or 3,5,6-((CH$_3$)$_3$benzimidazolyl)cobamide) could be studied, and the differential enthalpies and entropies of activation for formation of the two diastereomers determined [559]. Under these conditions, 87% of the α diastereomer is produced, whereas under equilibrium conditions there is <2% present [883]. Use of corrinoids with altered side chains showed the importance

of entropic factors due to differential side chain motion in controlling the product distribution [559].

7.3.7. The Cis influence

A number of ways of assessing the effect the corrin macrocycle has on the properties of Co(III) suggest themselves. One way is to perturb the electronic structure of the corrin; a second is to interrupt the 13-atom 14-π electron conjugated system of the corrin; a third is to cleave the macrocycle itself; and a fourth is to compare the properties of Co(III) in the corrins to its properties in other macrocyclic complexes but in which the inner coordination sphere of the metal bears a close resemblance to that in the cobalt corrinoids. The effect of these factors on equilibrium constants for substitution of H_2O is reviewed here; the consequences for the kinetics of the ligand substitution reactions are discussed later in this review.

Shown in Fig. 28 is the structure of (A) the standard corrin as in $[H_2OCbl]^+$, with the substituent at C10 marked as R; (B) cobyrinic acid heptamethyl ester, the cobester, [Cbs], again with the substituent at C10 marked as R; (C) (5*R*,6*R*)-5,6-dihydro-5-hydroxy-heptamethylcob(III) yrinate-c,6-lactone, or the stable yellow cobester, [SYCbs] [884–886]; (D) 5,6-dioxo-5,6-seco-heptamethyl-cob(III)yrinate, the 5-seco cobester, [5-secoCbs], in which the corrin ring has been cleaved between C5 and C6 [780,781]; (E) [10-(2-[[4-(1H-imidazol-1-ylmethyl)benzoyl]amino]-phenyl)-5,15-diphenylcorrolato]-cobalt(III), [DPTC-Co], a Co(III) corrole model for $[H_2OCbl]^+$ [111]; and (F) the 8 amino acid porphyrin-containing fragment obtained from the proteolysis of cytochrome *c*, referred to as *N*-acetylmicroperoxidase 8 ([NAcMP8]), and in which Fe (III) has been replaced by Co(III), [NAcCoMP8] [111,887].

Perhaps the simplest modification that can be made to the electronic structure of a corrin is to replace the C10H with a substituent. The red shift in the main bands in the uv-vis spectrum of $[H_2OCbl]^+$ on substituting the C10H with Cl or Br (from 351, 527 and 554 nm in $[H_2OCbl]^+$ to 355, 536 and 558 nm in $[H_2O\text{-}10ClCbl]^+$ [856] and to 356, 539 and 555 nm in $[H_2O\text{-}10BrCbl]^+$ [231,771] [231]) confirm that Cl and Br are resonance donating towards corrin. The substitution of C10H by Br alters the electronic structure of the ring and leads to differences between the resonance Raman spectra of [CNCbl] and [CN-10BrCbl] [151]. Available values of log *K*, which refer to Eq. 30, and in which charges are omitted for convenience, are given in Table 13.

$$L + [H_2O\text{-}10RCbl] \rightleftharpoons^{K} [L\text{-}10RCbl] + H_2O \quad (30)$$

The results compiled in Table 13 show that substitution of H by Cl or Br at C10 moderately favours the coordination of anionic ligands (log *K* increases by between 0.6 in the case of $S_2O_3^{2-}$ and 0.1 in the case of CNO^-) but decreases the affinity for neutral N-donor ligands (log *K* decreases by between 0.2 and 0.3). DFT calculations (BP86/TZVP) and an examination of the properties of the electron density using Bader's QTAIM model [869,870] on model complexes (all corrin substituents replaced by H; bzm modelled with imidazole) showed [231] that on changing the C10 substituent R from H to Cl or Br (i) the charge on the corrin nucleus (the 13 atoms of the macrocycle and Co) become more positive, while there is minimal effect on the imidazole axial ligand, and this is more pronounced with an anionic rather than neutral β ligand; (ii) Co becomes more electron-rich, an effect that is more marked if the β ligand is neutral; (iii) the charge on the donor atom of the β ligand becomes more negative; and (iv) an anionic β ligand causes the charge on

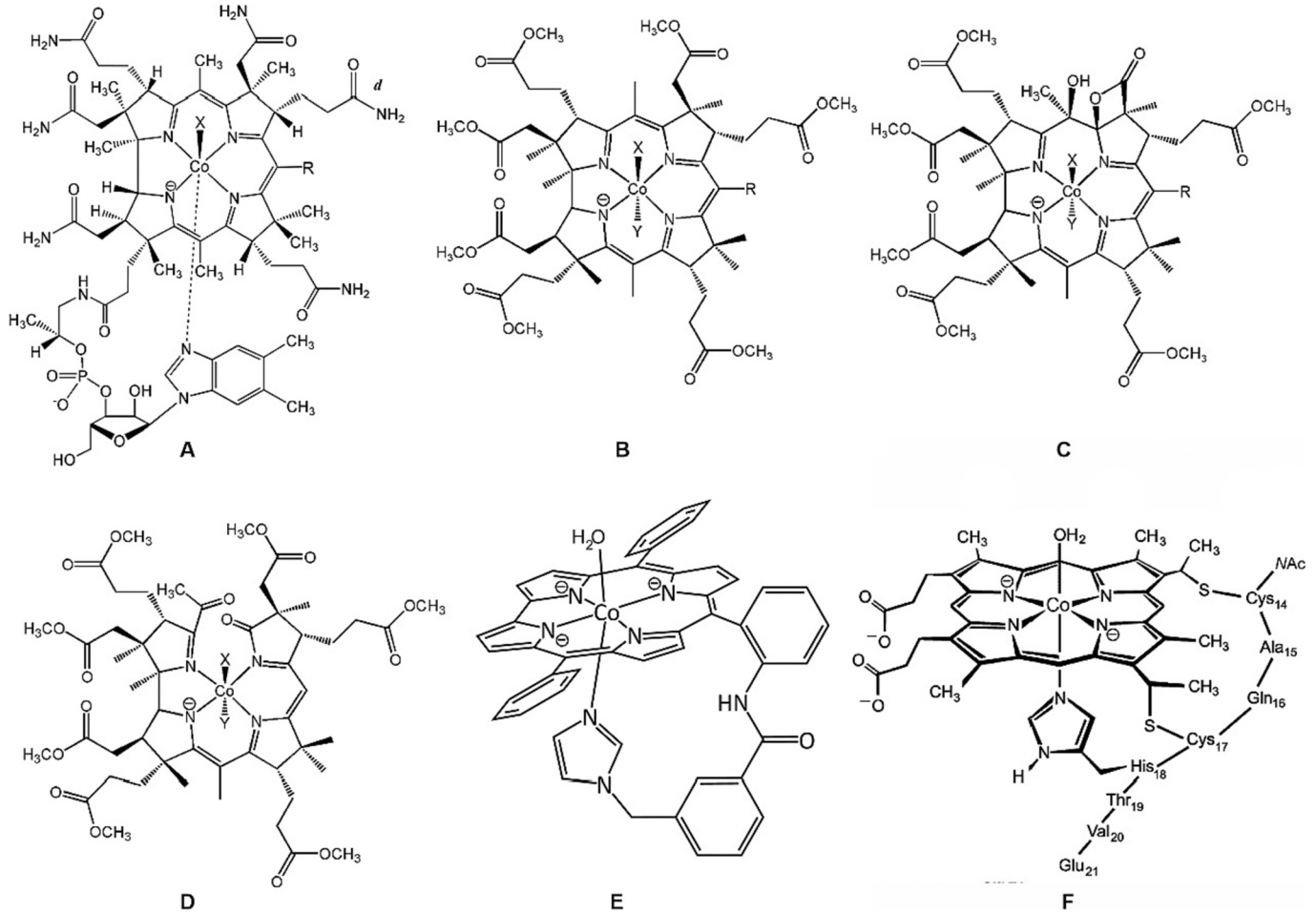

Fig. 28. Co(III) complexes that have been used to assess the cis influence of the corrin macrocycle on the chemistry of the Co(III)-axial ligand system (see text).

the C10 substituent R to become more negative, an effect that increases as R changes from H to Cl to Br. These effects suggest that when R = Cl or Br, $[H_2O\text{-}10RCbl]^+$ will disfavour coordination of a neutral ligand compared to an anionic ligand because the corrin nucleus is more positive, and Co is more electron-rich, hence less capable of accepting charge density from the axial donor. If the ligand is an anion, binding to the metal will be favoured because of electrostatic interaction with the corrin; moreover, charge donation by that ligand can be accepted by the corrin and be delocalised onto the C-10 R. Anions are therefore bound more favourably by $[H_2O\text{-}10RCbl]^+$, R = Cl or Br, than by $[H_2OCbl]^+$ itself, R = H.

These rationalisations help explain why there is a small, but significant, decrease in the pK_a of coordinated H_2O when R = Cl or Br (Table 13): since anionic OH^- coordinates preferentially to the 10-Cl and 10-Br derivatives, it will be a poorer Lewis base towards H^+.

Values of log *K* for substitution of H_2O trans to CN^- in cobester complexes of the type $[(H_2O)(CN)\text{-}10RCbs]^+$ (and which are for equilibrium mixtures of the α-H_2O,β-CN^- and β-H_2O,α-CN^- diastereomers) are given in Table 14.

The extent of the perturbation of the electronic structure of the corrin in now more pronounced. The NO_2 group is strongly electron-withdrawing (Hammett para constant, $\sigma_p = 0.78$ [789], and confirmed by the shift of the γ band from 354 nm to 345 nm), while NH_2 is electron-donating ($\sigma_p = -0.66$ [789], γ band at 371 nm).

There is a large error in the pK_as of these compounds because of hydrolysis of the ester groups of the corrin side chains, and no conclusions can be drawn as the values are unreliable. From DFT calculations (BP86/TZVP) and QTAIM analyses of the wavefunction, it was found that the metal becomes more positively charged, and hence harder, as R is varied from NH_2 to H to NO_2. Whilst $[(H_2O)(CN)\text{-}10NH_2Cbs]^+$ and $[(H_2O)(CN)Cbs]^+$ have a similar affinity for virtually all ligands, $[(H_2O)(CN)\text{-}10NO_2Cbs]^+$ has a lower affinity for the soft anions CN^- and SO_3^{2-} as well as 4-*N*,*N*-dimethylimidazole and imidazole, a similar affinity for CH_3NH_2, but a much higher affinity for the harder anions SCN^-, N_3^- and NO_2^-.

The values of log *K* listed in Tables 13 and 14 provide clear evidence that perturbing the electronic structure of the corrin by varying the substituent at C10 can have a significant effect on the ligand substitution reactions of Co(III), and are an illustration of the importance of cis effects in the chemistry of the cobalt corrinoids.

The reduction potentials of C10-modified aquacyanocobesters in acetonitrile as determined by cyclic voltammetry on a glassy carbon electrode are shown in Table 15 [666].

Given the electron-donating properties of C10Cl and C10Br towards the corrin (see above), the reduction potential of $[(CN)(H_2O)Cbs]^+$ shifts to less negative potentials, i.e., Co(II) and Co(I) becomes more accessible. It is surprising though, given the strong electron-donating properties of $C10NH_2$, that its reduction potential is not less negative. The markedly more negative potential of the $C10NO_2$ derivative is in line with the strong electron-withdrawing properties of this substituent, i.e., the Co(III) state is favoured in the case of the aquacyanocobester. However, this does not apply to the dicyanocobester for reasons that are not obvious.

Other ways of perturbing the electronic structure of the corrin are to interrupt the conjugation of the native macrocycle (for example, to form the so-called stable yellow cobester, Fig. 26C) or, more extreme, to actually cleave the corrin ring (as in the 5-seco-cobester of Fig. 26D). In [SYCbs] the C5 carbon is oxidized and the *c* side chain cyclized to form a lactone at C6; the 13 atom, 14 π-e^- delocalised system of the corrin is interrupted, giving a triazamethine system with four conjugated double bonds between N2 and N4 and an isolated double bond between N1 and C4.

A comparison of the ^{59}Co NMR resonance of $[(CN)_2Cbs]$ and $[(CN)_2SYCbs]$ with available ^{59}Co data for analogous systems suggests that the more π-conjugated corrin of $[(CN)_2Cbs]$ interacts more strongly with the metal than the less extensively conjugated macrocycle of $[(CN)_2SYCbs]$ [886]. Moreover, as the interaction between Co(III) and the equatorial macrocycle increases, ν_{CN} of axially coordinated CN^- shifts to lower frequency. The uv-vis spectral data and DFT-calculated MOs (at the PBE1PBE/6-311G(d,p) level of theory) are consistent with greater overlap between the corrin and the metal orbitals in $[(CN)_2Cbs]$ than in $[(CN)_2SYCbs]$, which gives the metal in the former a softer, more

Table 13
Equilibrium constants for the substitution of H_2O trans to bzm by incoming L in $[H_2O(10\text{-}R)Co]^+$.

L	R	log *K*[a]	Ref	L	R	log *K*[a]	Ref
OH^-	H	7.62[b]	[111]	$SeCN^-$	H	3.77(2)	[856]
	Cl	7.22[b]	[231]			3.92	[757]
	Br	7.28[b]	[231]		Cl	3.93(3)	[856]
CH_3NH_2	H	5.12(8)	[856]	SO_3^{2-}	H	4.10(8)	[231]
	Cl	4.82(6)	[856]		Cl	4.45(7)	[231]
imidazole	H	4.63(7)	[856]		Br	4.72(7)	[231]
	H	4.59	[888]	$SeCN^-$	H	3.77(2)	[856]
	Cl	4.32(7)	[856]			3.92	[757]
	Br	4.27(5)	[231]		Cl	3.93(3)	[856]
pyridine	H	1.23(7)	[856]	$S_2O_3^{2-}$	H	3.72(2)	[856]
	Cl	1.0(1)	[856]			3.76	[889]
4-*N*,*N*-$(CH_3)_2$aminopyridine	H	3.8(2)	[231]			3.86	[757]
	Cl	3.5(2)	[231]		Cl	4.35(5)	[856]
	Br	3.5(2)	[231]	SCN^-	H	3.21(3)	[231]
NO_2^-	H	5.32(6)	[231]			3.03(5)	[856]
		5.34(3)	[856]			3.36	[888]
		5.3	[787]			3.11	[889]
		5.93	[890]			3.08	[757]
	Cl	5.5(2)	[231]		Cl	3.29(6)	[231]
		5.5(1)	[856]			3.4(2)	[856]
	Br	5.8(1)	[231]		Br	3.26(4)	[231]
N_3^-	H	4.68(7)	[231]	CNO^-	H	2.57(4)	[856]
	Cl	4.85(3)	[231]			3.00	[888]
		4.97(8)	[856]			2.63	[889]
	Br	4.84(6)	[231]			2.72	[757]
SO_3^{2-}	H	4.10(8)	[231]		Cl	2.67(7)	[856]
	Cl	4.45(7)	[231]				
	Br	4.72(7)	[231]				

[a]25 °C unless otherwise indicated. [b]pK_a, 25 °C, $\mu = 0.50$ M, Na_2SO_4.

Table 14
Equilibrium constants for the substitution of H_2O trans to CN^- by incoming L in aquacyano-10Rcob(III)ester.

L	R	log $K^{a,b}$	ΔH /kJ mol^{-1}	ΔS /J K^{-1} mol^{-1}	Ref
OH^-	H	10.6	86(10)	85(34)	[891]
	NH_2	10.4	89(11)	100(39)	[891]
	NO_2	10.2	84(11)	87(39)	[891]
CH_3NH_2	H	3.2(1)			[891]
	NH_2	3.52(7)			[891]
	NO_2	3.13(6)			[891]
imidazole	H	4.66(6)			[891]
	NH_2	4.5(2)			[891]
	NO_2	4.37(4)			[891]
4-*N*,*N*-$(CH_3)_2$aminopyridine	H	4.97(3)			[891]
	NH_2	4.9(2)			[891]
	NO_2	2.91(9)			[891]
CN^-	H	6.13(5)[c]			[852]
		6.44(3)[d]			[852]
		9.05	−63(4)	−38(14)	[781]
		8.26	−23(2)	81(6)	[892]
		9.6(1)			[891]
	NH_2	10.0(3)			[891]
	NO_2	7.39(8)			[891]
NO_2^-	H	3.11	−21(3)	−11(10)	[781]
		2.88	−6.6(9)	33(3)	[892]
		4.2(1)			[891]
	NH_2	4.8(2)			[891]
	NO_2	5.22(3)			[891]
N_3^-	H	2.80	−16(2)	0(6)	[781]
		2.59	−9.4(7)	13(3)	[892]
		3.55(3)			[891]
	NH_2	4.27(7)			[891]
	NO_2	4.53(9)			[891]
SO_3^{2-}	H	6.13	10(2)	151(6)	[781]
		5.08	50(3)	265(9)	[892]
		7.94(6)			[891]
	NH_2	8.6(1)			[891]
	NO_2	6.04(6)			[891]
SCN^-	H	3.16(3)			[891]
	NH_2	3.1(2)			[891]
	NO_2	3.9(1)			[891]

[a]25 °C unless otherwise indicated. Log *K* values interpolated from values of ΔH and ΔS where available. [b] In 50% aqueous isopropanol unless otherwise indicated. [c]pH 7.5; 21 °C. [d]pH 9.5; 21 °C.

Table 15
Reduction potentials of C10-substituted aquacyanocobesters.

C10 subst	Redox couple[a]			
	$CNCo^{3+}OH_2$| $Co^{2+}OH_2$	$Co^{2+}OH_2$| Co^+	$CNCo^{3+}CN$| $Co^{2+}CN$	$Co^{2+}CN$| Co^+
H	−0.23	−0.44	−1.10	−1.31
Br	−0.15	−0.34	−0.98	−1.19
Cl	−0.14	−0.33	−0.93	−1.14
NH_2	−0.19	−0.42	−1.10	−1.34
NO_2	−0.28	–	−1.07	−1.33

[a]in V vs SHE; only axial ligands given.

covalent character [886].

The corrin cavity is quite small; the average diagonal N—N distance across the cavity in all Co(III) corrins is 3.79(4) Å [781] and is significantly smaller than the 3.92(4) Å found in Co(III) porphyrins (although the ability of corrin to accommodate larger metal ions, see Section 2.4, should be kept in mind). The small cavity size seems ideal for accommodating low spin Co(III) [893], but it is possible that Co(III) is in a compressed state in a corrin macrocycle; if so, this is very likely to significantly impact its chemistry [894]. Cleavage of the corrin ring, as achieved in [5-secoCbs] will relieve this putative strain. Values of log *K* for substitution of H_2O trans to CN^- in $[(H_2O)(CN)SYCbs]^+$ and in $[(H_2O)(CN)5\text{-seco-Cbs}]^+$ are collected in Table 16.

Focusing first on the ionic ligands listed in Table 16, it is clear that, consistent with the conclusion that Co(III) is softer in $[ACCbs]^+$ than in $[ACSYCbs]^+$ as a consequence of interruption of the delocalised π system in the latter, the results show that the ligands with a harder donor atom (N in N_3^- and NO_2^-) produce ΔH values that are more negative in their reactions with $[ACSYCbs]^+$ than with $[ACCbs]^+$. If the donor atom is softer (C in CN^-; S in $SO_3^{2-}$and $S_2O_3^{2-}$) then ΔH is less positive, or more negative, for reactions with $[ACCbs]^+$ than with $[ACSYCbs]^+$. The softer metal in $[ACCbs]^+$ has a preference for softer ligands and the harder metal in $[ACSYCbs]^+$ for the harder ligands.

The results with neutral ligands (Table 16) confirm the trend. Substitution of H_2O by the aliphatic amines with a harder donor atom produce ΔH values that are more negative in their reactions with $[ACSYCbs]^+$ than with $[ACCbs]^+$, while the softer, aromatic N donors produce more negative ΔH values with $[ACCbs]^+$ than with $[ACSYCbs]^+$. Modelling (DFT, M06L/SVP, and a QTAIM [869,896] analysis of the electron density) shows that complexes of the aliphatic amines with the stable yellow cobester produce shorter and stronger Co—N bonds with less ionic character than the Co—N bonds of these ligands with the cobester. Conversely, the Co—N bond to the aromatic N donors are found to be shorter, stronger, and somewhat less ionic in the complexes of the cobester than in those of the stable yellow cobester. The distinction between the harder Co(III) in $[ACSYCbs]^+$ and softer Co(III) in $[ACCbs]^+$ seen for the anionic ligands is maintained for neutral N-donor ligands.

Cleavage of the corrin between C5 and C6 to form $[(H_2O)(CN)5\text{-seco-Cbs}]^+$ ($[AC5\text{-seco-Cbs}]^+$) has a very marked effect on the pK_a of coordinated H_2O, decreasing it from ca. 10–11 in $[ACCbs]^+$ and in $[ACSYCbs]^+$ (the precise values are uncertain because of hydrolysis of the ester side chains in alkaline solution) to 7.28 at 25 °C. By comparison, the pK_a of H_2O coordinated to Co(III) in complexes such as [Co

Table 16
Equilibrium constants for the substitution of H_2O trans to CN^- by incoming L in Co(III) corrinoids.

L	Corrinoid	log K[a]	ΔH /kJ mol^{-1}	ΔS /J K^{-1} mol^{-1}	Ref
OH^-	cobester[b]	9.8[e]			[781]
		10.6[e]			[891]
	SYCbs[c]	≈ 11[e]			[892]
	5-seco-Cbs[d]	7.28[e]	−88(17)	−434(56)	[781]
CN^-	cobester	9.05	−63(4)	−38(14)	[781]
		8.26	−23(2)	81(6)	[892]
	SYCbs	7.16	−17(1)	80(5)	[892]
	5-seco-Cbs	5.38	−93(5)	−209(18)	[781]
NO_2^-	cobester	3.11	−21(3)	−11(10)	[781]
		2.88	−6.6(9)	33(3)	[892]
	SYCbs	2.34	−22.9(4)	−32(2)	[892]
	5-seco-Cbs	2.40	−82(3)	−229(11)	[781]
N_3^-	cobester	2.80	−16(2)	0(6)	[781]
		2.59	−9.4(7)	13(3)	[892]
	SYCbs	2.63	−18.6(7)	−12(2)	[892]
	5-seco-Cbs	2.96	−44(5)	−91(15)	[781]
SO_3^{2-}	cobester	6.13	10(2)	151(6)	[781]
		5.08	50(3)	265(9)	[892]
	SYCbs	2.88	59(1)	253(5)	[892]
	5-seco-Cbs	3.83	−83(10)	−205(33)	[781]
$S_2O_3^{2-}$	cobester	0.69	36(6)	134(19)	[781]
		0.50	21(3)	80(10)	[892]
	SYCbs	0.6(2)			[892]
	5-seco-Cbs	1.55	32(9)	137(30)	[781]
NH_3	cobester	2.75	−41(1)	−85(2)	[895]
	SYCbs	2.94			[895]
NH_2EtOH	cobester	1.91	−24(2)	−44(7)	[895]
	SYCbs	1.52			[895]
NH_2EtOMe	cobester	1.84	−51.2	−136(8)	[895]
	SYCbs	1.70			[895]
4MeIm[f]	cobester	4.29	−23(1)	5(4)	[895]
	SYCbs	1.56			[895]
4Mepy[f]	cobester	3.36	−29(2)	−33(8)	[895]
	SYCbs	0.38			[895]
4MeOpy	cobester	3.33	−25(1)	−19(3)	[895]
	SYCbs	g			[895]
$CF_3CH_2NH_2$	cobester	0.4[h]			[895]
	SYCbs	<−2[h]			[895]
NH_2OMe	cobester	1.93 (3)			[895]
	SYCbs	i			[895]

[a]25 °C unless otherwise indicated. Log K values interpolated from values of ΔH and ΔS where available. [b]Cobyrinic acid heptamethyl ester. [c](5*R*,6*R*)-aquacyano-5,6-dihydro-5-hydroxy-heptamethylcob(III)yrinate-*c*,6-lactone, or aquacyano-stable yellow cobester. [d]aquacyano-5,6-dioxo-5,6-seco-heptamethylcob(III)yrinate. [e]pK_a of coordinated H_2O. [f]Im = imidazole; py = pyridine. [g]Very slow reaction; no reliable value obtained. [g]Estimated. [i]Slow destruction of the corrin observed; no reliable value of log K obtained.

$(H_2O)_6]^{3+}$ (2.9 [897]), $[Co(cyclen)(H_2O)_2]^{3+}$ (cyclen = 1,4,7,11-tetraazacyclododecane; 5.6 [898]), and $[Co(NH_3)_5(H_2O)]^{3+}$ (6.36 [899]) may be noted. The pK_a of Co(II) complexes is significantly higher (9.7 in $[Co(H_2O)_6]^{2+}$ [900] and ≈ 12.1 in $[Co(Py5)(OH_2)]^{2+}$, Py5 = 2,6-(bis(bis-2-pyridyl)-methoxymethane)pyridine) [901]), reflecting the lower polarization of the O—H bond of coordinated H_2O by the metal ion. The pK_a values are clear evidence that Co is much less polarizing in $[ACCbs]^+$ than in $[AC5\text{-}seco\text{-}Cbs]^+$, or, it could be argued, the metal ion has acquired some Co(II) character in $[ACCbs]^+$.

A comparison of log K values for coordination of CN^-, SO_3^{2-}, NO_2^-, N_3^- and $S_2O_3^{2-}$ by $[ACCbs]^+$ and $[AC5\text{-}seco\text{-}Cbs]^+$ shows that cleavage of the corrin ring significantly decreases the affinity of Co(III) for the softer ligands CN^-, SO_3^{2-} and, more marginally, NO_2^-. However, $[AC5\text{-}seco\text{-}Cbs]^+$ has a higher affinity for N_3^- and $S_2O_3^{2-}$ than $[ACCbs]^+$. The observed trend in log K values correlates with the position of the ligands in the spectrochemical series ($N_3^- < S_2O_3^{2-} < NO_2^- < SO_3^{2-} < CN^-$). N_3^- and $S_2O_3^{2-}$ are π donors; the others are π acceptors. When the corrin is cleaved, the hardness of the metal ion increases and this decreases its affinity for π acceptors. The stability of its complexes with π donors increases as the metal ion becomes more Co(III)-like, and more capable of accepting electron density from the ligand. The temperature-dependence of log K values show very negative values for ΔH offset by ΔS values which are also large and negative.

It is unfortunate that the crystal structures of a 5-seco-cobester is not available. DFT modelling (BP86-D3/6-311G(d,p)) suggests that cleavage of the corrin does not unduly perturb the coordination sphere of the metal ion and it essentially retains an octahedral coordination geometry [781]. A QTAIM analysis of the topological properties of the electron density indicated that the sum of the partial charges on the metal and the entire coordination sphere, or the metal and the four equatorial donor N atoms, is less negative in the 5-seco-cobester complexes than in the cobesters themselves and supports the conclusion that cleavage of the corrin has made the metal and its immediate environment more positive. The cleavage of the corrin causes the bond lengths to the equatorial N donors closest to the site of ring cleavage to increase and permits a closer approach of the axial ligand to the metal ion. This rationalises the very negative ΔH values for substitution of H_2O by incoming L (Table 16). Generally, values of ΔS are also very negative, offsetting the enthalpic drive to complex formation.

There are several notable differences between corrins, corroles and porphyrins. Firstly, the corrin, porphyrin and corrole macrocycles, when coordinated to a metal, carry −1, −2 and − 3 formal charges, respectively; in the +3 oxidation state of Co, the immediate coordinate sphere of the metal ion in $[H_2OCbl]^+$ and its porphyrin and corrole analogues (Fig. 26) has a formal charge of +2, +1, and 0, respectively. (It is assumed that the charge on the phosphate in the cobalamins, some 9 Å away from the metal centre, and the charge on the propionate side chains of haem *c* – between 5.5 and 8.5 Å from the metal, depending on their orientation – will have little influence on the chemistry at the metal.) Secondly, with their delocalised 18 π-electron system, porphyrins and corroles are significantly more electron rich than corrins [902–904]. Thirdly (see Fig. 32 below), the upper face of a corrin is much more sterically hindered than the corresponding faces of a porphyrin and a corrole. There is therefore likely to be an interplay between electronic and steric factors in determining the stability of complexes of these macrocycles with anionic and neutral ligands, and sterically demanding and less demanding ligands. The available values of log K for substitution of H_2O trans to bzm, or an imidazole derivative (Fig. 28) are collected in Table 17. The values are plotted in Fig. 29.

The pK_a of coordinated H_2O increases as the charge on the immediate coordination sphere of the metal ion increases, viz., from 7.462(7) in $[H_2OCbl]^+$, to 7.81(3) in [NAcCoMP8], to 9.76(6) in [DPTC-Co]. However, the effect of solvent is probably not negligible; while the values for $[H_2OCbl]^+$ and [DPTC-Co] were measured in 80% CH_3OH, the value available for [NAcCoMP8] was determined in aqueous solution. Nevertheless, a comparison of the properties of the Co—OH_2 bond using a QTAIM analysis of the wavefunction of the DFT (BP86/TZVP) energy minimised structures of models for $[H_2OCbl]^+$ and [DPTC-Co] (all substituents on corrin replaced by H; imidazole used as the α ligand) offers a rationalisation for the trend [111]. There is ample evidence that QTAIM is useful for examining the properties of the metal—ligand bond of a complex of a metal ion from the first transition series [871,907–911]. The electron density, ρ_b (given in atomic units, au, where 1 au of $\rho = 6.7483$ e Å^{-3}) and the Laplacian $\nabla^2\rho_b$ (1 au of $\nabla^2\rho_b = 24.099$ e Å^{-5}) at the bond critical point (bcp) are a measure of bond strength [912,913]. The ratio of the potential (V_b) and kinetic (G_b) energy densities at the bond critical point, $|V_b|/G_b$, gives insight into the nature of a bond. For $|V_b|/G_b > 2$, the bond is predominantly covalent in nature; for $|V_b|/G_b < 1$ the bonding is essentially ionic; and $1 < |V_b|/G_b < 2$ is characteristic of a bond of intermediate character [914].

The modelling showed that the Co—OH_2 bond in $[H_2OCbl]^+$ is shorter (2.107 Å vs 2.128 Å), stronger ($\rho_b = 0.0551$ au vs 0.0538 au; $\nabla^2\rho_b = 0.297$ au vs 0.272 au) and less ionic ($|V_b|/G_b = 1.087$ vs 1.069) than in [DPTC-Co] [111]. An increase in the ionicity of the Co—OH_2

Table 17
Equilibrium constants for the substitution of H_2O trans to an imidazole derivative, Y, by incoming L in Co(III) macrocyclic complexes.[a]

L	Y	Macrocyle	log K[b]	ΔH /kJ mol^{-1}	ΔS /J K^{-1} mol^{-1}	Ref
OH^-	bzm	corrin	7.462(7)[f,g]			[111]
	His	porphyrin	7.81(3)[f]			[890]
	(*N*-R)im	corrole	9.76(6)[f,g]			[111]
$HONH_2$	bzm	corrin	4.83	100(9)	428(30)	[890]
	His	porphyrin	5.45	−105(13)	−248(44)	[890]
CH_3ONH_2	bzm	corrin	5.79	−81(7)	−161(23)	[890]
	His	porphyrin	4.01	−64(6)	−138(20)	[890]
$HOCH_2CH_2NH_2$	bzm	corrin	3.60(5)[g]			[111]
	(*N*-R)im	corrole	5.15(2)			[111]
(*N*-CH_3)imidazole	bzm	corrin	4.49	−62(3)	−122(11)	[890]
			3.99(5)[g]			[111]
	His	porphyrin	5.70	42(3)	250(11)	[890]
	(*N*-R)im	corrole	5.32(2)			[111]
pyridine	bzm	corrin	1.23(7)			[856]
			1.00	6.2(5)	40(2)	[890]
			0.48(4)[g]			[111]
	His	porphyrin	4.94	−30(3)	−6(9)	[890]
	(*N*-R)im	corrole	4.11(2)			[111]
4- *N,N*-$(CH_3)_2$aminopyridine	bzm	corrin	3.8(2)			[231]
			3.99(2)[g]			[111]
	(*N*-R)im	corrole	5.32(2)			[111]
Thiophene	bzm	corrin	1.0(2)[g]			[111]
	(*N*-R)im	corrole	1.09(4)			[111]
Thiourea	bzm	corrin	1.1			[787]
			1.76(2)[g]			[111]
	(*N*-R)im	corrole	2.1(1)			[111]
$P(OCH_3)_3$	bzm	corrin	5.0			[818]
			4.77(7)[g]			[111]
	(*N*-R)im	corrole	11.8(1)[c]			[111]
			10.4(1)[d]			[111]
cysteine	bzm	corrin	6.0			[905]
			6.5(1)[g]			[111]
	(*N*-R)im	corrole[k]	5.7(2)			[111]
CN^-	bzm	corrin	>12			[331]
			14.1			[906]
			12.53(7)[e,g]			[111]
			11.9(5)[f,g]			[111]
	(*N*-R)im	corrole	13.1(7)[c]			[111]
	His	porphyrin	6.02	–47(2)	−42(6)	[890]
NO_2^-	bzm	corrin	5.32(6)			[231]
			5.34(3)			[856]
			5.3			[787]
			6.7(4)[g]			[111]
			5.93	−47(3)	−44(9)	[890]
	(*N*-R)im	corrole	3.0(1)			[111]
	His	porphyrin	2.88	−20(2)	−12(8)	[890]
N_3^-	bzm	corrin	4.68(7)			[231]
			4.9(1)			[856]
			4.74			[888]
			4.75			[889]
			4.9			[787]
			5.03	−29(1)	−1(3)	[890]
			6.35(5)[g]			[111]
	(*N*-R)im	corrole	2.82(2)			[111]
	His	porphyrin	2.30	−20(1)	−23(5)	
HSO_3^-	bzm	corrin	6.3	156(9)	644(31)	[890]
	His	porphyrin	3.61	22(2)	143(7)	[890]
SCN^-	bzm	corrin	3.21(3)			[231]
			3.03(5)			[856]
			3.36			[888]
			3.11			[889]
			3.08			[757]
			4.73(4)			[111]
	(*N*-R)im	corrole	1.31(5)			[111]
I^-	bzm	corrin	1.4			[856]
			3.96(2)[g]			[111]
	(*N*-R)im	corrole	2.33(3)			[111]

[a]Refer to Fig. 28 for details of the structure of the complexes. [b]25 °C unless otherwise indicated in aqueous solution unless otherwise indicated. Log K values interpolated from values of ΔH and ΔS where available. All log K values for substitution of H_2O in the corrole, and the pK_a of coordinated H_2O, were determined in 80% CH_3OH. [c]In competition reaction with 4-*N,N*-$(CH_3)_2$aminopyridine. [d]In competition reaction with pyridine. [e]In competition reaction with azide. [f]In competition reaction with nitrite. [f]The pK_a of coordinated H_2O. [g]Determined in 80% CH_3OH.

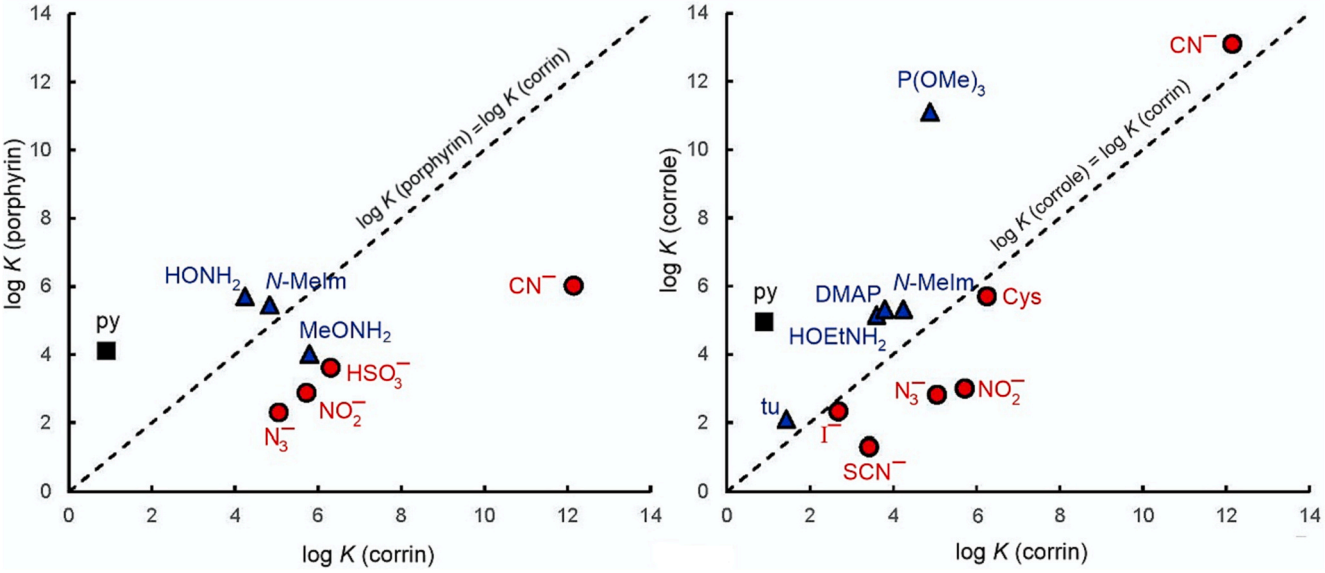

Fig. 29. Comparison of log *K* values for substitution of coordinated H_2O in (left) a Co(III) porphyrin and a Co(III) corrin, and (right) a Co(III) corrole and a Co(III) corrin (see text for details).

bond is expected to make the lone pair on coordinated OH^- more accessible to a proton from solution, hence increasing the pK_a. This effect is presumably a consequence of the differences in the positive charge on the immediate coordination sphere of the metal ion.

The equilibrium constants for substitution of H_2O by neutral and anionic ligands in corrin, porphyrin and corrole systems, collected in Table 17, are not directly comparable because of differences in the solvent used. The composition of the solvent is known to affect both the log *K* value for complex formation and (see later) the kinetics of the reaction. For example, log *K* for coordination of I^- by $[H_2OCbl]^+$ increases from 1.41 to 3.95 as the fraction of CH_3OH in varied from 0% to 100% [915]; log *K* for binding of SCN^- increases from 3.03 to 4.17 as the fraction of CH_3CN is increased from 0% to 70% [916]; but log *K* decreases from 4.32 to 3.99 for coordination of *N*-methylimidazole on going from aqueous solution to 80% CH_3OH [111]. The values in Table 17 indicate that log *K* values for neutral ligands are usually higher in aqueous solution than in 80% CH_3OH, but the converse is usually true for anionic ligands.

The broad trends (Fig. 29) are nevertheless clear. The corrin system binds anionic ligands more strongly than the porphyrin and the corrole systems, but binds neutral ligands less strongly, and the affinity trends parallel each other. The very low value of log *K* for coordination of pyridine by $[H_2OCbl]^+$, 1.00 or 1.23 in aqueous solution, 0.48 in 80% CH_3OH (Table 17) is noteworthy. There are no available crystal structures of pyridine coordinated to Co(III) in a cobalt corrinoid system. A survey of available Co(III) pyridine complexes in the CSD showed that in the relatively sterically undemanding environments of simple pentammine complexes, porphyrins, cobaloximes and corroles, the Co—N bond length to pyridine is very similar, on average 1.99(2) Å. A feature of the β face of the corrin is its steric crowding (see Fig. 30, details of which are discussed late) [211,258] where C26, C37, C46, C54 and C19H adopt sentinel-like positions to an incoming ligand. DFT modelling (BP86/TZVP [111]) produced a long Co—N bond (2.045 Å) compared to the Co—N bond length to imidazole (1.985 Å) or NO_2^- (1.966 Å). Pyridine was aligned along the C5—C15 vector of the corrin, with close contacts between its C2 and C6 H's and C5 and C15 of the corrin. By contrast, the planar structures and relatively sterically more accessible β coordination site of the porphyrin and corrole are much more accommodating to the steric demands of pyridine. The stronger base, 4-*N,N*—$(CH_3)_2$aminopyridine (pK_a = 9.15, cf. pK_a = 5.2 for pyridine itself [917]) binds much more strongly to the corrin (log *K* = 3.99(2) vs. 0.48(4) in 80% CH_3OH, Table 17), and, according to DFT modelling, has a somewhat shorter Co—N bond length (2.027 Å) than in its corrin complex (2.045 Å).

One factor that may be important is the net charge at the metal centre of these systems. The +2 charge on corrin may be a reason why it coordinates anionic ligands more strongly than a corrole or a porphyrin, although the very small differences in log *K* values for coordination of NO_2^- and N_3^- by the porphyrin (+1 residual charge) and the corrole (neutral) – but taking cognisance of the effect of the solvent – suggests that this is unlikely to be the only factor.

The order of log *K* for binding to Co(III) in all three systems approximately parallels the pK_a of their conjugate acids [917]: HCN, 9.04; H_2SO_3, 6.85; HN_3, 4.44; HNO_2, 2.93; HSCN, 0.93; HI, −0.93, i.e., the affinity of an anion for Co(III) in these systems parallels its affinity for the proton. By contrast, the affinity for a neutral N-donor ligand shows little correlation with the pK_a of the ligand (4-*N,N*-$(CH_3)_2$aminopyridine, 9.7; $HOCH_2CH_2NH_2$, 9.47; (*N*-CH_3)imidazole, 7.10;

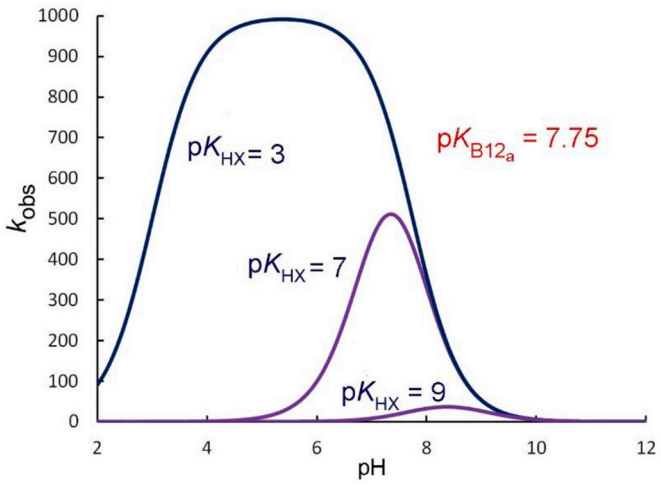

Fig. 30. An illustrative pH dependence of the apparent rate constant for the substitution of H_2O in $[H_2OCbl]^+$ by HX. This is a function of the separation of pK_{HX} and pK_{B12a}. For purposes of illustration, it is assumed that the pK_a of $[H_2OCbl]^+$ = 7.75, HX does not displace H_2O from H_2OCbl^+ and that the pH-independent rate constant for the reaction $X^- + H_2OCbl^+ \rightarrow XCbl + H_2O$ is $k = 10^3\ M^{-1}\ s^{-1}$.

$HONH_2$, 5.96; CH_3ONH_2, 4.60).

DFT calculations (M06L/SVP/SVPFit) on models of the corrin and porphyrin systems with a range of neutral and anionic ligands, L, in the β coordination site trans to imidazole showed that Co—L_β and Co—N_α bond lengths are longer in corrins than in porphyrins as might be anticipated given the greater steric constraints of the corrin [890]. The average difference of the Co—L_β bond lengths, $\Delta r_{\text{corrin–porphyrin}}$, for the neutral ligands was 0.025(3) Å, larger than $\Delta r_{\text{corrin–porphyrin}}$ for anionic ligands, 0.015(10) Å. Precisely the same was found in DFT modelling of corrin and corrole systems: $\Delta r_{\text{corrin–corrole}} = 0.038(15)$ Å for neutral ligands (pyridine, imidazole, trimethylphosphite) but $\Delta r_{\text{corrin–corrole}} = 0.013(7)$ Å for anionic ligands (CN^-, CH_3S^-, NO_2^-). This was attributed to the increased coulombic interaction between the anionic ligands and the greater charge on the metal centre in the corrin system. While the bonds to the axial anionic ligands are still longer in the corrin system than in the porphyrin and corrole systems, they are shorter than might have been expected based on the results obtained with the neutral ligands.

A fairly detailed QTAIM analysis of corrin and corrole model complexes with neutral (L = pyridine, imidazole, trimethylphosphite) and anionic (L = CN^-, CH_3S^-, NO_2^-) ligands gave further insights into the nature of the bonding in these complexes [111]. Not unexpectedly [912,913], a strong correlation between the electron density at the bond critical point, ρ_b, and the Co—L_β bond length was found. The bond between Co(III) and H_2O is long and weak (2.128 Å, 0.0538 au in corrole; 2.107 Å, 0.0551 au in corrin), rationalizing the ready replacement of H_2O by a very wide variety of ligands (for examples, see Table 17). The bonding between Co(III) and L is predominantly ionic (ρ_b close to zero; $\nabla^2\rho_b > 0$; $|V_b|/G_b$ close to 1). However, as the electron density on L increases (H_2O < imidazole < pyridine < NO_2^- < CN^- < trimethylphosphite < CH_3S^-), the bonding becomes significantly more covalent ($|V_b|/G_b$ increases as does the delocalization index, *DI*, which is a measure of the average number of electrons shared between the ligand and the metal).

The bonding to NO_2^- in both the corrin and the corrole systems has significant ellipticity. The ellipticity of a bond ε is defined as $|\lambda_1|/|\lambda_2| - 1$, where λ_1 and λ_2 are the eigenvalues of the Hessian matrix of the electron density at the bond critical point along mutually perpendicular axes, perpendicular to the bond path [869]. It is therefore a function of the ratio of the rate of electron density decrease in the two directions perpendicular to the bond path at the bond critical point. In the event of π bonding between two atoms, $|\lambda_1| > |\lambda_2|$ and ε will be significantly greater than 0. For the Co—NO_2^- bond in the corrin system, $\varepsilon = 0.107$ au and 0.109 au in the corrole system; this can be compared to a value of 0.273 for the C5—C6 (formally) double bond of the corrin, and a value of 0.001 for the C7—C8 (formally) single bond. This measure therefore points to a significant participation of the π^* frontier orbital of NO_2^- in the bonding with Co(III). In the case of CN^-, ε is small (0.018 and 0.002 in the corrin and corrole systems, respectively) but this masks the participation of *both*, mutually perpendicular frontier π^* orbitals in the bonding, as evidenced by large values of both λ_1 and λ_2. Very similar effects were found for the bonding in the porphyrin system [890].

7.3.8. Solvent effects

The uv-vis and fluorescence spectra of [CNCbl] show a modest dependence on solvent polarity [918]. The hexaalkylcobesters, in which all seven side chains have been hydrolysed to their corresponding acids and esterified, yield so-called hydrophobic corrinoids which are soluble in a wide range of solvents [919]. They have been quite extensively studied to probe the effect of solvent on their properties. The polarity of the solvent has a small but not insignificant effect on value of log *K* for the substitution of coordinated H_2O by a variety of incoming ligands. Generally, log *K* increases with an increase in solvent polarity (see Table A1 of the Appendix) (DMF < DMSO < methanol < water [861]; and toluene < ethyl acetate < acetonitrile < methanol < water [873]). There is a linear correlation [920] between log *K* and the cube of the empirical solvent polarity parameter, $E_T(30)$ [921] for substitution trans to coordinated SO_3^{2-} complex of the heptamethylester of sulfitocobyrinic acid. This was attributed to charge diffusion of coordinated SO_3^{2-} by hydrogen bonding or dipole interaction with the solvent, i.e., the greater the interaction between coordinated SO_3^{2-} and the solvent, the weaker the trans influence of the ligand.

A detailed study of the coordination of iodide by $[H_2OCbl]^+$ in methanol-water mixtures showed that log *K* at 25 °C varies linearly with the concentration of methanol (from log $K = 1.41$ in H_2O, $\mu = 0.15$ M, $NaClO_4$) to log $K = 3.96$ in pure methanol) [915]. Balt et al. observed a similar trend in the coordination of SCN^- by $[H_2OCbl]^+$, with log *K* varying from 3.30 in aqueous solution to 4.17 in 80% acetonitrile [922]. By contrast, there is a minimal increase in the affinity for a neutral ligand such as urea in water-dioxane mixtures, where *K* varies from 13 to 17 M^{-1} [923]. The effect is clearly a consequence of charge neutralization that occurs on coordination of an anionic ligand by $[H_2OCbl]^+$, a process favoured in non-aqueous solvents.

7.3.9. Substitution at the α coordination site

Many studies have been carried out on the cleavage of the Co—C bond in adenosylcobalamin [73], the first step in the mechanism of the [AdoCbl]-dependent enzymes [312], including reactions that entail ligand substitution. [AdoCbl] is very light-sensitive (Section 6) and the Co—C bond is also cleaved at elevated temperature; the Co—C bond dissociation energy in aqueous solution is approximately 125 kJ mol^{-1} [316] (and about 132 kJ mol^{-1} in ethylene glycol [315]). The bond dissociation energy of $[AdoCbi]^+$ is significantly larger, ca. 175 kJ mol^{-1} [924]. This value is reproduced within the experimental uncertainty (8 kJ mol^{-1}) by the BP86-D3 functional [925]. Thiols react with alkylcobalamins, to ultimately produce cob(I)alamin (Section 5.2.2), and cyanide reacts with [AdoCbl], forming $[(CN)_2Cbl]^-$ [926].

Arguably the first comprehensive study of the reaction between AdoCbl and CN^- was undertaken by van Eldik and co-workers [927], in which they attempted to resolve the conflicting reports about this reaction (see references in [927]). In the presence of 0.1 M CN^-, pH 11, $\mu = 1.0$ M ($NaClO_4$) there is clean conversion of [AdoCbl] to $[(CN)_2Cbl]^-$ as identified by its distinctive uv-vis spectrum and by ^1H and ^{13}C NMR. The NMR data identified the formation of adenine which arises from the cleavage in solution of the Ado ligand to adenine and a cyanohydrin [926]. From the rate dependence of the reaction on $[CN^-]$, a value of $k_2 = 7.4(1) \times 10^{-3}\ M^{-1}\ s^{-1}$ (pH 11) was obtained and the pH dependence of the reaction shows that CN^- and not HCN is the reactant. A study of the temperature-dependence of the reaction gave $\Delta H^\ddagger = 53.0(6)$ kJ mol^{-1} and $\Delta S^\ddagger = -127(3)$ J K^{-1} mol^{-1}, and from the pressure-dependence of the kinetics, $\Delta V^\ddagger = -10.0(4)$ cm^3 mol^{-1}. It was reasonably concluded that the initial (and only experimentally observable) step is the attack of CN^- on [AdoCbl], which is then followed by a fast uptake of a second equivalent of CN^- to produce the final product, $[(CN)_2Cbl]^-$. There was no clear evidence whether the rate-determining initial step was attack of CN^- on the β coordination site, displacing Ado from the metal, or its attack on the α coordination site, either displacing bzm or attacking a vacant or H_2O-occupied coordination site of the base-off form of [AdoCbl]. Given the very negative values of $\Delta S^\ddagger$ and $\Delta V^\ddagger$, which are indicative of a reaction under associative activation, van Eldik and co-workers favoured a mechanism where the rate determining step is attack of CN^- on the β coordination site (Scheme 31, red pathway). It was surprising to them, though, as reflected in a subsequent perspective [808], that the reaction would be so slow at such a labile Co(III) centre, and that it have a distinctly associative character.

When the same reaction was performed in 92:8 DMF:D_2O, ^1H NMR evidence was obtained of the rapid formation of $[(\beta\text{-Ado})(\alpha\text{-CN})Cbl]^-$ followed by Co—C bond cleavage to produce $[(CN)_2Cbl]^-$ [928] (Scheme 31, blue pathway). The cleavage of the Co—C bond to the Ado ligand trans to CN^- is rate-limiting with a saturating rate constant $k_1 = 9.3(3) \times 10^{-5}\ s^{-1}$; at low $[CN^-]$, $k_2 = kK = 2.1(5) \times 10^{-2}\ M^{-1}\ s^{-1}$, where *K* ($2.2(4) \times 10^2\ M^{-1}$) is the equilibrium constant for the formation

of [(β-Ado)(α-CN)Cbl]$^-$. From the temperature-dependence of the reaction, values of $\Delta H^{\ddagger} = 90.0(5)$ kJ mol^{-1} and $\Delta S^{\ddagger} = -20.5(2)$ J K^{-1} mol^{-1} were found. Increasing the percentage of D_2O in the solution causes an increase in the rate of the reaction, and the rate-determining step changes from cleavage of the Co—C bond in [(β-Ado)(α-CN)Cbl]$^-$ to formation of [(β-Ado)(α-CN)Cbl]$^-$. It is therefore likely that the mechanism in aqueous solution is not that shown in Scheme 31, but rather initial formation of [(β-Ado)(α-CN)Cbl]$^-$. Given the very negative values of $\Delta S^{\ddagger}$ and $\Delta V^{\ddagger}$ it seems likely that the reaction involves nucleophilic participation of entering CN$^-$ in the displacement of the bzm ligand.

The reaction of [(Ado)(OH)Cbi] with CN$^-$ at pH 11.0 proceeds by rapid, initial formation of [(Ado)(CN)Cbi] with CN$^-$ occupying the α coordination site, followed by slow ($k_1 = 2.91 \times 10^{-2}$ s^{-1} in H_2O, 25 °C, $\mu = 1.0$ M; $k_1 = 6.7 \times 10^{-5}$ s^{-1} in 92:8 DMF:D_2O, 25 °C, $\mu = 0.5$ M) solvent-assisted displacement of the β Ado ligand by CN$^-$ [929]. The equilibrium constant for formation of [(Ado)(CN)Cbi] is 5.6 M^{-1} in H_2O (25 °C, $\mu = 1.0$ M) and 2.8×10^3 M^{-1} in 92:8 DMF:D_2O (25 °C, $\mu = 0.5$ M).

Cyanide readily replaces bzm from the α coordination site trans to an alkyl ligand (see Section 7.3.1 in which the base-on/base-off equilibrium is discussed). Another example is the displacement of bzm by an imidazole derivative trans to imidazole to form a bis-imidazolylcobalamin, with log K ranging from < -1 for histidine, 0.6 for imidazole itself, and 1.4 for 1,5-dimethylimidazole [846]. One such reaction, the substitution of bzm by *N*-methylimidazole (NMI) trans to NMI has been reported in detail [930]. There is clear ^{1}H NMR and FAB-MS evidence for the formation of [$(NMI)_2$Cbl]$^+$ when [(H_2O)Cbl]$^+$/[(OH)Cbl] (p$K_a = 8.13$ under the conditions used) is added to 50 mM NMI. A value of log $K = 0.98(1)$ for substitution of bzm trans to NMI was determined by NMR, since the difference in absorbance between [NMICbl]$^+$ and [$(NMI)_2$Cbl]$^+$ is too small for reliable determination of the equilibrium constant using uv-vis spectroscopy. The kinetics are unusual, and are discussed in Section 9.

8. Organometallic chemistry of the cobalt corrinoids

Given the importance of [MeCbl] and [AdoCbl] in biology, and featuring as they do a Co—C bond which has to be heterolytically or homolytically cleaved during enzyme turnover, the organometallic chemistry of B_{12} and its derivatives has been extensively studied and comprehensive reviews are available (for example [6,34,931–933]). Only some selected, illustrative examples of the broad organometallic chemistry of the cobalt corrinoids is given in what follows in this section, and some has been covered elsewhere in this review, and particularly in Section 2 on the structure of the cobalt corrinoids, Section 3 on their biological chemistry, and in Section 6 on their photochemistry.

As mentioned in Section 2 and in Section 6, organometallic corrinoids are known with a Co—(sp^3 C) bond (such as [AdoCbl] [169], [MeCbl] [169], [ethylCb] [182] and [isoamylCbl] [173]), a Co—(sp^2 C) bond ([PhCbl] [174], [CH_2CHCbl] [633], [*cis*-CHClCHCbl] [633]) and a Co—(sp C) bond ([PhCCCbl] [170], [4NO_2PhCCCbl] [177], [2,4-F_2PhCCCbl] [716]).

Homolysis of the Co—C bond in the [AdoCbl]-dependent enzymes requires the reversible formation of [Cbl(II)] and Ado$^\bullet$, and suppression of irreversible side reactions involving β-alkoxide or β-hydride elimination [934–936], Scheme 32 [937]. [AdoCbl] is quite resistant to acid hydrolysis, and requires severe conditions (boiling in 1 M HCl) for it to be hydrolysed [934]. By contrast, tetrahydrofurfurylcobalamin, where the β ligand lacks the hydroxyl and base substituents of the Ado ligand, is rapidly hydrolysed (half-life of <5 min at 25 °C, pH 2.2 [938]). Even [2′,5′-dideoxyAdoCbl] which lacks the β hydroxyl group of Ado is significantly less stable than [AdoCbl]; in boiling 1 M HCl after 10 min, [AdoCbl] underwent approx. 30% hydrolysis whereas [2′,5′-dideoxyAdoCbl] was virtually completely hydrolysed [934]. A series of (alkoxylethyl)cobalamins were also shown to be readily hydrolysed in aqueous media, pH 0–4.4, 25 °C [939]. Acid hydrolysis of [MeCbl] is apparently unknown [933] although the bond is heterolytically cleaved by a soft Lewis acid such as Hg(II) to produce [H_2OCbl]$^+$ and CH_3Hg^+ [620].

As discussed in Section 5, [Cbl(I)]$^-$ is a very strong nucleophile ($n = 14.4$ on the Pearson scale [385]) and will react with a variety of alkylating agents such as methyl iodide [606] and trimethylsulfoxonium iodide, [$(CH_3)_3$SO]I [607] by an S_N2 reaction. The product is usually the β diastereomer, but depending on the alkylating agent, and reaction conditions, variable amounts of the α diastereomer can be produced

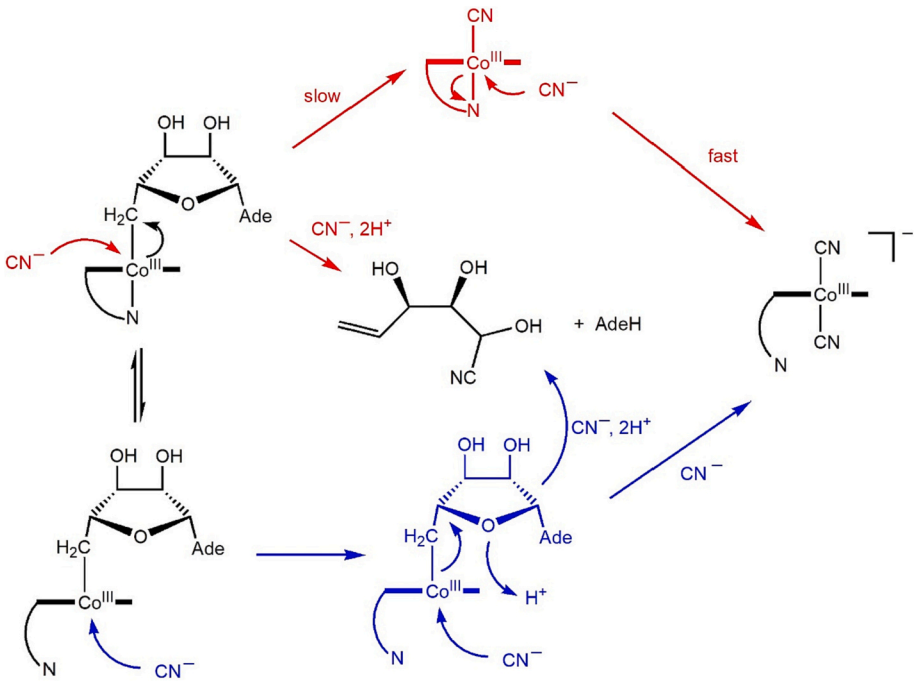

Scheme 31. The reaction of CN$^-$ and [AdoCbl].

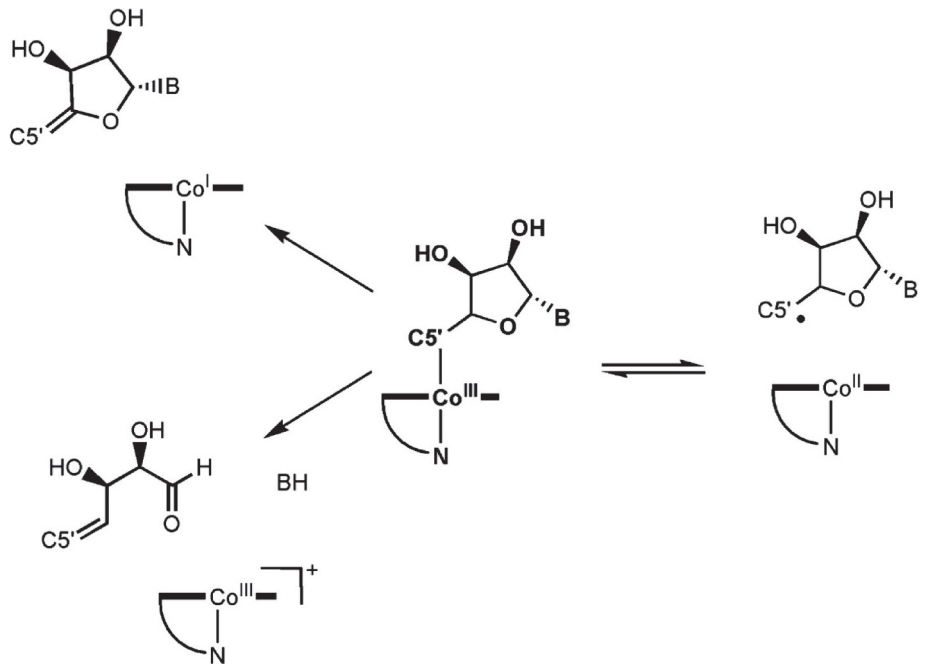

Scheme 32. The reversible and irreversible cleavage of the Co—C bond of [AdoCbl].

[133,316,744,874,939–941]. The products usually can be separated chromatographically. Under certain conditions, alkylation does occur through a two-step, one-electron transfer pathway; a Co(I) cobamide acts as a one-electron reductant and the reaction proceeds via a Co(II) intermediate [940]. Since Co(I) cobalamins exist predominantly as a four-coordinate complex, the presence or absence of the bzm base has virtually no effect on the reactivity pattern. The electrochemical synthesis of alkylcobalamins in well-established [439,463]. Co(I) is generated at controlled electrode potentials near that of Co(II)|Co(I) couple; it then reacts rapidly with a suitable alkylating agent [330,942–944].

[Cbl(II)] reacts efficiently with alkyl radicals to produce an alkylcobalamin stereospecifically on the β face [674,945–947]; this is ensured by the presence of bzm in the α coordination site, and appears to involve minimal rearrangement of the corrin [227]. Some alkylcobalamins, such as [CH_3OCOCH_2Cbl], are difficult to prepare by direct alkylation of $[Cbl]^-$ because they are easily reduced. An alternative procedure for their synthesis involves the reaction of [Cbl(II)], produced and maintained by controlled potential electrolytic reduction, or chemical reduction with formate, of $[H_2OCbl]^+$, with an excess of $BrCHCOOCH_3$ [557].

The reaction of a Co(III) cobamide with a nucleophilic alkylating agent such as an organomagnesium halide, a vinyl ether in a nucleophilic solvent, malononitrile, or phenylacetronitrile, will produce an alkylcobamide, but the route is seldom used as reductive alkylation is far more versatile [948].

As discussed in Section 6, alkylcobalamins are unusually light sensitive and dissociate to an alkyl radical and [Cbl(II)]. Homolysis of the Co—C bond of [AdoCbl] is of course key to its function as an enzymatic cofactor. The bond dissociation energy is relatively low, about 125 kJ mol^{-1} [315,384]; that of [MeCbl] is somewhat higher, 155 kJ mol^{-1} [464]. The absence of bzm increases the strength of the Co—C bond to ca. 185 and 175 kJ mol^{-1} in $[MeCbi]^+$ and $[AdoCbi]^+$ [924], although factors other than the trans influence of bzm (see Section 7) are the likely cause [462].

The Co—C bond of [MeCbl] can be cleaved homolytically by reaction with an alkyl radical $R^\bullet$ to produce [Cbl(II)] and RCH_3 [949,950]. Thermolysis of ethyl-, neopenty- and cyclohexylcobalamin (80 °C) proceed at similar rates, irrespective if the reaction involves homolytic fission (with neopentylcobalamin) or β-elimination (with cyclohexylcobalamin), suggesting that both reactions involve, as initial step, homolytic fission of the Co—C bond to form a caged radical pair [859].

Exposure of [MeCbl] (in a glass of $CD_3OD + D_2O$) to ionising radiation leads to electron capture and ultimately cleavage of the Co—C bond and formation of Co(II) and CH_3^-, which is then protonated; but the reaction sequence is complex [951]. The initial species is a π^* corrin anion; on annealing, EPR signals diagnostic of Co(II) appear, with electron density in $3d_x2_{-y}2$. Further annealing leads to reorganisation of the unpaired spin and the emergence of a Co(II) $(3d_z2)^1$ species. The conclusion was that this is the kinetically favoured reduction pathway – at least under the conditions of the experiment. The addition of an electron to [AdoCbl] also leads to initial formation of a π^* corrin anion, but the $(3d_x2_{-y}2)^1$ intermediate was not detected. Photolysis of [AdoCbl] in a frozen glass leads to the expected homolysis of the Co—C bond [951].

Thiolates demethylate $[MeCbi]^+$ and [MeCbl] to produce the Co(III) cobamides, the reaction with $[MeCbi]^+$ being much faster due to stabilisation of the Co—C bond in [MeCbl] by trans bzm [462,507]. The dealkylation of [MeCbl] with soft metal ions such as Hg(II) is well known (see Section 5.2.8). The exchange of a methyl ligand between a methylcobamide and a Co(II) cobamide has been observed [462,952].

9. Kinetics of the ligand substitution reactions

Co(III), along with Cr(III), is the classic example of an inert metal ion from the first row of the *d* block. For example, NMR methods show that the residence time of H_2O in Co_{aq}^{3+} [953] and Cr_{aq}^{3+} [954] is of the order of 10^5 s, compared to 10^{-5} s for Fe_{aq}^{3+} and Ti_{aq}^{3+} [955] and 10^{-8} s for Co_{aq}^{2+} [956]. In the cobalt corrinoids, however, the reactions are quite fast (sometimes described as “instantaneous” [757]) and their study has been a fruitful area of research for many years.

In line with the chemistry of Co(III) complexes in aqueous solution [957], from early work on the kinetics of ligand substitution on $[H_2OCbl]^+$ [518,888,958] and subsequently confirmed several times (for example [519,737,847,959,960]), it is well-established that the hydroxide ligand in [HOCbl] and also in aquahydroxocobinamide [568,737,888,961,962] is essentially inert to substitution by other ligands. There is evidence for the (slow) reaction of [HOCbl] with HNO

(which arises from the decomposition of Piloty's Acid, PA, benzenesulfonylhydroxamic acid, $PhSO_2NHOH$) between pH 10 and 12.4, to produce nitrosylcobalamin, [NOCbl], with a pH-independent initial rate of $4.33(9) \times 10^{-7}\,M\,s^{-1}$, [PA] = 130 mM, [HOCbl] = 85 μM [536].

Usually a ligand HX such as imidazole or NH_3 will only coordinate the metal ion if it is deprotonated (pK_a for imidazole = 6.93 [963] and 9.25 for NH_3 [917]). There are exceptions; for example, both HCN and CN^- [737] and HN_3 and N_3^- [888] will substitute H_2O on $[H_2OCbl]^+$, albeit the protonated ligand reacts more slowly – see below. Hence the observed rate constant for the reaction of HX with $[H_2OCbl]^+$ will increase with pH. On the other hand, since [HOCbl] is inert, the observed rate constant will decrease above the pK_a of $[H_2OCbl]^+$ (7.462(7) [111]). The net effect is a bell-shaped curve, the position of the maximum and the shape of which will depend on the separation of the pK_a of HX and $[H_2OCbl]^+$, and the inherent value of the rate of substitution of $[H_2OCbl]^+$ by the incoming ligand (Fig. 30).

One of the landmark papers in the inorganic chemistry of the cobalt corrinoids is the study by Reenstra and Jencks [737] of the reaction of $[H_2OCbl]^+$ and CN^- across a wide pH range. It is unfortunate that KCl was used to adjust the ionic strength. While the affinity of $[H_2OCbl]^+$ for Cl^- is low, it is not zero ($K = 3.3$ [331] or 1.3 [757]), and some [ClCbl] will have been present in the system. Hence, while the absolute values of the reported rate constants are suspect, the general conclusions are nevertheless valid.

Reactions with CN^- have proved very useful in cobalt corrinoid chemistry because of the very high affinity of the cobalt corrinoids for CN^-, the moderately fast kinetics of the reaction making their study by stopped flow methods (or even in some instances conventional spectrophotometric methods) feasible and, not least, the very distinctive changes in the uv-vis spectrum that accompany the reactions. The reaction of $[H_2OCbl]^+$ and CN^- is first order in cyanide and first order in Cbl, and Reenstra and Jencks rationalised the pH-dependence of the second order rate constant for formation of [CNCbl] by proposing that $[H_2OCbl]^+$ reacts with both HCN and CN^-; that the initial product of the reaction with HCN has the ligand bound through N, which then loses H^+ and isomerises to C-bound CN^-; and that [HOCbl] is inert to substitution. The reactions are summarised in Eq. 31.

$$CN^- + [H_2OCbl]^+ \xrightarrow{k_1} [NCCbl] + H_2O \quad (31a)$$

$$HCN + [H_2OCbl]^+ \underset{k_{-2}}{\overset{k_2}{\rightleftarrows}} [HCNCbl]^+ + H_2O \quad (31b)$$

$$[HCNCbl]^+ \overset{K_3}{\rightleftarrows} [CNCbl] + H^+ \quad (31c)$$

$$[CNCbl] \xrightarrow{k_4} [NCCbl] \quad (31d)$$

The observed second order rate constant, k_2^{obs} is related to the microscopic rate constants [519] by Eq. 31, where $\alpha = k_4K_3K_w/k_{-2}$ and K_{Co} refers to the dissociation of coordinated H_2O to produce substitution-inert [HOCbl] [518].

$$k_2^{obs} = \frac{k_1}{(1+[H^+]/K_{HCN})(1+K_{Co}/[H^+])} + \frac{k_2\alpha/[H^+]}{(1+K_{HCN}/[H^+])(1+K_{Co}/[H^+])(1+\alpha/[H^+])} \quad (32)$$

There are therefore two pathways to the product and the overall observed rate constant varies with pH in the form of a skewed bell-like curve (as in Fig. 28).

An alternative way of viewing the data is shown in Fig. 31 [519]. The second-order rate constants are expressed as corrected rate constants in terms of the addition of CN^- and the fraction of cobalamin present as $[H_2OCbl]^+$ (Eq. 33).

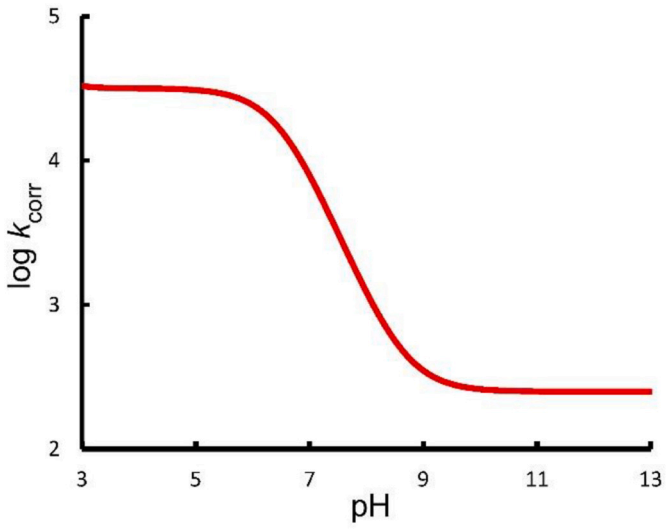

Fig. 31. The variation of k_{corr} (Eq. 33), the second order rate constant for the reaction of free $[H_2OCbl]^+$ with cyanide, corrected for the ionisation of the reactants.

$$k_{corr} = k_{II}^{obs}(1 + [H^+]/K_{HCN})(1 + K_{Co}/[H^+]) \quad (33)$$

The plot converges to k_1 at high pH, where addition of CN^- to $[H_2OCbl]^+$ is rate-limiting. As the pH decreases, there is an acid catalysed region (addition of HCN to $[H_2OCbl]^+$ to form the N-bound species is rate-limiting), which converges to $k_2\alpha/K_{HCN}$ at low pH (where isomerisation of the N-bound species is rate-limiting).

If the bzm base is absent, as in diaquacobinamide, $[(H_2O)_2Cbi]^{2+}$ ($[DAC]^{2+}$), the situation is much more complicated as both $[(H_2O)_2Cbi]^{2+}$ and $[(HO)(H_2O)Cbi]^+$ (pK_a = 5.9 [962]) will react with both HCN and CN^-. This is considered further below.

9.1. Distinguishing between a dissociative and a dissociative interchange mechanism

Given the steric crowding of Co(III) in the cobalt corrinoids, and in particular the effect of the *a, c* and *g* side chains, the "sentinel" methyl groups at C12 and C17, and the C-19 H (Fig. 32, from the crystal structure of $[H_2OCbl]^+$ [179]) it is most unlikely that the ligand substitution reactions of a ligand coordinated in the β coordination site of the metal will proceed through an associative (A) mechanism which would entail the formation of a seven-coordinate intermediate. It is also unlikely – but less improbable – that an interchange mechanism under associative activation (I_a), which would require very substantial bond formation with the incoming ligand whilst significant bonding between Co(III) and the departing ligand is retained, is operative. Simple steric arguments would (intuitively) suggest that the reaction proceeds through a purely dissociative (D) mechanism or an interchange mechanism under dissociative activation (I_d).

Thusius [889] pointed out that although stability constants vary by at least six orders of magnitude (from $K = 32\,M^{-1}$ for coordination of I^- by $[H_2OCbl]^+$ to $2.2 \times 10^7\,M^{-1}$ for coordination of SO_3^{2-} for the limited

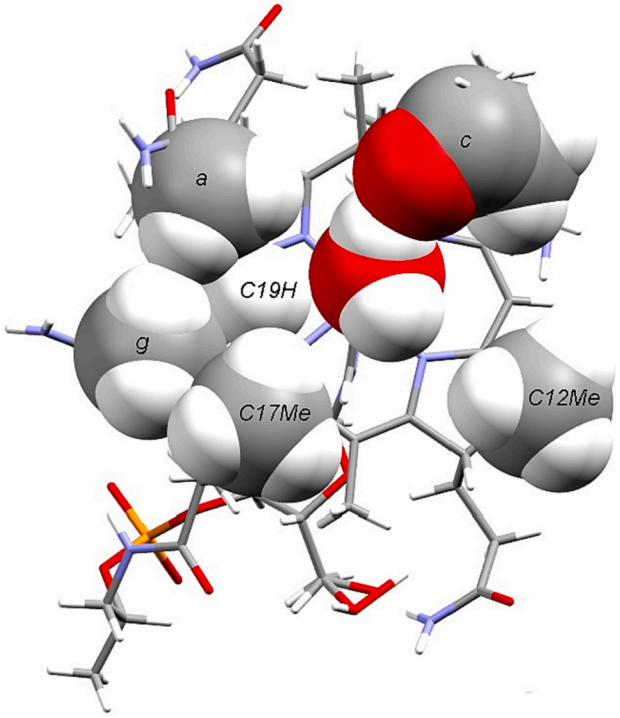

Fig. 32. The crowded upper face of a corrin, from the crystal structure of $[H_2OCbl]^+$ [179].

series of ligands that he studied) and much more if the value for CN^- is included, the second order rate constants k_2 vary only by an order of magnitude (from $1.7 \times 10^2\ M^{-1}\ s^{-1}$ for the reaction of $[H_2OCbl]^+$ with HSO_3^- to $2.3 \times 10^3\ M^{-1}\ s^{-1}$ for the reaction with SCN^-). The compilation of data by Poon [964] shows that equilibrium constants in fact vary by about 11 orders of magnitude but rate constants vary by only some 2 orders of magnitude. The very low dependence of the rate of ligand substitution on the nucleophilicity of the entering ligand suggests that bond formation between the entering ligand and the metal plays a relatively minor role in the transition state of the reaction, which is dominated by dissociation of departing H_2O. There is also a linear free energy relationship between log k_2 and log K with unit slope, suggestive of a mechanism that is dissociative in nature [964]. As discussed below, however, reliance on values of rate constants may be unwise because very significant differences in the reactivity of two species may be masked by compensation effects in the activation parameters, $\Delta H^{\ddagger}$ and $\Delta S^{\ddagger}$.

The unusual lability of Co(III) in the cobalamins was recognised early on [331,888,958]. Thusius seems to have been the first to point out that this lability appears to be due to $\Delta H^{\ddagger}$ which is some 45 kJ mol^{-1} lower than in typical Co(III) complexes [889], and a direct quote may be appropriate: "It would appear that some property common to both the corrin and porphyrin ring systems can dramatically alter the lability of axial ligands, but the nature and origin of the effect remain obscure". He also pointed out that comparison between different Co(III) complexes should be done with care. Thus, cobaloximes are some 10^7 times less reactive than the cobalamins, but the difference here seems to be largely a consequence of much more negative values of $\Delta S^{\ddagger}$, which *may* be indicative of a mechanism which is more associative in nature.

The anation of aquapentaamminecobalt(III) complexes is well-established to proceed by an I_d mechanism [965], and indeed an I_d mechanism appears to be the predominant mechanism of ligand substitution reaction in octahedral complexes of the metal ions of the later first transition series. So the early view was that the ligand substitution reactions of Co(III) in the corrinoids proceeded through a D mechanism, although it was pointed out [888] that since substitution of H_2O in $[H_2OCbl]^+$ by imidazole was significantly slower than by N_3^- and NCO^-, the reaction rate was unlikely to depend solely on the rate of unimolecular release of H_2O from the metal ion.

Reenstra and Jencks [737] advanced convincing reasons why a D mechanism in a coordinating solvent such as water is unlikely. Their elegant analysis is worth a brief reiteration (Scheme 33; only axial ligands are shown and charges are omitted for clarity. In the scheme, Z replaces H_2O trans to X). As already mentioned, the presence of Cl^- in their system (from the use of KCl to adjust ionic strength) makes the absolute values suspect but does not invalidate the overall conclusions.

The formation of the product [XCoZ] will normally proceed through the intermediate **1** in Scheme 33 which is formed either through the initial dissociation of H_2O, producing a species where departing H_2O is in the outer coordination sphere (red pathway in Scheme 33), followed by uptake of Z, or through the formation of an outer sphere complex with Z in an interchange mechanism (green pathway) in which bond formation to Z may be significant as bond breaking to departing H_2O occurs (an I_a mechanism), or bond breaking between the metal and departing H_2O occurs to a significant extent before bond formation to Z begins (an I_d mechanism). If there is incontrovertible experimental evidence for a seven coordinate intermediate (blue pathway) then the mechanism is an associative mechanism, A. No such evidence has been found to date in cobamide chemistry.

As mentioned above, in a sterically crowded environment with a relatively rigid equatorial ligand as in the cobalt corrinoids, an A mechanism is unlikely. Whether a D or an I mechanism is operative then depends on the lifetime of **1**. If **1** adds water faster than Z diffuses away (i.e., $k_r > k_{-a}$) then the pathway for reverting of **1** to reactants must proceed through the outer sphere complex [XCo(—OH_2)(···Z)] and therefore based on the principle of microscopic reversibility, the same pathway must be the lowest energy route for the formation of **1**.

If a D mechanism is operative, yet the reaction is second order and the rate constants vary by several orders of magnitude, then k_r must be smaller than k_{-a}, but k_r and k_{-1} must be larger than k_2 in order to maintain second order kinetics. This requires the metal to have a low selectivity as H_2O is not a particularly reactive ligand towards metal ions. A higher selectivity would mean that addition of Z and H_2O would become competitive and the reaction would no longer be second order. Such a mechanism in a coordinating solvent is unlikely to occur. In a non-coordinating solvent, the lifetime of the pentacoordinate intermediate may be long enough to permit diffusion of the departing ligand away before entry of the incoming ligand, favouring a D mechanism. This is found, for example, for alkylcobaloximes in chloromethane where the rate of ligand exchange is insensitive to the identity of the entering ligand [966].

Of course, there is no clear distinction between an I_a and an I_d mechanism; they form a continuum between a pure D and a pure A mechanism, and depend on the extent of participation of Z in the formation of **1**, i.e., the extent of participation of the incoming ligand in the transition state between reactants and products.

There is another way of distinguishing between a D and an I mechanism. In general terms, for a reaction in which Y in an octahedral (or pseudo octahedral) complex, L_5MY, is replaced by Z, and where the reaction proceeds through a D mechanism, the elementary steps of the reaction are shown in Eq. 34.

$$L_5MY \underset{k_{-1}}{\overset{k_1}{\rightleftarrows}} L_5M + Y \tag{34a}$$

$$L_5M + Z \xrightarrow{k_2} L_5MZ \tag{34b}$$

It is then readily shown that Eq. 35 applies.

$$\frac{d[P]}{dt} = \frac{k_1 k_2 [L_5MY][Z]}{k_{-1}[Y] + k_2[Z]} \tag{35}$$

In the case of an interchange mechanism, the elementary steps may

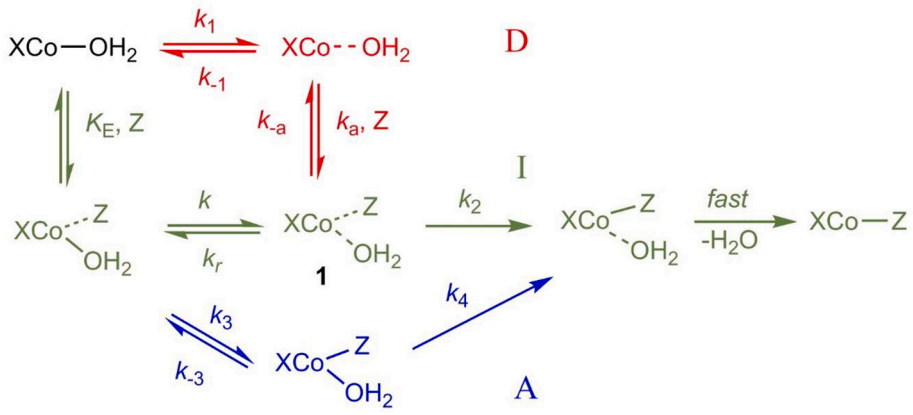

Scheme 33. Possible routes to the substitution of H_2O in a Co(III) corrinoid by an incoming ligand, Z, trans to X.

be written as in Eq. 36 where K_E is the equilibrium constant for formation of the encounter complex (L_5MY,Z) in which the entering ligand Z is in the outer coordination sphere.

$$L_5MY + Z \overset{K_E}{\rightleftarrows} (L_5MY, Z) \tag{36a}$$

$$(L_5MY, Z) \overset{k}{\rightarrow} (L_5MZ, Y) \tag{36b}$$

$$(L_5MZ, Y) \overset{fast}{\rightarrow} L_5MZ + Y \tag{36c}$$

Eq. 37 then follows.

$$\frac{d[P]}{dt} = \frac{kK_E[L_5MY]_0[Z]}{1 + K_E[Z]} \tag{37}$$

Since $\frac{d[P]}{dt} = k_{obs}[L_5MY][Z]$ and if, as is usually the case in cobalt corrinoid chemistry, $[Z] >> [L_5MY]$, under pseudo first-order conditions, Eq. 38 is applicable, where $k'_{obs} = k_{obs}[Z]$.

$$\frac{d[P]}{dt} = k'_{obs}[L_5MY] \tag{38}$$

The microscopic and macroscopic rate constants can then be related. For simplicity, suppose $Y = H_2O$ and the reaction is carried out in aqueous solution so that [Y] is invariant. Then for a D mechanism, Eq. 39 applies, while for an I mechanism, the applicable equation is Eq. 40.

$$k'_{obs} = k_{obs}[Z] = \frac{k_1k_2[Z]}{k_{-1} + k_2[Z]} \tag{39a}$$

$$\lim_{[Z]\to 0} k'_{obs} = \frac{k_1k_2[Z]}{k_{-1}} \tag{39b}$$

$$\lim_{[Z]\to \infty} k'_{obs} = k_1 \tag{39c}$$

$$k'_{obs} = \frac{kK_E[Z]}{1 + K_E[Z]} \tag{40a}$$

$$\lim_{[Z]\to 0} k'_{obs} = kK_E[Z] \tag{40b}$$

$$\lim_{[Z]\to \infty} k'_{obs} = k \tag{40c}$$

Hence if a D mechanism is operating, the saturating rate constant is the rate for the dissociation of Y from the coordination sphere and this must be *strictly independent* of the entering group. For an I mechanism, the saturating rate constant is the rate of interchange of Y and Z and will depend on the nature of Z (Fig. 33). Therefore, even if there is no direct experimental evidence for the existence of a five coordinate intermediate, which would be incontrovertible proof for a D mechanism, a D and an I mechanism can be distinguished provided saturation kinetics are observed. In the absence of such definitive proof, it is probably reasonable to assume an interchange mechanism. Of course, the underlying assumption is that the same mechanism is operative for all ligands in a particular study – and that may or may not be the case.

Conclusive evidence for the operation of an I_d mechanism in the substitution of H_2O in $[H_2OCbl]^+$ was provided by Meier and van Eldik [967,968] when they showed that the rate of reaction of $[H_2OCbl]]^+$ with pyridine reaches a saturating value of 34(7) s^{-1} in aqueous solution (25 °C, $\mu = 0.1$ M, $NaClO_4$) whereas no saturation is observed with stronger nucleophiles such as thiourea and dimethylthiourea. Saturation effects with other ligands (imidazole, 33 s^{-1}; hydroxylamine, 8.3 s^{-1}; pyridine, 8.2 s^{-1}; 4-methylpyridine, 6.2 s^{-1}; histamine, 2.3 s^{-1}; and methylglycinate, 1.1 s^{-1}) had been observed before [960], but the use of KCl as ionic strength adjustor, which will inevitably lead to the formation of some [ClCbl] in solution ($K = 3.3$ [331] or 1.3 [757]), compromises the reliability of the data [969]. The values of $\Delta V^{\ddagger}$ for the substitution of H_2O by a series of ligands (in cm^3 mol^{-1}: pyridine, 9(1) [967]; 4-methylpyridine, 8.2(5) [970]; 3-acetylpyridine, 10(1); thiourea, 9.9(9) [968]; dimethylthiourea, 7(1) [968]; I^{-1}, 5.5(8) [889,971]; $S_2O_3^{2-}$, 6.0(8) [889]; N_3^-, 6.9(3) [972]; HN_3, 9.4(8) [972]) are all positive, rather similar, and significantly smaller than values for ligand substitutions on the Co(III) porphyrin complexes $[Co(TMPP)(H_2O)_2]^{5+}$ and $[Co(TPPS)(H_2O)_2]^{3-}$, which proceed through a limiting D mechanism (14(4) and 15.4(6) cm^3 mol^{-1}, respectively [973,974]). This is as expected for an interchange mechanism under dissociative activation where the most significant event in the rate determining step is cleavage of the Co—OH_2 bond. An I_d mechanism persists even if H_2O is replaced

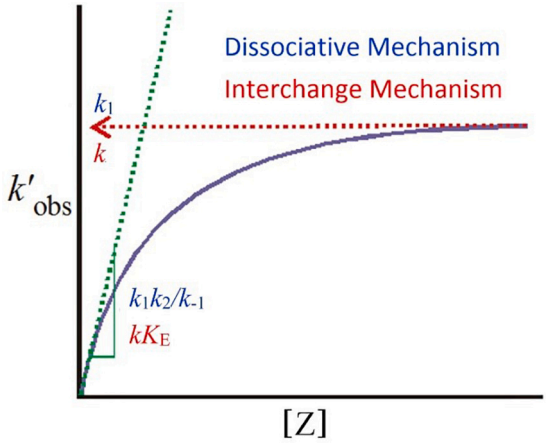

Fig. 33. The dependence of the pseudo first order rate constant, k_{obs}', on [Z] for the reaction $L_5MY + Z \rightleftharpoons L_5MZ + Y$.

by a bulkier I^- ligand [772].

There is other, albeit indirect, evidence against a limiting D mechanism. For example, the transition state for substitution of H_2O in $[H_2OCbl]^+$ by incoming Z = CN^- is some 25 kJ mol^{-1} more stable than when Z = HCN [519]; the rate at which H_2O in $[H_2OCbl]^+$ is replaced by Z = a substituted imidazole increases with the basicity – and hence the nucleophilicity – of incoming Z [847]; and the activation parameters for substitution of H_2O in $[H_2OCbl]^+$ by small neutral and anionic ligands varies with the ligand (Table 18). Saturating rate constants (see Fig. 29) were found for substitution of H_2O in aquahydroxocobinamide, $[(H_2O)(OH)Cbi^+]$. The activation parameters show a strong dependence on the nature of the incoming ligand which means the saturating rate constant cannot be due to unimolecular dissociation of H_2O from the metal (Table 19).

There is a compensation effect between values of $\Delta H^{\ddagger}$ and $\Delta S^{\ddagger}$ [980]; an increase in $\Delta H^{\ddagger}$, making the reaction enthalpically less favourable, is compensated by an increase in $\Delta S^{\ddagger}$, and the reaction becomes entropically more favourable. This is discussed further below. Therefore, the similarity in rate constants determined at a single temperature cannot be used as the basis of assigning a limiting D mechanism to the reaction, as was originally proposed [889,964].

In aqueous solutions in which salts of non-coordinating anions such as ClO_4^- or NO_3^- have been used to adjust the ionic strength, saturation behaviour (see Fig. 29) is usually not observed; hence the only information generally available is a second order rate constant, k_2, which, for an I_d mechanism, corresponds to kK_E (Fig. 29). If one assumes that K_E, the equilibrium constant for formation of the outer sphere complex, does not change significantly whether the cobalamin is present strictly as the aqua complex, or whether there is some [ClCbl] present so that saturation behaviour is observed, then it is possible to determine K_E from a plot of $k_2/[Z]$ against k_2 [960]. Values of K_E for a wide range of ligands including substituted pyridines, NH_2OH, methyl glycinate, imidazole and a number of anions are available [969] and range between 0.2 and 4.2 M^{-1}.

Another example of a kinetic trans effect in cobamide chemistry comes from the thermolysis of the Co—C bond of an alkylcobalamin, which leads to its homolytic cleavage [981]. The reaction is faster in the presence of oxygen as the oxidation of the metal to Co(III) competes effectively with radical recombination [982]. The results of a study of the rate of homolysis of *p*-X-benzylcobalamins are summarised in Table 20 [982]. The rate of the homolysis reaction is virtually independent of the identity of the alkyl ligand. What is very evident is the very marked difference in the kinetic trans effect of bzm and H_2O.

The presence of two readily available coordination sites on diaquacobinamide, $[DAC]^{2+}$, which exists is solution as the diaqua, aquahydroxo or dihydroxo complex, depending on pH (pK_as = 5.9 and 10.2 [961]), with a reactant that itself has multiple protonation states can lead to complex kinetics. A good example [522] is that of the reaction of $[DAC]^{2+}$ with H_2S (pK_as = 7.04 and 11.96 [983]).

Coordinated OH^- in aquahydroxocobinamide, $[AHCbi]^+$, and in dihydroxocobinamide, [DACbi], is substitution-inert [961,962]. $[DAC]^{2+}$ reacts with two equivalents of H_2S to sequentially produce $[(HS)(H_2O)Cbi]^+$ and $[(HS)_2Cbi]$ (Scheme 34, adapted from [522]). The value of pK_{a2} is >10.5, the limit of the pH range of the study.

Coordinated HS^- in $[(HS)(H_2O)Cbi]^+$ reduces Co(III) to Co(II) to form $[HS^{\bullet}Cbi(II)]^+$ which deprotonates (pK_a = 5.2(6)) to produce [SCbl(II)]. This species reacts further with H_2S, as well as HS^-, to form [HSSCbi(II)] (Scheme 35, adapted from [522]).

The complexity of the system required several assumptions to be made, and the fitting of multi-parameter expressions to the experimental data, determined as a function of temperature and pH. This inevitably resulted in significant uncertainty in the activation parameters. Nevertheless, the results (summarised in Table 21) give a clear indication of the validity of the proposed mechanism (Schemes 34 and 35) and the conclusions that follow.

The reaction of $[DAC]^{2+}$ with H_2S depends on the concentration of H_2S. At low concentrations, one equivalent reacts with $[DAC]^{2+}$ to form $[HSCbi]^+$; at higher concentrations, a second equivalent reacts to form $[(HS)_2Cbi]$ (Scheme 34). HS^- reacts faster than H_2S, and $[DAC]^{2+}$ is more labile than $[AHC]^+$ towards anionic HS^-. The values of $\Delta S^{\ddagger}$ for the reverse reactions (k_{-1}, k_{-4}, k_{-5}) tend to be positive, indicative of a reactions under dissociative activation. Those for the forward reactions are either indistinguishable from zero within the uncertainty in the experimental values (k_4), somewhat negative (k_1) or strongly positive (k_5) suggesting (k_4, k_1) an interchange mechanism is operative, while substitution of H_2O by HS^- trans to HS^- would appear to be a dissociative process, consonant with the strong trans effect of HS^-.

Coordinated HS^- reduces Co(III) to Co(II) to form the long-lived radical intermediate $[(HS)^{\bullet}Cbi(II)]^+$ (which equilibrates with its deprotonated form $[S^{\bullet}Cbi(II)]$ (pK_{a5} = 5.2(6)). H_2O is released from the coordination sphere in the process, as reflected by positive value of $\Delta V^{\ddagger}$. The formation of the radical intermediate, however, is hindered by the formation of $[(HS)_2Cbi]$. $[(HS)^{\bullet}Cbi(II)]$ and $[S^{\bullet}Cbi(II)]$ react with H_2S and with HS^- to form $[(HSS)^{-\bullet}Cbi(II)]$, the reactions with H_2S (k_7, k_9) being slower than with HS^- (k_8, k_{10}).

9.2. The influence of the corrin ring and the Cis effect

A notable feature of the corrin macrocycle is its effect on the rate of the ligand substitution reactions on Co(III). Low spin Co(III), along with Cr(III), is the quintessential kinetically inert metal ion from the first row of the d block because of the high ligand field contribution to the activation energy [984,985]. Yet in the cobalt corrinoids Co(III) undergoes ligand substitution reactions that are relatively fast. This suggests that the corrin macrocycle imparts significant lability to the metal ion, perhaps conferring on it some measure of Co(II)-like character. Indeed,

Table 18
Activation parameters from the temperature dependence of the second order rate constants for the substitution of H_2O in $[H_2OCbl]^+$ by incoming Z.[a]

Z	$\Delta H^{\ddagger}$ /kJ mol^{-1}	$\Delta S^{\ddagger}$ /J K^{-1} mol^{-1}	Ref	Z	$\Delta H^{\ddagger}$ /kJ mol^{-1}	$\Delta S^{\ddagger}$ /J K^{-1} mol^{-1}	Ref
NH_3	77.0(4)	27(1)	[975]	NH_2Me	81(2)	46(7)	[975]
NH_2OH	72.0(5)	21(2)	[975]	$NH_2CH_2CO_2Me$	66(2)	−21(6)	[975]
$NH_2CH_2CH(OH)CH_2OH$	60(1)	−44(4)	[975]	$NH_2(CH_2)_2OH$	59.7(3)	−46(1)	[975]
$NH_2(CH_2)_3OH$	68.3(6)	−15(2)	[975]	NH_2Et	64(2)	−21(7)	[975]
Aspartate	99(2)	27(6)	[976]	Asparagine	97(2)	43(6)	[976]
Glutamate	100(2)	30(6)	[976]	Glutamine	103(2)	53(6)	[976]
NH_2Pr	65(1)	−21(4)	[975]	SCN^-	63(1)	26(4)	[977]
$S_2O_3^{2-}$	68.5(7)	23(2)	[977]	NO_2^-	67(1)	26(3)	[977]
SO_3^{2-}	79.9(5)	33(1)	[977]	HSO_3^-	67.2(4)	20(1)	[977]
CN^-	52(1)	−25(4)	[519]	HCN	72(2)	50(1)	[519]
N_3^-	65.9(7)	28(2)	[978]	HN_3	70(1)	27(4)	[978]
N_3^- [a]	65(2)	30(5)	[979]	$[Fe(II)(CN)_5NO]^{2-}$ [b]	56(2)	10(8)	[979]
$[Fe(II)(CN)_6]^{4-}$ [c]	84(5)	101(16)	[979]	$[Fe(III)(CN)_5(OH_2)]^{2-}$ [d]	88(15)	119(49)	[979]

Values of $\Delta V^{\ddagger}$ (cm^3 mol^{-1}): [a] 6.9(2); [b] 8.9(5); [c] 16(1); [d] 8.2(8)

Table 19
Activation parameters from the temperature dependence of the saturating rate constant[a] the substitution of H_2O in $[(H_2O)(OH)Cbi]^+$ by incoming Z.[b]

Z	$\Delta H^{\ddagger}$ /kJ mol^{-1}	$\Delta S^{\ddagger}$ /J K^{-1} mol^{-1}	Z	$\Delta H^{\ddagger}$ /kJ mol^{-1}	$\Delta S^{\ddagger}$ /J K^{-1} mol^{-1}
CN^-	53.0(9)	9(3)	N_3^-	45(2)	−14(6)
pyridine	81(4)	106(13)	N-methylimidazole	79(5)	106(18)

[a]See Fig. 29. [b]All data from [961].

Table 20
Activation parameters and interpolated rate constants (aqueous aerobic solution, 25 °C) for the thermolysis of para-substituted benzylcobalamins and cobinamides.

X	axial ligand	$\Delta H^{\ddagger}$ /kJ mol^{-1}	$\Delta S^{\ddagger}$ /J K^{-1} mol^{-1}	k_1 / s^{-1}
H	bzm	90(1)	10(4)	2.59×10^{-3}
Me	bzm	93(2)	18(7)	2.44×10^{-3}
MeO	bzm	98(3)	32(8)	2.11×10^{-3}
Br	bzm	98(2)	34(7)	2.18×10^{-3}
^-O_2C	bzm	105(2)	54(7)	1.85×10^{-3}
H	H_2O	120(5)	60(17)	9.50×10^{-6}
Me	H_2O	114(6)	42(20)	1.16×10^{-5}

the problem of assigning a formal oxidation state to a metal ion in a complex with ligands that have a delocalised electronic structure has long been recognized [986–988]. Some second order rate constant for the substitution of X by L trans to Y in Co(III) systems with four N-donor equatorial ligands (N_4) are given in Table 22.

In almost all cases substitution occurs faster on Co(III) in a corrin than in cobaloxime, porphyrin, tetrammine or bisethylenediamine systems. (The one exception is where $L = NO_2^-$ for reasons that are not obvious). The ratio $k_{II}^{corrin}/k_{II}^{N_4}$ varies from 7.6×10^8 to 6.5×10^2 for $N_4 = (NH_3)_4$, $(en)_2$ and $BQDI_2$; 10^3 for N_4 = porphyrin; and between 114 and 2 for N_4 = cobaloxime.

It is clear that the corrin is responsible for imparting on Co(III) the unusual lability of the cobalt corrinoids. There are two immediately obvious ways of verifying this. The first is to compare the kinetics of ligand substitution reactions in corrins and other N_4 macrocycles such as porphyrins and corroles, or pseudo macrocycles such as the cobaloximes, expanding the data of Table 22. The second is to modify the electronic and structural properties of the corrin and see what effect this has on the kinetics of the ligand substitution reactions on Co(III). These cis effects have received less attention than the trans effect in cobalt corrinoid chemistry.

Saturation kinetics have been observed in the reaction of the diaqua-Co(III)hematoporphyrin, $[(H_2O)_2Co(HP)]^+$, with SCN^- (pH 7.2) and with CN^- (pH 13) [988]. Since the pK_a of $[(H_2O)_2Co(HP)]^+$ is 10.5 [988], the reaction with SCN^- was for substitution of H_2O trans to H_2O and the reaction with CN^- was for substitution of H_2O trans to OH^-. Although the authors interpreted the data in terms of a D mechanism, they provided no definitive proof of the existence of a five coordinate intermediate. In the absence of such evidence, it is reasonable to conclude that the rate constant at low ligand concentrations, k_2, corresponds to kK_E of an interchange mechanism (Fig. 33), whereas the saturating rate constant corresponds to k, the rate constant for the interchange of H_2O and the entering ligand. The substitution of H_2O trans to H_2O by SCN^- has $k_2 = 1.85 \times 10^3$ M^{-1} s^{-1} and $k = 17.4$ s^{-1}; for substitution of H_2O trans to OH^- by CN^-, $k_2 = 65$ M^{-1} s^{-1} and $k = 11$ s^{-1}.

The rate of substitution of H_2O by SCN^- in $[H_2OCbl]^+$ (i.e., trans to bzm) is of the same order of magnitude as for the porphyrin system (between $1.319(5) \times 10^3$ M^{-1} s^{-1} with $\mu = 2.2$ M (KNO_3) [969] and 7.1×10^3 M^{-1} s^{-1} with $\mu = 0.054$ M [958]), but saturating kinetics (i.e., a value of k) was not observed. The substitution of H_2O by SCN^- trans to H_2O appears not to have been reported.

As mentioned before, the absence of the bzm ligand, as in diaquacobinamide, $[(H_2O)_2Cbi]^{2+}$ ($[DAC]^{2+}$), complicates matters. Both $[DAC]^{2+}$ (pK_a = 5.9 [962]) and aquahydroxocobinamide $[(HO)(H_2O)Cbi]^+$ ($[AHC]^+$) will react with both HCN and CN^-; OH^- is inert to substitution, but displacement of H_2O by CN^- in $[AHC]^+$ will lead to protonation of OH^- trans to CN^- (pK_a of $[AHC]^+ = 11.0$ [331]); and the two diastereomers of $[DAC]^{2+}$ and $[AHC]^+$ may well react at different rates. The kinetics have been examined between pH 4.5 and 12.0 [962], but no attempt appears to have been made to derive microscopic rate

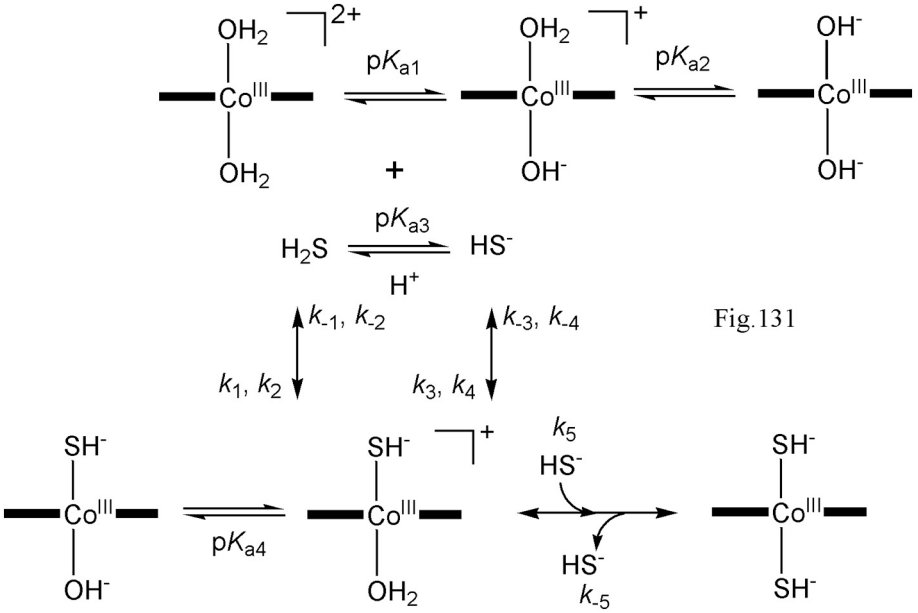

Scheme 34. The reaction of $[DAC]^{2+}$ and $[AHC]^+$ with H_2S and HS^-. (Adapted from [522].)

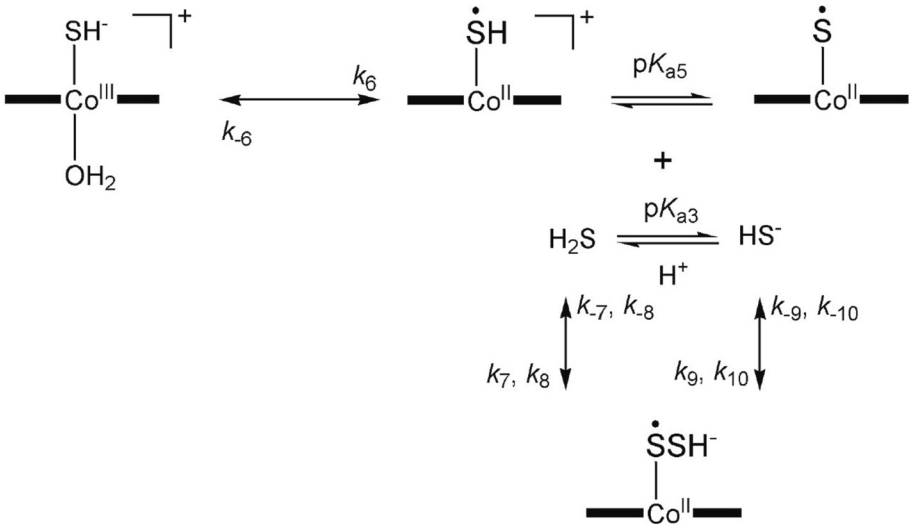

Scheme 35. The reduction of Co(III) to Co(II) by coordinated HS^- in $[(HS)(H_2O)Cbi]^+$ (see Scheme 34) and its subsequent reaction with H_2S/HS^-. (Adapted from [522].)

Table 21
Activation parameters and rate constants for the reaction of $[DAC]^{2+}$ and $[AHC]^+$ with H_2S and HS^- (Schemes 34 and 35).

pK_as					
pK_{a3}	7.3(1)	pK_{a4}	10.0(1)	pK_{a5}	5.2(6)
Activation parameters and second order rate constants (25 °C)[a]					
Rate constant	**$\Delta H^{\ddagger}$/kJ mol^{-1}**	**$\Delta S^{\ddagger}$/J K^{-1} mol^{-1}**	**$\Delta V^{\ddagger}$/cm^3 mol^{-1}**	**k (25 °C) M^{-1} s^{-1}**	
k_1	46(4)	−26(12)		2.4×10^3	
k_{-1}	85(4)	59(12)		9.5	
k_4	58(8)	26(24)		1×10^4	
k_{-4}	100(11)	124(34)		55	
k_5	109(12)	158(36) [c]		87	
k^b_{-5}	82(6)	42(20)		4	
	90(1)	65(3)		3	
k^b_6	72(6)	−8(28)	22(1)	0.6	
	108(10)	110(30)		0.4	
k^b_{-6}	28(4)	−155(12)		0.6	
	77(1) [d]	11(3)		0.2	
Observed first order rate constants (/s^{-1})[e]					
k'_7	0.07(5)				
k'_8	0.49				
k'_9	0.29				
k'_{10}	1.77(3)				

[a]Interpolated from values of $\Delta H^{\ddagger}$ and $\Delta S^{\ddagger}$. Several errors in the text ([522]) have been corrected. [b]Determined by two different methods. [c]Incorrectly given as −158(36) M^{-1} s^{-1} in the publication. [d] Incorrectly given as 7(1) kJ mol^{-1} in the publication. [e] 25 °C, pH 4.0 to 10.5; $[Cbi]_{total} = 50$ μM; $[H_2S]_{total} = 6.25$ mM.

constants from the data, no doubt because of the complexity of the system. We have attempted to fit the kinetic data, but without success, as the variables (i.e., the rate constants and pK_a values) are heavily cross-correlated.

Terphasic kinetics were observed between pH 5 and 7, and biphasic kinetics (i.e., the fastest phase presumably occurred within the dead time of the stopped flow spectrometer used) between pH 7 and 12. The existence of multiphasic kinetics was attributed to the presence of different isomers in solution, depending on the hydrogen bonding between the side chains of the corrin and the axial ligands, but no convincing evidence was presented for this supposition. It is likely that the fastest phase (which produced relatively small changes in the uv-vis spectrum) was due to the formation of an outer sphere complex between the cobamide and the incoming ligand. Ligand exchange with coordinated H_2O then proceeded at different rates for the substitution of the α and β ligands, with the more sterically hindered α face presumably undergoing ligand substitution more slowly. At pH 12.01 (the highest pH value of the study) the only reaction of consequence will be substitution of H_2O trans to OH^- in $[AHC]^+$ by CN^-. The observed rate constants for the faster and the slower phase were 2.2×10^3 M^{-1} s^{-1} and 4.2×10^2 M^{-1} s^{-1}, respectively. Correcting for the fraction of inert dihydroxocobinamide, $[(OH)_2Cbi]$, (the pK_a of $[AHC]^+$ is 10.3 ± 0.2 [962]) then leads to $k_2 = 1.2 \times 10^5$ M^{-1} s^{-1} and 2.2×10^4 M^{-1} s^{-1} for the two phases observed, or at least two orders of magnitude faster than for a porphyrin. Although saturating kinetics for this system have been observed [961], with $k = 9.6(6) \times 10^3$ s^{-1}, or nearly three orders of magnitude faster than for the porphyrin system, the use of KCl to adjust ionic strength to 1.0 M makes the actual value suspect.

The reaction of $[(H_2O)_2Cbi]^{2+}$ and I^- has also been studied [962]. The pH-dependence of the rate of substitution of H_2O by I^- could not be explained, and the authors suggest that ion pairing may be a factor, but made no attempt to resolve the issue; the results are unreliable as it is unclear what reaction was monitored. The reaction of I^- at pH 1 and 2 (i.e, where the only cobalt species is $[(H_2O)_2Cbi]^{2+}$) produced results that, as expected, are within experimental error independent of pH; the two rate constants, $2.2(3) \times 10^3$ M^{-1} s^{-1} and $2.7(4) \times 10^2$ M^{-1} s^{-1} are presumably for the substitution of H_2O by I^- on each of the two faces of the corrin (but see below).

Table 22
Second order rate constants for substitution of ligand X trans to Y by incoming L in some Co(III) complexes.[a]

Equatorial ligand	L	X	Y	$k_{II}^{298}/M^{-1}\,s^{-1}$	$k_{II}^{corrin}/k_{II}^{N_4}$ [b]	Ref
Corrin	SCN^-	H_2O	H_2O	8.20×10^2		[989]
$(NH_3)_4$	SCN^-	H_2O	H_2O	8.60×10^{-7}		[990]
$(NH_3)_4$	SCN^-	H_2O	NH_3	1.30×10^{-6}	7.6×10^8	[804]
Corrin	CN^-	Me	H_2O	very fast [c]		[991]
$(en)_2$	CN^-	Me	H_2O	198		[991]
cobaloxime	CN^-	Me	H_2O	14	2×10^7	[992]
Corrin	im	H_2O	bzm	212		[847]
$(o\text{-BQDI})_2$ [e]	im	PPh_3	–	9.50×10^{-4}	2.2×10^5	[993]
Corrin	MeGly	H_2O	bzm	1.3		[975]
$(NH_3)_4$	Gly	H_2O	NH_3	2.00×10^{-3}	6.5×10^2	[994]
Corrin	NO_2^-	H_2O	bzm	4.50×10^2		[995]
$(NH_3)_4$	NO_2^-	H_2O	NH_3	8.00×10^3	0.06	[531]
Corrin	I^-	H_2O	H_2O	2.20×10^3		[989]
Corrin	I^-	H_2O	bzm	1.40×10^3		[915]
(4-N-Methyl-pyridyl)porphyrin	I^-	H_2O	H_2O	1.62	1.1×10^3	[996]
Corrin	$histam^0$	H_2O	bzm	1.14		[847]
Cobaloxime	$histam^0$	H_2O	CH_2Cl	0.01	114	[997]
Corrin	H_2O	thiourea	bzm	15 [d]		[916]
Cobaloxime	H_2O	thiourea	CH_3	2 [d]	8	[916]
Corrin	$histam^+$	H_2O	bzm	7.5		[847]
Cobaloxime	$histam^+$	H_2O	CH_2Cl	2.58	3	[997]
Corrin	thiourea	H_2O	bzm	223		[916]
Cobaloxime	thiourea	H_2O	CH_3	113	2	[916]

[a] Abbreviations: cobaloxime, bis(dimethylglyoximato); bzm, 5,6-dimethylbenzimidazole; $histam^0$ and $histam^+$, neutral and cationic histamine with neutral and protonated pendant amino groups, respectively; im, imidazole. [b] Ratio of k_{II} for corrin to k_{II} for an N_4 equatorial system at 298 K. [c] Reaction too fast to measure by stopped flow methods. Assuming a typical instrument dead time of 2 ms, this suggests $t_{1/2} < 2$ ms or $k_{obs} > 10^6\,s^{-1}$. Assuming $[(H_2O)(CN)Cbi]^+ = 50\,\mu M$, this requires $[CN^-] > 500\,\mu M$ for pseudo first order conditions, or $k_{II} > 2 \times 10^9\,M^{-1}\,s^{-1}$. [d] Aquation rate constant, s^{-1}.
[e] o-benzosemiquinondiiime,

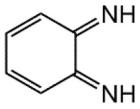

There are limited data for the hydrolysis of cobalt corrinoids so direct comparison with other Co(III) macrocyclic complexes is difficult, not least because of different trans ligands. Nevertheless, is may be noted that the rate of hydrolysis of [BrCbl] (Br^- trans to bzm), $5.90 \times 10^2\,s^{-1}$ [889], is considerably faster than hydrolysis of $[Br_2Co(tet\mathit{a})]^+$ (i.e., Br^- trans Br^-; tet*a* = 5,7,7,12,14,14-hexamethyl-1,4,8,11-tetraazacyclotetradecane), $3.8 \times 10^{-2}\,s^{-1}$ [998], although the rate of hydrolysis of [SCNCbl] ($1.8\,s^{-1}$ [958]) is very similar to that of hydrolysis of $[(SCN)_2Co(tet\mathit{a})]^+$ ($1.5\,s^{-1}$ [998]). Poon pointed out that cyanide and chloride have very similar trans labilising effects in cyclam complexes (cyclam = 1,4,8,11-tetra-azacyclo-tetradecane) [964]; it may therefore be reasonable to compare the rate constant of aquation (substitution of NH_3) of trans-$[Co(cyclam)Cl(NH_3)]^{2+}$, $k_{aq} = 4.6 \times 10^{-11}\,s^{-1}$ (25 °C) [999] and $[(NH_3)(CN)Cbi]^+$, $k_{aq} > 0.3\,s^{-1}$ [625], indicating the nearly 10 orders of magnitude greater reactivity of the corrinoid complex.

Further evidence for the lability imparted on Co(III) compared to other N_4 equatorial donor systems is given in Table 23.

Direct evidence of the cis effect of the corrin ligand can be obtained by perturbing the electronic structure of the corrin. Replacing the C10H by electron-withdrawing NO in 10-nitrosoaquacobalamin completely deactivates the metal ion towards ligand substitution by 1.2 M pyridine (no observable reaction after 72 h, 1.2 M pyridine) or 0.7 M N_3^- [772].

The replacement of the C10H by Cl [856] to form $[H_2O\text{-}10ClCbl]^+$ (Table 24) and by Br to form $[H_2O\text{-}10BrCbl]^+$ [231] (Table 25) results in a decrease in the rate of H_2O substitution by an incoming ligand, Z.

Saturating kinetics were observed for the reaction of $[H_2O\text{-}10ClCbl]^+$ with pyridine but not with N_3^-, indicative that an interchange mechanism is operative. Both $\Delta H^‡$ and $\Delta S^‡$ values are more positive for the reactions between these ligands and $[H_2OCbl]^+$ than for the reactions with $[H_2O\text{-}10ClCbl]^+$, which suggests that the transition state in the latter occurs earlier along the reaction coordinate than the former.

Table 23
Second order rate constants for substitution of Y *trans* to X in $X\text{–}Co^{III}(N_4)\text{–}Y$ systems by entering Z.

Equatorial ligand	Y	Z	X	$k_2/M^{-1}\,s^{-1}$	Ref
corrin	H_2O	I^-	H_2O	2.2×10^3	[989]
(4-*N*-methyl-pyridyl)-porphyrin	H_2O	I^-	H_2O	1.62	[996]
corrin	H_2O	SCN^-	H_2O	8.2×10^2	[989]
$(NH_3)_4$	H_2O	SCN^-	H_2O	8.6×10^{-7}	[990]
corrin	Me	CN^-	H_2O	very fast	[991]
$(en)_2$	Me	CN^-	H_2O	198	[991]
cobaloxime	Me	CN^-	H_2O	14	[992]
corrin	H_2O	imidazole	bzm	212	[847]
(*o*-benzosemi-quinonediiminato)$_2$	PPh_3	imidazole	none	9.5×10^{-4}	[993]
corrin	H_2O	$histamine^0$	bzm	1.14	[847]
cobaloxime	H_2O	$histamine^0$	CH_2Cl	0.01	[997]
corrin	H_2O	$histamine^+$	bzm	7.5	[847]
cobaloxime	H_2O	$histamine^+$	CH_2Cl	2.58	[997]

Single point semi-empirical MO calculations (RHF, ZINDO/1) showed that as the Co—OH_2 bond length is increased, the charge density on Co in $[H_2O\text{-}10ClCbl]^+$ is always more positive than in $[H_2OCbl]^+$; the former is therefore the better electrophile towards the incoming ligand, rationalising the observed kinetics results.

The results for $[H_2O\text{-}10BrCbl]^+$ are similar. Replacement of C10H with Br results in slower substitution reactions that are a consequence of smaller values of $\Delta H^‡$ but which do not compensate for more negative values of $\Delta S^‡$, again indicative of an earlier transition state. That the transition state occurs earlier along the reaction coordinate of the reaction with the 10-Cl and 10-Br derivatives than with $[H_2OCbl]^+$ was

Table 24
Kinetics data for the substitution of H_2O in $[H_2OCbl]^+$ and $[H_2O\text{-}10ClCbl]^+$.

	Z = py			$Z = N_3^-$		
	k /s^{-1} [a]	$\Delta H^‡$ /kJ mol^{-1}	$\Delta S^‡$ /J K^{-1} mol^{-1}	k /s^{-1} [b]	$\Delta H^‡$ /kJ mol^{-1}	$\Delta S^‡$ /J K^{-1} mol^{-1}
$[H_2OCbl^+]$ [c]	16.8	80(2)	47(8)	15.7×10^3	92(2)	125(8)
$[H_2OCbl^+]$ [d]	28.0	85(3)	68(10)			
$[H_2O\text{-}10ClCbl^+]$ [c]	3.8	70(1)	1(4)	8.0×10^2	74(1)	58(5)

[a]Saturating rate constant for interchange of py and H_2O in an I_d mechanism (see Fig. 33). [b]Estimated from the values of kK_E; for K_E, $\Delta H = -24$ kJ mol^{-1} and $\Delta S = -90$ J K^{-1} mol^{-1} [980]. [c] $\mu = 2.2$ M [856],. [d] $\mu = 0.5$ M [967]. $\Delta H^‡ = 73(3)$ jkJ mol^{-1}, $\Delta S^‡ = 21(11)$ J K^{-1} mol^{-1}, and $k_2 = 12.5$ M^{-1} s^{-1} $\Delta H^‡ = 73(3)$ jkJ mol^{-1}, $\Delta S^‡ = 21(11)$ J K^{-1} mol^{-1}, and $k_2 = 12.5$ M^{-1} s^{-1}.

Table 25
Kinetics data for the substitution of H_2O in $[H_2OCbl]^+$ and $[H_2O\text{-}10BrCbl]^+$. (Data from [231] unless otherwise indicated.)

	Z = imidazole				$Z = N_3^-$			
	k_2(25 °C)[a] /M^{-1} s^{-1}	$\Delta H^‡$ /kJ mol^{-1}	$\Delta S^‡$ /J K^{-1} mol^{-1}		k_2 /M^{-1} s^{-1}	$\Delta H^‡$ /kJ mol^{-1}	$\Delta S^‡$ /J K^{-1} mol^{-1}	
$[H_2OCbl^+]$ [b, c]	24.9	82(2)	57(8)	[960]	4.47×10^2	68(2)	34(8)	[969]
$[H_2O\text{-}10BrCbl]^+$	6.4	66(4)	−8(15)		3.62×10^2	54(5)	−13(17)	d

[a]Second order rate constant k_2. No saturation behaviour observed. [b] $\mu = 1.0$ M. [c]For Z = *N*-methylimidazole, $\Delta H^‡ = 73(3)$ jkJ mol^{-1}, $\Delta S^‡ = 21(11)$ J K^{-1} mol^{-1}, and $k_2 = 12.5$ M^{-1} s^{-1} [890]. [d]Reverse reaction: $\Delta H^‡ = 89(5)$ kJ mol^{-1}, $\Delta S^‡ = 20(17)$ J K^{-1} mol^{-1}, and $k_r = 1.7$ s^{-1}.

suggested to be a consequence of the lower charge density on the metal in the 10-Cl and 10-Br derivatives, making them better electrophiles both towards the incoming and the departing ligand.

The rate constants and activation parameters for the substitution of H_2O by CN^- in aquacyanocobester ($[ACCbs]^+$) and aquacyano-stable yellow cobester ($[ACSYCbs]^+$, see Fig. 27) (which exist in aqueous solution as an equilibrium mixture of the *α*-cyano,*β*-aqua and *α*-aqua,*β*-cyano diastereomers) have been determined using stopped-flow spectrophotometry [892]. Biphasic kinetics were observed, and the results are summarised in Table 26.

The two rate constants could correspond to the reactions of the two diastereomers with entering CN^-. However, the reaction of the two diastereomers of aquacyanocobinamide ($[ACCbi]^+$) with CN^- ($k_2 = 2.1 \times 10^5$ M^{-1} s^{-1}) [1000] and the reaction of aquahydroxocobinamide ($[AHCbi]^+$) with CN^-, N_3^-, pyridine, *N*-methylimidazole and 3-aminopropan-1-ol gave only monophasic kinetics [961]. Only in the case of the reaction of aquacyanocobyrinic acid (with all amide side chains hydrolysed) were biphasic kinetics observed by Zelder and co-workers, with $k_2 = 1.56(4) \times 10^4$ and $4.22(5) \times 10^3$ and M^{-1} s^{-1}; this was assumed to be due to the reaction of the two diastereomers [1001].

In a subsequent study, the same group [108] were able to produce diastereomerically pure aquacyano corrinoids and measure the kinetics of substitution of H_2O by CN^-. The results obtained are summarised in Table 27.

Perhaps surprisingly, substitution of H_2O on the *α* face of the corrin proceeds over five times faster than on the sterically less hindered *β* face, with a significant difference of some 5 kJ mol^{-1} in the value of $\Delta H^‡$, indicative of more significant bonding between the metal and the incoming CN^- ligand. There is no statistically significant difference in the values of $\Delta S^‡$. The slower reaction of CN^- with the cobester containing a *c* side chain monocarboxylic acid was tentatively attributed to the effects of hydrogen bonding with the H_2O on the *β* face of the corrin,

Table 27
Kinetics data for the reaction of cyanide with diasteromerically pure aquacyano corrinoids.

	$\Delta H^‡$ /kJ mol^{-1}	$\Delta S^‡$ /J K^{-1} mol^{-1}	k_2 /M^{-1} s^{-1}
[(*β*-H_2O,*α*-CN)Cbi]$^+$	58(1)	50(1)	1.73×10^5
[(*β*-CN,*α*-H_2O)Cbi]$^+$	53(1)	47(5)	9.09×10^5
[(*β*-H_2O,*α*-CN)Cbs-cCA] [a]	51(1)	19(1)	7.03×10^4

[a]Cobester with all side chain terminating in —OCH_3 except for the *c* side chain, which is a carboxylic acid.

perhaps stabilising the bonding between Co(III) and H_2O, and conferring on the reaction a more associative character as reflected in the significantly less positive value of $\Delta S^‡$.

$[AHCbs]^+$ reacts with CN^- (pH 9.0) with a change in absorbance at 367 nm which very nearly – but not quite – conformed to a single-exponential process [892]. The absorbance changes could not be fitted to a double-exponential because of the high cross-correlation of the variables. Clearly the two diastereomers of $[AHCbs]^+$ react at very similar rates, with $k_2 = 5.3(5) \times 10^3$ M^{-1} s^{-1} at 25 °C, identical to the value of 5.39×10^3 M^{-1} s^{-1} of the slower phase of the reaction of $[ACCbs]^+$ with CN^- (Table 26). There is evidence (spectroscopic and chromatographic) that dicyanocobester ([DCCbs]) and dicyano stable yellow cobester ([DCSYCbs]) are present in aqueous solutions of $[ACCbs]^+$ and $[ACSYCbs]^+$ [892]. An analogous observation has been made about solutions of aquacyanocobinamide ($[ACCbi]^+$) [989]. It is therefore likely $[ACCbs]^+$ and $[ACSYCbs]^+$ (and indeed $[ACCbi]^+$) exist in solution as an equilibrium mixture of the aquahydroxo, the aquacyano and the dicyano complexes. Given that CN^- has a greater trans effect than OH^- and that the slower phase of the reaction of $[ACCbs]^+$ with CN^- is identical to that of $[AHCbs]^+$ with CN^-, it was reasonably concluded that the k_2^I values in Table 26 are for substitution of H_2O by CN^- trans to CN^-, and k_2^{II} for substitution of H_2O by CN^- trans to OH^-.

Table 26
Kinetics data for the substitution of H_2O in $[ACCbs]^+$ and $[ACSYCbs]^+$ by CN^-.

	$\Delta H^‡$ /kJ mol^{-1}	$\Delta S^‡$ /J K^{-1} mol^{-1}	k_2^I [a] /M^{-1} s^{-1}	$\Delta H^‡$ /kJ mol^{-1}	$\Delta S^‡$ /J K^{-1} mol^{-1}	k_2^{II} [b] /M^{-1} s^{-1}
[ACCbs]	46(3)	−2(9)	4.23×10^4	52(7)	1(24)	5.39×10^3
[ACSYCbs]	57(6)	29(3)	2.08×10^4	72(5)	50(18)	6.10×10^2

[a]For the faster of the two reactions observed. [b]For the slower of the two reactions. The values of k_2 are interpolated from the activation parameters.

The value of of k_2^I at 25 °C for the reaction of CN^- with $[ACCbs]^+$ is just over twice that for its reaction with $[ACSYCbs]^+$. The apparent similarity requires careful consideration, however. There is a compensation effect between the values of $\Delta H^‡$ and $\Delta S^‡$ (as $\Delta H^‡$ decreases, $\Delta S^‡$ increases). As noted above, $k_2^I = kK_E$, where, in an I_d mechanism k is the rate constant for interchange between CN^- and H_2O and K_E is the equilibrium constant for the formation of the outer sphere complex. According to the Fuoss-Eigen model, K_E is a function of the molar volume and the charge of the outer sphere complex; these are likely to be very similar for $[ACCbs]^+ + CN^-$, and for $[ACSYCbs]^+ + CN^-$. Hence it is reasonable to suppose that differences in $\Delta H^‡$ and $\Delta S^‡$ reflect differences in the transition state for the interchange reaction.

The transition state will feature an elongated Co—OH_2 bond, and the formation of a Co—CN^- bond. Differences in the electronic structure of two systems are expected to manifest predominantly as differences in $\Delta H^‡$ [1002]. That the value of $\Delta H^‡$ for the reaction of CN^- with $[ACCbs]^+$ is some 11 kJ mol^{-1} smaller than for its reaction with $[ACSYCbs]^+$ reflects a transition state that occurs earlier along the reaction coordinate, with better bonding between the soft incoming ligand and the softer metal centre on $[ACCbs]^+$. Interruption of the conjugation of the corrin makes the Co(III) harder and hence have a lower affinity for entering CN^-. The consequence of this is a more negative value of $\Delta S^‡$ because of loss of freedom of the entering ligand which has not been wholly compensated for by the increasing freedom of the departing ligand. A late transition state, on the other hand, will have a large $\Delta H^‡$ value because bond breaking to the departing ligand has not been significantly compensated for by bond formation to the entering ligand, and this will be offset by a positive value of $\Delta S^‡$ because of a more disordered transition state with significant freedom of the departing ligand and with only a small loss of freedom of the entering ligand – and hence the more positive value of $\Delta S^‡$ for the reaction of CN^- with $[ACSYCbs]^+$. Indeed, if the values of $\Delta S^‡$ were the same, $[ACCbs]^+$ would react one hundred times, and not twice, as fast with CN^-. Values of $\Delta H^‡$ are more informative than values of k_2 and indicate the significant increase in the inertness of Co(III) upon interruption of the conjugation of the corrin ring.

The reaction of CN^- with $[ACCbs]^+$, aquacyano(10-nitro)cobester ($[AC\text{-}10NO_2Cbs]^+$) and aquacyano(10-amino)cobester ($[AC\text{-}10NH_2Cbs]^+$) in 50% isopropanol also produced biphasic kinetics, with the faster phase attributed to the substitution of H_2O trans to CN^- by CN^-, and the slower phase to substitution of H_2O trans by OH^- by CN^- [891] (Table 28).

There is a small, but significant difference in the values of k_2^I, but a difference which is again masked by the compensation effect between $\Delta H^‡$ and $\Delta S^‡$. If all three reactions had the same value of $\Delta S^‡$ the values of k_2^I would vary in the approximate ratio 109:106:1 for the C10 substituent Z = NH_2, H and NO_2, respectively.

The results in Table 28 are consistent with an early transition state for the reaction between CN^- and $[AC\text{-}10NH_2Cbs]^+$, a somewhat later transition state for the reaction between CN^- and $[ACCbs]^+$, and an even later transition state when CN^- reacts with $[AC\text{-}10NO_2Cbs]^+$. This is a consequence of the hardness of the metal ion increasing as the C10 substituent changes from electron-donating NH_2 to strongly electron-withdrawing NO_2, and concomitant decrease in the affinity of the metal ion for the soft entering ligand, CN^-. This is an illustration of what a profound effect altering the electronic structure of the equatorial ligand in a Co(III) macrocycle will have on the reactivity of the metal ion.

Biphasic kinetics were also observed for the substitution of H_2O in the aquacyano complex of 5-seco-cobester $[AC\text{-}5\text{-}seco\text{-}Cbs]^+$ (see Fig. 27) [781]. For this system as well there was clear evidence of the presence of the dicyano and the diaqua complexes in solution in equilibrium with the aquacyano complex. The faster phase was attributed to substitution of H_2O trans to CN^-, and the slower phase to substitution of H_2O trans to H_2O. Only an estimate of the rate constant for the substitution of H_2O in $[AC\text{-}5\text{-}seco\text{-}Cbs]^+$ by CN^- could be obtained because of the rather poor reproducibility of the data; the value of k_2 was estimated to be 10^2 M^{-1} s^{-1}. The value of k_2 for substitution of H_2O in $[ACCbs]^+$ and $[ACSYCbs]^+$ is $4.8(3) \times 10^4$ M^{-1} s^{-1} and $1.53(2) \times 10^4$ M^{-1} s^{-1}, respectively in aqueous solution [892]. In 50% isopropanol, k_2 for substitution of H_2O by CN^- in the aquacyano complexes of 10-Z-Cbs, where Z is the substituent at the C10 position of corrin, is 7.8×10^4 M^{-1} s^{-1} for X = H (i.e., for $[ACCbs]^+$ itself); 3.0×10^4 M^{-1} s^{-1} for Z = NH_2; and 1.7×10^2 M^{-1} s^{-1} for Z = NO_2 [891]. Despite the uncertainty in the value of k_2 for the substitution of H_2O by CN^- in $[AC\text{-}5\text{-}seco\text{-}Cbs]^+$, it is clear that interrupting the delocalised electronic system of the corrin causes a very marked decrease in the rate constants. Perturbing the electron density of the macrocyclic ligand, and the size of the macrocyclic cavity, affects the lability of Co(III); the metal ion becomes more inert and Co(III)-like in its behaviour.

The kinetics data for substitution of H_2O in $[H_2OCbl]^+$ and the Co(III) porphyrin analogue of $[H_2OCbl]^+$, NAcCoMP8 (see Fig. 27) are shown in Table 29.

The value of $\Delta H^‡$ for the reaction of CN^- with $[H_2OCbl]^+$ is much smaller than for its reaction with NAcCoMP8, although the much more negative value of $\Delta S^‡$ masks the very considerable difference in the behaviour of the metal ion towards incoming CN^- if only the value of k_2 is considered. If the values of $\Delta S^‡$ were the same, then k_2 would be some 10^4 times larger for the reaction of CN^- with $[H_2OCbl]^+$. The opposite is true for the reaction with NMeIm, a consequence of a smaller value of $\Delta H^‡$ and a somewhat larger values of $\Delta S^‡$. This parallels values of log K for coordination of CN^- by the two Co(III) complexes: log $K = 14.1$ for $[H_2OCbl]^+$ [444] but 6.04 for NAcCoMP8 [890]; in the case of NMeIm, log $K = 4.49$ for coordination by $[H_2OCbl]^+$ but 5.70 for coordination by NAcCoMP8 [890]. The relative lability of Co(III) in a porphyrin and a corrin is clearly influenced by their relative affinity for the incoming ligand.

Another factor that may influence the values of $\Delta S^‡$ are the effects of electrostriction; this was the main argument advanced to rationalise the activation parameters in a comparative study of the kinetics of the substitution of H_2O in $[H_2OCbl]^+$ and $[H_2O\text{-}DPTC\text{-}Co]$, a Co(III) corrole analogue of $[H_2OCbl]^+$ (Fig. 27) by CN^- in 80:20 MeOH:H_2O and low ionic strength (30 mM) [1003]. For the reaction with $[H_2OCbl]^+$, $\Delta H^‡ = 82(5)$ kJ mol^{-1} and $\Delta S^‡ = 96(19)$ J K^{-1} mol^{-1}, giving k_2 (25 °C) $= 2.72 \times 10^3$ M^{-1} s^{-1} while for $[H_2O\text{-}DPTC\text{-}Co]$, $\Delta H^‡ = 41(1)$ kJ mol^{-1} and $\Delta S^‡ = -50(3)$ J K^{-1} mol^{-1}, and $k_2 = 9.\ 90 \times 10^2$ M^{-1} s^{-1}. In this case, $\Delta H^‡$ is much smaller for the corrole system than for the corrin system – but again differences in k_2 are masked by a compensation effect with $\Delta S^‡$ very negative and very positive, respectively, for the two systems. $[H_2O\text{-}DPTC\text{-}Co]$ has a higher affinity for CN^- in 80% MeOH than does $[H_2OCbl]^+$ (log $K = 13.1(7)$ compared to 12.53(7) [1003]), a consequence of which is the difference in values of $\Delta H^‡$. A factor controlling $\Delta S^‡$ is the position of the transition state along the reaction coordinate, as was argued in several instances reviewed above, reflected in

Table 28
Kinetics data for the substitution of H_2O in $[ACCbs]^+$, $[AC\text{-}10NO_2Cbs]^+$ and $[AC\text{-}10NH_2Cbs]^+$ by CN^-.

	$\Delta H^‡$ /kJ mol^{-1}	$\Delta S^‡$ /J K^{-1} mol^{-1}	$k_2^{I\,a}$ /M^{-1} s^{-1}	$\Delta H^‡$ /kJ mol^{-1}	$\Delta S^‡$ /J K^{-1} mol^{-1}	$k_2^{II\,b}$ /M^{-1} s^{-1}
$[ACCbs]$	58(3)	43(12)	7.8×10^4	92(19)	150(66)	3.3×10^4
$[AC\text{-}10\text{-}NO_2Cbs]^+$	90(3)	119(12)	1.7×10^3	77(8)	53(28)	1.3×10^2
$[AC\text{-}10\text{-}NH_2Cbs]^+$	40(3)	−27(11)	3.0×10^4	34(3)	−71(9)	1.1×10^3

[a]For the faster of the two reactions observed. [b]For the slower of the two reactions. The values of k_2 are interpolated from the activation parameters.

Table 29
Kinetics data for the reaction of $[H_2OCbl]^+$ and NAcCoMP8 with CN^- and *N*-methylimidazole.

Entering ligand	Co(III) complex	$\Delta H^‡$ /kJ mol^{-1}	$\Delta S^‡$ /J K^{-1} mol^{-1}	k_2 /M^{-1} s^{-1}	$\Delta H^‡$ /kJ mol^{-1}	$\Delta S^‡$ /J K^{-1} mol^{-1}	k_{-2} /s^{-1}	Ref
CN^-	$[H_2OCbl]^+$	52(1)	−25(4)	2.37×10^2				[737]
	NAcCoMP8	75(3)	46(9)	1.12×10^2				[890]
NMeIm	$[H_2OCbl]^+$	73(3)	21(11)	1.2×10^1	146(26)	196(83)	1.2×10^{-2}	[890]
	NAcCoMP8	66(5)	34(16)	1.0×10^3	86(25)	−5(99)	3.3×10^{-3}	[890]

a substantially more negative value for $\Delta S^‡$ for the corrole system than for the corrin system. The effect of electrostriction was advanced as an additional factor to be considered [1003]. $[H_2OCbl]^+$ has a net charge of +2 at the metal centre (the charge on phosphate, some 9 Å away from the metal, is unlikely to influence matters). On the other hand, the corrole system has a net charge of 0 at the metal centre, with the 3+ charge on the metal balanced by the negative charges on the N donors of the macrocycle. The reaction between CN^- and $[H_2OCbl]^+$ would involve some neutralisation of charge at the metal centre; this would lead to a significant release of solvent electrostriction, contributing to the large, positive values of $\Delta S^‡$. The entering of CN^- into the coordination sphere of Co(III) in [H$_2$O-DPTC-Co] results in an anionic species, leading to the electrostriction of the solvent, and a contribution to a negative value of $\Delta S^‡$.

The rationalisation of kinetics data is not a straight forward matter; it is clear, though, that the examination of values of $\Delta H^‡$, $\Delta S^‡$ and (where available) $\Delta V^‡$ is likely to provide more insight that simply comparing values of rate constants.

9.3. The effect of solvent

The effect of the solvent on the kinetics of the ligand substitution reactions of the cobalt corrinoids has received some – if limited – attention. Perhaps the most comprehensive investigations were carried out by Balt et al. [916,922,923,1004]. They measured the rate of the reaction of $[H_2OCbl]^+$ with $S_2O_3^{2-}$ as a function of ionic strength and solvent composition [1004]. The second order rate constant k_2 (a composite of the interchange rate constant k and the equilibrium constant K_E for formation of the outer sphere complex in an interchange mechanism, Fig. 33) decreases with increasing ionic strength, $\mu(NaClO_4)$, presumably reflecting the competition of the non-coordinating anion with $S_2O_3^{2-}$ for the outer coordination sphere of the metal complex [1002]. A plot of k_2 against $\mu^{½}$ yields a good straight line (not shown in the original paper) in accordance with simple Debye-Hückel theory.

Increasing the percentage of (non-coordinating) dioxane in dioxane-water mixtures marginally decreases the rate of anation (from k_2 = ca. 5.0×10^2 M^{-1} s^{-1} in aqueous solution, $\mu = 0.1$ M to ca. 2.0×10^2 M^{-1} s^{-1} in 70% dioxane). Since this does not parallel the solubility pattern of [H$_2$OCbl]Cl in the solvent mixtures, it was concluded that the transition state resembles the ground state and that the reaction has a dissociative character.

Qualitatively similar results were obtained for substitution of H_2O in $[H_2OCbl]^+$ by thiourea in dioxane-water mixtures. The rate is only moderately sensitive to the composition of the solvent, decreasing with an increase in the fraction of dioxane ($k_2 = 235$ M^{-1} s^{-1}, $\Delta H^‡ = 69$ kJ mol^{-1}, $\Delta S^‡ = 32$ J K^{-1} mol^{-1} in aqueous solution, $\mu = 0.1$ M ($NaClO_4$); and $k_2 = 97$ M^{-1} s^{-1}, $\Delta H^‡ = 70$ kJ mol^{-1}, $\Delta S^‡ = 28$ J K^{-1} mol^{-1} in 80% dioxane), leading to the conclusion that $[H_2OCbl]^+$ creates its own solvent micro-environment that makes its ligand substitution reactions rather insensitive to the bulk solvent composition [923].

A study of the kinetics of substitution of H_2O in $[H_2OCbl]^+$ by a series of neutral S-donor thiourea derivatives in H_2O solvent and in 50% dioxane-water solvent show that (i) reaction rates in H_2O are about 4 times faster than in the mixed solvent system, (ii) decrease with the steric bulk of the incoming ligand, as expected, and (iii) it was speculated, are influenced by whether the incoming ligand is capable of hydrogen bonding with the acetamide side chains of the corrin [916]. Equilibrium constants for the formation of these complexes are rather insensitive to the composition of the solvent.

The reaction of $[H_2OCbl]^+$ with SCN^- occurs in two steps. The first was assumed to be the displacement of H_2O by SCN^- to produce the thiocyanato-*κ*–S isomer, which then isomerises to the thiocyanato-*κ*–N isomer. (There is more recent NMR evidence that SCN-Cbl exists as a mixture of the two isomers in solution [799].) It is unclear which is the primary kinetic product but the assumption that it is the *κ*–S isomer seems reasonable given that the initial uv-vis spectrum is reminiscent of complexes with S-donor ligands while the final spectrum is similar to complexes with N-donors. The *κ*–N isomer is well-known in the solid state [799,800,1005], although there is a report of the existence of the *κ*–S isomer as well [1006]. The equilibrium constant for formation of [(SCN)Cbl] increases from log $K = 3.30$ in H_2O to 4.17 in 80% MeCN-H_2O, while the rate of the anation reaction decreases from 3.24×10^3 M^{-1} s^{-1} to 1.67×10^3 M^{-1} s^{-1} in these solvents.

Very similar trends were found for the reaction of pyridine and $[H_2OCbl]^+$ in 70% EtOH [1007]. Saturation kinetics are observed, as first reported by van Eldik et al. [967,968]. The non-aqueous solvent mixture decreases the observed rate constant at 25 °C from 16.8 s^{-1} to 9.5 s^{-1}. This very small difference belies the significant differences in the activation parameters for the reaction. The values of $\Delta H^‡$ for the rate constant for interchange of H_2O and pyridine are 80(2) and 99(8) kJ mol^{-1} in water and ethanol–water, respectively, while $\Delta S^‡$ values are 47 (8) and 106(27) J K^{-1} mol^{-1}, respectively. There is therefore a compensation effect between the two parameters, emphasizing, as stated above, that a comparison of rate constants (and for that matter, equilibrium constants) determined at a single temperature is unlikely to be very meaningful. The compensation effect between the two activation parameters is interpreted in terms of the position of the transition state along the reaction coordinate; this occurs later in an ethanol–water mixture, probably because the outer sphere complex that precedes the ligand exchange is less favoured than in pure water. These results, together with those of Balt and co-workers, suggest that this may be a general feature of the ligand substitution reactions of $[H_2OCbl]^+$ in mixed solvents.

9.4. The base-on/base-off equilibrium: kinetics

The kinetics of the base-on/base-off equilibrium in alkylcobalamins have been studied by pH-jump stopped flow measurements [802]. The observed rate constants decrease with increasing $[H^+]$ up to $[H^+] \approx 0.1$ M, and then increase as an acid-catalysed pathway from dissociation of bzm becomes important, $k_H = k_{-1}/K$ (Scheme 36). The results obtained with $X^- = CF_3^-$, $NCCH_2^-$ and CN^- are summarised in Table 30, illustrating the kinetic trans effect order $NCCH_2^- > CF_3^- > CN^-$.

The rate constants for the dechelation of bzm in $[CF_3Cbl]$ were determined by pH jump experiments [802]; the assumed reactions of the system are shown in Scheme 37. (Where precisely the site of protonation of *base-on* **2** is, is unclear.) The ratio k_{-1}/K_4 was defined as k_H, the rate constant for the acid-catalysed dechelation of bm and its substitution by CN^-; k_{-3} is the rate constant for the replacement of bzm by solvent H_2O. The observed first order rate constant is related to the microscopic rate and equilibrium constants by Eq. 41; $k^H = k_{-1} K_4$.

$$k_{obs} = k_{-3} + \frac{k_3 K_2}{K_2 + [H^+]} + k^H[H^+] \quad (41)$$

As the pH decreases, the contribution of the second term to k_{obs}

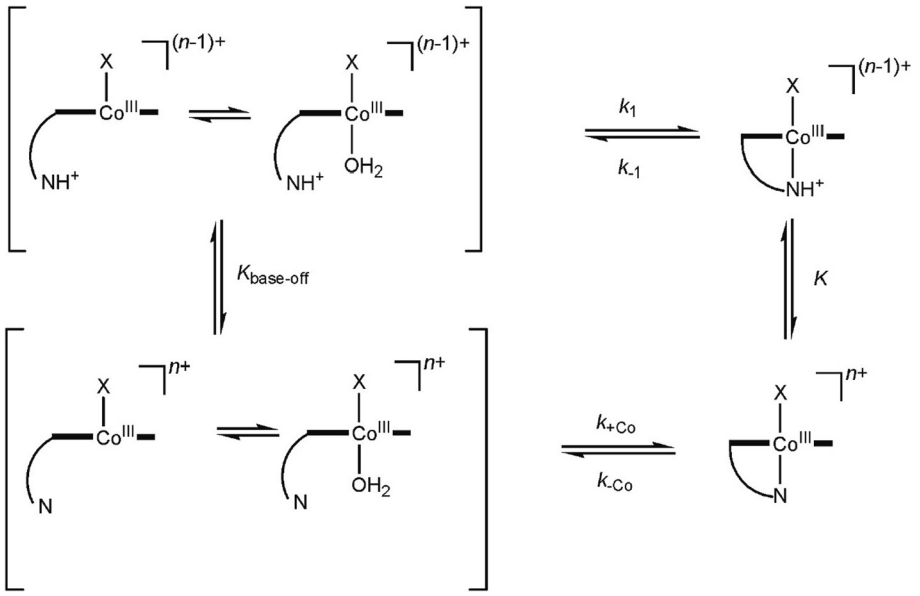

Scheme 36. Kinetic scheme for the base-on/base-off equilibrium of the cobalamins.

Table 30
Rate constants for coordination of bzm in alkylcobalamins[a].

X^-	$pK_{base\text{-}off}$	k_{+Co}/s^{-1}	k_{-Co}/s^{-1}	$k_H/M^{-1}\,s^{-1}$
$NCCH_2^-$	1.81	$4.4(3)\times10^5$	83(13)	$9.1(7)\times10^2$
CF_3^-	1.44	$7.80(7)\times10^4$	7.7(2)	31.8(4)
CN^-	0.1	$9.2(6)\times10^3$	0.19(4)	0.28(6)

[a]See Scheme 36.

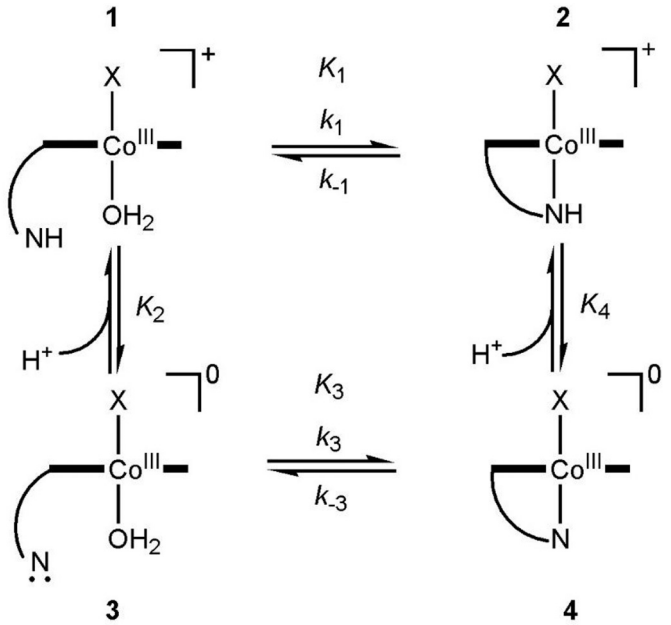

Scheme 37. Reaction scheme for the substitution of bzm trans to X by CN^- as defined by van Eldik and co-workers [802].

decreases and k_{obs} drops (for example, from $365\,s^{-1}$ with $[HClO_4]=0.01$ M to $130\,s^{-1}$ when $[HClO_4]=0.025$ M for the reaction of $[NCCH_2Cbl]$ with $HClO_4$ (5 °C, $\mu=1.0$ M) [802]. With increasing $[HClO_4]$ the rate rises as the k^H term becomes more important ($k_{obs}=360\,s^{-1}$ with $[HClO_4]=0.30$ M).

The values of k^H (25 °C, $M^{-1}\,s^{-1}$) for $[NCCH_2Cbl]$ $(9.1(7)\times10^2)$, $[CF_3Cbl]$ (31.8(4)) and [CNCbl] (0.28(6)] reflect the trans effect order of the β ligand. Based on this [802] and evidence from other studies [516,927,1008], the trans effect of alkyl ligands in alkylcobalamins was determined to be $Pr \geq Et \geq Ado \geq Me > CF_3CH_2 > CF_2H > NCCH_2 > CF_3 > CN^-$.

9.5. Kinetics of the displacement of bzm

The mechanism of the substitution of bzm coordinated in the α coordination site by CN^- trans to an alkyl group in alkylcobalamins [516,1008] and of imidazole trans to CN^- in cyanoimidazolylcobamide in which the axial base is imidazole rather than bzm [812], has been studied. The kinetic evidence points to a D [516] or I_d [812,1008] mechanism involving rate-limiting dechelation of the axial base to form an alkylaqua intermediate, followed by replacement of H_2O by CN^- (Scheme 38, $X=R^-$ or CN^-). For $X=CH_3^-$, the apparent equilibrium constant for substitution of bzm by CN^- is 0.38 M^{-1} [1008] (or 0.35 M^{-1} [1009]).

The substitution of the base (bzm or imidazole) with CN^- shows saturation kinetics in a plot of the observed first order rate constant against $[CN^-]$, and a non-zero intercept. The saturating rate constant could then correspond to the rate of dissociation of H_2O in a D mechanism (k_1 in Scheme 38) or to the rate constant for the interchange of the base and H_2O in an I_d mechanism. The intercept is the rate constant for the reverse reaction.

For $X=NCCH_2$, $\Delta H^{\ddagger}=85(2)$ kJ mol^{-1}, $\Delta S^{\ddagger}=97$ (6) J K^{-1} mol^{-1} and $\Delta V^{\ddagger}=12.7(5)$ cm^3 mol^{-1}; and for $X=CN^-$, $\Delta H^{\ddagger}=105(2)$ kJ mol^{-1}, $\Delta S^{\ddagger}=81(6)$ J K^{-1} mol^{-1} and $\Delta V^{\ddagger}=13.1(3)$ cm^3 mol^{-1} [516]. For $X=CF_3$ trans to bzm, $\Delta H^{\ddagger}=77(3)$ kJ mol^{-1}, $\Delta S^{\ddagger}=44(11)$ J K^{-1} mol^{-1} and $\Delta V^{\ddagger}=14.8(8)$ cm^3 mol^{-1}; and for $X=CH_2CF_3$, $\Delta H^{\ddagger}=71(1)$ kJ mol^{-1}, $\Delta S^{\ddagger}=-25(4)$ J K^{-1} mol^{-1} and $\Delta V^{\ddagger}=9(1)$ cm^3 mol^{-1} [1008]. The range of values of $\Delta V^{\ddagger}$ and $\Delta S^{\ddagger}$ suggests the mechanism of the reactions ranges from purely dissociative in character (replacement of bzm by CN^- trans to CF_3) to significant participation of incoming solvent in the transition state (replacement of bzm by CN^- trans to CH_2CF_3).

In the case where the axial base is imidazole rather than bzm [812], its substitution by CN^- trans to CN^- has $\Delta H^{\ddagger}=111(2)$ kJ mol^{-1}, $\Delta S^{\ddagger}=97(6)$ J K^{-1} mol^{-1} and $\Delta V^{\ddagger}=9.3(3)$ cm^3 mol^{-1}. The displacement of imidazole proceeds more slowly than does displacement of bzm from [CNCbl]. This accords with a smaller equilibrium constant for

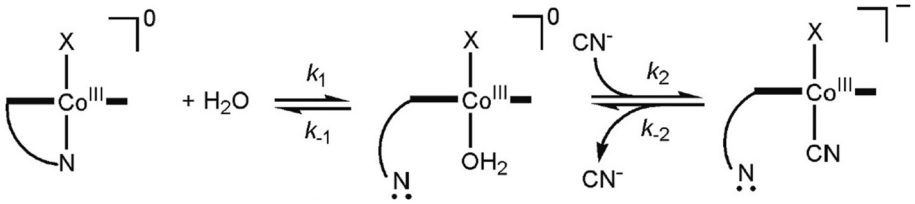

Scheme 38. The probable mechanism of the substitution of bzm by CN^- trans to an alkyl group, X. The first step may proceed in a purely dissociative manner with initial dechelation, or involve entering H_2O in the transition state.

displacement of imidazole from the α coordination site by CN^- (log $K = 2.9$) than when the base is bzm (log $K = 4$). The smaller value of $\Delta V^{\ddagger}$ for the reaction with cyanoimidazolylcobamide compared to that for [CNCbl] is also indicative of a reaction that is less dissociative in character.

The reaction of [AdoCbl] with CN^- proceeds by rapid initial displacement of bzm, followed by rate-determining heterolysis of the Co—C bond ($\Delta H^{\ddagger} = 55(1)$ kJ mol^{-1}, $\Delta S^{\ddagger} = -98(3)$ J K^{-1} mol^{-1} and $\Delta V^{\ddagger} = -5.7(3)$ cm^3 mol^{-1}) and formation of $[(CN)_2Cbl]^-$ [928,1010]. In 92% DMF-8% D_2O, rather different activation parameters were found, $\Delta H^{\ddagger} = 90.0(5)$ kJ mol^{-1}, $\Delta S^{\ddagger} = -20.5(2)$ J K^{-1} mol^{-1} and $\Delta V^{\ddagger} = -8.2(3)$ cm^3 mol^{-1}, strong evidence for the participation of H_2O solvent in Co—C bond cleavage by, it was suggested, protonation of the O atom of the ribosole [1010].

9.6. Kinetics of the reaction of Co(II) and Co(I) corrinoids

As mentioned in Section 6, the flash photolysis of [MeCbl] in deaerated aqueous and isopropanol solutions generates the [Cbl(II)]:$CH_3^{\bullet}$ caged radical pair. The rate constant for their recombination was found to be ca. $2 \times 10\,M^{-1}\,s^{-1}$ [697]. $CH_3^{\bullet}$ which escapes recombination rapidly dimerises ($k_2 \approx 10^{10}\,M^{-1}\,s^{-1}$ [1011]). In aerated solutions, $CH_3^{\bullet}$ reacts rapidly with O_2 ($k_2 = 4.7 \times 10^9\,M^{-1}\,s^{-1}$ [698]) to produced $CH_3O_2^{\bullet}$ which then reacts with [Cbl(II)] ($k_2 \approx 2.4 \times 10^9\,M^{-1}\,s^{-1}$) to form the peroxo complex [CH_3O_2Cbl] [697].

Pulse radiolysis methods have been used to generate the carbonate radical anion, $CO_3^{\bullet-}$. It oxidises [Cbl(II)] rapidly ($k_2 = 2.0 \times 10^9\,M^{-1}\,s^{-1}$) to form [HOCbl] and HCO_3^- [555]. [Cbl(II)] also reacts rapidly with NO_2 ($k = 3.5 \times 10^8\,M^{-1}\,s^{-1}$ at room temperature, pH 7.0 and 9.0) producing [NO_2Cbl] [599].

HOCl rapidly oxidises [Cbl(II)] to [HOCbl] with apparent rate constants decreasing from $1.38(2) \times 10^6\,M^{-1}\,s^{-1}$ at pH 8.60 to $2.28(2) \times 10^3\,M^{-1}\,s^{-1}$ at pH 12.00 [554]. Fits of the data taking into account the pK_1 of HOCl (7.40) and assuming that the rate constant for reaction with OCl^- is the value observed at pH 12, gave $k_2 = 2.6(1) \times 10^7\,M^{-1}\,s^{-1}$ (25 °C) for the oxidation of [Cbl(II)] by HOCl. Small amounts of other corrinoids, from which two to four H atoms had been extracted by $Cl^{\bullet}$ formed from the oxidation of HOCl by [Cbl(II)], were detected. High concentrations of HOCl (up to 0.9 M) cause extensive destruction of the corrin.

As mentioned in Section 5.2.6, at pH 1, SO_2 reacts with [Cbl(II)] to form the (protonated, base-off) $[^{-}SO_2Cbl(III)]^{2+}$ complex [575] which then reacts with a second equivalent of SO_2 to produce $[^{-}S_2O_4Cbl(III)]^{2+}$. The reaction with cob(II)inamide, $[Cbi]^+$, produces an equivalent product. The rate of the reaction of [Cbl(II)] and $[Cbi]^+$ with SO_2 depends strongly on pH, and increases as pH decreases, with [Cbl(II)] reacting more slowly. The reactive form of SO_2 is therefore SO_2(aq) rather than HSO_3^- (p$K = 1.9$). The reactions are first order in [SO_2(aq)] and first order in [corrinoid]. The rate of reaction of the two species approaches a value of $3.2 \times 10^4\,M^{-2}\,s^{-1}$ at pH 2. Clearly, bzm has a marked retarding effect on the rate of the reaction (for [Cbl(II)], $pK_{base\text{-}off} = 2.9$ [116,522]).

The oxidation of [Cbl(II)] by complexes of the type $[Co(III)(NH_3)_5\times]^{n+}$ and by $[Co(III)(bipy)_3]^{3+}$ [573] is described in Section 5.2.6. Also described there is the reaction of [Cbl(II)] with $O_2^{\bullet}$ (in the presence of catalase to scavenge the H_2O_2 produced) [568,569]. The rate constant is $\approx 7(1) \times 10^8\,M^{-1}\,s^{-1}$, which approaches that of superoxide dismutase ($2 \times 10^9\,M^{-1}\,s^{-1}$) suggesting [568] that [Cbl(II)] may play a role in biology to scavenge of $O_2^{\bullet}$, modulating intracellular signal transduction and protecting against chronic inflammation.

Cbl(II)] reacts with I_2 to produce [ICbl], $k_2 = 6(1) \times 10^4\,M^{-1}\,s^{-1}$, which is then rapidly hydrolysed to $[H_2OCbl]^+$ [1012]. The analogous reaction with Br_2 has $k_2 = 6(1) \times 10^6\,M^{-1}\,s^{-1}$. The initial reaction of [Cbl(II)] and H_2O_2 has $k_2 = 1.32(8) \times 10^2\,M^{-1}\,s^{-1}$, and the products formed include a significant amount of stable yellow corrinoids.

Cbl(II)] reacts directly with organic halides, RX, in methanol (and with chlorides and bromides in aqueous solution) with the stoichiometry 2Cbl(II)] + RX + $H_2$0 (or CH_3OH) → $[H_2OCbl]^+$ + [RCbl] + X^- [561], refuting an earlier inference that the attacking nucleophile is $[Cbl]^-$, generated from the disproportionation of two equivalents of [Cbl(II)] [1013]. The results were interpreted in terms of the initial rate-determining formation of [XCbl] and $R^{\bullet}$; the alkyl radical then rapidly reacts with a second equivalent of [Cbl(II)] to produce [RCbl]. Hydrolysis of [XCbl] produces $[H_2OCbl]^+$ (or $[CH_3OCbl]$). Rate constants (25 °C) vary from 0.8(1) $M^{-1}\,s^{-1}$ for the reaction of [Cbl(II)] with $CCl_3CO_2CH_3$ to $6(1) \times 10^{-5}\,M^{-1}\,s^{-1}$ for its reaction with $CH_2BrCO_2CH_3$ in methanol. The latter reacts faster with [Cbl(II)] in aqueous solution ($k_2 = 2.6(3) \times 10^{-3}\,M^{-1}\,s^{-1}$).

In aqueous solution the proposed mechanism of the reaction of an alkyliodide entails initial formation of a complex between RI and [Cbl(II)] which then reacts with a second equivalent of [Cbl(II)] forming [RCbl], $[H_2OCbl]^+$ and I^-. The reactions are second order in [Cbl(II)] and first order in RI. Rate constants vary from 14(3) $M^{-2}\,s^{-1}$ for the reaction with $CH_2ICO_2^-$ to $1.0(1) \times 10^4\,M^{-2}\,s^{-1}$.

[Cbl(II)] reacts with NO to form [NOCbl] which can be formally described as $[NO^{-}Cbl(III)]$ [116]. NMR data (^1H, ^{31}P, ^{15}N) are consistent with a six coordinate species with weakly bound bzm and a bent Co—NO bond. As discussed in Section 5.2.3, the pK_a of the base-on/base-off equilibrium shifts from 2.9 in [Cbl(II)] to 5.1 in [NOCbl], indicative of a weakening of the bond between the metal and bzm due to the strong trans labilising effect of NO. Flash photolysis of [NOCbl] (532 nm) in the pH range 4–6 produces base-off [Cbl(II)] and NO. Base-off [Cbl(II)] picks up an H_2O ligand ($k = 10^7\,s^{-1}$) and then equilibrates with the base-on form. (The rate of H_2O exchange on base-off [Cbl(II)], 25 °C, 0.1 M $HClO_4$, is $4(1) \times 10^7\,s^{-1}$). Above the pK_a of [NOCbl] (5.1), photolysis leads to the 5-coordinate base-on [Cbl(II)] with a weakened Co—bzm bond. This presumably then shortens and strengthens, and the resulting 5 coordinate [Cbl(II)] equilibrates with six-coordinate [H_2OCbl(II)] with H_2O in the β coordinate site. These Co(II) species then recombine with NO, and the kinetics of the recombination reaction were investigated. The recombination occurs with $k_2 = 7.4(2) \times 10^8\,M^{-1}\,s^{-1}$ (25 °C, pH 7.4) and increases marginally with pH (from $5.0(2) \times 10^8\,M^{-1}\,s^{-1}$ at pH 1.0), indicative of the small trans labilising effect of coordinated bzm. The activation parameters found (pH 7.4) were $\Delta H^{\ddagger} = 24.5(7)$ kJ mol^{-1}, $\Delta S^{\ddagger} = 7(2)$ J K^{-1} mol^{-1}, and $\Delta V^{\ddagger} = 5.4(2)$ cm^3 mol^{-1}, consistent with an I_d mechanism for the interchange of H_2O and NO.

Cob(I)alamin, $[Cbl]^-$ reacts rapidly with CH_3I ($k_2 = 3.4(2) \times 10^4\,M^{-1}\,s^{-1}$) to form [$CH_3Cbl$] [289]. The ratio of the rate

constants for the attack of $[Cbl]^-$ and of CH_3OH on CH_3I, $\eta = \log (k_{B12s}/k_{MeOH}) = 14.4$ makes $[Cbl]^-$ one of the most powerful nucleophiles known [385]. Whilst powerful nucleophiles in their own right, Co(I) cobaloximes and Co(I) compounds with cobaloxime-like equatorial ligands have a lower nucleophilicity with η values between 12.2 and 14.3.

The reaction of $[Cbl]^-$ with NO_3^- was studied between pH 1.5 and 2.5 and the rate law found was rate $= k_3[Cbl]^-[NO_3^-][H^+]$, yielding $k_3 = 1.2 \times 10^4\ M^{-2}\ s^{-1}$ (25 °C) [610]. The pH dependence of the reaction might suggest that the corrinoid reactant is [HCbl(I)]. Alternatively, HNO_3 is more rapidly reduced than NO_3^- ($pK_a = -1.38$ [1014]). A study over a wider pH range, including below the pK_a of [HCbl(I)] would be required to elucidate this more clearly. A more recent study, of the reaction between $[Cbl]^-$ and NO_2^- and NO_3^- [608] was discussed in Section 5.2.8. The reaction between $[Cbl]^-$ and N_2O is complex [609]. $[Cbl]^-$ was produced by pulse radiolysis of aqueous solutions of [Cbl(II)] and formate in the presence of N_2O which produces initially $OH^\bullet$, e^- and $H^\bullet$. A sequence of reactions (Eq. 42) then leads to formation of CO_2^-, which reacts with [Cbl(II)] to from $[Cbl]^-$.

$$H_2O + N_2O + e^- \rightarrow OH^\bullet + OH^- + N_2, k = 8.7 \times 10^9\ M^{-1}\ s^{-1} \quad (42a)$$

$$OH^\bullet + HCOO^- \rightarrow H_2O + CO_2^-\ k = 3.5 \times 10^9\ M^{-1}\ s^{-1} \quad (42b)$$

$$H^\bullet + HCOO^- \rightarrow H_2 + CO_2^-\ k = 2.3 \times 10^8\ M^{-1}\ s^{-1} \quad (42c)$$

$$CO_2^- + [Cbl(II)] \rightarrow CO_2 + [Cbl]^- \qquad k = 8.2 \times 10^8\ M^{-1}\ s^{-1} \quad (42d)$$

$[Cbl]^-$ is then oxidised by N_2O to $[H_2OCbl]^+$, the rate constant varying from $1.4 \times 10^3\ M^{-1}\ s^{-1}$ at pH 3.5 to $1.5 \times 10^2\ M^{-1}\ s^{-1}$ at pH 8 (Eq. 43). The increase in the rate of the reaction with a decrease in pH suggests that [HCbl(I)] may be the reductant. The decrease in rate in alkaline solutions was attributed to the formation of $[N_2OCbl]^-$.

$$[Cbl]^- + N_2O + 2H^+ \rightarrow [H_2OCbl]^+ + N_2 \quad (43)$$

$[H_2OCbl]^+$ rapidly reacts with $[Cbl]^-$ to form two equivalents of [Cbl(II)]. Rate constants for this reaction are virtually independent of pH between pH 5.8 and 11, with $k \approx 3.2 \times 10^7\ M^{-1}\ s^{-1}$.

$[Cbl]^-$ is rapidly oxidised to [Cbl(II)] by peroxynitrous acid, ONOOH (or perxoynitrite, since pK_a of ONOOH = 6.8) [611], a reaction that may have biological significance since elevated levels of peroxynitrite have been linked to chronic inflammatory disorders. The second order rate constant for the reaction varies with pH, increasing sharply. The rate of reaction is independent of pH above 10.5, and increases sharply as pH is decreased. Assuming the two oxidants of $[Cbl]^-$ are $ONOO^-$ and ONOOH, fitting the experimental data (confined to above pH 8 as the reaction became too fast to monitor at lower pH under the experimental conditions used) gave $k_{ONOOH} = 1.60(3) \times 10^8\ M^{-1}\ s^{-1}$ and $k_{ONOO^-} = 1.36 \times 10^5\ M^{-1}\ s^{-1}$ (the average of the values obtained at pH 11.67 and 12.23). Two possible mechanisms for the reactions that oxidised $[Cbl]^-$ to [Cbl(II)] were discussed [611]. The first envisages the first step is oxidation of $[Cbl]^-$ to [Cbl(II)] by $ONOO^-$ (or ONOOH), producing NO_2 and OH^-; NO_2 the reacts with $[Cbl]^-$ through multiple (unspecified) fast reactions to form [Cbl(II)], N_2 and OH^-. The second entails a two electron oxidation of $[Cbl]^-$ to [HOCbl] and NO_2^-. Comproportionation of Co(III) and Co(I) yields the observed Co(II) product. The second mechanism does not accord with the experimental observations of the study.

That the rate of reduction of hydroxylamines and hydroxylaminesulfonic acids by $[Cbl]^-$ (Eq. 44, R, R′ = H, Me, Et, SO_3^-; R″ = H, Me, SO_3^-) is independent of pH in the pH range 1.0–2.0 suggests that the reductant is indeed $[Cbl]^-$ [613].

$$RR'NHOR''^+ + 2[Cbl]^- + 2H^+ \rightarrow RR'NH + R''OH + 2[Cbl(II)] \quad (44)$$

Rate constants vary by at most an order of magnitude (between 4.1 and 48 $M^{-1}\ s^{-1}$, 25 °C) and are pH independent, except for the reactions with sulfonic acids which are strongly pH-dependent. For example, the reaction with $HON(SO_3)_2^{2-}$ has $k_2 = (0.20 + 5.4[H^+])\ M^{-1}\ s^{-1}$. NH_2OSO_3H is rapidly oxidised by $[Cbl]^-$ with $k_2 > 2 \times 10^4\ M^{-1}\ s^{-1}$ (at $[H^+] = 0.04$ M). The proposed mechanism entails nucleophilic attack of $[Cbl]^-$ on the OR″ moiety (Eq. 44) to generate the Co(III) species [ROCbl] which rapidly hydrolyses to $[H_2OCbl]^+$. Comproportionation between Co(III) and Co(I) generates the observed two equivalents of Co(II).

Two equivalents of $[Cbl]^-$ reduce disulfides RSSR to thiolates, producing [Cbl(II)] [528], as discussed in Section 5.2.6. The oxides of sulfur are also oxidants of $[Cbl(I)]^-$(and [Cbi]), as also discussed in Section 5.2.8.

10. Concluding remarks

Much has been written about the chemistry of the cobalt corrinoids, and entire conferences held to discuss aspects of their chemistry. The effect the corrin ligand has on controlling and modifying the chemistry of cobalt has attracted, continues to attract, and undoubtedly will continue to attract in the future the attention of coordination chemists in particular, and organic and inorganic chemists in general. Our understanding of the role these compounds play in biology continues to grow, and it would come as no surprise if even more discoveries are made of the role they play in nature. The advent of computational methods during the last thirty years or so has shed new light on their chemistry. More rigorous, *ab initio* methods are likely to provide even greater insight in the future as accessibility to computational resources continues to grow.

Table of Abbreviations

$[ACCbi]^+$	aquacyanocobinamide (Factor B).
AdoMet	S-adenosylmethionine
$[AHC]^+$	aquahydoxocobinamide
B_{12a}	aquacobalamin
B_{12s}	cob(I)alamin
BDHC	8,12-diethyl- 1,2,3,7,13,17,18,19-octamethyl-*AD*-didehydrocorrin
CASPT2	complete active space second-order perturbation theory
$[Cbl(I)]^-$	cob(I)alamin (B_{12s})
CFeSP	a corrinoid iron-sulfur protein
$[CH_3Cbl]$	methylcobalamin
CH_3–THF	5-methyltetrahydrofolate
[ClRhbl]	chlororhodibalamin
$[(CN)_2Cbl]^-$	dicyanocobalamin
cobamide	all side chains terminating in amides, and with the *f* side chain lacking bzm and terminating with 3′-phosphoryl-D-ribose
cobinamide	all side chains terminating in amides except for the *f* side chain = $CH_2CH_2CONHCH_2CH(OH)CH_3$
cobyric acid	all side chains terminating in amides except for the *f* side chain = CH_2CH_2COOH.
coenzyme M	2-mercaptanmethanesulfonate, $HS(CH_2)_2SO_3^-$
$[DAC]^{2+}$	diaquacobinamide
DFT	density functional theory
[DPTC-Co]	10-(2–4-(1H-imidazol-1-ylmethyl)benzoylamino-phenyl)-5,15-diphenylcorrolato-cobalt(III), a Co(III) corrole model of $[H_2OCbl]^+$.
ECD	electronic circular dichroism
ENDOR	electron nuclear double resonance
EXAFS	x-ray absorption fine structure
GIF	gastric intrinsic factor.
$[H_2OCbl]^+$	aquacobalamin (B_{12a})
$[(H_2O)(OH)Cbi]^+$	aquahydroxocobinamide
[Hbl]	hydrogenobalamin
Hcy	homocysteine
IF	intrinsic factor
[IRhbl	iodorhodiblamin
MCD	magnetic circular dichroism
MC-XQDPT2	a modified variant of the second-order multi-configurational quasi-degenerate perturbation theory
$[MeCbl]^+$	methylcob(IV)alamin
MLCT	metal to ligand charge transfer

(*continued on next page*)

(*continued*)

MP2	second order Møller-Plesset perturbation theory
MSR	methionine synthase reductase
[Nibl]	nibalamin, the Ni(II) analogue of cob(I)alamin
QM/MM	combined quantum mechanics and molecular mechanics
[R-10XCbl]	a cobalamin with axial ligand R, and X substituting for H at the C10 position of the corrin ring.
RDases	reductive dehalogenases
rR	resonance Raman
SAH	S-adenosylhomocysteine
[5-secoCbs]	the 5-seco cobester, 5,6-dioxo-5,6-seco-heptamethyl-cob(III) yrinate
SHE	standard hydrogen electrode
SNG	S-nitrosoglutathione
[SYCbs]	the stable yellow cobester, (5*R*,6*R*)-5,6-dihydro-5-hydroxy-heptamethylcob(III)yrinate-c,6-lactone
TDHC	tetradehydrocorrin
TMA	Thrombotic microangiopathy
WOC	water oxidation catalyst
XMCQDPT2	second-order extended multiconfiguration quasi-degenerate perturbation theory
[Znby]	zincobyric acid
[AdoCbl]	5′-adenosylcobalamin (coenzyme B_{12}).
[AdoRhbl]	5′-adenosylrhodibalamin
B_{12}	vitamin B_{12}, cyanocobalamin
B_{12r}	cob(II)alamin
BDE	bond dissociation energy
bzm	5,6-dimethylbenzimidazole
CASSCF	complete active space self-consistent field
Cbl(II)]	cob(II)alamin (B_{12r}).
$[CH_3Cbi]^+$	methylcobinamide
$[CH_3Rhbl]$	methylrhodibalamin
[ClCbl]	chlorocobalamin
[CNCbl]	cyanocobalamin, vitamin B_{12}
cobamic acid	all side chains hydrolysed to carboxylic acid, and with the *f* side chain lacking bzm and terminating with 3′-phosphoryl-D-ribose
cobester	heptamethyl cobyrinate
cobinic acid	all side chains hydrolysed to carboxylic acids but with the *f* side chain = $CH_2CH_2CONHCH_2CH(OH)CH_3$
cobyrinic acid	nucleotide-free corrinoid with all amide side chains hydrolysed to carboxylic acids
COSMO	COnductor-like Screening MOdel.
DDHC	didehydrocorrin
DHA	dehydroascorbic acid
DTT	dithiothreitol
EC-LTEM	electrochemical liquid transmission electron microscopy
EPR	electron paramagnetic resonance
FTO	fluorine-doped tin oxide
[GSCbl]	glutathionylcobalamin
$[H_2ORhbl]^+$	aquarhodibalamin
$[(H_2O)_2Cbi]^{2+}$	diaquacobinamide
[Hby]	hydrogenobyric acid
[HOCbl]	hydroxocobalamin
ISC	inter system crossing
LMCT	ligand to metal charge transfer
MCM	methylmalonyl–coenzyme A mutase (methylmalonyl-CoA isomerase)
[MeCbl]	methylcobalamin
MFE	magnetic field effect
MM	molecular mechanics
MS	methionine synthase (5-methyltetrahydrofolate-homocysteine methyltransferase)
[NAcCoMP8]	the 8 amino acid porphyrin-containing fragment obtained from the proteolysis of cytochrome *c*, referred to as *N*-acetylmicroperoxidase 8 (NAcMP8), and in which Fe(III) has been replaced by Co(III).
nOe	nuclear Overhauser effect
QTAIM	quantum theory of atoms in molecules
$[RCbl]^{m+1}$	a cob(III)alamin with R^{m-} axial ligand
ROS	reactive oxygen species
rROA	resonance Raman optical activity
SAM	S–adenosylmethionine
SERS	surface-enhanced Raman scattering
SNAP	S-nitroso-N-acetylpenicillamine
SORCI	Spectroscopy ORiented Configuration Interaction
TD-DFT	time-dependent density functional theory
TDHC	the tetradehydro analogue of BDHC
TTP	thrombotic thrombocytopenic purpura
XANES	x-ray absorption near edge structure
XRD	x-ray diffraction
[ZnCbl]	zincobalamin

(*continued on next column*)

(*continued*)

Declaration of Competing Interest

The author declares there are no conflicts of interest.

Data availability

No data was used for the research described in the article.

Acknowledgments

Sincere thanks to colleagues for their willingness to read through an early draft of this manuscript and who offered valuable comments and insights: Ilia Dereven'kov, Dorota Gryko, Bernhard Kräutler, Sergei Markov, and Rudi van Eldik.

Appendix A. Supplementary data

Supplementary data to this article can be found online at https://doi.org/10.1016/j.jinorgbio.2023.112154.

References

[1] B. Kräutler, D. Arigoni, B. Golding (Eds.), Vitamin B_{12} and B_{12}-Proteins, Wiley-VCH, Weinheim, 1998.
[2] R. Banerjee (Ed.), Chemistry and Biochemistry of B_{12}, Wiley, New York, 1999.
[3] E. Mutti (Ed.), Vitamin B_{12}: Chemical Aspects, Transport, Cause and Symptoms of Deficiency, Dietary Sources, and Health Benefits, Nova Science Publishers, New York, NY, 2015.
[4] R. Obeid (Ed.), Vitamin B_{12}: Advances and Insights, CRC Press, Boca Raton, FL, 2017.
[5] P.P. Govender (Ed.), Molecular Modelling of Vitamin B_{12} and Its Analogues, Jenny Stanford Publishing, Singapore, 2022.
[6] L. Randaccio, S. Geremia, N. Demitri, J. Wuerges Molecules 15 (2010) 3228–3259.
[7] K.L. Brown, Chem. Rev. 105 (2005) 2075–2149.
[8] R. Banerjee, Chem. Biol. 4 (1997) 175–186.
[9] T. Toraya, Cell. Mol. Life Sci. 57 (2000) 106–127.
[10] E.N.G. Marsh, Bioorg. Chem. 28 (3) (2000) 176–189.
[11] M.J. Warren, E. Raux, H.L. Schubert, J.C. Escalante-Semerena, Nat. Prod. Rep. 19 (2002) 390–412.
[12] T. Toraya, Chem. Rec. 2 (2002) 352–366.
[13] R. Banerjee, Chem. Rev. 103 (2003) 2083–2094.
[14] R. Banerjee, S.W. Ragsdale, Annu. Rev. Biochem. 72 (2003) 209–247.
[15] T. Toraya, Chem. Rev. 103 (2003) 2095–2127.
[16] B. Kräutler, Biochem. Soc. Trans. 33 (2005) 806–810.
[17] S.W. Ragsdale, Vitam. Horm. 79 (2008) 293–324.
[18] R.G. Matthews, M. Koutmos, S. Datta, Curr. Opin. Struct. Biol. 18 (2008) 658–666.
[19] R.G. Matthews, Met. Ions Life Sci. 6 (2009) 53–114.
[20] E.N. Marsh, D.P. Patterson, L. Li, ChemBioChem 11 (2010) 604–621.
[21] G.M. Sandala, D.M. Smith, L. Radom, Acc. Chem. Res. 43 (2010) 642–651.
[22] P.A. Frey, in: L. Mander, H.-W. Lui (Eds.), Comprehensive Natural Products II: Chemistry and Biology Vol. 7, Elsevier, Oxford, UK, 2010, pp. 501–546.
[23] K. Gruber, B. Puffer, B. Kräutler, Chem. Soc. Rev. 40 (2011) 4346–4363.
[24] D.P. Dowling, A.K. Croft, C.L. Drennan, Annu. Rev. Biophys. 41 (2012) 403–427.
[25] B. Kräutler, Subcell. Biochem. 56 (2012) 323–346.
[26] K. Yamada, in: A. Sigel, H. Sigel, S. R (Eds.), Interrelations between Essential Metal Ions and Human Diseases. Metal Ions in Life Sciences vol. 13, Springer, Dordrecht, Germany, 2013.
[27] T. Toraya, Arch. Biochem. Biophys. 544 (2014) 40–57.
[28] B. Kräutler, in: R.A. Scott (Ed.), Encyclopedia of Inorganic and Bioinorganic Chemistry, John Wiley & Sons, Inc., Hoboken, NJ, 2022, pp. 1–26.
[29] R. Banerjee, C. Gherasim, D. Padovani, Curr. Opin. Chem. Biol. 13 (2009) 484–491.
[30] V. Cracan, R. Banerjee, in: L. Banci (Ed.), Metallomics and the Cell, Metal Ions in Life Sciences vol. 12, Springer, Dordrecht, Germany, 2013, pp. 333–374.
[31] B. Kräutler, Chem. Eur. J. 26 (2020) 15438–15445.
[32] B. Kräutler, in: G. Litwack (Ed.), Vitamins and Hormones vol. 119, Academic Press, Cambridge, Mass., 2022, pp. 221–240.
[33] B. Kräutler, Chem. Eur. J. 21 (2015) 11280–11287.
[34] M. Giedyk, K. Goliszewska, D. Gryko, Chem. Soc. Rev. 44 (2015) 3391–3404.

[35] A.R. Jones, Photochem. Photobiol. Sci. 16 (2017) 820–834.
[36] M.J. Toda, P. Lodowski, A.A. Mamun, M. Jaworska, P.M. Kozlowski, Coord. Chem. Rev. 385 (2019) 20–43.
[37] R.K.O. Sigel, S. Gallo, CHIMIA 64 (2010) 126–131.
[38] S. Gallo, M. Oberhuber, R.K.O. Sigel, B. Kräutler, ChemBioChem 9 (2008) 1408–1414.
[39] K.J. Kennedy, F.J. Widner, O.M. Sokolovskaya, L.V. Innocent, R.R. Procknow, K. C. Mok, M.E. Taga, mBio 13 (5) (2022) e0112122.
[40] R. Obeid, S.G. Heil, M.M.A. Verhoeven, E.G.H.M. van den Heuvel, L.C.P.G.M. de Groot, S.J.P.M. Eussen, Front. Nutr. 6 (2019).
[41] B. Wolffenbuttel, H. Wouters, M. Heiner-Fokkema, M.M.V.D. Klauw, Mayo Clin. Proc. Innov. Quality Outcomes 3 (2019) 200–214.
[42] L.Z. Bozidarka, O. Milan, B. Vladan, A.H. Mohamed, J. Milos, R.I. Esma, Curr. Med. Chem. 26 (2019) 2948–2961.
[43] E. Andrès, A.-A. Zulfiqar, T. Vogel, QJM: Int. J. Med. 113 (2019) 5–15.
[44] E. Kouroglou, P. Anagnostis, A. Daponte, A. Bargiota, Endocrine 66 (2019) 149–156.
[45] D.S. Socha, S.I. DeSouza, A. Flagg, M. Sekeres, H.J. Rogers Cleve, Clin. J. Med. 87 (2020) 153–164.
[46] P. Lyon, V. Strippoli, B. Fang, L. Cimmino, Nutrients 12 (2020) 2867.
[47] D. Watkins, D.S. Rosenblatt, Curr. Opin. Clin. Nutr. Metab. Care 23 (2020) 241–246.
[48] J. Aly, O. Engmann, Front. Neurosci. 14 (2020).
[49] W. Herrmann, R. Obeid, in: O. Stanger (Ed.), Water Soluble Vitamins, Springer, Dordrecht, Germany, 2012.
[50] S. Kather, N. Grützner, P.H. Kook, F. Dengler, R.M. Heilmann, J. Vet. Intern. Med. 34 (2020) 13–28.
[51] J.-R. González-Montaña, F. Escalera-Valente, A.J. Alonso, J.M. Lomillos, R. Robles, M.E. Alonso, Animals 10 (2020) 1855.
[52] J.W. McFadden, C.L. Girard, S. Tao, Z. Zhou, J.K. Bernard, M. Duplessis, H. M. White, J. Dairy Sci. 103 (2020) 5668–5683.
[53] P.H. Degnan, M.E. Taga, A.L. Goodman, Cell Metab. 20 (2014) 769–778.
[54] O.M. Sokolovskaya, A.N. Shelton, M.E. Taga, Science 369 (2020) eaba0165.
[55] D. Lison, in: G.F. Nordberg, B.A. Fowler, M. Nordberg, L.T. Friberg (Eds.), Handbook of the Toxicology of Metals, Elsevier, Amsterdam, The Netherlands, 2007, pp. 511–528.
[56] K. Czarnek, S. Terpiłowska, A.K. Siwicki, Central Eur. J. Immunol. 40 (2015) 236–242.
[57] R. Danzeisen, D. Weight, M. Blakeney, D. Boyle, Regul. Toxicol. Pharmacol. 130 (2022), 105125.
[58] J.M. Pratt, The Inorganic Chemistry of Vitamin B_{12}, Academic Press, London, 1972.
[59] M. Kobayashi, S. Shimizu, Eur. J. Biochem. 261 (1999) 1–9.
[60] M. Odaka, M. Kobayashi, in: R.H. Kretsinger, V.N. Uversky, E.A. Permyakov (Eds.), Encyclopedia of Metalloproteins, Springer, New York, New York, NY, 2013, pp. 670–678.
[61] J.S. Combe, Transcripts of the Medical-Chirurgical Society, Edinburgh 1, 1824, pp. 193–198.
[62] T. Addison, London Med. Gazette 43 (1849) 517–518.
[63] L. SInclair, J. Roy. Soc. Med. 101 (2008) 262–264.
[64] M.A. Biermer, Schweizer Aerzte (Basel) 2 (1872) 15–18.
[65] G.H. Whipple, F.S. Robscheit-Robbins, Am. J. Phys. 72 (1925) 408–418.
[66] G.R. Minot, L. Murphy, P. J. Am. Med. Assoc. 87 (1926) 470–476.
[67] D.H. Alpers, G. Russell-Jones, Biochimie 95 (2013) 989–994.
[68] L.R. McDowell, Vitamins in Animal and Human Nutrition, Iowa State University Press, Ames, IA, 2000.
[69] E.L. Smith, Nature 162 (1948) 144–145.
[70] E.L. Rickes, N.G. Brink, F.R. Koniuszy, T.R. Wood, K. Folkers, Science 107 (1948) 396–397.
[71] A.A. Yaroshevsky, Geochem. Int. 44 (2006) 48–55.
[72] D.C. Hodgkin, J. Kamper, M. Mackay, J. Pickworth, K.N. Trueblood, J.G. White, Nature (London) 178 (1956) 64–66.
[73] P.G. Lenhert, D.C. Hodgkin, Nature 192 (1961) 937–938.
[74] A. Eschenmoser, C.E. Wintner, Science 196 (1977) 1410–1420.
[75] Anon, Vitamin B_{12} total synthesis. Wikipedia. https://en.wikipedia.org/wiki/Vitamin_B12_total_synthesis. Last accessed 20 January 2023.
[76] S. Okamoto, L.D. Eltis, Metallomics 3 (2011) 963–970.
[77] D.G. Barceloux, D. Barceloux, J. Toxicol. Clin. Toxicol. 37 (1999) 201–216.
[78] L. Leyssens, B. Vinck, C. Van Der Straeten, F. Wuyts, L. Maes, Toxicology 387 (2017) 43–56.
[79] D. Lison, S. van den Brule, G. Van Maele-Fabry, Crit. Rev. Toxicol. 48 (2018) 522–539.
[80] S. Mahey, R. Kumar, M. Sharma, V. Kumar, R. Bhardwaj, SN Appl. Sci. 2 (2020) 1279.
[81] J.M. Ortiz-Guerrero, M.C. Polanco, F.J. Murillo, S. Padmanabhan, M. Elías-Arnanz, Proc. Natl. Acad. Sci. U. S. A. 108 (2011) 7565–7570.
[82] R. Gräsbeck, Hematology 10 (2005) 227–228.
[83] A. Miller, M. Korem, R. Almog, Y. Galboiz, J. Neurol. Sci. 233 (2005) 93–97.
[84] G. Scalabrino, M. Peracchi, Trends Mol. Med. 12 (2006) 247–254.
[85] R. Green, Blood 129 (2017) 2603–2611.
[86] G. Rizzo, A.S. Laganà, in: V.B. Patel (Ed.), Molecular Nutrition, Academic Press, London, UK, 2020, pp. 105–129.
[87] A. Ankar, A. Kumar, Vitamin B_{12} Deficiency, StatPearls [Internet], StatPearls Publishing, 2022. https://www.ncbi.nlm.nih.gov/books/NBK441923/. Last accessed November.
[88] N.M. Rodriguez, K. Shackelford, Pernicious Anemia. StatPearls [Internet], StatPearls Publishing, 2022. https://www.ncbi.nlm.nih.gov/books/NBK540989/. Last accessed November.
[89] U. Gröber, K. Kisters, J. Schmidt Nutrients 5 (2013) 5031–5045.
[90] D.K. Dror, L.H. Allen, Nutr. Rev. 66 (2008) 250–255.
[91] Z.P. Wang, X.X. Shang, Z.T. Zhao, J. Matern. Fetal Neonatal Med. 25 (2012) 389–934.
[92] B. Troesch, P. Weber, M.H. Mohajeri, Nutrients 8 (2016) 803.
[93] R. Rathod, A. Kale, S. Joshi, J. Biomed.Science 23 (2016) 17.
[94] E. Moore, A. Mander, D. Ames, R. Carne, K. Sanders, D. Watters, Int. Psychogeriatr. 24 (2012) 541–556.
[95] F. Yousaf, B. Spinowitz, C. Charytan, M. Galler, Case Rep. Med. 2017 (2017) 9410727.
[96] A. Gerrard, C. Dawson, J. Clin. Pathol. 75 (2022) 744.
[97] R. Pawlak, S.E. Lester, T. Babatunde, Eur. J. Clin. Nutr. 68 (2014) 541–548.
[98] L.E. Chapman, A.L. Darling, J.E. Brown, Diabetes Metab. 42 (2016) 316–327.
[99] K. Gopinath, A. Moosa, V. Mizrahi, D.F. Warner, Future Microbiol. 8 (2013) 1405–1418.
[100] M.O. Senge, A.A. Ryan, K.A. Letchford, S.A. MacGowan, T. Mielke, Symmetry 6 (2014) 781–843.
[101] K.P. Jensen, K.V. Mikkelsen, Inorg. Chim. Acta 323 (2001) 15-May.
[102] P. Renz, in: R. Banerjee (Ed.), Chemistry and Biochemistry of B12, Wiley, New York. NY, 1999, pp. 557–576.
[103] E. Stupperich, H.J. Eisinger, B. Kräutler, Eur. J. Biochem. 186 (1989) 657–661.
[104] N.N. Greenwood, A. Earnshaw, Chemistry of the Elements, Elsevier, Oxford, UK, 1997.
[105] K.A. Rubinson, E. Itabashi, H.B. Mark, Inorg. Chem. 21 (1982) 3571–3573.
[106] N. Kumar, J. Kuta, W. Galezowski, P.M. Kozlowski, Inorg. Chem. 52 (2013) 1762–1771.
[107] K. Zhou, F. Zelder, Eur. J. Inorg. Chem. (2011) 53–57.
[108] B. Aebli, C. Männel-Croisé, F. Zelder, Inorg. Chem. 53 (2014) 2516–2520.
[109] G.P. Moss, Pure Appl. Chem. 59 (1987) 779–832.
[110] B. Kräutler, in: B. Kräutler, D. Arigoni, B.T. Golding (Eds.), Vitamin B_{12} and B_{12}-Proteins, Wiley-VCH, Weinheim, 1998, pp. 517–522.
[111] C.F. Zipp, J.P. Michael, M.A. Fernandes, S. Mathura, C.B. Perry, I. Navizet, P. P. Govender, H.M. Marques, Inorg. Chem. 53 (2014) 4418–4429.
[112] K.L. Brown, J.M. Hakimi, D.W. Jacobsen, J. Am. Chem. Soc. 106 (1984) 7894–7899.
[113] K.L. Brown, J.M. Hakimi, D.M. Nuss, Y.D. Montejano, D.W. Jacobsen, Inorg. Chem. 23 (1984) 1463–1471.
[114] C.L. Drennan, S. Huang, J.T. Drummond, R.G. Matthews, M.L. Ludwig, Science 266 (1994) 1669–1674.
[115] E.Z. Kurmaev, A. Moewes, L. Ouyang, L. Randaccio, P. Rulis, W.Y. Ching, M. Bach, M. Neumann, Europhys. Lett. 62 (2003) 582–587.
[116] M. Wolak, A. Zahl, T. Schneppensieper, G. Stochel, R. van Eldik, J. Am. Chem. Soc. 123 (2001) 9780–9791.
[117] I.A. Dereven'kov, D.S. Salnikov, S.V. Makarov, M. Surducan, R. Silaghi-Dumitrescu, G.R. Boss, J. Inorg. Biochem. 125 (2013) 32–39.
[118] D.S. Salnikov, R. Silaghi-Dumitrescu, S.V. Makarov, R. van Eldik, G.R. Boss, Dalton Trans. 40 (2011) 9831–9834.
[119] S. Van Doorslaer, G. Jeschke, B. Epel, D. Goldfarb, R.-A. Eichel, B. Krautler, A. Schweiger, J. Am. Chem. Soc. 125 (2003) 5915–5927.
[120] J. Yan, M. Bi, A.K. Bourdon, A.T. Farmer, P.-H. Wang, O. Molenda, A.T. Quaile, N. Jiang, Y. Yang, Y. Yin, B. Şimşir, S.R. Campagna, E.A. Edwards, F.E. Löffler, Nat. Chem. Biol. 14 (2018) 8–14.
[121] B. Hoffmann, M. Oberhuber, E. Stupperich, H. Bothe, W. Buckel, R. Konrat, B. Kräutler, J. Bacteriol. 182 (2000) 4773–4782.
[122] P.J. Anderson, J. Lango, C. Carkeet, A. Britten, B. Kräutler, B.D. Hammock, J. R. Roth, J. Bacteriol. 190 (2007) 1160–1171.
[123] L.G. Ljungdahl, J. LeGall, J.-P. Lee, Biochemistry 12 (1973) 1802–1808.
[124] R. Bonnett, D.G. Redman, Proc. Roy. Soc. Lond. A. 228 (1965) 342–343.
[125] D. Doddrell, A. Allerhand, Proc. Natl. Acad. Sci. U. S. A. 68 (1971) 1083–1088.
[126] O.D. Hensens, H.A.O. Hill, J.M. Thornton, A.M. Turner, R.J.P. Williams, A. Neuberger, G.W. Kenner Phil, Trans. Roy. Soc. London B 273 (1976) 353–357.
[127] J.D. Satterlee, Inorg. Chim. Acta 46 (1980) 157–166.
[128] T.G. Pagano, L.G. Marzilli, Biochemistry 28 (1989) 7213–7223.
[129] A.M. Calafat, L.G. Marzilli, J. Am. Chem. Soc. 115 (1993) 9182–9190.
[130] K.L. Brown, in: R. Banerjee (Ed.), Chemistry and Biochemistry of B_{12}, John Wiley & Sons, Inc., New York, 1999, pp. 197–237.
[131] R.A. Horton, J.D. Bagnato, C.B. Grissom, J. Organomet. Chem. 68 (2003) 7108–7111.
[132] H.A. Hassanin, L. Hannibal, D.W. Jacobsen, K.L. Brown, H.M. Marques, N. E. Brasch, Dalton Trans. (2009) 424–433.
[133] C.B. Perry, N. Shin, M.A. Fernandes, H.M. Marques, Dalton Trans. 42 (2013) 7555–7561.
[134] S.M. Chemaly, Polyhedron 174 (2019), 114162.
[135] J. Shen, V. Terskikh, G. Wu, ChemPhysChem 20 (2019) 268–275.
[136] Q. Sun, Y. Zhai, W. Wang, N. Gan, S. Zhang, Z. Suo, H. Li, Spectrochim. Acta A 258 (2021), 119828.
[137] R.A. Firth, H.A.O. Hill, J.M. Pratt, R.J.P. Williams, W.R. Jackson, Biochemistry 6 (1967) 2178–2189.
[138] E. Mayer, D.J. Gardiner, R.E. Hester, Biochim. Biophs. Acta 297 (1973) 568–570.
[139] E. Mayer, D.J. Gardiner, R.E. Hester, Mol. Phys. 26 (1973) 783–787.
[140] I. Sagi, M.R. Chance, J. Am. Chem. Soc. 114 (1992) 8061–8066.
[141] M.R. Chance, in: R. Banerjee (Ed.), Chemistry and Biochemistry of B_{12}, John Wiley & Sons, Inc., New York, NY, 1999, pp. 43–71.

[142] T.A. Stich, A.J. Brooks, N.R. Buan, T.C. Brunold, J. Am. Chem. Soc. 125 (2003) 5897–5914.
[143] T.A. Stich, N.R. Buan, T.C. Brunold, J. Am. Chem. Soc. 126 (2004) 9735–9749.
[144] N.A. Miller, A. Deb, R. Alonso-Mori, B.D. Garabato, J.M. Glownia, L.M. Kiefer, J. Koralek, M. Sikorski, K.G. Spears, T.E. Wiley, D. Zhu, P.M. Kozlowski, K. J. Kubarych, J.E. Penner-Hahn, R.J. Sension, J. Am. Chem. Soc. 139 (2017) 1894–1899.
[145] J.R. Pilbrow, in: B. Zagalak, W. Friedrich (Eds.), Vitamin B_{12}: Proceedings of the 3rd European Symposium on Vitamin B_{12} and Intrinsic Factor, University of Zurich, Zurich, Switzerland, De Gruyter, Berlin, 2019, pp. 505–510. March 5–8, 1979.
[146] S. Dong, R. Padmakumar, R. Banerjee, T.G. Spiro, J. Am. Chem. Soc. 118 (1996) 9182–9183.
[147] S. Hirota, L.G. Marzilli, in: R. Banerjee (Ed.), Chemistry and Biochemistry of B_{12}, John Wiley & Sons, Inc., New York, NY, 1999, pp. 239–260.
[148] A.J. Brooks, M. Vlasie, R. Banerjee, T.C. Brunold, J. Am. Chem. Soc. 126 (2004) 8167–8180.
[149] T.C. Brunold, CHIMIA 58 (2004) 186–193.
[150] K. Park, T.C. Brunold, J. Phys. Chem. B 117 (2013) 5397–5410.
[151] E. Machalska, G. Zajac, A. Gruca, F. Zobi, M. Baranska, A. Kaczor, J. Phys. Chem. Lett. 11 (2020) 5037–5043.
[152] C.B. Perry, H.M. Marques, S. Afr, J. Sci. 100 (2004) 368–380.
[153] L. Randaccio, S. Geremia, G. Nardin, J. Wuerges, Coord. Chem. Rev. 250 (2006) 1332–1350.
[154] C. Kratky, B. Kräutler, in: R. Banerjee (Ed.), Chemistry and Biochemistry of B_{12}, John Wiley & Sons, New York, 1999, pp. 9–41.
[155] M. Ociepa, A.J. Wierzba, J. Turkowska, D. Gryko, J. Am. Chem. Soc. 142 (2020) 5355–5361.
[156] N. Bresciani-Pahor, M. Porcolin, L.G. Marzilli, L. Randaccio, M.F. Summers, P. J. Toscano, Coord. Chem. Rev. 63 (1985) 1–125.
[157] L. Randaccio, N. Bresciani-Pahor, E. Zangrando, Chem. Soc. Rev. 18 (1989) 225–250.
[158] L. Randaccio, S. Geremia, M. Stener, D. Toffoli, E. Zangrando, Eur. J. Inorg. Chem. (2002) 93–103.
[159] L. Randaccio, S. Geremia, E. Zangrando, C. Ebert, Inorg. Chem. 33 (1994) 4641–4650.
[160] N. Marino, A.E. Rabideau, R.P. Doyle, Inorg. Chem. 50 (2011) 220–230.
[161] C. Rovira, P.M. Kozlowski, J. Phys. Chem. B 111 (2007) 3251–3257.
[162] A.J. Wierzba, A. Wincenciuk, M. Karczewski, V.I. Vullev, D. Gryko, Chem. Eur. J. 24 (2018) 10344–10356.
[163] A. Medek, L. Frydman, J. Am. Chem. Soc. 122 (2000) 684–691.
[164] M. Tollinger, R. Konrat, B. Kräutler, Helv. Chim. Acta 82 (1999) 1596.
[165] H. Savage, Biophys. J. 50 (1986) 947–965.
[166] J.P. Bouquiere, J.L. Finney, H.F.J. Savage, Acta Crystallogr. Sec. B B50 (1994) 566–578.
[167] F.P.A. Fabbiani, G. Buth, B. Dittrich, H. Sowa, CrystEngComm 12 (2010) 2541–2550.
[168] B. Dittrich, T. Koritsanszky, A. Volkov, S. Mebs, P. Luger, Angew. Chem. Int. Ed. 46 (2007) 2935–2938.
[169] S. Mebs, J. Henn, B. Dittrich, C. Paulmann, P. Luger, J. Phys. Chem. A 113 (2009) 8366–8378.
[170] M. Ruetz, R. Salchner, K. Wurst, S. Fedosov, B. Kräutler, Angew. Chem. Int. Ed. 52 (2013) 11406–11409.
[171] L. Randaccio, M. Furlan, S. Geremia, M. Šlouf, Inorg. Chem. 37 (1998) 5390–5393.
[172] S.M. Chemaly, C.B. Perry, H.M. Marques, Acta Crystallogr. Sec C60 (2004) m88-m90.
[173] C.B. Perry, M.A. Fernandes, H.M. Marques, Acta Crystallogr. Sec. C60 (2004) m165–m167.
[174] C. Brenig, M. Ruetz, C. Kieninger, K. Wurst, B. Kräutler, Chem. Eur. J. 23 (2017) 9726–9731.
[175] K.L. Brown, D.R. Evans, J.D. Zubkowski, E.J. Valente, Inorg. Chem. 35 (1996) 415–423.
[176] S. Gallo, E. Freisinger, R.K.O. Sigel, Inorg. Chim. Acta 360 (2007) 360–368.
[177] M. Chrominski, A. Lewalska, D. Gryko, Chem. Commun. 49 (2013) 11406–11408.
[178] K.L. Brown, S. Cheng, X. Zou, J.D. Zubkowski, E.J. Valente, L. Knapton, H. M. Marques, Inorg. Chem. 36 (1997) 3666–3675.
[179] C. Kratky, G. Farber, K. Gruber, K. Wilson, Z. Dauter, H.F. Nolting, R. Konrat, B. Kräutler, J. Am. Chem. Soc. 117 (1995) 4654–4670.
[180] L. Randaccio, M. Furlan, S. Geremia, M. Slouf, I. Srnova, D. Toffoli, Inorg. Chem. 39 (2000) 3403–3413.
[181] K. Zelenka, H. Brandl, B. Spingler, F. Zelder, Dalton Trans. 40 (2011) 9665–9667.
[182] L. Hannibal, C.A. Smith, J.A. Smith, A. Axhemi, A. Miller, S. Wang, N.E. Brasch, D.W. Jacobsen, Inorg. Chem. 48 (2009) 6615–6622.
[183] H.A. Hassanin, M.F. El-Shahat, S. DeBeer, C.A. Smith, N.E. Brasch, Dalton Trans. 39 (2010) 10626–10630.
[184] T.C. Brunold, K.S. Conrad, M.D. Liptak, K. Park, Coord. Chem. Rev. 253 (2009) 779–794.
[185] K.P. Jensen, U. Ryde, J. Phys. Chem. A 107 (2003) 7539–7545.
[186] R.A. Kwiecien, M. Rostkowski, A. Dybala-Defratyka, P. Paneth, J. Inorg. Biochem. 98 (2004) 1078–1086.
[187] J. Kuta, J. Wuerges, L. Randaccio, P.M. Kozlowski, J. Phys. Chem. A 113 (2009) 11604–11612.
[188] T. Andruniow, J. Kuta, M.Z. Zgierski, P.M. Kozlowski, Chem. Phys. Lett. 410 (2005) 410–416.
[189] N. Dölker, F. Maseras, A. Lledós, J. Phys. Chem. B 105 (2001) 7564–7571.
[190] N. Dölker, F. Maseras, A. Lledós, J. Phys. Chem. B 107 (2003) 306–315.
[191] P. George, P.E. Siegbahn, J.P. Glusker, C.W. Bock, J. Phys. Chem. B 103 (1999) 7531–7541.
[192] D.M. Smith, B.T. Golding, L. Radom, J. Am. Chem. Soc. 123 (2001) 1664–1675.
[193] T. Andruniow, M.Z. Zgierski, P.M. Kozlowski, J. Phys. Chem. B 104 (2000) 10921–10927.
[194] K.P. Jensen, S.P.A. Sauer, T. Liljefors, P.-O. Norrby, Organometallics 20 (2001) 550–556.
[195] T. Andruniow, P.M. Kozlowski, M.Z. Zgierski, J. Chem. Phys. 115 (2001) 7522–7533.
[196] T. Andruniow, M.Z. Zgierski, P.M. Kozlowski, J. Am. Chem. Soc. 123 (2001) 2679–2680.
[197] M. Torrent, D.G. Musaev, K. Morokuma, S.-C. Ke, K. Warncke, J. Phys. Chem. B 103 (1999) 8618–8627.
[198] S.C. Ke, M. Torrent, D.G. Museav, K. Morokuma, K. Warncke, Biochemistry 38 (1999) 12681–12689.
[199] A.J. Reig, K.S. Conrad, T.C. Brunold, Inorg. Chem. 51 (2012) 2867–2879.
[200] H.M. Marques, K.L. Brown, Coord. Chem. Rev. 225 (2002) 123–158.
[201] N.L. Allinger, J. Am. Chem. Soc. 99 (1977) 8127–8134.
[202] S.J. Weiner, P.A. Kollman, D.A. Case, U.C. Singh, C. Ghio, G. Alagona, S. Profeta, P. Weiner, J. Am. Chem. Soc. 106 (1984) 765–784.
[203] S.J. Weiner, P.A. Kollman, D.T. Nguyen, D.A. Case, J. Comput. Chem. 7 (1986) 230–252.
[204] W.D. Cornell, P. Cieplak, C.J. Bayly, I.R. Gould, K.M. Merz, D.M. Ferguson, D. C. Spellmeyer, T. Fox, J.W. Caldwell, P.A. Kollman, J. Am. Chem. Soc. 117 (1995) 5179–5197.
[205] H.M. Marques, K.L. Brown, J. Mol. Struct. (THEOCHEM) 340 (1995) 97–124.
[206] H.M. Marques, B. Ngoma, T.J. Egan, K.L. Brown, J. Mol. Struct. 561 (2001) 71–91.
[207] H.M. Marques, K.L. Brown, Coord. Chem. Rev. 192 (1999) 127–153.
[208] H.M. Marques, K.L. Brown, Inorg. Coord. Chem. 34 (1995) 3733–3740.
[209] K.L. Brown, H.M. Marques, Polyhedron 15 (1996) 2187–2197.
[210] H.M. Marques, R.P. Hicks, K.L. Brown, J. Chem. Soc. Chem. Commun. (1996) 1427–1428.
[211] K.L. Brown, X. Zou, H.M. Marques, J. Mol. Struct. (THEOCHEM) 453 (1998) 209–224.
[212] H.M. Marques, in: R. Banerjee (Ed.), Chemistry and Biochemistry of B_{12}, John Wiley & Sons, Inc., New York, 1999, pp. 289–313.
[213] H.M. Marques, X. Zou, K.L. Brown, J. Mol. Struct. 520 (2000) 75–95.
[214] C.B. Perry, K.L. Brown, X. Zou, H.A. Marques, J. Mol. Struct. 737 (2005) 245–258.
[215] A.K. Rappé, C.J. Casewit, K.S. Colwell, W.A. Goddard, W.M. Skiff, J. Am. Chem. Soc. 14 (1992) 10024–10035.
[216] J.M. Sirovatka, A.K. Rappe, R.G. Finke Inorg. Chim. Acta 300-302 (2000) 545-555. https://doi.org/10.1016/S0020-1693(00)00025-6.
[217] A.K. Petrus, D.G. Allis, R.P. Smith, F.T.J.R.P. Doyle, ChemMedChem 4 (2009) 297.
[218] D.G. Allis, T.J. Fairchild, R.P. Doyle, Mol. BioSyst. 6 (2010) 1611–1618.
[219] C. Kandt, Z.T. Xu, D.P. Tieleman, Biochemistry 45 (2006) 13284–13292.
[220] J. Gumbart, M.C. Wiener, E. Tajkhorshid, J. Mol. Biol. 393 (2009) 1129–1142.
[221] T. Pieńko, A.J. Wierzba, M. Wojciechowska, D. Gryko, J. Trylska, J. Phys. Chem. B 121 (2017) 2968–2979.
[222] E.D. Greenhalgh, C. Kunze, T. Schubert, G. Diekert, T.C. Brunold, Biochemistry 60 (2021) 2022–2032.
[223] E.D. Greenhalgh, W. Kincannon, V. Bandarian, T.C. Brunold, Biochemistry 61 (2022) 195–205.
[224] V.B. Pett, M.N. Liebman, P. Murray-Rust, K. Prasad, J.P. Glusker, J. Am. Chem. Soc. 109 (1987) 3207–3215.
[225] L. Werthemann, PhD Thesis, ETH, Zurich, Switzerland, 1968.
[226] B. Kräutler, W. Keller, M. Hughes, C. Caderas, C. Kratky, J. Chem. Soc. Chem. Commun. (1987) 1678–1680.
[227] B. Kräutler, W. Keller, C. Kratky, J. Am. Chem. Soc. 111 (1989) 8936–8938.
[228] P. Langan, M. Lehmann, C. Wilkinson, G. Jogl, C. Kratky, Acta Cryst. D 55 (1999) 51–59.
[229] G. Jogl, X. Wang, S.A. Mason, A. Kovalevsky, M. Mustyakimov, Z. Fisher, C. Hoffman, C. Kratky, P. Langan, Acta Cryst D67 (2011) 584–591.
[230] L.Z. Ouyang, P. Rulis, W.Y. Ching, M. Slouf, G. Nardin, L. Randaccio, Spectrochim. Acta 61 (2005) 1647–1652.
[231] N. Ghadimi, C.B. Perry, M. Fernandes, P.P. Govender, H.M. Marques, Inorg. Chim. Acta 436 (2015) 29–38.
[232] M.D. Liptak, A.S. Fleischhacker, R.G. Matthews, J. Telser, T.C. Brunold, J. Phys. Chem. B 113 (2009) 5245–5254.
[233] C. Kieninger, K. Wurst, M. Podewitz, M. Stanley, E. Deery, A.D. Lawrence, K. R. Liedl, M.J. Warren, B. Kräutler, Angew. Chem. Int. Ed. 59 (2020) 20129–20136.
[234] R.D. Shannon, Acta Cryst A32 (1976) 751–767.
[235] G.H. Beaven, E.A. Johnson, Nature 176 (1955) 1264–1265.
[236] C. Giannotti, in: D. Dolphin (Ed.), B_{12} vol. 1, Wiley, New York, NY, 1982, pp. 418–419.
[237] D. Lexa, J.M. Savéant, J. Am. Chem. Soc. 98 (1976) 2652–2658.
[238] D. Lexa, J.M. Savéant, Acc. Chem. Res. 16 (1983) 235–243.
[239] M.D. Wirt, I. Sagi, M.R. Chance, Biophys. J. 63 (1992) 412–417.
[240] M. Giorgetti, I. Ascone, M. Berrettoni, P. Conti, S. Zamponi, R. Marassi, J. Biol. Inorg. Chem. 5 (2000) 156–166.
[241] K.P. Jensen, U. Ryde, ChemBioChem 4 (2003) 413–424.
[242] D.A. Pratt, W.A. van der Donk, J. Am. Chem. Soc. 127 (2005) 384–396.
[243] M.D. Liptak, T.C. Brunold, J. Am. Chem. Soc. 128 (2006) 9144–9156.

[244] M. Jaworska, P. Lodowski, THEOCHEM 631 (2003) 209–223.
[245] K.P. Jensen, J. Phys, Chem. B 109 (2005) 10505–10512.
[246] M. Kumar, P.M. Kozlowski, Coord. Chem. Rev. 333 (2017) 71–81.
[247] K.P. Jensen, U. Ryde, J. Porphyrins Phthalocyanines 9 (2005) 581–606.
[248] K.P. Jensen, U. Ryde, Coord. Chem. Rev. 254 (2009) 769–778.
[249] V.B. Koppenhagen, B. Elsenhans, F. Wagner, J.J. Pfiffner, J. Biol. Chem. 249 (1974) 6532–6540.
[250] V.B. Koppenhagen, E. Warmuth, G. Schlingmann, B. Dresow, in: B. Zagalak, W. Friedrich (Eds.), Vitamin B_{12} (Proceedings of the Third European Symposium on Vitamin B_{12} and Intrinsic Factor. University of Zurich, March 5-8, 1979; Zurich, Switzerland), Walter de Gruyter, Berlin, 1979, pp. 635–646.
[251] C. Kieninger, E. Deery, A.D. Lawrence, M. Podewitz, K. Wurst, E. Nemoto-Smith, F.J. Widner, J.A. Baker, S. Jockusch, C.R. Kreutz, K.R. Liedl, K. Gruber, M. J. Warren, B. Kräutler, Angew. Chem. Int. Ed. 58 (2019) 10756–10760.
[252] B. Dresow, G. Schlingmann, L. Ernst, W.S. Sheldrick, V.B. Koppenhagen, Liebigs Annal. Chem. 1980 (1980) 1699–1710.
[253] B. Dresow, G. Schlingmann, G.M. Sheldrick, V.B. Koppenhagen, Angew. Chem. Int. Ed. Eng. 19 (1980) 321.
[254] F.J. Widner, C. Kieninger, K. Wurst, E. Deery, A.D. Lawrence, M.J. Warren, B. Kräutler, Synthesis 53 (2021) 332–337.
[255] F.J. Widner, A.D. Lawrence, E. Deery, D. Heldt, S. Frank, K. Gruber, K. Wurst, M. J. Warren, B. Kräutler, Angew Chem. Int. Edn 55 (2016) 11281–11286.
[256] G. Schlingmann, B. Dresow, V.B. Koppenhagen, W. Becker, W.S. Sheldrick, Angew. Chem. Int. Ed. Eng. 19 (1980) 321–322.
[257] M. Bröring, E. Cónsul Tejero, A. Pfister, C.D. Brandt, J.J. Pérez, Torrente Chem. Commun. (2002) 3058–3059.
[258] J.P. Glusker, in: D. Dolphin (Ed.), B_{12} vol. 1, Wiley-Interscience, New York, 1982, pp. 23–107.
[259] J.D. Dunitz, E.F. Meyer, Helv. Chim. Acta 54 (1971) 77–89.
[260] M. Dobler, J.D. Dunitz, Helv. Chim. Acta 54 (1971) 90–98.
[261] C. Kieninger, J.A. Baker, M. Podewitz, K. Wurst, S. Jockusch, A.D. Lawrence, E. Deery, K. Gruber, K.R. Liedl, M.J. Warren, B. Kräutler, Angew. Chem. Int. Ed. 58 (2019) 14568–14572.
[262] H. Rollinson, J. Adetunji, in: W.M. White (Ed.), Encyclopedia of Geochemistry: A Comprehensive Reference Source on the Chemistry of the Earth, Springer International Publishing, Cham, 2018, pp. 738–743.
[263] L.Z. Ouyang, P. Rulis, W.Y. Ching, G. Nardin, L. Randaccio, Inorg. Chem. 43 (2004) 1235–1241.
[264] M. Currie, J.D. Dunitz, Helv. Chim. Acta 54 (1971) 98–112.
[265] A. Fischli, A. Eschenmoser, Angew Chem. Int. Edn. Engl. 6 (1967) 866–868.
[266] A. Eschenmoser, Pure Appl. Chem. 20 (1969) 1–14.
[267] A. Eschenmoser, Q. Rev. Chem. Soc. 24 (1970) 366–415.
[268] R.B. Woodward, Pure Appl. Chem. 33 (1973) 145–177.
[269] V.B. Koppenhagen, J.J. Pfiffner, J. Biol. Chem. 245 (1970) 5865–5867.
[270] V.B. Koppenhagen, J.J. Pfiffner, J. Biol. Chem. 246 (1971) 3075–3077.
[271] K.A. Rubinson, J. Am. Chem. Soc. 101 (1979) 6105–6110.
[272] C. Brenig, L. Prieto, R. Oetterli, F. Zelder, Angew. Chem. Int. Ed. 57 (2018) 16308–16312.
[273] E.N.G. Marsh, D.E. Holloway, Subcell. Biochem. 35 (2000) 351–403.
[274] E.N.G. Marsh, C.L. Drennan, Curr. Op. Chem. Biol. 5 (2001) 499–505.
[275] P.A. Frey, Annu. Rev. Biochem. 70 (2001) 121–148.
[276] R. Banerjee, Biochemistry 40 (2001) 6191–6198.
[277] J.H. Martens, H. Barg, M. Warren, D. Jahn, Appl. Microbiol. Biotechnol. 58 (2002) 275–285.
[278] K. Gruber, C. Kratky, Curr. Op. Chem. Biol. 6 (2002) 598–603.
[279] D. Heldt, A.D. Lawrence, M. Lindenmeyer, E. Deery, P. Heathcote, S.E. Rigby, M. J. Warren, Biochem. Soc. Trans. 33 (2005) 815–819.
[280] S.J. Moore, M.J. Warren, Biochem. Soc. Trans. 40 (2012) 581–586.
[281] S.J. Moore, A.D. Lawrence, R. Biedendieck, E. Deery, S. Frank, M.J. Howard, S.E. J. Rigby, M.J. Warren, Proc. Natl. Acad. Sci. U. S. A. 110 (2013) 14906–14911.
[282] J. Bridwell-Rabb, C.L. Drennan, Curr. Opin. Chem. Biol. 37 (2017) 63–70.
[283] T.A. Mattes, E. Deery, M.J. Warren, J.C. Escalante-Semerena, in: R.A. Scott (Ed.), Encyclopedia of Inorganic and Bioinorganic Chemistry, John Wiley & Sons, Hoboken, NJ, 2017, pp. 1–24.
[284] D.R. Monteverde, L. Gómez-Consarnau, C. Suffridge, S.A. Sañudo-Wilhelmy, Geobiology 15 (2017) 3–18.
[285] H. Fang, J. Kang, D. Zhang, Microb. Cell Factories 16 (2017) 15.
[286] M.L. Ludwig, C.L. Drennan, R.G. Matthew, Structure (London) 4 (1996) 505–512.
[287] N. Sukumar, Biochimie 95 (2013) 976–988.
[288] W. Ding, A. Li, Y. Jia, X. Ji, H. Qianzhu, Q. Zhang, ChemBioChem 17 (2016) 1191–1197.
[289] G.N. Schrauzer, E. Deutsch, J. Am. Chem. Soc. 91 (1969) 3341–3350.
[290] M.L. Ludwig, R.G. Matthews, Annu. Rev. Biochem. 66 (1997) 269–313.
[291] M. Kumar, H. Hirao, P.M. Kozlowski, J. Biol. Inorg. Chem. 17 (2012) 1107–1121.
[292] R.G. Matthews, Acc. Chem. Res. 34 (2001) 681–689.
[293] K.R. Wolthers, N.S. Scrutton, Biochemistry 46 (2007) 6696–6709.
[294] M.M. Haque, M. Bayachou, J. Tejero, C.T. Kenney, N.M. Pearl, S.C. Im, L. Waskell, D.J. Stuehr, FEBS J. 281 (2014) 5325–5340.
[295] K.R. Wolthers, N.S. Scrutton, FEBS J. 276 (2009) 1942–1951.
[296] C.D. Fyfe, N. Bernardo-García, L. Fradale, S. Grimaldi, A. Guillot, C. Brewee, L.M. G. Chavas, P. Legrand, A. Benjdia, O. Berteau, Nature 602 (2022) 336–342.
[297] Y. Kung, N. Ando, T.I. Doukov, L.C. Blasiak, G. Bender, J. Seravalli, S. W. Ragsdale, C.L. Drennan, Nature 484 (2012) 265–269.
[298] M. Can, F.A. Armstrong, S.W. Ragsdale, Chem. Rev. 114 (2014) 4149–4174.
[299] H. Ogawa, T. Tsuruoka, S. Inouye, T. Niida, Sci. Rep. Meiji Seika Kaisha 13 (1973) 42–48.
[300] S. Omura, M. Murata, H. Hanaki, K. Hinotozawa, R. Oiwa, H. Tanaka, J. Antibiot. (Tokyo) (1984) 829–835.
[301] E. Bayer, K.H. Gugel, K. Hägele, H. Hagenmaier, S. Jessipow, W.A. König, H. Zähner, Helv. Chim. Acta 55 (1972) 224–239.
[302] K.D. Allen, S.C. Wang, Biochim. Biophys. Acta 1844 (2014) 2135–2144.
[303] U. Ryde, Curr. Opin. Chem. Biol. 7 (2003) 136–142.
[304] M.J. Toda, A.P. Ghosh, S. Parmar, P.M. Kozlowski, in: E.N.G. Marsh (Ed.), Methods in Enzymology vol. 669, Academic Press, New York, NY, 2022, pp. 119–150.
[305] N. Kumar, P.M. Kozlowski, J. Phys. Chem. B 117 (2013) 16044–16057.
[306] N. Kumar, M. Alfonso-Prieto, C. Rovira, P. Lodowski, M. Jaworska, P. M. Kozlowski, J. Chem. Theory Comput. 7 (2011) 1541–1551.
[307] V. Bandarian, R.G. Matthews, Biochemistry 40 (2001) 5056–5064.
[308] E.N.G. Marsh, G.D. Román Meléndez, Biochim. Biophs. Acta 1824 (2012) 1154–1164.
[309] E.N.G. Marsh, D.E. Holloway, FEBS Lett. 310 (1992) 167–170.
[310] A. Ratnatilleke, J.W. Vrijbloed, J.A. Robinson, J. Biol. Chem. 274 (1999) 31679–31685.
[311] B. Beatrix, O. Zelder, D. Linder, W. Buckel, Eur. J. Biochem. 221 (1994) 101–109.
[312] S. Chowdhury, R. Banerjee, Biochemistry 39 (2000) 7998–8006.
[313] G.H. Reed, Curr. Op. Chem. Biol. 8 (2004) 477–483.
[314] R. Padmakumar, R. Banerjee, Biochemistry 36 (1997) 3713–3718.
[315] R.G. Finke, B.P. Hay, Inorg. Chem. 23 (1984) 3041–3043.
[316] B.P. Hay, R.G. Finke, J. Am. Chem. Soc. 108 (1986) 4820–4829.
[317] B.P. Hay, R.G. Finke, J. Am. Chem. Soc. 109 (1987) 8012–8018.
[318] L.G. Marzilli, P.J. Toscano, L. Randaccio, N. Bresciani-Pahor, M. Calligaris, J. Am. Chem. Soc. 101 (1979) 6754–6756.
[319] F.T.T. Ng, G.L. Rempel, J. Am. Chem. Soc. 104 (1982) 621–623.
[320] M.K. Geno, J. Halpern, J. Am. Chem. Soc. 109 (1987) 1238–1240.
[321] K.L. Brown, H.B. Brooks, Inorg. Chem. 30 (1991) 3420–3430.
[322] B. Kräutler, R. Konrat, E. Stupperich, G. Färber, K. Gruber, C. Kratky, Inorg. Chem. 33 (1994) 4128–4139.
[323] R. Banerjee, S. Chowdhury, in: R. Banerjee (Ed.), Chemistry and Biochemistry of B_{12}, Wiley Interscience, New York, 1999, pp. 707–729.
[324] P.K. Sharma, Z.T. Chu, M.H.M. Olsson, A. Warshel, Proc. Natl. Acad. Sci. U. S. A. 104 (2007) 9661–9666.
[325] K. Gruber, V. Csitkovits, A. Łyskowski, C. Kratky, B. Kräutler, Angew Chem. Int. Edn 61 (2022), e202208295.
[326] E. Brunk, W.F. Kellett, N.G.J. Richards, U. Rothlisberger, Biochemistry 53 (2014) 3830–3838.
[327] M. Wang, K. Warncke, J. Am. Chem. Soc. 135 (2013) 15077–15084.
[328] S.S. Licht, C.C. Lawrence, J. Stubbe Biochemistry 38 (4) (1999) 1234–1242.
[329] K.L. Brown, X. Zou, R.R. Banka, C.B. Perry, H.M. Marques, Inorg. Chem. 43 (2004) 8130–8142.
[330] M. Fasching, W. Schmidt, B. Kräutler, E. Stupperich, A. Schmidt, C. Kratky, Helv. Chim. Acta 83 (2000) 2295–2316.
[331] G.C. Hayward, H.A.O. Hill, J.M. Pratt, N.J. Vanston, R.J.P. Williams, J. Chem. Soc. A (1965) 6485–6493.
[332] K.S. Conrad, C.D. Jordan, K.L. Brown, T.C. Brunold, Inorg. Chem. 54 (2015) 3736–3747.
[333] W. Buckel, P. Friedrich, B.T. Golding, Angew. Chem. Int. Ed. 51 (2012) 9974–9976.
[334] K.P. Jensen, U. Ryde, J. Am. Chem. Soc. 127 (2005) 9117–9128.
[335] K.A.P. Payne, C.P. Quezada, K. Fisher, M.S. Dunstan, F.A. Collins, H. Sjuts, C. Levy, S. Hay, S.E.J. Rigby, D. Leys, Nature 517 (2015) 513–516.
[336] E. Miller, G. Wohlfarth, G. Diekert, Arch. Microbiol. 166 (1996) 379–387.
[337] M. Fincker, A.M. Spormann, Annu. Rev. Biochem. 86 (2017) 357–386.
[338] C. Holliger, D. Hahn, H. Harmsen, W. Ludwig, W. Schumacher, B. Tindall, F. Vazquez, N. Weiss, A.J.B. Zehnder, Arch. Microbiol. 169 (1998) 313–321.
[339] R.-Z. Liao, S.-L. Chen, P.E.M. Siegbahn, ACS Catal. 5 (2015) 7350–7358.
[340] F. Alonso, I.P. Beletskaya, M. Yus, Chem. Rev. 102 (2002) 4009–4091.
[341] C.J. Gantzer, L.P. Wackett, Environ. Sci. Technol. 25 (1991) 715–722.
[342] R.G. Matthews, in: R.L. Blakely (Ed.), Methionine Biosynthesis in Folates and Pterins vol. 1, John Wiley & Sons, New York, NY, USA, 1984, pp. 497–550.
[343] E. Stupperich, FEMS Microbiol. Rev. 12 (1993) 349–366.
[344] F. Mancia, N.H. Keep, A. Nakagawa, P.F. Leadlay, S. McSweeney, B. Rasmussen, P. Bösecke, O. Diat, E. P.R. Structure 4 (1996) 339–350.
[345] R. Reitzer, K. Gruber, G. Jogl, V.G. Wagner, H. Bothe, W. Buckel, C. Kratky, Structure (1999) 891–899.
[346] F. Berkovitch, E. Behshad, K.H. Tang, E.A. Enns, P.A. Frey, C.L. Drennan, Proc. Natl. Acad. Sci. U. S. A. 101 (2004) 15870–15875.
[347] M. Yamanishi, S. Yamada, H. Muguruma, Y. Murakami, T. Tobimatsu, A. Ishida, J. Yamauchi, T. Toraya, Biochemistry 37 (1998) 4799–4803.
[348] M. Yamanishi, S. Yamada, A. Ishida, J. Yamauchi, T. Toraya, J. Biochem. (Tokyo) 124 (1998) 598–601.
[349] A. Abend, R. Nitsche, E. Bandarian, E. Stupperich, J. Retey, Angew. Chem. Int. Ed. Eng. 37 (1998) 625–627.
[350] M. Yamanishi, M. Yunoki, T. Tobimatsu, H. Sato, J. Matsui, A. Dokiya, Y. Iuchi, K. Oe, K. Suto, N. Shibata, Y. Morimoto, N. Yasuoka, T. Toraya, Eur. J. Biochem. 269 (2002) 4484–4494.
[351] K. Akita, N. Hieda, N. Baba, S. Kawaguchi, H. Sakamoto, Y. Nakanishi, M. Yamanishi, K. Mori, T. Toraya, J. Biochem. (Tokyo) 147 (2010) 83–93.
[352] A. Abend, V. Bandarian, R. Nitsche, E. Stupperich, J. Retey, G.H. Reed, Arch. Biochem. Biophys. 370 (1999) 138–141.
[353] N. Shibata, Y. Sueyoshi, Y. Higuchi, T. Toraya, Angew. Chem. 130 (2018) 7956–7961.

[354] K.-M. Larsson, D.T. Logan, P. Nordlund, ACS Chem. Biol. 5 (2010) 933–942.
[355] B. Durbeej, G.M. Sandala, D. Bucher, D.M. Smith, L. Radom, Chem. Eur. J. 15 (2009) 8578–8585.
[356] P. Friedrich, U. Baisch, R.W. Harrington, F. Lyatuu, Z. Zhou, F. Zelder, W. McFarlane, W. Buckel, G.B.T. Chem, Eur. J. Dermatol. 18 (2012) 16114–16122.
[357] R.T. Batey, Curr. Opin. Struct. Biol. 16 (2006) 299–306.
[358] A. Serganov, D.J. Patel, Annu. Rev. Biophys. 41 (2012) 343–370.
[359] R.R. Breaker, Biochemistry 61 (2022) 137–149.
[360] M. Mandal, R.R. Breaker, Nat. Rev. Mol. Cell Biol. 5 (2004) 451–463.
[361] A. Nahvi, J.E. Barrick, R.R. Breaker, Nucleic Acids Res. 32 (2004) 143–150.
[362] A. Nahvi, N. Sudarsan, M.S. Ebert, X. Zou, K.L. Brown, R.R. Breaker, Chem. Biol. 9 (2002) 1043–1049.
[363] J.E. Johnson, F.E. Reyes, J.T. Polaski, R.T. Batey, Nature 492 (2012) 133–137.
[364] Z. Cheng, K. Li, L.A. Hammad, J.A. Karty, C.E. Bauer, Mol. Microbiol. 91 (2014) 649–664.
[365] G. Klug, Mol. Microbiol. 91 (2014) 635–640.
[366] M. Fang, C.E. Bauer, mBio 8 (2017) e00261-00217.
[367] S. Padmanabhan, M. Jost, C.L. Drennan, M. Elías-Arnanz, Annu. Rev. Biochem. 86 (2017) 485–514.
[368] S.M. Chemaly, S. Afr. J. Sci. 112 (2016), 2016-0106.
[369] M. Elías-Arnanz, S. Padmanabhan, F.J. Murillo, Curr. Opin. Microbiol. 14 (2011) 128–135.
[370] H. Takano, K. Mise, K. Hagiwara, N. Hirata, S. Watanabe, M. Toriyabe, H. Shiratori-Takano, K. Ueda, J. Bacteriol. 197 (2015) 2301–2315.
[371] H. Takano, M. Kondo, N. Usui, T. Usui, H. Ohzeki, R. Yamazaki, M. Washioka, A. Nakamura, T. Hoshino, W. Hakamata, T. Beppu, K. Ueda, J. Bacteriol. 193 (2011) 2451–2459.
[372] H. Takano, K. Hagiwara, K. Ueda, Appl. Microbiol.Biotech. 99 (2015) 2329–2337.
[373] M. Elías-Arnanz, M. Fontes, S. Padmanabhan, in: D.E. Whitworth (Ed.), Myxobacteria: Multicellularity and Differentiation, ASM Press, Washington, D.C., U.S.A, 2008, pp. 211–255.
[374] H. Takano, T. Beppu, K. Ueda, Biosci. Biotechnol. Biochem. 70 (2006) 2320–2324.
[375] A.I. Díez, J.M. Ortiz-Guerrero, A. Ortega, M. Elías-Arnanz, S. Padmanabhan, J. G. de la Torre Eur, Biophys. J. 42 (2013) 463–476.
[376] H. Takano, Y. Agari, K. Hagiwara, R. Watanabe, R. Yamazaki, T. Beppu, A. Shinkai, K. Ueda, Microbiology 160 (2014) 2650–2660.
[377] M. Jost, J. Fernández-Zapata, M. Polanco, J.M. Ortiz-Guerrero, P.Y. Chen, G. Kang, S. Padmanabhan, M. Elías-Arnanz, C.L. Drennan, Nature 526 (2015) 536–541.
[378] M. Jost, J.H. Simpson, C.L. Drennan, Biochemistry 54 (2015) 3231–3234.
[379] R.J. Kutta, S.J.O. Hardman, L.O. Johannissen, B. Bellina, H.L. Messiha, J.M. Ortiz-Guerrero, M. Elías-Arnanz, S. Padmanabhan, P. Barran, N.S. Scrutton, A.R. Alex, R. Jones, Nat. Commun. 6 (2015) 7907.
[380] S. Padmanabhan, R. Pérez-Castaño, M. Elías-Arnanz, Curr. Op. Chem. Biol. 57 (2019) 47–55.
[381] M.C. Pérez-Marín, S. Padmanabhan, M.C. Polanco, F.J. Murillo, M. Elías-Arnanz, Mol. Microbiol. 67 (2008) 804–819.
[382] C.D. Garr, R.G. Finke, Inorg. Chem. 32 (1993) 4414–4421.
[383] C.D. Garr, R.G. Finke, J. Am. Chem. Soc. 114 (1992) 10440–10445.
[384] R.G. Finke, in: B. Krautler, D. Arigoni, B.J. Golding (Eds.), Vitamin B_{12} and B_{12}-Proteins, Wiley-VCH, Weinheim, 1998, pp. 383–402.
[385] G.N. Schrauzer, E. Deutsch, R.J. Windgassen, J. Am. Chem. Soc. 90 (1968) 2441–2442.
[386] S.M. Chemaly, J.M. Pratt, J. Chem. Soc. Dalton Trans. (1984) 595–599.
[387] M.F. Romine, D.A. Rodionov, Y. Maezato, L.N. Anderson, P. Nandhikonda, I. A. Rodionova, A. Carre, X. Li, C. Xu, T.R.W. Clauss, Y.-M. Kim, T.O. Metz, A. T. Wright, Proc. Natl. Acad. Sci. U. S. A. 114 (2017) E1205–E1214.
[388] M.F. Romine, D.A. Rodionov, Y. Maezato, A.L. Osterman, W.C. Nelson, ISME J. 11 (2017) 1434–1446.
[389] A. Ankar, S.S. Bhimjii, Vitamin B_{12} (Cobalamin) Deficiency, StatPearls Publishing LLC, Treasure Island, FL, 2017.
[390] R. Green, L.H. Allen, A.L. Bjørke-Monsen, A. Brito, J.L. Guéant, J.W. Miller, A. M. Molloy, E. Nexo, S. Stabler, B.H. Toh, P.M. Ueland, C. Yajnik, Nat. Rev. Dis. Primers 3 (2017) 17040.
[391] C.Q. Chan, L.L. Low, K.H. Lee, Front. Med. (Lausanne) 3 (2016) 38.
[392] A.D. Smith, H. Refsum, Annu. Rev. Nutr. 36 (2016) 211–239.
[393] J. Du, M. Zhu, H. Bao, B. Li, Y. Dong, C. Xiao, G.Y. Zhang, I. Henter, M. Rudorfer, B. Vitiello, Crit. Rev. Food Sci. Nutr. 56 (2016) 2560–2578.
[394] M.J. Shipton, J. Thachil, Clin. Med. (London) 15 (2015) 145–150.
[395] F. Zelder, Chem. Commun. 51 (2015) 14004–14017.
[396] A. Sobczyńska-Malefora, E. Delvin, A. McCaddon, K.R. Ahmadi, D.J. Harrington, Crit. Rev. Clin. Lab. Sci. 58 (2021) 399–429.
[397] O.A. Gromova, I.Y. Torshin, L.A. Maiorova, O.I. Koifman, D.S. Salnikov, J. Porphyrins Phthalocyanines 25 (2021) 835–842.
[398] G. Rizzo, A.S. Laganà, in: V.B. Patel (Ed.), Molecular Nutrition, Academic Press, London, UK, 2020, pp. 105–129.
[399] L.K. Butola, P.K. Kute, A. Anjankar, A. Dhok, N. Gusain, A. Vagga, J. Evolution Med. Dent. Sci. 9 (2020) 3139–3146.
[400] A.D. Smith, M.J. Warren, H. Refsum, in: N.A.M. Eskin (Ed.), Advances in Food and Nutrition Research vol. 83, Academic Press, Cambridge, MA, 2018, pp. 215–279.
[401] R.G. Matthews, in: R. Banerjee (Ed.), Chemistry and Biochemistry of B_{12}, Wiley, New York, 1999, pp. 681–706.
[402] B.-H. Ban-Hock Toh, I.R. van Driel, P.A. Gleeson, N. Engl. J. Med. 337 (1997) 1441–1448.
[403] J. Kim, C. Gherasim, R. Banerjee, Proc. Natl. Acad. Sci. U. S. A. 105 (2008) 14551–14554.
[404] P.E. Mera, J.C. Escalante-Semerena, Appl. Microbiol. Biotechnol. 88 (2010) 41–48.
[405] C. Gherasim, M. Lofgren, R. Banerjee, J. Biol. Chem. 288 (2013) 13186–13193.
[406] G. Shepherd, L.I. Velez, Ann. Pharmacother. 42 (2008) 661–669.
[407] A. Chan, J. Jiang, A. Fridman, L.T. Guo, G.D. Shelton, M.-T. Liu, C. Green, K. J. Haushalter, H.H. Patel, J. Lee, D. Yoon, T. Burney, D. Mukai, S.B. Mahon, M. Brenner, R.B. Pilz, G.R. Boss, J. Med. Chem. 58 (2015) 1750–1759.
[408] I.A. Dereven'kov, V.S. Osokin, P.A. Molodtsov, A.S. Makarova, S.V. Makarov, React. Kinet. Mech. Catal. 135 (2022) 1469–1483.
[409] M. Laforge, F. Buneaux, P. Houeto, F. Bourgeois, R. Bourdon, P. Levillain, J. Anal. Toxicol. 18 (1994) 173–175.
[410] J. Ma, S.I. Ohira, S.K. Mishra, M. Puanngam, P.K. Dasgupta, S.B. Mahon, M. Brenner, W. Blackledge, G.R. Boss, Anal. Chem. 83 (2011) 4319–4324.
[411] J. Ma, P.K. Dasgupta, F.H. Zelder, G.R. Boss, Anal. Chim. Acta 736 (2012) 78–84.
[412] C. Aebersold, B. Amstutz, A.E. Steuer, T. Kraemer, F. Zelder, Anal. Methods 7 (2015) 9707–9712.
[413] M.T. Chaudhary, M. Sarwar, A.M. Tahir, M.A. Tahir, G. Mustafa, S.A. Wattoo, M. Imran, A. Subhani, Aust. J. Forensic Sci. 48 (2015) 42–49.
[414] S.M. Clardy, D.G. Allis, T.J. Fairchild, R.P. Doyle, Expert Opin. Drug Deliv. 8 (2011) 127–140.
[415] F. Zelder, R. Alberto, in: K.M. Kadish, K.M. Smith, R. Guilard (Eds.), The Porphyrin Handbook vol. 25, Elsevier Science, San Diego, CA, 2012, pp. 83–130.
[416] K.Ó. Proinsias, M. Giedyk, D. Gryko, Chem. Soc. Rev. 42 (2013) 6605–6619.
[417] A.K. Renfrew, E.S. O'Neill, T.W. Hambley, E.J. New, Coord. Chem. Rev. 375 (2018) 221–233.
[418] A. Pettenuzzo, R. Pigot, L. Ronconi, Eur. J. Inorg. Chem. 2017 (2017) 1625–1638.
[419] J. Wuerges, G. Garau, S. Geremia, S.N. Fedosov, T.E. Petersen, L. Randaccio, Proc. Natl. Acad. Sci. U. S. A. 103 (2006) 4386–4391.
[420] P.M. Pathare, D.S. Wilbur, S. Heusser, E.V. Quadros, P. McLoughlin, A.C. Morgan, Bioconjug. Chem. 7 (1996) 217–232.
[421] T.A. Shell, J.R. Shell, Z.L. Rodgers, D.S. Lawrence, Angew. Chem. Int. Ed. 53 (2014) 875–878.
[422] O.F. Ikotun, B.V. Marquez, C.H. Fazen, A.R. Kahkoska, R.P. Doyle, S.E. Lapi, Chem. Med. Chem. 9 (2014) 1244–1251.
[423] B.-R. Sah, R. Schibli, R. Waibel, L. von Boehmer, P. Blauenstein, E. Nexo, A. Johayem, E. Fischer, E. Muller, J.D. Soyka, A.K. Knuth, S.K. Haerle, P. A. Schubiger, N.G. Schaefer, I.A. Burger, J. Nucl. Med. 55 (2014) 43–49.
[424] K.E. Henry, C.T. Elfers, R.M. Burke, O.G. Chepurny, G.G. Holz, J.E. Blevins, C. L. Roth, R.P. Doyle, Endocrinology 156 (2015) 1739–1749.
[425] S. Mundwiler, B. Spingler, P. Kurz, S. Kunze, R. Alberto, Chem. Eur. J. 11 (2005) 4089–4095.
[426] S. Kunze, F. Zobi, P. Kurz, B. Spingler, R. Alberto, Angew. Chem. 116 (2004) 5135–5139.
[427] D. Porębska, Ł. Orzeł, D. Rutkowska-Zbik, G. Stochel, R. van Eldik, Int. J. Mol. Sci. 22 (2021) 7973.
[428] A.R. Vortherms, A.R. Kahkoska, A.E. Rabideau, J. Zubieta, L.L. Andersen, M. Madsen, R.P. Doyle, Chem. Commun. 47 (2011) 9792–9794.
[429] F. Zobi, L. Quaroni, G. Santoro, T. Zlateva, O. Blacque, B. Sarafimov, M.C. Schaub, A.Y. Bogdanova, J. Med. Chem. 56 (2013) 6719–6731.
[430] N. Viola-Villegas, A.E. Rabideau, M. Bartholoma, J. Zubieta, R.P. Doyle, J. Med. Chem. 52 (2009) 5253–5261.
[431] N. Viola-Villegas, A.E. Rabideau, J. Cesnavicious, J. Zubieta, R.P. Doyle, Chem. Med. Chem. 3 (2008) 1387–1394.
[432] C.A. Hall, P.D. Colligan, Exp. Cell Res. 183 (1989) 159–167.
[433] E. Mutti, M. Ruetz, H. Birn, B. Kräutler, E. Nexo, PLoS One 8 (2013), e75312.
[434] F. Zelder, M. Sonnay, L. Prieto, Chem Bio Chem 16 (2015) 1264–1278.
[435] M. Ruetz, C. Gherasim, K. Gruber, S. Fedosov, R. Banerjee, B. Kräutler, Angew. Chem. Int. Ed. 52 (2013) 2606–2610.
[436] N.A. Miller, T.E. Wiley, K.G. Spears, M. Ruetz, C. Kieninger, B. Kräutler, R. J. Sension, J. Am. Chem. Soc. 138 (2016) 14250–14256.
[437] P. Lodowski, K. Ciura, M.J. Toda, M. Jaworska, P.M. Kozlowski, Phys. Chem. Chem. Phys. 19 (2017) 30310–30315.
[438] J.M. Pratt, in: D. Dolphin (Ed.), B_{12} vol. 1, John Wiley & Sons, New York, N.Y., 1982, pp. 325–392.
[439] B. Kräutler, in: R. Banerjee (Ed.), Chemistry and Biochemistry of B_{12}, John Wiley and Sons, Inc., New York, 1999, pp. 315–339.
[440] I.A. Dereven'kov, D.S. Salnikov, R. Silaghi-Dumitrescu, S.V. Makarov, O. I. Koifman, Coord. Chem. Rev. 309 (2016) 68–83.
[441] D. Lexa, J.M. Savéant, J. Zickler, J. Am. Chem. Soc. 102 (1980) 4851–4852.
[442] K.A. Rubinson, H.V. Parekh, E. Itabashi, H.B. Mark, Inorg. Chem. 22 (1983) 458–463.
[443] R.C. Johnston, J. Zhou, J.C. Smith, J.M. Parks, J. Phys. Chem. B 120 (2016) 7307–7318.
[444] D. Lexa, J.M. Savéant, J. Zickler, J. Am. Chem. Soc. 102 (1980) 2654–2663.
[445] D. Lexa, J.M. Savéant, J. Am. Chem. Soc. 100 (1978) 3220–3222.
[446] T. Spataru, R.L. Birke, J. Electroanal. Chem. 593 (2006) 74–86.
[447] R.L. Birke, Q. Huang, T. Spataru, D.K. Gosser, J. Am. Chem. Soc. 128 (2006) 1922–1936.
[448] H. Vetter, J. Knappe, Z. Physiol. Chem. 352 (1971) 433–446.
[449] M. Kumar, W. Galezowski, P.M. Kozlowski Int, J. Quant. Chem. 113 (2013) 479–488.
[450] T.A. Stich, M. Yamanishi, R. Banerjee, T.C. Brunold, J. Am. Chem. Soc. 127 (2005) 7660–7661.

[451] T.A. Stich, N.R. Buan, J.C. Escalante-Semerena, T.C. Brunold, J. Am. Chem. Soc. 127 (2005) 8710–8719.
[452] M. Koutmos, S. Datta, K.A. Pattridge, J.L. Smith, R.G. Matthews, Proc. Natl. Acad. Sci. U. S. A. 106 (2009) 18527–18532.
[453] M. Kumar, P.M. Kozlowski, Angew. Chem. Int. Ed. 50 (2011) 8702–8705.
[454] M. Kumar, N. Kumar, H. Hirao, P.M. Kozlowski, Inorg. Chem. 51 (2012) 5533–5538.
[455] T. Doukov, J. Seravalli, J.J. Stezowski, S.W. Ragsdale, Structure 8 (2000) 817–830.
[456] T. Svetlitchnaia, V. Svetlitchnyi, O. Meyer, H. Dobbek, Proc. Nail. Acad. Sci. USA 103 (2006) 14331–14336.
[457] J.T. Jarrett, D.M. Hoover, M.L. Ludwig, R.G.R.G. Matthews, Biochemistry 37 (1998) 12649–12658.
[458] M.D. Liptak, S. Datta, R.G. Matthews, T.C. Brunold, J. Am. Chem. Soc. 130 (2008) 16374–16381.
[459] M. Kumar, P.M. Kozlowski, J. Inorg. Biochem. 126 (2013) 26–34.
[460] T.A. Stich, J. Seravalli, S. Venkateshrao, T.G. Spiro, S.W. Ragsdale, T.C. Brunold, J. Am. Chem. Soc. 128 (2006) 5010–5020.
[461] H.P.C. Hogenkamp, J.E. Rush, C.A. Swenson, J. Biol. Chem. 240 (1965) 3641–3644.
[462] B. Kräutler, Helv. Chim. Acta 70 (1987) 1268–1278.
[463] B. Kräutler, Met. Ions Life Sci. 6 (2009) 1–51.
[464] B.D. Martin, R.G. Finke, J. Am. Chem. Soc. 114 (1992) 585–592.
[465] Y. Morita, K. Oohora, A. Sawada, T. Kamachi, K. Yoshizawa, T. Hayashi, Inorg. Chem. 56 (2017) 1950–1955.
[466] G. Costa, G. Mestroni, E. de Savorgnani, Inorg. Chim. Acta 3 (1969) 323–328.
[467] D.G. Brown, in: S.J. Lippard (Ed.), Progress in Inorganic Chemistry vol. 18, John Wiley & Sons, Inc., New York, 1973, pp. 177–286.
[468] C.M. Elliott, E. Hershenhart, R.G. Finke, B.L. Smith, J. Am. Chem. Soc. 103 (1981) 5558–5566.
[469] D. Lexa, J.M. Savéant, J. Zickler, J. Am. Chem. Soc. 99 (1977) 2786–2790.
[470] N.B. Nazhat, B.T. Golding, G.R.A. Johnson, P. Jones, J. Inorg. Biochem. 36 (1989) 75–81.
[471] D.E. Linn, E.S. Gould, Inorg. Chem. 27 (1988) 1625–1628.
[472] F. Nome, J.H. Fendler, J. Chem. Soc. Dalton Trans. (1976) 1212–1219.
[473] M. Lehene, D. Plesa, S. Ionescu-Zinca, S.D. Iancu, N. Leopold, S.V. Makarov, A.M. V. Brânzanic, R. Silaghi-Dumitrescu, Inorg. Chem. 60 (2021) 12681–12684.
[474] R. Banerjee, ACS Chem. Biol. 1 (2006) 149–159.
[475] C. Paul, D.M. Brady, Integr. Med. (Encinitas) 16 (2017) 42–49.
[476] L. Hannibal, P.M. DiBello, D.W. Jacobsen, Clin. Chem. Lab. Med. 51 (2013) 477–488.
[477] I.A. Dereven'kov, K.A. Ugodin, S.V. Makarov, Russ. J. Phys. Chem. 95 (2021) 2020–2024.
[478] D.A. Ryan, D. Meyerstein, W.A. Mulac, J.H. Espenson, Inorg. Chem. 17 (1978) 3725–3726.
[479] L. Ernst, G. Holze, H.H. Inhoffen, Liebigs Ann. Chem. (1981) 198–201.
[480] B. Kräutler, R. Stepánek, G. Holze, Helv. Chim. Acta 66 (1983) 44–49.
[481] B. Kräutler, R. Stepánek, Helv. Chim. Acta 66 (1983) 1493–1512.
[482] B. Kräutler, R. Stepánek, Angew Chem. Int. Edn. Engl. 24 (1985) 62–64.
[483] B. Kräutler, R. Stepanek, Photochem. Photobiol. 54 (1991) 585–592.
[484] E.H. Pezacka, R. Green, D.W. Jacobsen, Biochim. Biophys. Res. Commun. 169 (1990) 443–450.
[485] L. Xia, A.G. Cregan, L.A. Berben, N.E. Brasch, Inorg. Chem. 43 (2004) 6848–6857.
[486] W.P. Watson, T. Munter, B.T. Golding, Chem. Res. Toxicol. 17 (2004) 1562–1567.
[487] A. McCaddon, B. Regland, P. Hudson, G. Davies, Neurology 58 (2002) 1395–1399.
[488] C.A. de Jager, Neurobiol. Aging 35 (Suppl. 2) (2014) S35–S39.
[489] E.H. Reynolds, Handb. Clin. Neurol. 120 (2014) 927–943.
[490] A. McCaddon, Biochimie 95 (2013) 1066–1076.
[491] T.-L.C. Hsu, N.E. Brasch, R.G. Finke, Inorg. Chem. 37 (20) (1998) 5109–5116.
[492] E. Suarez-Moreira, L. Hannibal, C.A. Smith, R.A. Chavez, D.W. Jacobsen, N. E. Brasch, Dalton Trans. (2006) 5269–5277.
[493] L. Hannibal, C.A. Smith, D.W. Jacobsen, Inorg. Chem. 49 (2010) 9921–9927.
[494] R.K. Suto, N.E. Brasch, O.P. Anderson, R.G. Finke, Inorg. Chem. 40 (2001) 2686–2692.
[495] R. Mukherjee, A. McCaddon, C.A. Smith, N.E. Brasch, Inorg. Chem. 48 (2009) 9526–9534.
[496] S. Ramasamy, T.K. Kundu, W. Antholine, P.T. Manoharan, J.M. Rifkind, J. Porphyrins Phthalocyanines 16 (2012) 25–38.
[497] L.A. Schumacher, R. Mukherjee, J.M. Brown, H. Subedi, N.E. Brasch, Eur. J. Inorg. Chem. (2011) 4717–4720.
[498] I.A. Dereven'kov, L.V. Tsaba, E.A. Pokrovskaya, S.V. Makarov, J. Coord. Chem. 71 (2018) 3194–3206.
[499] I.A. Dereven'kov, A.Y. Polyakova, S.V. Makarov, Eur. J. Inorg. Chem. 2017 (2017) 4174–4179.
[500] I.A. Dereven'kov, S.V. Makarov, T.T. Bui Thi, A.S. Makarova, O.I. Koifman, Eur. J. Inorg. Chem. 2018 (2018) 2987–2992.
[501] S. Chang, J. Tat, S.P. China, H. Kalyanaraman, S. Zhuang, A. Chan, C. Lai, Z. Radic, E.A. Abdel-Rahman, D.E. Casteel, R.B. Pilz, S.S. Ali, G.R. Boss, PNAS Nexus 1 (2022) 1–13.
[502] Z. Li, A. Shanmuganathan, M. Ruetz, K. Yamada, N.A. Lesniak, B. Kräutler, T. C. Brunold, M. Koutmos, R. Banerjee, J. Biol. Chem. 292 (2017) 9733–9744.
[503] N.E. Brasch, T.-L.C. Hsu, K.M. Doll, R.G. Finke, J. Inorg. Biochem. 76 (1999) 197–209.
[504] N. Adler, T. Medwick, T.J. Poznanski, J. Am. Chem. Soc. 88 (1966) 5018–5020.
[505] I.A. Dereven'kov, S.V. Makarov, J. Coord. Chem. 72 (2019) 1298–1306.
[506] K. Tahara, A. Matsuzaki, T. Masuko, J.-I. Kikuchi, Y. Hisaeda, Dalton Trans. 42 (2013) 6410–6416.
[507] H.P.C. Hogenkamp, G.T. Bratt, S.Z. Sun, Biochemistry 24 (1985) 6428–6432.
[508] H.P.C. Hogenkamp, G.T. Bratt, A.T. Kotchevar, Biochemistry 26 (1987) 4723–4727.
[509] D. Zheng, R.L. Birke, J. Am. Chem. Soc. 124 (2002) 9066–9067.
[510] K. Mieda-Higa, A.A. Mamun, T. Ogura, T. Kitagawa, P.M. Kozlowski, J. Raman Spectrosc. 51 (2020) 1331–1342.
[511] D.S. Salnikov, I.A. Dereven'kov, S.V. Makarov, E.S. Ageeva, A. Lupan, M. Surducan, R. Silaghi-Dumitrescu, Rev. Roum. Chim. 57 (2012) 353–359.
[512] I.A. Dereven'kov, PhD Thesis, Ivanovo State University of Chemistry and Technology, 2013.
[513] D.S. Salnikov, S.V. Makarov, O.I. Koifman, New J. Chem. 45 (2021) 535–543.
[514] R.A. Pugina, E.A. Denisova, P.A. Ivlev, D.S. Salnikov, S.V. Makarov, J. Porphyrins Phthalocyanines 22 (2018) 1092–1098.
[515] D.S. Salnikov, I.A. Dereven'kov, E.N. Artyushina, S.V. Makarov, Russ. J. Phys. Chem. A 87 (2013) 44–48.
[516] M.S.A. Hamza, X. Zou, K.L. Brown, R. van Eldik, J. Chem. Soc. Dalton Trans. (2002) 3832–3839.
[517] D.S. Salnikov, P.N. Kucherenko, I.A. Dereven'kov, S.V. Makarov, R. van Eldik, Eur. J. Inorg. Chem. (2014) 852–862.
[518] J.B. Conn, T.G. Wartman, Science 115 (1952) 72–73.
[519] H.M. Marques, K.L. Brown, D.W. Jacobsen, J. Biol. Chem. 263 (1988) 12378–12383.
[520] D.S. Salnikov, I.A. Dereven'kov, S.V. Makarov, E.N. Artyushina Izv, Vyssh. Uchebn. Zaved. Khim. Khim. Tekhnol. 54 (2011) 43–46.
[521] I.A. Dereven'kov, D.S. Salnikov, N.I. Shpagilev, S.V. Makarov, E.V. Tarakanova, Macroheterocycles 5 (2012) 260–265.
[522] D.S. Salnikov, S.V. Makarov, R. van Eldik, P.N. Kucherenko, G.R. Boss, Eur. J. Inorg. Chem. (2014) 4123–4133.
[523] P.M. Kozlowski, J. Kuta, W. Galezowski, J. Phys. Chem. B 111 (2007) 7638–7645.
[524] D.W. Jacobsen, E.H. Pezacka, K.L. Brown, J. Inorg. Biochem. 50 (1993) 47–63.
[525] M. Alfonso-Prieto, X. Biarnés, M. Kumar, C. Rovira, P.M. Kozlowski, J. Phys. Chem. B 114 (2010) 12965–12971.
[526] T. Spataru, R.L. Birke, J. Phys. Chem. A 110 (2006) 8599–8604.
[527] A.P. Ghosh, P. Lodowski, A. Chmielowska, M. Jaworska, P.M. Kozlowski, J. Catal. 376 (2019) 32–43.
[528] G. Chithambarathanu Pillai, E.S. Gould, Inorg. Chem. 25 (1986) 3353–3356.
[529] S.A. Svarovsky, R.H. Simoyi, S.V. Makarov, J. Chem. Soc. Dalton Trans. (2000) 511–514.
[530] S.V. Makarov, E.V. Kudrik, R. van Eldik, E.V. Naidenko, J. Chem. Soc. Dalton Trans. (2002) 4074–4076.
[531] M. Wolak, G. Stochel, M. Hamza, R. Van Eldik, Inorg. Chem. 39 (2000) 2018–2019.
[532] C. Selçuki, R. van Eldik, T. Clark, Inorg. Chem. 43 (2004) 2828–2833.
[533] D. Zheng, R.L. Birke, J. Am. Chem. Soc. 123 (2001) 4637–4638.
[534] V.S. Sharma, R.B. Pilz, G.R. Boss, D. Magde, Biochemistry 42 (2003) 8900–8908.
[535] F. Roncaroli, T.E. Shubina, T. Clark, R. van Eldik, Inorg. Chem. 45 (2006) 7869–7876.
[536] J. Polaczek, H. Subedi, Ł. Orzeł, L.S. Lisboa, R.B. Cink, G. Stochel, N.E. Brasch, R. van Eldik, Inorg. Chem. 60 (2021) 2964–2975.
[537] K.S. Conrad, T.C. Brunold, Inorg. Chem. 50 (2011) 8755–8766.
[538] Z.L. Rodgers, T.A. Shell, A.M. Brugh, H.L. Nowotarski, M.D.E. Forbes, D. S. Lawrence, Inorg. Chem. 55 (2016) 1962–1969.
[539] L.K. Keefer, ACS Chem. Biol. 6 (2011) 1147–1155.
[540] L. Hannibal, C.A. Smith, D.W. Jacobsen, N.E. Brasch, Angew. Chem. Int. Ed. Eng. 46 (2007) 5140–5143.
[541] H.A. Hassanin, L. Hannibal, D.W. Jacobsen, M.F. El-Shahat, M.S.A. Hamza, N. E. Brasch, Angew Chem. Int. Edn. 48 (2009) 8909–8913.
[542] F. Doctorovich, D. Bikiel, J. Pellegrino, S.A. Suárez, A. Larsen, M.A. Martí, Coord. Chem. Rev. 255 (2011) 2764–2784.
[543] H. Subedi, H.A. Hassanin, N.E. Brasch, Inorg. Chem. 53 (2014) 1570–1577.
[544] N. Paolocci, M.I. Jackson, B.E. Lopez, K. Miranda, C.G. Tocchetti, D.A. Wink, A. J. Hobbs, J.M. Fukuto, Pharmacol. Therap. 113 (2007) 442–458.
[545] H.N. Sabbah, C.G. Tocchetti, M. Wang, S. Daya, R.C. Gupta, R.S. Tunin, R. Mazhari, E. Takimoto, N. Paolocci, D. Cowart, W.S. Colucci, D.A. Kass, Circ. Heart Fail. 6 (2013) 1250–1258.
[546] B.K. Kemp-Harper, J.D. Horowitz, R.H. Ritchie, Drugs 76 (2016) 1337–1348.
[547] M. Wolak, G. Stochel, R. van Eldik, Inorg. Chem. 45 (2006) 1367–1379.
[548] H.M. Abu-Soud, D. Maitra, J. Byun, C.E.A. Souza, J. Banerjee, G.M. Saed, M. P. Diamond, P.R. Andreana, S. Pennathur, Free Radic. Biol. Med. 52 (2012) 616–625.
[549] D. Maitra, I. Ali, R.M. Abdulridha, F. Shaeib, S.N. Khan, G.M. Saed, S. Pennathur, H.M. Abu-Soud, PLoS One 9 (2014), e110595.
[550] N. Okamoto, T. Bito, N. Hiura, A. Yamamoto, M. Iida, Y. Baba, T. Fujita, A. Ishihara, Y. Yabuta, F. Watanabe, ACS Omega 5 (2020) 6207–6214.
[551] I.A. Dereven'kov, V.S. Osokin, L. Hannibal, S.V. Makarov, I.A. Khodov, O. I. Koifman, J. Biol. Inorg. Chem. 26 (2021) 427–434.
[552] B. Kormányos, I. Nagypál, G. Peintler, A.K. Horváth, Inorg. Chem. 47 (2008) 7914–7920.
[553] I.A. Dereven'kov, S.V. Makarov, N.I. Shpagilev, D.S. Salnikov, O.I. Koifman, BioMetals 30 (2017) 757–764.
[554] R.S. Dassanayake, M.M. Farhath, J.T. Shelley, S. Basu, N.E. Brasch, J. Inorg. Biochem. 163 (2016) 81–87.
[555] R.S. Dassanayake, J.T. Shelley, D.E. Cabelli, N.E. Brasch, Chem. Eur. J. 21 (2015) 6409–6419.

[556] J.M. Pratt, M.S.A. Hamza, G.J. Buist, J. Chem. Soc. Chem. Commun. (1993) 701–702.
[557] M. Puchberger, R. Konrat, B. Kräutler, U. Wagner, C. Kratky, Helv. Chim. Acta 83 (2003) 1453–1466.
[558] J.H. Espenson, A.H. Martin, J. Am. Chem. Soc. 99 (1977) 5953–5957.
[559] K.L. Brown, D.Q. Zhao, S.F. Cheng, X. Zou, Inorg. Chem. 36 (1997) 1764–1771.
[560] D.H. Dolphin, A.W. Johnson, J. Chem. Soc. (1965) 2174–2181.
[561] H.-U. Blaser, J. Halpern J. Am. Chem. Soc. 102 (1980) 1684–1689.
[562] C. Wedemeyer-Exl, T. Darbre, R.R. Keese, Org. Biomol. Chem. 5 (2007) 2119–2128.
[563] J.H. Bayston, N.K. King, F.D. Looney, M.E. Winfield, J. Am. Chem. Soc. 91 (1969) 2775–2779.
[564] A. von Zelewsky, Helv. Chim. Acta 55 (1972) 2941–2947.
[565] E. Jórin, A.A. Schweiger, H.H. Günthard, J. Am. Chem. Soc. 105 (1983) 4277–4286.
[566] S. Van Doorslaer, A. Schweiger, B. Kräutler, J. Phys. Chem. B 105 (2001) 7554–7563.
[567] E. Hohenester, C. Kratky, B. Kräutler, J. Am. Chem. Soc. 113 (1991) 4523–4530.
[568] E. Suarez-Moreira, J. Yun, C.S. Birch, J.H.H. Williams, A. McCaddon, N.E. Brasch, J. Am. Chem. Soc. 131 (2009) 15078–15079.
[569] R.S. Dassanayake, D.E. Cabelli, N.E. Brasch, ChemBioChem 14 (2013) 1081–1083.
[570] H.M. Marques, J.C. Bradley, K.L. Brown, H. Brooks, Inorg. Chim. Acta 209 (1993) 161–169.
[571] I.A. Dereven'kov, S.V. Makarov, A.S. Makarova, React. Kinet. Mech. Catal. 133 (2021) 73–84.
[572] M.E. Solovieva, Y.V. Shatalin, V.V. Solovyev, A.V. Sazonov, V.P. Kutyshenko, V. S. Akatov, Redox Biol. 20 (2019) 28–37.
[573] P.N. Balasubramanian, E.S. Gould, Inorg. Chem. 24 (1985) 1791–1793.
[574] M. Wolak, G. Stochel, R. van Eldik, J. Am. Chem. Soc. 125 (2003) 1334–1351.
[575] I.A. Dereven'kov, P.A. Ivlev, C. Bischin, D.S. Salnikov, R. Silaghi-Dumitrescu, S. V. Makarov, O.I. Koifman, J. Biol. Inorg. Chem. 22 (2017) 969–975.
[576] I.A. Dereven'kov, N.I. Shpagilev, S.V. Makarov, Russ. J. Phys. Chem. A 92 (2018) 2182–2186.
[577] H. Subedi, N.E. Brasch, Dalton Trans. 45 (2016) 352–360.
[578] C.S. Birch, N.E. Brasch, A. McCaddon, J.H.H. Williams, Free Radic. Biol. Med. 57 (2009) 184–188.
[579] H. Jamaati, E. Mortaz, Z. Pajouhi, G. Folkerts, M. Movassaghi, M. Moloudizargari, I.M. Adcock, J. Garssen Front. Microbiol 8 (2017) 2008.
[580] M.A. Altinoz, İ. Elmaci, Nitric Oxide 79 (2017) 68–83.
[581] J.R. Klinger, P.J. Kadowitz, Am. J. Cardiol. 120 (2017) S71–S79.
[582] I.E. García, H.A. Sánchez, A.D. Martínez, R.M.A. Biochim, Biophs. Acta 1860 (2017) 91–95.
[583] K. Yarlagadda, J. Hassani, I.P. Foote, J. Markowitz Biochim. Biophys. Acta 1868 (2017) 500–509.
[584] P. Wigner, P. Czarny, P. Galecki, K.P. Su, T. Sliwinski, Psychiatry Res. 262 (2017) 566–574.
[585] B. Salimian Rizi, A. Achreja, D. Nagrath, Trends Cancer 3 (2017) 659–672.
[586] B.C.M. Stephan, S.L. Harrison, H.A.D. Keage, A. Babateen, L. Robinson, M. Siervo, Curr. Cardiol. Rep. 19 (2017) 87.
[587] D.J. Stuehr Biochim, Biophys. Acta 1411 (1999) 217–230.
[588] S. Nicolaou, S.H. Kenyon, J.M. Gibbons, T. Ast, W.A. Gibbons, Eur. J. Clin. Investig. 26 (1996) 167–170.
[589] A. Kambo, V.S. Sharma, D.E. Casteel, V.L. Woods, R.B. Pilz, G.R. Boss, J. Biol. Chem. 280 (2005) 10073–10082.
[590] M. Brouwer, W. Chamulitrat, G. Ferruzzi, D. Sauls, J. Weinberg, Blood 88 (1996) (1857) 1857–1864.
[591] D. Zheng, L. Yan, R.L. Birke, Inorg. Chem. 41 (2002) 2548–2555.
[592] J.T. Drummond, R.G. Matthews, Biochemistry 33 (1994) 3732–3741.
[593] J.T. Drummond, R.G. Matthews, Biochemistry 33 (1994) 3742–3750.
[594] D. Rutkowska-Zbik, M. Witko, G. Stochel, Theor. Chem. Accounts 120 (2008) 411–419.
[595] H. Subedi, N.E. Brasch, Inorg. Chem. 52 (2013) 11608–11617.
[596] V.S. Osokin, I.A. Dereven'kov, S.V. Makarov, A. Gaina-Gardiuta, R. Silaghi-Dumitrescu, J. Coord. Chem. (2022) 1–11.
[597] J. Polaczek, L. Orzel, G. Stochel, R. van Eldik, J. Biol. Inorg. Chem. 20 (2015) 1069–1078.
[598] C.D. Hubbard, D. Chatterjee, M. Oszajca, J. Polaczek, O. Impert, M. Chrzanowska, A. Katafias, R. Puchta, R. van Eldik, Dalton Trans. 49 (2020) 4599–4659.
[599] R.S. Dassanayake, D.E. Cabelli, N.E. Brasch, J. Inorg. Biochem. 142 (2015) 54–58.
[600] R. Mukherjee, N.E. Brasch, Chem. Eur. J. 17 (2011) 11805–11812.
[601] H. Subedi, N.E. Brasch, Eur. J. Inorg. Chem. (2015) 3825–3834.
[602] O. Augusto, M.G. Bonini, A.M. Amanso, E. Linares, C.C.X. Santos, S.L.L. De Menezes, Free Radic. Biol. Med. 32 (2002) 841–859.
[603] I.A. Dereven'kov, T.T.B. Thi, D.S. Salnikov, S.V. Makarov, Russ. J. Phys. Chem. A 90 (2016) 596–600.
[604] D. Zheng, T. Darbre, R. Keese, J. Inorg. Biochem. 73 (1999) 273–275.
[605] D. Lexa, J.M. Savéant, J. Chem. Soc. Chem. Commun. (1975) 872–874.
[606] D. Dolphin, in: D.B. McCormick, L.D. Wright (Eds.), Methods in Enzymology vol. 18, Academic Press, New York, NY, 1971, pp. 34–52.
[607] Y. Hisatake, T. Tanakam, T. Tsurugi, H. Kuroda, Process for producing methylcobalamin. International patent number PCT/JP2002/005510. European Patent Office, 2004.
[608] N.T. Plymale, R.S. Dassanayake, H.A. Hassanin, N.E. Brasch, Eur. J. Inorg. Chem. (2012) 913–921.
[609] R. Blackburn, M. Kyaw, A.J. Swallow, J. Chem. Soc. Faraday Trans. 1 (73) (1977) 250–255.
[610] P.N. Balasubramanian, E.S. Gould, Inorg. Chem. 22 (1983) 2635–2637.
[611] R. Mukherjee, N.E. Brasch, Chem. Eur. J. 17 (2011) 11723–11727.
[612] J.M. Pratt, P.R. Norris, M.S.A. Hamza, R. Bolton, J. Chem. Soc. Chem. Commun. (1994) 1333–1334.
[613] P.N. Balasubramanian, E.S. Gould, Inorg. Chem. 23 (1984) 824–828.
[614] I.A. Dereven'kov, D.S. Salnikov, S.V. Makarov, G.R. Boss, O.I. Koifman, Dalton Trans. 42 (2013) 15307–15316.
[615] H.V. Motwani, S. Qiu, B.T. Golding, H. Kylin, M. Törnqvist, Food Chem. Toxicol. 49 (2011) 750–757.
[616] H.V. Motwani, C. Fred, J. Haglund, B.T. Golding, M. Törnqvist, Chem. Res. Toxicol. 22 (2009) 1509–1516.
[617] D.L. Rabenstein, J. Chem. Ed. 55 (1978) 292.
[618] J.E. Fergusson, The heavy elements : chemistry, environmental impact and health effects, Pergamon Press, Oxford, UK, 1990.
[619] R.P. Mason, J.M. Benoit, in: P.G. Craig (Ed.), Organometallic Compounds in the Environment, John Wiley & Sons, Ltd., Chichester, UK, 2003, pp. 57–99.
[620] R.E. DeSimone, M.W. Penley, L. Charbonneau, S.G. Smith, J.M. Wood, H.A. O. Hill, J.M. Pratt, S. Ridsdale, R.J.P. Williams, Biochim. J. Chem. Biophs. Acta 304 (1973) 851–863.
[621] J.M. Wood, Science 183 (1974) 1049–1052.
[622] V.C.W. Chu, D.W. Gruenwedel, Z. Naturforsch. C 31 (1976) 753–755.
[623] J.M. Pratt, J. Aron, S.M. Chemaly, H.M. Marques, in: P.J. Craig, F. Glockling (Eds.), The Biological Alkylation of Heavy Elements, Royal Society of Chemistry, London, 1988, pp. 44–61.
[624] S.M. Chemaly, S. Afr. J. Sci. 98 (2002) 568–572.
[625] G.C. Hayward, H.A.O. Hill, J.M. Pratt, R.J.P. Williams, J. Chem. Soc. A (1971) 196–200.
[626] J. Zhou, D. Riccardi, A. Beste, J.C. Smith, J.M. Parks, Inorg. Chem. 53 (2014) 772–777.
[627] T.B. Demissie, B.D. Garabato, K. Ruud, P.M. Kozlowski, Angew Chem. Int. Edn 55 (2016) 11503–11506.
[628] H. Shimakoshi, Y. Hisaeda, Chem Plus Chem 82 (2017) 18–29.
[629] H. Shimakoshi, Y. Hisaeda, Curr. Op. Electrochem. 8 (2018) 24–30.
[630] M. Giedyk, J. Turkowska, S. Lepak, M. Marculewicz, K.Ó. Proinsias, D. Gryko, Org. Lett. 19 (2017) 2670–2673.
[631] H.A.O. Hill, J.M. Pratt, M.P. O'Riordan, F.R. Williams, R.P.J. Williams, J. Chem. Soc. A (1971) 1859–1862.
[632] D. Lexa, J.M. Savéant, J.P. Soufflet, J. Electroanal. Chem. 100 (1979) 159–172.
[633] K.M. McCauley, D.A. Pratt, S.R. Wilson, J. Shey, T.J. Burkey, W.A. van der Donk, J. Am. Chem. Soc. 127 (2005) 1126–1136.
[634] H. Shimakoshi, Z. Luo, T. Inaba, Y. Hisaeda, Dalton Trans. 45 (2016) 10173–10180.
[635] Y. Sun, W. Zhang, J. Tong, S. Wu, D. Liu, H. Shimakoshi, Y. Hisaeda, X.M. Song, RSC Adv. 7 (2017) 19197–19204.
[636] H. Tian, H. Shimakoshi, K. Imamura, Y. Shiota, K. Yoshizawa, Y. Hisaeda, Chem. Commun. 53 (2017) 9478–9481.
[637] Y. Sun, W. Zhang, T.-Y. Ma, Y. Zhang, H. Shimakoshi, Y. Hisaeda, X.-M. Song, RSC Adv. 8 (2018) 662–670.
[638] H. Shimakoshi, Z. Luo, K. Tomita, Y. Hisaeda, J. Organomet. Chem. 839 (2017) 71–77.
[639] M.J. Hossain, T. Ono, K. Wakiya, Y. Hisaeda, Chem. Commun. 53 (2017) 10878–10881.
[640] T. Wdowik, D. Gryko, ACS Catal. 12 (2022) 6517–6531.
[641] L. Auer, C. Weymuth, R. Scheffold, Helv. Chim. Acta 76 (1993) 810–818.
[642] R. Scheffold, S. Abrecht, R. Rflnski, H.-R. Ruf, P. Stamouli, O. Tinembart, L. Walder, C. Weymuth, Pure Appl. Chem. 59 (1987) 363–372.
[643] S. Busato, O. Tinembart, Z.-D. Zhang, R. Scheffold, Tetrahedron 46 (1990) 3155–3166.
[644] Y. Chen, X.P. Zhang, J. Organomet. Chem. 69 (2004) 2431–2435.
[645] P. Bonhôte, R. Scheffold, Helv. Chim. Acta 74 (1991) 1425–1444.
[646] H. Su, L. Walder, Z.-D. Zhang, R. Scheffold, Helv. Chim. Acta 71 (1988) 1073–1078.
[647] Z.D. Zhang, R. Scheffold, Helv. Chim. Acta 76 (1993) 2602–2615.
[648] A. Fischli, J.J. Daly, Helv. Chim. Acta 63 (1980) 1628–1643.
[649] M. Guo, Y. Chen, Rev. Environ. Sci. Biotechnol. 17 (2018) 259–284.
[650] H. Shimakoshi, Y. Hisaeda, Chem. Rec. 21 (2021) 2080–2094.
[651] H. Shimakoshi, M. Tokunaga, Y. Hisaeda, Dalton Trans. (2004) 878–882.
[652] S. Hisashi, M. Yasunori, K. Takeshi, M. Takashi, M. Eiki, N. Yoshinori, H. Yoshio, Bull. Chem. Soc. Japan 78 (2005) 859–863.
[653] D.R. Burris, C.A. Delcomyn, M.H. Smith, A.L. Roberts, Environ. Sci. Technol. 30 (1996) 3047–3052.
[654] M.C. Lagunas, D.S. Silvester, L. Aldous, R.G. Compton, Electroanalysis 18 (2006) 2263–2268.
[655] H. Shimakoshi, M. Tokunaga, T. Baba, Y. Hisaeda, Chem. Commun. (2004) 1806–1807.
[656] M. Yukito, H. Yoshio, K. Akiro, O. Teruhisa, Bull. Chem. Soc. Japan 57 (1984) 405–411.
[657] K. Tahara, K. Mikuriya, T. Masuko, J. Kikuchi, Y. Hisaeda, J. Porphyrins Phthalocyanines 17 (2013) 135–141.
[658] T. Keishiro, S. Hisashi, T. Akihiro, H. Yoshio, Bull. Chem. Soc. Japan 83 (2010) 1439–1446.
[659] H. Shimakoshi, L. Li, M. Nishi, Y. Hisaeda, Chem. Commun. 47 (2011) 10921–10923.
[660] J. Xu, H. Shimakoshi, Y. Hisaeda, J. Organomet. Chem. 782 (2015) 89–95.

[661] W. Cheng, R.G. Compton, Angew. Chem. Int. Ed. Eng. 55 (2016) 2545–2549.
[662] C. Kunze, M. Bommer, W.R. Hagen, M. Uksa, H. Dobbek, T. Schubert, G. Diekert, Nat. Commun. 8 (2017) 15858.
[663] H.M. Shahadat, H.A. Younus, N. Ahmad, S. Zhang, S. Zhuiykov, F. Verpoort, Chem. Commun. 56 (2020) 1968–1971.
[664] Y.-Y. Li, R.-Z. Liao Chin, Chem. Lett. 33 (2022) 358–361.
[665] Z. Abdi, S.E. Balaghi, A.S. Sologubenko, M.-G. Willinger, M. Vandichel, J.-R. Shen, S.I. Allakhverdiev, G.R. Patzke, M.M. Najafpour, ACS Sustain. Chem. Eng. 9 (2021) 9494–9505.
[666] M. Karczewski, M. Ociepa, K. Pluta, K.Ó. Proinsias, D. Gryko, Chem. Eur. J. 23 (2017) 7024–7030.
[667] C. Jia, K. Ching, P.V. Kumar, C. Zhao, N. Kumar, X. Chen, B. Das, ACS Appl. Mater. Interfaces 12 (2020) 41288–41293.
[668] W.-F. Huang, S.-T. Chang, H.-C. Huang, C.-H. Wang, L.-C. Chen, K.-H. Chen, M. C. Lin, J. Phys. Chem. C 124 (2020) 4652–4659.
[669] S.A. Bhat, N. Rashid, M.A. Rather, S.A. Pandit, P.P. Ingole, M.A. Bhat, Electrochim. Acta 337 (2020) 135730.
[670] J. Francisco Silva, S. Griveau, C. Richard, J.H. Zagal, F. Bedioui, Electrochem. Commun. 9 (2007) 1629–1634.
[671] S.C. Eady, M.M. MacInnes, N. Lehnert, Inorg. Chem. 56 (2017) 11654–11667.
[672] H.P.C. Hogenkamp, Biochemistry 5 (1966) 417–422.
[673] P.Y. Law, J.M. Wood, Biochim. Electrochim. Biophys. Acta 331 (1973) 451–454.
[674] J. Endicott, F.T.L. Netzel, J. Am. Chem. Soc. 101 (1979) 4000–4002.
[675] L.A. Walker, J.T. Jarrett, N.A. Anderson, S.H. Pullen, I.G. Matthews, R.J. Sension, J. Am. Chem. Soc. 120 (1998) 3597–3603.
[676] L.A. Walker, J.J. Shiang, N.A. Anderson, S.H. Pullen, R.J. Sension, J. Am. Chem. Soc. 120 (1998) 7286–7292.
[677] P.A. Schwartz, P.A. Frey, Biochemistry 46 (2007) 7284–7292.
[678] A.R. Jones, H.J. Russell, G.M. Greetham, M. Towrie, S. Hay, N.S. Scrutton, J. Phys. Chem. A 116 (2012) 5586–5594.
[679] A.S. Rury, T.E. Wiley, R.J. Sension, Acc. Chem. Res. 48 (2015) 860–967.
[680] A.P. Ghosh, A.A. Mamun, P. Lodowski, M. Jaworska, P.M. Kozlowski, J. Photochem. Photobiol. B 189 (2018) 306–317.
[681] T.A. Shell, D.S. Lawrence, Acc. Chem. Res. 48 (2015) 2866–2874.
[682] J.F. Endicott, Inorg. Chem. 16 (1977) 494–496.
[683] C.Y. Mok, J.F. Endicott, J. Am. Chem. Soc. 100 (1978) 123–129.
[684] C.Y. Mok, J.F. Endicott, J. Am. Chem. Soc. 99 (1977) 1276–1277.
[685] T.E. Wiley, N.A. Miller, W.R. Miller, D.L. Sofferman, P. Lodowski, M.J. Toda, M. Jaworska, P.M. Kozlowski, R.J. Sension, J. Phys. Chem. A 122 (2018) 6693–6703.
[686] P. Lodowski, M. Jaworska, T. Andruniów, B.D. Garabato, P.M. Kozlowski, Phys. Chem. Chem. Phys. 16 (2014) 18675–18679.
[687] T.A. Shell, D.S. Lawrence, J. Am. Chem. Soc. 133 (2011) 2148–2150.
[688] B. Kräutler, B. Puffer, Angew Chem. Int. Edn 50 (2011) 9791–9792.
[689] A. Arsalan, I. Ahmad, S.A. Ali, K. Qadeer, S. Mahmud, F. Humayun, A.E. Beg, Int. J. Chem. Kinet. 52 (2020) 207–217.
[690] N.A. Miller, A. Deb, R. Alonso-Mori, J.M. Glownia, L.M. Kiefer, A. Konar, L. B. Michocki, M. Sikorski, D.L. Sofferman, S. Song, M.J. Toda, T.E. Wiley, D. Zhu, P.M. Kozlowski, K.J. Kubarych, J.E. Penner-Hahn, R.J. Sension, J. Phys. Chem. A 122 (2018) 4963–4971.
[691] T.E. Wiley, B.C. Arruda, N.A. Miller, M. Lenard, R.J. Sension, Chin. Chem. Lett. 26 (2015) 439–443.
[692] D.A. Harris, A.B. Stickrath, E.C. Carroll, R.J. Sension, J. Am. Chem. Soc. 129 (2007) 7578–7585.
[693] J.J. Shiang, A.G. Cole, R.J. Sension, K. Hang, Y. Weng, J.S. Trommel, L. G. Marzilli, T. Lian, J. Am. Chem. Soc. 128 (2006) 801–808.
[694] I. Ahmad, K. Qadeer, A. Hafeez, S. Zahid, M.A. Sheraz, S. Ur Rehman Khattak, J. Photochem. Photobiol. A 332 (2017) 92–100.
[695] F.H.M. Vaid, S. Zahid, A. Faiyaz, K. Qadeer, W. Gul, Z. Anwar, I. Ahmad, J. Photochem. Photobiol. A 362 (2018) 40–48.
[696] A.B. Stickrath, E.C. Carroll, X. Dai, D.A. Harris, A. Rury, B. Smith, K. Tang, J. Wert, R.J. Sension, J. Phys. Chem. A 113 (2009) 8513–8522.
[697] J.F. Endicott, G.J. Ferraudi, J. Am. Chem. Soc. 99 (1977) 243–245.
[698] J.K. Thomas, J. Phys. Chem. (1967) 1919–1925.
[699] J. Peng, K.-C. Tang, K. McLoughlin, Y. Yang, D. Forgach, R.J. Sension, J. Phys. Chem. B 114 (2010) 12398–12405.
[700] J. Gomes, B.D. Castro, M. Rangel, Organometallics 27 (2008) 2536–2543.
[701] H.P.C. Hogenkamp, J.N. Ladd, H.A. Barker, J. Biol. Chem. 237 (1962) 1950–1952.
[702] H.P. Hogenkamp, J. Biol. Chem. 238 (1963) 477–480.
[703] R.J. Sension, D.A. Harris, A.G. Cole, J. Phys. Chem. B 109 (2005) 21954–21962.
[704] L.M. Yoder, A.G. Cole, W.L. A, R.J. Sension, J. Phys. Chem. B 105 (2001) 12180–12188.
[705] E. Chen, M.R. Chance, Biochemistry 32 (1993) 1480–1487.
[706] L.E.H. Gerards, H. Bulthuis, M.W.G. de Bolster, S. Balt, Inorg. Chim. Acta 190 (1991) 47–53.
[707] N.R. Walker, S. Firth, A.J. Stace, Chem. Phys. Lett. 292 (1998) 125–132.
[708] A.G. Cole, L.M. Yoder, J.J. Shiang, N.A. Anderson, L.A. Walker, M.M. Banaszak Holl, R.J. Sension, J. Am. Chem. Soc. 124 (2002) 434–441.
[709] P.M. Kozlowski, B.D. Garabato, P. Lodowski, M. Jaworska, Dalton Trans. 45 (2016) 4457–4470.
[710] R.T. Taylor, L. Smucker, M.L. Hanna, J. Gill, Arch. Biochem. Biophys. 156 (1973) 521–533.
[711] J.J. Shiang, L.A. Walker, N.A. Anderson, A.G. Cole, R.J. Sension, J. Phys. Chem. B 103 (1999) 10532–10539.
[712] M. Jaworska, P. Lodowski, T. Andruniów, P.M. Kozlowski, J. Phys. Chem. B 111 (2007) 2419–2422.
[713] K. Kornobis, N. Kumar, P. Lodowski, M. Jaworska, P. Piecuch, J.J. Lutz, B. M. Wong, P.M. Kozlowski, J. Comput. Chem. 34 (2013) 987–1004.
[714] P. Lodowski, M. Jaworska, T. Andruniów, M. Kumar, P.M. Kozlowski, J. Phys. Chem. B 113 (2009) 6898–6909.
[715] M. Chromiński, A. Lewalska, M. Karczewski, D. Gryko, J. Org. Chem. 79 (2014) 7532–7542.
[716] M. Ruetz, A. Shanmuganathan, C. Gherasim, A. Karasik, R. Salchner, C. Kieninger, K. Wurst, R. Banerjee, M. Koutmos, B. Kräutler, Angew. Chem. Int. Ed. 56 (2017) 7387–7392.
[717] J. Rossier, S. Nasiri Sovari, A. Pavic, S. Vojnovic, T. Stringer, S. Bättig, G.S. Smith, J. Nikodinovic-Runic, F. Zobi, Molecules 24 (2019) 2310.
[718] P. Lodowski, M.J. Toda, K. Ciura, M. Jaworska, P.M. Kozlowski, Inorg. Chem. 57 (2018) 7838–7850.
[719] E.V. Salerno, N.A. Miller, A. Konar, R. Salchner, C. Kieninger, K. Wurst, K. G. Spears, B. Kräutler, R.J. Sension, Inorg. Chem. 59 (2020) 6422–6431.
[720] A.R. Jones, J.R. Woodward, N.S. Scrutton, J. Am. Chem. Soc. 131 (2009) 17246–17253.
[721] J.R. Woodward, T.J. Foster, A.R. Jones, A.T. Salaoru, N.S. Scrutton, Biochem. Soc. Trans. 37 (2009) 358–362.
[722] A.R. Jones, C. Levy, S. Hay, N.S. Scrutton, FEBS J. 280 (2013) 2997–3008.
[723] A.R. Jones, Mol. Phys. 114 (2016) 1691–1702.
[724] N.A. Miller, L.B. Michocki, A. Konar, R. Alonso-Mori, A. Deb, J.M. Glownia, D. L. Sofferman, S. Song, P.M. Kozlowski, K.J. Kubarych, J.E. Penner-Hahn, R. J. Sension, J. Phys. Chem. B 124 (2020) 199–209.
[725] G. Subramanian, X. Zhang, G. Kodis, Q. Kong, C. Liu, A. Chizmeshya, U. Weierstall, J. Spence, J. Chem. Phys. Lett 9 (2018) 1542–1546.
[726] W.D. Robertson, A.M. Bovell, K. Warncke, J. Biol. Inorg. Chem. 18 (2013) 701–713.
[727] T. Lazarides, T. McCormick, P. Du, G. Luo, B. Lindley, R. Eisenberg, J. Am. Chem. Soc. 131 (2009) 9192–9194.
[728] R.R. Hung, J.J. Grabowski, J. Am. Chem. Soc. 121 (1999) 1359–1364.
[729] A.S. Eisenberg, I.V. Likhtina, V.S. Znamenskiy, R.L. Birke, J. Phys. Chem. A 116 (2012) 6851–6869.
[730] J. Aron, D.A. Baldwin, H.M. Marques, J.M. Pratt, P.A. Adams, J. Inorg. Biochem. 27 (1986) 227–243.
[731] S.M. Chemaly, Polyhedron 175 (2020), 114203.
[732] G. Tsiminis, E.P. Schartner, J.L. Brooks, M.R. Hutchinson, Appl. Spectrosc. Rev. 52 (2017) 439–455.
[733] H.A. Barker, R.D. Smyth, H. Weissbach, J.I. Toohey, J.N. Ladd, B.E. Volcani, J. Biol. Chem. 235 (1960) 480–488.
[734] H.A. Barker, R.D. Smyth, H. Weissbach, A. Munch-Petersen, J.I. Toohey, J. N. Ladd, B.E. Volcani, M.R. Wilson, J. Biol. Chem. (1960) 181–190.
[735] D. Cavallini, R. Scandurra, in: B.M. Donald, D.W. Lemuel (Eds.), Methods in Enzymology, Academic Press: Waltham, MA, 1971; Vol. 18, Part C, p. 3.
[736] Q. Yuan, L.L. Pearce, J. Peterson Chem. Res. Toxicol. 30 (2017) 2197–2208.
[737] W.W. Reenstra, W.P. Jencks, J. Am. Chem. Soc. 101 (1979) 5780–5791.
[738] C.L. Evans, Br. J. Pharmacol. 23 (1964) 455–475.
[739] C. Männel-Croisé, F. Zelder, ACS Appl. Mater. Interfaces 4 (2012) 725–729.
[740] L. Tivana, J. Da Cruz Francisco, F. Zelder, B. Bergenstahl, P. Dejmek, Food Chem. 158 (2014) 20–27.
[741] F. Zelder, L. Tivana, Org. Biomol. Chem. 13 (2015) 14–17.
[742] P. Lawrence, Vitamin B_{12} - A review of analytical methods for use in food. UK National Measurement Office, Report no. LGC/R/2014/378, 2015.
[743] D.D. Erbahar, I. Gürol, F. Zelder, M. Harbeck, Sensors Actuators B Chem. 207 (2015) 297–302.
[744] K.L. Brown, D.R. Evans, Inorg. Chem. 29 (1990) 2559–2561.
[745] S.H. Ford, A. Nichols, J.M. Gallery, J. Chromatogr. A 536 (1991) 185–191.
[746] S.H. Ford, J. Gallery, A. Nichols, M. Shambee, J. Chromatogr. A 537 (1991) 235–247.
[747] M.J. Dunphy, A.M. Sysel, J.A. Lupica, K. Griffith, T. Sherrod, J.A. Bauer, Chromatographia 77 (2014) 581–589.
[748] A.H. Chamle, N.J.L. Shane, A. Pal, B.S. Muddukrishna, Indian J. Pharm. Sci. 81 (2019) 57–62.
[749] J. Van Wyk, T.J. Britz, Dairy Sci. Technol. 90 (2010) 509–520.
[750] N.E. Brasch, R.G. Finke, J. Inorg. Biochem. 73 (1999) 215–219.
[751] C. Tian, N. Zhao, X. Jiang, D. Wan, Y. Xie, Water 13 (2021) 1790.
[752] A. Sharma, S. Arya, D. Chauhan, P.R. Solanki, S. Khajuria, A. Khosla, J. Mat. Res. Tech. 9 (2020) 14321–14337.
[753] S.V. Tymoshuk, O.S. Fedyshyn, L.O. Kobryn, I.O. Patsay, L.V. Oleksiv, O. S. Tymoshuk, J. Chem. Tech. 29 (2021) 179–191.
[754] S.S. Harke, R.V. Patil, M.A. Dar, S.R. Pandit, K.D. Pawar, Food Chem. Adv. 1 (2022), 100017.
[755] J. Haglund, A.-L. Magnusson, L. Ehrenberg, M. Törnqvist, Toxicol. Environ. Chem. 85 (2003) 81–94.
[756] C. Fred, J. Haglund, T. Alsberg, P. Rydberg, J. Minten, M. Törnqvist, J. Sep. Sci. 27 (2004) 607–612.
[757] J.M. Pratt, R.G. Thorp, J. Chem. Soc. A (1966) 187–191.
[758] S.M. Chemaly, Dalton Trans. (2008) 5766–5773.
[759] C.K. Jørgensen, in: F.A. Cotton (Ed.), Progress in Inorganic Chemistry Vol. 4, John Wiley & Sons, Inc, New York, NY, 1962, pp. 73–124.
[760] J.M. Pratt, R.G. Thorp, in: H.J. Emeléus, A.G. Sharpe (Eds.), Advances in Inorganic Chemistry and Radiochemistry Vol. 12, Academic Press, New York, NY, 1969, pp. 375–427.
[761] C.B. Perry, H.M. Marques, S. Afr. J. Chem. 58 (2005) 9–15.

[762] S. Salama, T.G. Spiro, J. Raman Spectrosc. 6 (1977) 57–60.
[763] J.M. Pratt, in: R. Banerjee (Ed.), Chemistry and Biochemistry of B_{12}, John Wiley & Sons, New York, 1999, pp. 113–164.
[764] P. Lodowski, M. Jaworska, K. Kornobis, T. Andruniów, P.M. Kozlowski, J. Phys. Chem. B 115 (2011) 13304–13319.
[765] H. Solheim, K. Kornobis, K. Ruud, P.M. Kozlowski, J. Phys. Chem. B 115 (2011) 737–748.
[766] J.D. Handali, K.F. Sunden, B.J. Thompson, N.A. Neff-Mallon, E.M. Kaufman, T. C. Brunold, J.C. Wright, J. Phys. Chem. A 122 (2018) 9031–9042.
[767] E.V. Salerno, N.A. Miller, A. Konar, Y. Li, C. Kieninger, B. Kräutler, R.J. Sension, J. Phys. Chem. B 124 (2020) 6651–6656.
[768] K. Kornobis, N. Kumar, B.M. Wong, P. Lodowski, M. Jaworska, T. Andruniów, K. Ruud, P.M. Kozlowski, J. Phys. Chem. A 115 (2011) 1280–1292.
[769] A.C. Banciu, Rev. Roum. Chim. 46 (2001) 349–355.
[770] F. Wagner, K. Bernhauer, Ann. N. Y. Acad. Sci. 112 (1964) 580–589.
[771] F. Wagner, Proc. Roy. Soc. Lond. A 288 (1965) 344–347.
[772] H.M. Marques, L. Knapton, X. Zou, K.L. Brown, J. Chem. Soc. Dalton Trans. (2002) 3195–3200.
[773] H. Shimakoshi, T. Inaoka, Y. Hisaeda, Tetrahedron Lett. 44 (2003) 6421–6424.
[774] C. Brenig, L. Mosberger, K. Baumann, O. Blacque, F. Zelder, Helv. Chim. Acta 104 (2021), e2100067.
[775] R. Bonnett, J. Cannon, V. Clark, A. Johnson, L. Parker, E.L. Smith, A. Todd, J. Chem. Soc. (1957) 1158–1168.
[776] D.L. Anton, H.P.C. Hogenkamp, T.E. Walker, N.A. Matwiyoff, J. Am. Chem. Soc. 102 (1980) 2215–2219.
[777] S.N. Fedosov, M. Ruetz, K. Gruber, N.U. Fedosova, B. Kräutler, Biochemistry 50 (2011) 8090–8101.
[778] R. Bonnett, J.R. Cannon, A.W. Johnson, A. Todd, J. Chem. Soc. (1957) 1148–1158.
[779] D. Salnikov, S. Makarov, New J. Chem. 43 (2019) 7708–7715.
[780] B. Kräutler Helv, Chim. Acta 65 (1982) 1941–1948.
[781] M. Nowakowska, S.M. Chemaly, A.L. Rousseau, P.P. Govender, P.R. Varadwaj, A. Varadwaj, K. Yamashita, H.M. Marques, Inorg. Chim. Acta 484 (2019) 402–413.
[782] R.M. Oetterli, L. Prieto, B. Spingler, F. Zelder, Org. Lett. 15 (2013) 4630–4633.
[783] S. Kurcoń, K.Ó. Proinsias, D. Gryko, J. Organomet. Chem. 78 (2013) 4115–4122.
[784] K.Ó. Proinsias, M. Giedyk, R. Loska, M. Chromiński, D. Gryko, J. Organomet. Chem. 76 (2011) 6806–6812.
[785] K.Ó. Proinsias, J.L. Sessler, S. Kurcoń, D. Gryko, Org. Lett. 12 (2010) 4674–4677.
[786] K. Zhou, F. Zelder, Angew. Chem. Int. Ed. 49 (2010) 5178–5180.
[787] R.A. Firth, H.A.O. Hill, J.M. Pratt, R.G. Thorp, R.J.P. Williams, J. Chem. Soc. A (1969) 381–386.
[788] L. Prieto, J. Rossier, K. Derszniak, J. Dybas, R.M. Oetterli, E. Kottelat, S. Chlopicki, F. Zelder, F. Zobi, Chem. Commun. 53 (2017) 6840–6843.
[789] C. Hansch, A. Leo, R.W. Taft, Chem. Rev. 91 (1991) 165–195.
[790] Y. Murakami, Y. Aoyama, K. Tokumaga, J. Am. Chem. Soc. 102 (1980) 6736–6744.
[791] Y. Murakami, in: D. Dolphin, C. McKenna, Y. Murakami, I. Tabushi (Eds.), Biomimetic Chemistry vol. 191, American Chemical Society, Washington, D.C, Advances in Chemistry, 1980, pp. 179–199.
[792] I. Navizet, C.B. Perry, P.P. Govender, H.M. Marques, J. Phys. Chem. B 116 (2012) 8836–8846.
[793] P.P. Govender, I. Navizet, C.B. Perry, H.M. Marques, Chem. Phys. Lett. 550 (2012) 150–155.
[794] B.J. Coe, S.J. Glenwright, Coord. Chem. Rev. 203 (2000) 5–80.
[795] P.M. Kozlowski, M.Z. Zgierski, J. Phys. Chem. B 108 (2004) 14163–14170.
[796] P.P. Govender, I. Navizet, C.B. Perry, H.M. Marques, J. Phys. Chem. A 117 (2013) 3057–3068.
[797] Cambridge Structural Database, V.5.43, Cambridge Crystallographic Data Centre (CCDC), Cambridge, UK, 2022.
[798] S. Balt, A.M. Van Herk, Inorg. Chim. Acta 125 (1986) 27–30.
[799] C.B. Perry, M.A. Fernandes, K.L. Brown, X. Zou, E.J. Valente, H.M. Marques, Eur. J. Inorg. Chem. (2003) 2095–2107.
[800] G. Garau, S. Geremia, L.G. Marzilli, G. Nardin, L. Randaccio, G. Tauzher, Acta Cryst., Sec. B (2003) 51–59.
[801] A.D. McNaught, A. Wilkinson. Compendium of Chemical Terminology (the "Gold Book"), 2nd. ed., Blackwell Scientific Publications, Oxford, UK, 1997.
[802] M.S.A. Hamza, X. Zou, K.L. Brown, R. van Eldik, Eur. J. Inorg. Chem. (2003) 268–276.
[803] M.S.A. Hamza, R. van Eldik, P.L.S. Harper, J.M. Pratt, E.A. Betterton, Eur. J. Inorg. Chem. (2002) 580–583.
[804] F. Basolo, R.G. Pearson, Mechanisms of Inorganic Reactions, Wiley, New York, NY, 1967.
[805] T.G. Appleton, H.C. Clark, L.E. Manzer Coord, Chem. Rev. 10 (1973) 335–422.
[806] J. Burgess, C.D. Hubbard, in: C.D. Hubbard, R. van Edik (Eds.), Advaces in Inorganic Chemistry vol. 54, Academic Press, New York, 2003, pp. 71–155.
[807] S. Aśperger, Chemical Kinetics and Inorganic Reaction Mechanisms, Springer, Boston, MA, 2003.
[808] M.S.A. Hamza, R. van Eldik, Dalton Trans. (2004) 1–12.
[809] R.H. Crabtree, The Organometallic Chemistry of the Transition Metals, Wiley-Interscience, Hoboken, NJ, 2005.
[810] M. De March, N. Demitri, S. Geremia, N. Hickey, L. Randaccio, J. Inorg. Biochem. 116 (2012) 215–227.
[811] R.F. See, D. Kozina, J. Coord. Chem. 66 (2013) 490–500.
[812] M.S.A. Hamza, X. Zou, R. Banka, K.L. Brown, R. van Eldik, Dalton Trans. (2005) 782–787.
[813] R.A. Firth, H.A.O. Hill, B.E. Mann, J.M. Pratt, R.G. Thorp, J. Chem. Soc. Chem. Commun. (1967) 1013–1014.
[814] R.A. Firth, H.A.O. Hill, B.E. Mann, J.M. Pratt, R.G. Thorp, R.J.P. Williams, J. Chem. Soc. A (1968) 2419–2428.
[815] H.A.O. Hill, J.M. Pratt, R.J.P. Williams, Discuss. Faraday Soc. 47 (1969) 165–171.
[816] S.M. Chemaly, J.M. Pratt, J. Chem. Soc. Dalton Trans. (1980) 2259–2266.
[817] S.M. Chemaly, J.M. Pratt, J. Chem. Soc. Dalton Trans. (1980) 2267–2273.
[818] S.M. Chemaly, J. Inorg. Biochem. 44 (1991) 1–15.
[819] M.D. Wirt, M.R. Chance, J. Inorg. Biochem. 49 (1993) 265–273.
[820] K.L. Brown, G.Z. Wu, Inorg. Chem. 33 (1994) 4122–4127.
[821] K.L. Brown, J. Am. Chem. Soc. 109 (1987) 2277–2284.
[822] K.L. Brown, D.R. Evans, Inorg. Chim. Acta 197 (1992) 101–106.
[823] J.D. Satterlee, Biochem. Biophys. Res. Commun. 89 (1979) 272–278.
[824] K.L. Brown, J.M. Hakimi, Inorg. Chem. 23 (1984) 1756–1764.
[825] K.L. Brown, J.M. Hakimi, D.S. Marynick, Inorg. Chim. Acta 79 (1983) 120–122.
[826] K.L. Brown, S. Peck-Siler, Inorg. Chem. 27 (1988) 3548–3555.
[827] K.L. Brown, J.M. Hakimi, J. Am. Chem. Soc. 108 (1986) 496–503.
[828] Y. Sulfab, M.S. El-Ezaby, Inorg. Chim. Acta 26 (1978) 177–181.
[829] S.M. Chemaly, E.A. Betterton, J.M. Pratt, J. Chem. Soc. Dalton Trans. (1987) 761–767.
[830] S.M. Chemaly, J. Inorg. Biochem. 44 (1991) 17–25.
[831] E.A. Betterton, S.M. Chemaly, J.M. Pratt, J. Chem. Soc. Dalton Trans. (1985) 1619–1622.
[832] R. Bieganowski, W. Friedrich, Naturforsch. 35b (1980) 1335–1340.
[833] H.-L. Chen, Z.-H. Liu, Transit. Met. Chem. 22 (1997) 326–329.
[834] H. Chen, H. Yan, W. Tang, J. Inorg. Biochem. 52 (1993) 109–120.
[835] J.H. Grate, G.N. Schrauzer, J. Am. Chem. Soc. 101 (1979) 4601–4611.
[836] M. Sonnay, F. Zelder, Dalton Trans. 47 (2018) 10443–10446.
[837] A. Drljaca, C.D. Hubbard, R. van Eldik, T. Asano, M.V. Basilevsky, W.J.L. Noble, Chem. Rev. 98 (1998) 2167–2290.
[838] E.A. Kaczka, D.E. Wolf, F.A. Kuehl, K. Folkers, Science (1950) 354–355.
[839] E.A. Kaczka, D.E. Wolf, F.A. Kuehl, K. Folkers, J. Am. Chem. Soc. 73 (1951) 3569–3573.
[840] G. Cooley, B. Ellis, V. Petrow, G.H. Beaven, E.R. Holiday, E.A. Johnson, J. Pharm. Pharmacol. 3 (1951) 271–285.
[841] P. George, D.H. Irvine, S.C. Glauser Ann, New York Acad. Sci. 88 (1960) 393–415.
[842] R.P. Buhs, E.G. Newstead, N.R. Renner, Science 113 (1851) 625–626.
[843] E. Lester Smith, S. Ball, D.M. Ireland, Biochem. J. 52 (1952) 395–400.
[844] B. Ellis, V. Petrow, J. Pharm. Pharmacol. 4 (1952) 152.
[845] G.I.H. Hanania, D.H. Irvine, J. Chem. Soc. (1964) 5694–5697.
[846] H.M. Marques, J.H. Marsh, J.R. Mellor, O.Q. Munro, Inorg. Chim. Acta 170 (1990) 259–269.
[847] H.M. Marques, T.J. Egan, J.H. Marsh, J.R. Mellor, O.Q. Munro, Inorg. Chim. Acta 166 (1989) 249–255.
[848] D.A. Baldwin, V.M. Campbell, L.A. Carleo, H.M. Marques, J.M. Pratt, J. Am. Chem. Soc. 103 (1981) 186–188.
[849] D.A. Baldwin, V.M. Campbell, H.M. Marques, J.M. Pratt, FEBS Lett. 167 (1984) 339–342.
[850] D.A. Baldwin, H.M. Marques, J.M. Pratt, S. Afr. J. Chem. 39 (1986) 189–196.
[851] W.H. Pailes, H.P.C. Hogenkamp, Biochemistry 7 (1968) 4160–4166.
[852] C. Männel-Croisé, F. Zelder, Inorg. Chem. 48 (2009) 1272–1274.
[853] D.A. Baldwin, E.A. Betterton, J.M. Pratt, J. Chem. Soc. Dalton Trans. (1983) 2217–2222.
[854] W.R. Bauriedel, J.C. Picken, L.A. Underkofler, Proc. Soc. Exp. Biol. Med. 91 (1956) 377–381.
[855] J.D. Brodie, Proc. Natl. Acad. Sci. U. S. A. 62 (1969) 461–467.
[856] L. Knapton, H.M. Marques, Dalton Trans. (2005) 889–895.
[857] G.I.H. Hanania, D.H. Irvine, in: V. Gutmann (Ed.), 8th Int. Conf. Coord. Chem., Vienna, Springer, Vienna, 1964, p. 418.
[858] M.S.A. Hamza, J.M. Pratt, J. Chem. Soc. Dalton Trans. (1994) 1377–1382.
[859] D.A. Baldwin, E.A. Betterton, S.M. Chemaly, J.M. Pratt, J. Chem. Soc. Dalton Trans. (1985) 1613–1618.
[860] S.O. Tumakov, I.A. Dereven'kov, D.S. Salnikov, S.V. Makarov, Russ. J. Phys. Chem. A 91 (2017) 1839–1844.
[861] H.A. Hassanin, M.F. El-Shahat, M.S.A. Hamza, J. Coord. Chem. 63 (2010) 2431–2439.
[862] D.A. Baldwin, E.A. Betterton, J.M. Pratt, J. Chem. Soc. Dalton Trans. (1983) 225–229.
[863] C.D. Garr, J.M. Sirovatka, R.G. Finke, Inorg. Chem. 35 (1996) 5912–5922.
[864] K.L. Brown, B.D. Gupta, Inorg. Chem. 29 (1990) 3854–3860.
[865] K.L. Brown, S. Satyanarayana, Inorg. Chem. 31 (1992) 1366–1369.
[866] C.D. Garr, J.M. Sirovatka, R.G. Finke, J. Am. Chem. Soc. 118 (1996) 11142–11154.
[867] J.M. Sirovatka, R. Finke, J. Am. Chem. Soc. 119 (1997) 3057–3067.
[868] J.M. Sirovatka, R.G. Finke, Inorg. Chem. 38 (8) (1999) 1697–1707.
[869] R.F.W. Bader, Acc. Chem. Res. 18 (1985) 9–15.
[870] R.F.W. Bader, P.V. Schleyer (Eds.), Encyclopedia of Computational Chemistry vol. 1, John Wiley and Sons, Chichester, UK, 1998, pp. 64–86.
[871] P.R. Varadwaj, A. Varadwaj, H.M. Marques, J. Phys. Chem. A 115 (2011) 5592–5601.
[872] M.S.A. Hamza, J. Inorg. Biochem. 69 (1998) 269–274.
[873] M.S.A. Hamza, M.A. Elawady, H.M. Marques, S. Afr. J. Chem. 61 (2008) 68–73.
[874] K.L. Brown, X. Zou, L. Salmon, Inorg. Chem. 30 (1991) 1949–1953.
[875] K.L. Brown, X. Zou, Inorg. Chem. 31 (1992) 2541–2547.
[876] X.A. Zou, D.R. Evans, K.L. Brown, Inorg. Chem. 34 (1995) 1634–1635.
[877] T.W. Koenig, B.P. Hay, R.G. Finke, Polyhedron 7 (1988) 1499–1516.

[878] T. Koenig, R.G. Finke, J. Am. Chem. Soc. 110 (1988) 2657–2658.
[879] K.L. Brown, S.F. Cheng, H.M. Marques, Inorg. Chem. 34 (1995) 3038–3049.
[880] K.L. Brown, L.X. Zhou, Inorg. Chem. 35 (1996) 5032–5039.
[881] K.L. Brown, S. Cheng, J.D. Zubkowski, E.J. Valente, Inorg. Chem. 36 (1997) 1772–1781.
[882] K.L. Brown, M.S.A. Hamza, J. Inorg. Biochem. 70 (1998) 171–174.
[883] X. Zou, K.L. Brown, C. Vaughn, Inorg. Chem. 31 (1992) 1552.
[884] A. Gossauer, B. Grüning, L. Ernst, W. Becker, W.S. Sheldrick, Angew. Chem. Int. Ed. 16 (1977) 481–482.
[885] B. Grüning, G. Holze, T. Jenny, P. Nesvadba, A. Gossauer, L. Ernst, W.S. Sheldrick, Helv. Chim. Acta 68 (1985) 1754–1770.
[886] S.M. Chemaly, K.L. Brown, M.A. Fernandes, O.Q. Munro, C. Grimmer, H. M. Marques, Inorg. Chem. 50 (2011) 8700–8718.
[887] H.M. Marques, Dalton Trans. (2007) 4371–4385.
[888] W.C. Randall, R.A. Alberty, Biochemistry 6 (1967) 1520–1525.
[889] D. Thusius, J. Am. Chem. Soc. 93 (1971) 2629–2635.
[890] S. Mathura, D. Sannasy, A.S. de Sousa, C.B. Perry, I. Navizet, H.M. Marques, J. Inorg. Biochem. 123 (2013) 66–79.
[891] N. Ghadimi, C.B. Perry, P.P. Govender, H.M. Marques, Inorg. Chim. Acta 450 (2016) 269–278.
[892] S.M. Chemaly, M. Florczak, H. Dirr, H.M. Marques, Inorg. Chem. 50 (2011) 8719–8727.
[893] C. Rovira, K. Kunc, J. Hutter, M. Parrinello, Inorg. Chem. 40 (2001) 11–17.
[894] J.C.A. Boeyens, J. Chem. Soc. Faraday Trans. 90 (1994) 3377–3381.
[895] S.M. Chemaly, L. Kendall, M. Nowakowska, D. Pon, C.B. Perry, H.M. Marques, Inorg. Chem. 52 (2013) 1077–1083.
[896] R.F. Bader, Atoms in Molecules: A Quantum Theory, Oxford University Oress, Oxford, UK, 1990.
[897] M.J. Sisley, R.B. Jordan, Inorg. Chem. 45 (2006) 10758–10763.
[898] J.H. Lee, J. Britten, J. Chin J. Am. Chem. Soc. 115 (1993) 3618–3622.
[899] F. Yajima, A. Yamasaki, S. Fujiwara, Inorg. Chem. 10 (1971) 2350–2352.
[900] W. Grzybkowski, Pol. J. Environ. Stud. 15 (2006) 655–663.
[901] D.J. Wasylenko, C. Ganesamoorthy, J. Borau-Garcia, C.P. Berlinguette, Chem. Commun. 47 (2011) 4249–4251.
[902] I. Aviv-Harel, Z. Gross, Chem. Eur. J. 15 (2009) 8382–8394.
[903] I. Aviv-Harel, Z. Gross, Coord. Chem. Rev. 255 (2011) 717–736.
[904] T.D. Lash, J. Porphyrins Phthalocyanines 15 (2011) 1093–1115.
[905] H.A.O. Hill, J.M. Pratt, R.G. Thorp, B. Ward, R.J.P. Williams, Biochem. J. 120 (1970) 263–269.
[906] N.R. de Tacconi, D. Lexa, J.M. Saveant, J. Am. Chem. Soc. 101 (1979) 467.
[907] P.R. Varadwaj, I. Cukrowski, H.M. Marques, J. Phys. Chem. A 112 (2008) 10657–10666.
[908] P.R. Varadwaj, H.M. Marques, Phys. Chem. Chem. Phys. 12 (2010) 2126–2138.
[909] P.R. Varadwaj, H.M. Marques, Theor. Chem. Accounts 127 (2010) 711–725.
[910] P.R. Varadwaj, I. Cukrowski, C.B. Perry, H.M. Marques, J. Phys. Chem. A 115 (2011) 6629–6640.
[911] P.R. Varadwaj, A. Varadwaj, G.H. Peslherbe, H.M. Marques, J. Phys. Chem. A 115 (2011) 13180–13190.
[912] R.F.W. Bader, C.F. Matta, J. Phys. Chem. A 108 (2004) 8385–8394.
[913] L. Sobczyk, S.J. Grabowski, T.M. Krygowski, Chem. Rev. 105 (2005) 3513–3560.
[914] E. Espinosa, I. Alkorta, J. Elguero, E. Molins, J. Chem. Phys. 117 (2002) 5529–5542.
[915] R. Moreno-Esparza, M. Lopez, K.H. Pannell, J. Chem. Soc. Dalton Trans. (1992) 1791–1795.
[916] S. Balt, M.W.G. de Bolster, C.J. van Garderen, A.M. van Herk, K.R. Lammers, E. G. van Der Velde, Inorg. Chim. Acta 106 (1985) 43–47.
[917] A.E. Martell, R.M. Smith, R.J. Motekaites, NIST Standard Database 46. Criticially Selected Stability Constants of Metal Complexes, V. 8.0, IST, Gaithersburg, MD, 2004.
[918] M.S. Zakerhamidi, L. Zare Haghighi, S.M. Seyed Ahmadian, J. Mol. Struct. 1144 (2017) 265–272.
[919] M. Yukito, H. Yoshio, K. Akiro, Bull. Chem. Soc. Japan 56 (1983) 3642–3646.
[920] M.S.A. Hamza, J.M. Pratt, J. Chem. Soc. Dalton Trans. (1996) 3721–3725.
[921] C. Reichardt, Angew. Chem. Int. Ed. 18 (1979) 98–110.
[922] S. Balt, M.W.G. de Bolster, A.M. van Herk, Inorg. Chim. Acta 107 (1985) 13–17.
[923] S. Balt, A.M. van Herk, W.E. Koolhaas, Inorg. Chim. Acta 92 (1984) 67–74.
[924] I.J. Kobylianskii, F.J. Widner, B. Kräutler, P. Chen, J. Am. Chem. Soc. 135 (2013) 13648–13651.
[925] K.P. Kepp, J. Phys. Chem. A 118 (2014) 7104–7117.
[926] A.W. Johnson, N. Shaw, J. Chem. Soc. A (1962) 4608–4614.
[927] N.E. Brasch, M.S.A. Hamza, R. Van Eldik, Inorg. Chem. 36 (1997) 3216–3222.
[928] N.E. Brasch, R. Haupt, Inorg. Chem. 39 (2000) 5469–5474.
[929] N.E. Brasch, A.G. Cregan, M.E. Vanselow, J. Chem. Soc. Dalton Trans. (2002) 1287–1294.
[930] A.G. Cregan, N.E. Brasch, R. van Eldik, Inorg. Chem. 40 (7) (2001) 1430–1438.
[931] P.A. Butler, B. Kräutler, in: G. Simonneaux (Ed.), Bioorganometallic Chemistry. Topics in Organometallic Chemistry vol. 17, Springer, Berlin, Heidelberg, 2006.
[932] B. Kräutler, in: S. Helmut, S. Astrid, K.O.S. Roland (Eds.), Organometallic Chemistry of B_{12} Coenzymes, De Gruyter, 2015, pp. 1–52.
[933] B. Kräutler, in: T. Hirao, T. Moriuchi (Eds.), Advances in Bioorganometallic Chemistry, Elsevier, 2019, pp. 399–430.
[934] H.P.C. Hogenkamp, T.G. Oikawa, J. Biol. Chem. 239 (1964) 1911–1916.
[935] L.E.H. Gerards, S. Balt, Rec. Trav. Chim. des Pays-Bas 113 (1994) 137–144.
[936] W.B. Lott, A.M. Chagovetz, C.B. Grissom, J. Am. Chem. Soc. 117 (1995) 12194–12201.
[937] M.P. Jensen, J. Halpern, J. Am. Chem. Soc. 121 (10) (1999) 2181–2192.
[938] S.H. Kim, H.L. Chen, N. Feilchenfeld, J. Halpern J. Am. Chem. Soc. 110 (1988) 3120–3126.
[939] K.L. Brown, L. Salmon, J.A. Kirby, Organometallics 11 (1992) 422–432.
[940] B. Kräutler, C. Caderas, Helv. Chim. Acta 67 (1984) 1891–1896.
[941] K.L. Brown, X. Zou, J. Am. Chem. Soc. 114 (1992) 9643–9651.
[942] W. Fieber, B. Hoffmann, W. Schmidt, E. Stupperich, R. Konrat, B. Kräutler, Helv. Chim. Acta 85 (2002) 927–944.
[943] G. Kontaxis, D. Riether, R. Hannak, M. Tollinger, B. Krautler, Helv. Chim. Acta 82 (1999) 848–869.
[944] S. Gschösser, R.B. Hannak, R. Konrat, K. Gruber, C. Mikl, B. Kräutler, Chem. Eur. J. 11 (2005) 81–93.
[945] B. Kräutler, Helv. Chim. Acta 67 (1984) 1053–1059.
[946] H. Fischer, J. Am. Chem. Soc. 108 (1986) 3925–3927.
[947] J. Halpern, Science 227 (1985) 869–875.
[948] K.L. Brown, in: M.I. Page (Ed.), New Comprehensive Biochemistry: The Chemistry of Enzyme Action vol. 6, Elsevier, Amsterdam, 1984, pp. 433–459.
[949] B. Kräutler, T. Dérer, P. Liu, W. Mühlecker, M. Puchberger, K. Gruber, C. Kratky, Angew. Chem. Int. Ed. Eng. 34 (1995) 84–86.
[950] H. Mosimann, B. Krautler, Angew. Chem. Int. Ed. Eng. 39 (2000) 393–395.
[951] M.C.R. Symons, in: M. Chanon, M. Julliard, J.C. Poite (Eds.), Paramagnetic Organometallic Species in Activation/Selectivity, Catalysis, NATO ASI Series vol. 257, Springer, Dordrecht, Netherlands, 1989, pp. 447–461.
[952] B. Kräutler, M. Hughes, C. Caderas, Helv. Chim. Acta 69 (1986) 1571–1575.
[953] A.C. Rutenberg, H. Taube, J. Chem. Phys. 20 (1952) 825–826.
[954] J. Hunt, R.A. Plane, J. Am. Chem. Soc. 76 (1954) 5960–5962.
[955] D. Fiat, R.E. Connick, J. Am. Chem. Soc. 90 (1968) 608–615.
[956] T.J. Swift, R.E. Connick, J. Chem. Phys. 37 (1962) 307–320.
[957] F.A. Posey, H. Taube, J. Am. Chem. Soc. 79 (1957) 255–262.
[958] W.C. Randall, R.A. Alberty, Biochemistry 5 (1966) 3189–3193.
[959] H.M. Marques, S. Afr. J. Chem. 44 (1991) 114–117.
[960] H.M. Marques, J.C. Bradley, L.A. Campbell, J. Chem. Soc. Dalton Trans. (1992) 2019–2027.
[961] H.M. Marques, J.C. Bradley, K.L. Brown, H. Brooks, J. Chem. Soc. Dalton Trans. (1993) 3475–3478.
[962] D.A. Baldwin, E.A. Betterton, J.M. Pratt, J. Chem. Soc. Dalton Trans. (1983) 217–223.
[963] D.D. Perrin, Dissociation Constants of Organic Bases in Aqueous Solution, Butterworths, London, UK, 1965.
[964] C.K. Poon, Coord. Chem. Rev. 10 (1973) 1–35.
[965] R.G. Wilkins, The study of kinetics and mechanism of reactions of transition metal complexes, Allyn & Bacon, Boston, MA, 1974.
[966] R.C. Stewart, L.G. Marzilli, J. Am. Chem. Soc. 100 (1978) 817–822.
[967] G. Stochel, R. Van Eldik, Inorg. Chem. 29 (1990) 2075–2077.
[968] M. Meier, R. van Eldik, Inorg. Chem. 32 (1993) 2635–2639.
[969] H.M. Marques, L. Knapton, J. Chem. Soc. Dalton Trans. (1997) 3827–3833.
[970] F.F. Prinsloo, M. Meier, R. Vaneldik, Inorg. Chem. 33 (1994) 900–904.
[971] B.B. Hasinoff, Can. J. Chem. 52 (1974) 910–914.
[972] F.F. Prinsloo, E.L.J. Breet, R. van Eldik, J. Chem. Soc. Dalton Trans. (1995) 685–688.
[973] S. Funahashi, M. Inamo, K. Ishihara, M. Tanaka, Inorg. Chem. 21 (1982) 447–449.
[974] J.G. Leipoldt, R. van Eldik, H. Kelm, Inorg. Chem. 22 (1983) 4146–4149.
[975] H.M. Marques, J. Chem. Soc. Dalton Trans. (1991) 1437–1442.
[976] T.T.T. Bui, D.S. Sal'nikov, I.A. Dereven'kov, S.V. Makarov, Russ. J. Phys. Chem. A 91 (2017) 658–661.
[977] H.M. Marques, J. Chem. Soc. Dalton Trans. (1991) 339–341.
[978] H.M. Marques, E.L.J. Breet, F.F. Prinsloo, J. Chem. Soc. Dalton Trans. (1991) 2941–2944.
[979] G. Stochel, R. van Eldik, H. Kunkely, A. Vogler, Inorg. Chem. 28 (1989) 4314–4318.
[980] H.M. Marques, O.Q. Munro, B.M. Cumming, C. de Nysschen, J. Chem. Soc. Dalton Trans. (1994) 297–303.
[981] G.N. Schrauzer, J.H. Grate, J. Am. Chem. Soc. 103 (1981) 541–546.
[982] F. Nome, M.C. Rezende, C.M. Sabóia, A.C. Da Silva, Can. J. Chem. 65 (1987) 2095–2099.
[983] M.J. O'Neil (Ed.), The Merck Index - An Encyclopedia of Chemicals, Drugs, and Biologicals, Merck & Co., Inc, Whitehouse Station, NJ, 2006.
[984] C.L. Rollinson, J.C. Bailar, H.J. Emeléus, R. Nyholm, The Chemistry of Chromium, Pergamon Press, Oxord UK, Molybdenum and Tungsten, 2015.
[985] F. Basolo, R.G. Pearson, Mechanisms of Inorganic Reactions: A Study of Metal Complexes in Solution, Wiley, New York, NY, 1958.
[986] R. Williams, E. Billig, J.H. Waters, H.B. Gray, J. Am. Chem. Soc. 88 (1966) 43–50.
[987] F. Röhrscheid, A.L. Balch, R.H. Holm, Inorg. Chem. 5 (1966) 1542–1551.
[988] E.B. Fleischer, S. Jacobs, L. Mestichelli, J. Am. Chem. Soc. 90 (1968) 2527–2531.
[989] E.A. Betterton, PhD Thesis, University of the Witwatersrand, Johannesburg, South Africa, 1982.
[990] W.G. Jackson, S.S. Jurisson, B.C. McGregor, Inorg. Chem. 24 (1985) 1788–1790.
[991] M.S.A. Hamza, C. Dücker-Benfer, R. Van Eldik, Inorg. Chem. 39 (2000) 3777–3783.
[992] A.L. Crumbliss, W.K. Wilmarth, J. Am. Chem. Soc. 92 (1970) 2593.
[993] B.M. Alzoubi, M.S.A. Hamza, C. Dücker-Benfer, R. van Eldik, Eur. J. Inorg. Chem. (2003) 2972–2978.
[994] B. Banerjea, J. Roy, Z. Anorg. Allg. Chem. 400 (1973) 89–96.
[995] H. Ghazi-Bajat, R. van Eldik, H. Kelm, Inorg. Chim. Acta 60 (1982) 81–85.
[996] K.R. Ashley, M. Berggren, M. Cheng, J. Am. Chem. Soc. 97 (1975) 1422–1426.
[997] D.S. Reddy, S. Satyanarayana, Proc. Indian Acad Sci. Chem. Sci. 115 (2003) 175–183.

[998] J.A. Kernohan, J.F. Endicott, Inorg. Chem. 9 (1970) 1504–1512.
[999] W.K. Lee, PhD Thesis, University of Hong Kong, 1972.
[1000] D.A. Baldwin, E.A. Betterton, J.M. Pratt, S. Afr. J. Chem. 35 (1982) 173–175.
[1001] C. Männel-Croisé, B. Probst, F. Zelder, Anal. Chem. 81 (2009) 9493–9498.
[1002] C.H. Langford, H.B. Gray, Ligand Substitution Processes, W. A. Benjamin, Inc., New York, NY, 1965.
[1003] C.F. Zipp, J.P. Michael, M.A. Fernandes, M. Nowakowska, H.W. Dirr, H. M. Marques, Inorg. Chem. Commun. 57 (2015) 15–17.
[1004] S. Balt, A.M. Van Herk, Transit. Met. Chem. 8 (1983) 152–154.
[1005] J. Wiese, G. Klar, W. Hinrichs, CCDC 771320, 2016.
[1006] J.M. Pratt, Inorganic Chemsitry of Vitamin B_{12}, Academic Press, London, UK, 1972.
[1007] L. Knapton, H.M. Marques, S. Afr. J. Chem. 59 (2006) 43–47.
[1008] M.S.A. Hamza, X. Zou, K.L. Brown, R. Van Eldik, Inorg. Chem. 40 (2001) 5440–5447.
[1009] S.J. Brodie, A.G. Cregan, R. van Eldik, N.E. Brasch, Inorg. Chim. Acta 348 (2003) 221–224.
[1010] M.S.A. Hamza, A.G. Cregan, N.E. Brasch, R. Van Eldik, Dalton Trans. (2003) 596–602.
[1011] W.A. Pryor, Free Radicals, McGraw-Hill, New York, NY, 1966.
[1012] R.A. Heckman, J.H. Espenson, Inorg. Chem. 18 (1979) 38–43.
[1013] R. Yamada, S. Shimizu, S. Fukui, Biochemistry 7 (1968) 1713–1719.
[1014] J.A. Dean (Ed.), Lange's Handbook of Chemistry, McGraw-Hill, New York, NY, 1985.